SIMULTANEOUS MEASUREMENT OF ELASTIC CONSTANTS OF

ENGINEERED WOOD-BASED PANELS BY MODAL TESTING

by

Jianhui Zhou

Master of Engineering (MSc.Eng.), South China Agricultural University, 2014

Bachelor of Engineering (BSc.Eng.), South China Agricultural University, 2011

A Dissertation Submitted in Partial Fulfillment
of the Requirements for the Degree of

Doctor of Philosophy

in the Graduate Academic Unit of Faculty of Forestry & Environmental Management

Supervisor: Ying Hei Chui, PhD, Structural Eng., University of Alberta
Co-supervisor: Meng Gong, PhD, Forestry & Env. Mgt.

Examining Board: Phil Garland, PhD, Mechanical Eng.
                 Fan-Rui Meng, PhD, Forestry & Env. Mgt.
                 Ling Li, PhD, Forestry & Env. Mgt.

External Examiner: Pierre Blanchet, PhD, Université Laval

This dissertation is accepted by the
Dean of Graduate Studies

THE UNIVERSITY OF NEW BRUNSWICK

June, 2018

ABSTRACT

With the advent of mass timber panels and the development of mid- to high-rise wood constructions, the renaissance of wood construction is underway from Europe to North America and throughout the world. Engineered wood-based panel products, especially mass timber panels, play an important role in the evolution of wood construction. Elastic properties are not only fundamental mechanical properties for structural design but also important indicators for quality control purposes. Accurate measurement of the global elastic properties of full-size panels is critical for their applications as load-bearing building components. An efficient and reliable non-destructive technique is required for the purposes both of characterizing elastic properties and of grading engineered wood-based panel products in the production line before processing for all kinds of structural applications.

In this study, two vibrational non-destructive techniques employing modal testing for natural frequencies and other modal parameters were developed for simultaneous measurement of elastic constants of engineered wood-based panels. Both vibrational methods adopted modal testing of a rectangular plate with the boundary condition of a pair of opposite edges in the width direction simply supported and the other pair free. Compared with the elastic constant values by conventional static tests, both vibrational methods generally showed close agreement.

The first method was developed for measuring the moduli of elasticity in both major and minor strength directions and the in-plane shear modulus of a panel based on free transverse vibration of rectangular thin orthotropic plates. A simplified modal testing

procedure together with frequency identification methodology based on sensitivity analysis and an iterative algorithm were proposed as the means of achieving an efficient and reliable measurement with three and/ or four sensitive natural frequencies from only three impacts. The method was first verified with standard static test values in laboratory for full-size cross laminated timber, oriented strand board and medium density fibreboard. Then, 55 full-size cross laminated timber panels with different characteristics and from three manufacturers were tested in factory environments. The results showed that non-edge bonding and gap size had a negative effect on both E_y and G_{xy} and led to a large variation compared with edge bonded panels as well as with their corresponding prediction models (i.e., k-method, gamma method and shear analogy method). The second vibrational method was developed for determination of effective bending and shear stiffness values based on Mindlin plate theory with an exact frequency solution and a genetic algorithm for the inverse problem. The results showed that the transverse shear moduli of cross laminated timber panels can be accurately determined with proper shear correction factors and were verified by planar shear test values.

According to an in-depth comparative study, the first vibrational method shows great potential for future development of a standard testing method and on-line quality control over other existing vibrational methods in terms of setup implementation, frequency identification, accuracy and the calculation efforts required. The second vibrational method is suggested for engineered wood-based panels with small transverse shear moduli and/ or small length/ width to thickness ratio. Both methods are deemed to be applicable to all kinds of composite plates.

ACKNOWLEDGEMENTS

Foremost, I would like to express my sincere gratitude to my supervisor and mentor Prof. Ying Hei Chui for his continuous support of my study and research, for his patience, motivation and kindness. His broad knowledge and rich experience in wood engineering pave the way of this study. I very much appreciate all the guidance, valuable suggestions, academic freedom and opportunities provided by him. I am also grateful to my advisory committee members Dr. Meng Gong, who is a co-supervisor, teacher and friend to me, and Dr. Lin J. Hu, who is a passionate role model to me, for their insightful suggestions, careful reviews and much encouragement throughout my whole research.

A very special thanks goes out to Dean McCarthy for preparing test specimens and test setup at Wood Science and Technology Centre, Prof. Gerhard Schickhofer and his research team at Graz University of Technology in Austria for hosting me as a visiting student and conducting research at their institute, Mr. Hermann Kirchmayr and the staff at Stora Enso in Austria, Ms. Julie Frappier and the staff at Nordic Structures in Quebec for their supports for mill tests of CLT panels. Without their help, the research on full-size CLT panels in Chapter 5 could not have been done.

Table of Contents

viii

Curriculum Vitae

List of Tables

List of Figures

xiv

List of Abbreviations Nomenclature and Symbols

Abbreviations

BC	boundary condition
CCCC	all four edges of a rectangular plate are clamped
CCCF	three edges of a rectangular plate are clamped and one is free
CFFF	three edges of a rectangular plate are free and one is clamped
CFCF	a pair of opposite edges of a rectangular plate are clamped and the other pair are free
CLT	cross laminated timber
COV/ CV	coefficient of variation
DAQ	data acquisition
df	degree of freedom
DMDF	double-layer medium density fiberboard
DOSB	double-layer oriented strand board
EWPs	engineered wood products
FE	finite element
FEM	finite element method
FFFF	all four edges of a rectangular plate are free
FRF	frequency response function
GA	genetic algorithm
GLT	glued-laminated timber
GM	gamma method
LVL	laminated veneer lumber
LSL	laminated strand lumber

MC	moisture content
MDF	medium density fiberboard
MNET	mixed numerical-experimental technique
MOE	moduli/ modulus of elasticity
MOR	modulus of rupture
MSWP	multi-ply solid wood panel
NDT	non-destructive technique/ test
NLT	nail laminated timber
OSB	oriented strand board
OSL	oriented strand lumber
PB	particleboard
PSL	parallel strand lumber
SAM	shear analogy method
SCF	shear correction factor
SCL	structural composite lumber
SFSF	a rectangular plate in which one pair of opposite edges are simply supported and the other pair are free
Sig.	significance
SPF	spruce-pine-fir
SSSS	a rectangular plate in which all four edges are simply supported
2D	two-dimensional
3D	three-dimensional

Nomenclature and Symbols

a	plate length
b	plate width
f_{mn}	natural frequency of mode (m, n)
f_{expi}	i^{th} experimental natural frequency
f_{cali}	i^{th} calculated natural frequency
h	plate thickness
k	aspect ratio
k_{xz}	shear correction factor with respect to xz plane
k_{yz}	shear correction factor with respect to yz plane
m	the number of node lines including the simply supported sides in the y direction
n	the number of node lines including the simply supported sides in the x direction
t	time
w	transverse deflection of a plate
σ_1	orthotropic ratio E_y/E_x
σ_2	orthotropic ratio G_{xy}/E_x
ρ	plate density
ν_{xy}	major Poisson's ratio
ν_{yx}	minor Poisson's ratio
A_{gross}	gross cross sectional area
ψ_x	angle of rotation of a normal line due to plate bending with respect to x coordinate

ψ_y	angle of rotation of a normal line due to plate bending with respect to y coordinate
D_x or D_{11}	flexural rigidity with respect to E_x
D_y or D_{22}	flexural rigidity with respect to E_y
D_{12} or D_{21}	flexural rigidity
D_{xy} or D_{66}	torsional rigidity with respect to G_{xy}
C_{44}	shear stiffness with respect to G_{yz}
C_{55}	shear stiffness with respect to G_{xz}
E	modulus of elasticity
$E_{eff,\,GM}$	effective modulus of elasticity by gamma method
$E_{app,\,SA}$	apparent modulus of elasticity by shear analogy method
E_x	modulus of elasticity in the x axis
$E_{x,eff,k}$	effective modulus of elasticity in the x axis by k-method
E_y	modulus of elasticity in the y axis
$E_{y,eff,k}$	effective modulus of elasticity in the y axis by k-method
E_0	modulus of elasticity of lumber parallel to grain
E_{90}	modulus of elasticity of lumber perpendicular to grain
$EI_{eff,0}$	effective bending stiffness in the major strength direction
$EI_{eff,90}$	effective bending stiffness in the minor strength direction
$EI_{app,SA}$	apparent bending stiffness by shear analogy method
$EI_{eff,GM}$	effective bending stiffness by gamma method
G	shear modulus
$GA_{eff,SA}$	effective shear stiffness by shear analogy method
$GA_{eff,Timo}$	effective shear stiffness by Timoshenko beam theory

G_{090}	shear modulus of lumber parallel to grain
G_r	rolling shear modulus of lumber
G_{xy}	shear modulus with respect to xy plane, in-plane shear modulus
$G_{xy,eff,k}$	effective in-plane shear modulus by k-method
$G_{xy,\,CLT,\,est}$	estimated in-plane shear modulus of cross laminated timber
G_{xz}	shear modulus with respect to xz plane, transverse shear modulus
G_{yz}	shear modulus with respect to yz plane, transverse shear modulus
$G_{transverse}$	transverse or planar shear modulus
I	second moment of area
I_{gross}	gross second moment of area
J	area axial moment of inertia
K_s	shear factor for shear analogy method
M_x, M_y	bending moment terms
M_{xy}	twisting moment term
Q_x, Q_y	transverse shear terms

CHAPTER 1 INTRODUCTION

1.1 Background

Wood has been a building material throughout history due to its unique mechanical and machining characteristics. With the development of wood science, adhesion science and modern manufacturing technologies as well as the changes in wood resources, engineered wood products (EWPs) which optimize properties to meet the specific needs of structural design have been widely used in modern wood constructions. EWPs are a high-performance, consistent, reliable, and environmentally responsible choice for everything from construction to materials handling applications to home projects (APA, 2017). Research also showed that building with wood, especially engineered wood equivalents, would drastically reduce global carbon dioxide emissions and fossil fuel consumption (Oliver et al., 2014).

Wood structural panels are an important category of EWPs includes all-veneer plywood, composite panels containing a combination of veneer and wood-based material, and mat-formed panels such as oriented strand board (OSB). Plywood and OSB are often used in light frame wood construction as wall and roof sheathing and subfloors. Recently, the latest and popular massive timber panels, especially cross laminated timber (CLT), nail laminated timber (NLT) and structural composite lumber (SCL), have gained lots of attention and popularity around the world with the trend of mid- to high- rise wood constructions.

Figure 1.1 Engineered wood-based panel products (Source: APA)

Mass timber panels not only can be used as load-carrying plate elements in structural systems such as walls, floors and roofs but also are perfect building materials for prefabrication with computer numerical controlled machining. They are engineered to have high strength and dimensional stability, which can be used as an alternative to concrete, masonry and steel in many building types and make wood skyscrapers possible. Of all the mass timber panels, CLT has been gaining popularity in residential and non-residential applications as an innovative wood product worldwide, which was first introduced in the early 1990s in Austria and Germany (Brandner et al., 2016; Brandner, 2013). It is composed of crosswise layers of structural lumber laminates usually glued together by a structural adhesive (Gagnon and Pirvu, 2011). The edge surfaces of adjacent lumber in one layer can be bonded, known as edge bonding, or left without bonding or even with very small gaps. CLT has been used or proposed to be used in several tall wood buildings such

as the 14-storey TREET project in Norway (Malo et al., 2016) and the 18-storey Brock

Commons building in Canada. It is also the main objective material in this study.

TREET - Bergen, Norway   UBC Brock Commons - Vancouver, Canada

Figure 1.2 14-storey TREET and 18-storey Brock Commons (Source: WoodSkyscrapers)

Wood as a natural material has directional properties that also vary by species, growing

conditions, wood quality and so on. Therefore, EWPs are developed and engineered to

meet the specific needs of structural design, especially better homogeneity in physical and

mechanical properties than solid wood. Even though EWPs are expected to be more

homogenous than solid wood, each individual panel of the same type from the same production line varies in properties to different extends associated with different quality control levels, such as the uniformity of raw material properties, adhesive spread, layup etc. The studies on quality control of traditional wood-based panels were extensively conducted and can be found in classical handbooks and monograph (Forest Products Laboratory, 2010; Thoemen et al., 2010; Williamson, 2002).

Elastic properties are the basic mechanical properties of EWPs for their structural application as well as important indicators for quality control. It is known that the design of structural assemblies built with mass timber panels can be governed by serviceability limit states. Serviceability limit states design checks require elastic properties as input parameters. In order to evaluate the elastic properties of a EWP, conventional static testing methods including bending test and shear test are commonly used for testing elastic properties of small-sized beam-like samples cut from full-sized panels. However, static tests are tedious and sometimes destructive, which provides limited and local properties rather than global properties of a full-sized panel. As being said, the properties of full-sized wood-based panels also vary with the lay-up, raw material and many other manufacturing parameters. Moreover, mass timber panel, which is usually large in dimension, is always used as a whole floor or roof individually. Therefore, a non-destructive method rather than static tests is desired for testing full-size engineered wood-based panels, especially mass timber panels, for quality control and grading of the fabricated panel in the production line before processing for all kinds of applications.

Vibrational methods employing experimental modal testing and analysis seem to be an efficient non-destructive approach for the determination of the elastic constants of panel products (Ayorinde and Yu, 2005). The application of transverse and longitudinal beam vibration for property evaluation of beam-like wood materials was investigated thoroughly (Biechle et al., 2011; Brashaw et al., 2009; Bucur, 2006; Chui, 1991; Chui and Smith, 1990; Yoshihara, 2013), while such method has not been widely used for wood-based panel products. Research studies of evaluating the elastic constants of wood-based panels by use of modal testing could be traced back to the late 1980s. The in-plane elastic constants were frequently determined, namely the moduli of elasticity in major and minor strength directions loaded in bending (E_x and E_y) and in-plane shear modulus (G_{xy}), of solid wood plate (Martínez et al., 2011; Sobue & Kitazumi, 1991), OSB (Coppens, 1988; Larsson, 1996, 1997), medium density fiberboard (MDF) (Bos and Casagrande, 2003; Carfagni and Mannucci, 1996), plywood (Sobue and Katoh, 1992), and CLT (Gsell et al., 2007; Gülzow, 2008; Gülzow et al., 2008). These studies laid the foundation for the potential development of non-destructive technique (NDT) for on-line quality control of wood-based panel products. Further details are provided in Chapter 2.

The ultimate goal is to apply vibration-based testing method for on-line evaluation of full-size composite components during the manufacturing process. However, there are many aspects of this method that has important bearing on accuracy, ease of use, and computational efficiency (Ayorinde and Yu, 2005; Gagneja et al., 2001). This study is aimed to tackle the difficulties in measuring elastic constants by modal testing and develop a vibration-based NDT for engineered wood-based panels. The method is expected be

suitable for quality control and structural grading of engineered wood-based panels in the production line before processing for all kinds of applications.

1.2 Objectives

The ultimate goal of this study is to develop a NDT that can be used as a testing tool to evaluate the in-plane elastic constants, namely E_x, E_y, G_{xy} and transverse shear moduli (G_{xz} and G_{yz}) of full-size engineered wood-based panels. However, prior to that, a number of technical issues need to be addressed. The specific objectives of this project are:

1) To first propose a supporting system for modal testing of engineered wood-based panels and develop a sensitive frequency identification procedure that allows direct identification of natural frequencies of interests from a few measured spectra; then to develop an algorithm to extract in-plane elastic constants from measured frequencies and verify the proposed method by comparing its results with those measured using conventional static methods.

2) To compare the proposed method with existing vibrational methods, and provide general recommendations on selecting proper boundary conditions, forward solutions and inverse techniques for the measurement of elastic constants of wood-based panels products.

3) To apply the proposed method for measuring full-size CLT panels with different characteristics both in laboratories and mills, and use the obtained data to verify current CLT structural design models including k-method based on compound theory, gamma method based on mechanical jointed beam theory and shear analogy method.

6

4) To develop the proposed method for evaluating transverse shear moduli for wood-based panels with low transverse shear moduli and/ or small length/ width to thickness ratio, such as CLT, based on Mindlin plate theory and to verify the results with static test results.

1.3 Thesis Organization

To achieve the objectives and get as close as possible to the ultimate goal, a series of studies were conducted. The dissertation is presented in an articles-format considering the broad contents it covers, which consists of eight chapters in total. Chapter 1 serves as an overall introduction of the dissertation and Chapter 8 gives general conclusions and recommendations for future research and the rest chapters are outlined as followings.

Chapter 2 briefly reviews the identification of elastic properties of composite materials as well as wood composites using vibrational methods. The theory of transverse vibration of rectangular orthotropic thin and moderate thick plates, their frequency solutions and inverse techniques are also reviewed for a better understanding of the whole dissertation.

Chapter 3 presents an efficient non-destructive test method for simultaneous measurement of effective elastic constants of orthotropic wood-based panel products based on a modal testing technique. An algorithm is developed based on an improved approximate frequency equation of transverse vibration of orthotropic plates under the boundary condition, in which two opposite sides are simply supported and the other two are free (SFSF). The in-

plane elastic constants of full-size engineered wood-based panels including cross laminated timber (CLT), oriented strand board (OSB) and medium density fiberboard (MDF) were measured and verified.

Chapter 4 presented a comparative study on measurement of elastic constants of wood-based panels using modal testing. Three boundary conditions with corresponding calculation methods are investigated for measuring the elastic constants of wood-based panels. Standard static tests were performed to provide reference values for comparison. Recommendations are given for the choice of boundary condition and corresponding calculation procedures for different test scenarios and needs.

Chapter 5 applied the proposed method in Chapter 3 for measuring elastic constants including E_x, E_y, G_{xy} of 55 full-size mass timber panels in both laboratory and mills. The modal test measured values were used to examine the influence of structural characteristics such as layup, edge bonding and gaps on measured elastic properties as well to verify the effective stiffness prediction models of CLT and MSWP, including k-Method, gamma method and shear analogy method.

Chapter 6 further develop the proposed method by employing modal testing for the measurement of natural frequencies and genetic algorithm for minimizing the difference between calculated and measured natural frequencies for the inverse determination of in-plane and out-of-plane elastic constants of CLT panels. Based on the exact solution of free transverse vibration of orthotropic Mindlin plates under boundary condition of SFSF, the

effective bending and shear stiffness values were determined for three-layer and five-layer symmetric CLT panels. Chapter 7 verified the elastic constants, especially transverse shear moduli of CLT, with static test values. Planar shear tests have been conducted to verify the shear correction factors adopted for the CLT panels in this study.

Chapters 3, 4, and 5 have been published in *Holzforschung*, *Journal of Wood Science* and *Composites Part B: Engineering*, respectively, while Chapters 6 and 7 are both currently under review. Parts of the dissertation were also presented at academic conferences, including the World Conference of Timber Engineering in 2014 and 2016 and the International Nondestructive Testing and Evaluation of Wood Symposium in 2015.

References

APA. (2017). Engineered Wood Products for Superior Performance. Retrieved from http://www.apawood.org/level_b.cfm?content=prd_main

Ayorinde, E. O., and Yu, L. (2005). On the elastic characterization of composite plates with vibration data. *Journal of Sound and Vibration*, *283*(1–2), 243–262.

Biechle, T., Chui, Y. H., and Gong, M. (2011). Comparison of NDE techniques for assessing mechanical properties of unjointed and finger-jointed lumber. *Holzforschung*, *65*(3), 397–401.

Bos, F., and Casagrande, S. B. (2003). On-line non-destructive evaluation and control of wood-based panels by vibration analysis. *Journal of Sound and Vibration*, *268*(2), 403–412.

Brandner, R. (2013). Production and Technology of Cross Laminated Timber (CLT): A State-of-the-art Report. In *Focus Solid Timber Solutions - European Conference on CLT* (pp. 3–36). Graz.

Brandner, R., Flatscher, G., Ringhofer, A., … Thiel, A. (2016). Cross laminated timber (CLT): overview and development. *European Journal of Wood and Wood Products*, *74*(3), 331–351.

Brashaw, B. K., Bucur, V., Divos, F., … Yin, Y. (2009). Nondestructive testing and evaluation of wood: a worldwide research update. *Forest Products Journal*, *59*(3), 7–14.

Bucur, V. (2006). *Acoustics of Wood*. Boca Raton: CRC Press.

Carfagni, M., and Mannucci, M. (1996). A simplified dynamic method based on experimental modal analysis for estimating the in-plane elastic properties of solid

wood panels. In J. L. Sandoz (Ed.), *International symposium on nondestructive testing of wood* (pp. 247–258). Lausanne: Presses polytechniques et universitaires romandes.

Chui, Y. H. (1991). Simultaneous evaluation of bending and shear moduli of wood and the influence of knots on these parameters. *Wood Science and Technology*, *25*(2), 125–134.

Chui, Y. H., and Smith, I. (1990). Influence of rotatory inertia, shear deformation and support condition on natural frequencies of wooden beams. *Wood Science and Technology*, *24*(3), 233–245.

Coppens, H. (1988). Quality control of particleboards by means of their oscillation behavior. In *FESYP Technical Conference* (pp. 143–165). Munich.

Forest Products Laboratory. (2010). *Wood Handbook - Wood as an Engineering Material*. (R. J. Ross, Ed.) (Centennial). Madison: United States Department of Agriculture Forest Service.

Gagneja, S., Gibson, R. F., and Ayorinde, E. O. (2001). Design of test specimens for the determination of elastic through-thickness shear properties of thick composites from measured modal vibration frequencies. *Composites Science and Technology*, *61*(5), 679–687.

Gagnon, S., and Pirvu, C. (2011). *CLT Handbook*. (S. Gagnon & C. Pirvu, Eds.). Quebec City: FPInnovations.

Gsell, D., Feltrin, G., Schubert, S., … Motavalli, M. (2007). Cross-Laminated Timber Plates: Evaluation and Verification of Homogenized Elastic Properties. *Journal of Structural Engineering*, *133*(1), 132–138.

11

Gülzow, A. (2008). *Zerstörungsfreie Bestimmung der Biegesteifigkeiten, von Brettsperrholzplatten*. ETH Zürich.

Gülzow, A., Gsell, D., and Steiger, R. (2008). Non-destructive evaluation of elastic parameters of square-shaped cross-laminated solid wood panels, built up symmetrically with 3 layers. *Holz Als Roh-Und Werkstoff*, *66*(1), 19–37.

Larsson, D. (1996). Stiffness characterization of wood based panels by modal testing. In J. Sandoz (Ed.), *International symposium on nondestructive testing of wood* (pp. 237–246). Lausanne: Presses polytechniques et universitaires romandes.

Larsson, D. (1997). Using modal analysis for estimation of anisotropic material constants. *Journal of Engineering Mechanics*, *222–229*(123), 3.

Malo, K. A., Abrahamsen, R. B., and Bjertnæs, M. A. (2016). Some structural design issues of the 14-storey timber framed building "Treet" in Norway. *European Journal of Wood and Wood Products*, *74*(3), 407–424.

Martínez, M. P., Poletti, P., and Espert, L. G. (2011). Vibration Testing for the Evaluation of the Effects of Moisture Content on the In-Plane Elastic Constants of Wood Used in Musical Instruments. In C. M. A. Vasques & J. Dias Rodrigues (Eds.), *Vibration and Structural Acoustics Analysis* (pp. 21–57). Springer Netherlands.

Oliver, C. D., Nassar, N. T., Lippke, B. R., and McCarter, J. B. (2014). Carbon, Fossil Fuel, and Biodiversity Mitigation With Wood and Forests. *Journal of Sustainable Forestry*, *33*(3), 248–275.

Sobue, N., and Katoh, A. (1992). Simultaneous determination of orthotropic elastic constants of standard full-size plywoods by vibration method. *Mokuzai Gakkaishi*,

38(10), 895–902.

Sobue, N., and Kitazumi, M. (1991). Identification of power spectrum peaks of vibrating completely-free wood plates and moduli of elasticity measurements. *Mokuzai Gakkaishi*, *37*(1), 9–15.

Thoemen, H., Irle, M., and Sernek, M. (2010). *Wood-Based Panels An Introduction for Specialists*. London England: Brunel University Press.

Williamson, T. G. (2002). *APA Engineered Wood Handbook*. New York: McGraw-Hill.

Yoshihara, H. (2013). Comparison of results obtained by static 3- and 4-point bending and flexural vibration tests on solid wood, MDF, and 5-plywood. *Holzforschung*, *67*(8), 941–948.

CHAPTER 2 LITERATURE REVIEW

2.1 Introduction

Engineered composite materials have been widely used in almost every engineering industry and still keep growing and developing at a very high speed. Elastic properties are the very basic mechanical properties for their various applications. In structural and aerospace engineering fields, the use of orthotropic plate materials such as sandwich, laminated material and fiber-reinforced composites is very popular. Elastic constants, namely the modulus of elasticity in major (E_x) and minor (E_y) directions, in-plane shear modulus (G_{xy}), out-of-plane/ transverse shear moduli (G_{xz} and G_{yz}) and the major Poisson's ratio (v_{xy}), are essential for their structural application as plate components. For instance, engineered wood-based panel products, especially mass timber panels, are often used as load-bearing plates and shear panels in wood constructions. The evaluation of serviceability criteria like maximum deflections and vibration susceptibility requires elastic constants as input parameters. Therefore, the characterization of elastic properties of composite materials is highly demanded and of great importance to their applications.

The measurement of elastic constants can be realised by both static and dynamic test methods. Standard static test methods based on quasi-static solid mechanics such as bending, tension, compression, shear, and torsional tests have been developed and established for various materials in official standards by national and international originations. Standard static test methods are commonly aimed at obtaining stress-strain or load-displacement data while dynamic test methods including vibration and acoustic based

14

methods are aimed at measuring natural frequencies and velocities, respectively. Vibrational methods based on plate theories tend to be the least expensive dynamic test methods presently utilized compared with static test methods. Vibrational methods can provide effective or global elastic properties of a full-size orthotropic plates at one time rather than local properties measured by separated static tests. Also, vibrational methods tend to be non-destructive and efficient while static tests generally require longer set-up and testing time. This chapter briefly reviews the vibration theory of orthotropic plates, the vibrational methods of determination of elastic constants of orthotropic materials and the research work of vibration-based NDT for wood materials.

2.2 Forward Solution for Free Transverse Vibration of Thin and Moderate Thick Rectangular Orthotropic Plates

Composites including sandwich and laminated plates are often assumed continuous orthotropic plates. Their vibrational behavior is controlled by the overall stiffness, also known as effective or global stiffness, of the composite material rather than the stiffness of their individual layer (Lauwagie, 2005). Based on such assumptions, the determination, sometimes called identification or measurement, of elastic constants of orthotropic plates by vibrational methods are based on the theory of free transverse vibration of thin/ moderately thick rectangular orthotropic plates, namely Kirchhoff plate and Mindlin plate theories, respectively.

It is well known that obtaining the free vibration frequencies and mode shapes of rectangular plates with different boundary conditions (BCs) of simple support (S), clamp (C) or free (F) at four edges is a classical problem in applied mechanics. Numerous studies have been conducted for this family of problems. The forward solutions of free transverse vibration of thin and thick orthotropic plates are of great importance to the inverse determination process. Without a suitable forward solution for calculating the natural frequencies with input of elastic constants, the inverse problem of determining elastic constants cannot be formulated.

For thin orthotropic plates with orthogonal material properties, only the plate with boundary condition of a pair of opposite edges simply supported achieves exact solutions, while no exact solutions were reported for the other boundary conditions before Xing and Liu (2009). Numerical methods such as Rayleigh–Ritz, superposition and finite element method (FEM) have shown adequate accuracy in solving this problem. Leissa conducted an extensive review of the research works up to 1985 in his monograph (Leissa, 1969) and a series of review articles (Leissa, 1973, 1977, 1978, 1981, 1987). Several typical studies were reviewed below.

Of all the available solutions, only exact solutions satisfy both the governing equations and the boundary conditions rigorously, which show theoretical importance and computational efficiency over numerical solutions. Huffington and Hoppmann (1958) reported the Levy-type exact frequency characteristic equation for free vibration of thin orthotropic plates with one pair of opposite edges simply supported and the other two edges being the

combination of free, simply supported and/ or clamped. Numerical methods are needed to solve the transcendental frequency characteristic equations to obtain frequencies. Ng and Kulkarni (1972) computed the natural frequencies of bridge slabs which was regarded as an orthotropic thin plate under boundary condition of SFSF based on the frequency equation by Huffington and Hoppmann (1958). They set the Poisson's ratio to zero and calculated a set of empirical relationships between the plate parameters for a simple frequency calculation process. The effects of a variety of boundary conditions, material orthotropic, Winkler foundation modulus and aspect ratio for the first several modes were studied numerically for rectangular orthotropic plates with a pair of parallel edges simply supported (Jayaraman et al., 1990). However, it turns out to still be tedious to use these methods for practical application.

Rayleigh-Ritz methodwas the most popular method before FEM became popular and affordable for obtaining approximate natural frequencies of thin rectangular orthotropic plates due to its versatility and conceptual simplicity. Hearmon (1946) might be the first who reported the frequency equation of rectangular orthotropic plate by Rayleigh-Ritz method and verified the fundamental natural frequencies with experimental results of wood and plywood plates with four edges clamped (CCCC) and simply supported edges (SSSS). Results showed that the experimental fundamental natural frequencies were on average about 23% lower than calculated ones for clamped edges and were similar or higher for simply supported edges. Warburton (1954) demonstrated that Rayleigh method could be used to derive simple approximate frequency expressions for all modes of free transverse vibrations of isotropic rectangular plates with all possible boundary conditions. Hearmon

17

(1959, 1961) extended Warburton's method to thin orthotropic plates under different boundary conditions. Kim and Dickinson (1985) provided the improved approximate expressions derived for the natural frequencies of isotropic and orthotropic rectangular plates with one or more free edges and high in-plane forces using Rayleigh-Ritz method with three terms in the shape function. Their simple closed-form frequency equations appear to be accurate and the most feasible for practical application.

Gorman (1978, 1982) first extended the superposition method to the free transverse vibration of isotropic plates and then orthotropic plates (Gorman, 1993; Gorman and Ding, 2003), and laminated symmetric cross-ply rectangular plates (Gorman and Ding, 1996). In his monograph (Gorman, 1999), the superposition method was extensively discussed and proved to be powerful for solving plate vibration problems. Experimental verification was conducted for free vibration of rectangular plates with classical edge conditions, namely FFFF, CFFF, CFCF and CCCF using aluminum plates (Singal et al., 1992).

Xing and Liu (2009) applied a novel method of separation of variables to solve the problem of free transverse vibration of thin rectangular orthotropic plates for all possible combinations of boundary conditions. Exact normal eigenfunctions and eigenvalue equations were obtained and a solution method of the transcendental eigenvalue equations was provided. Their study is the first of its kind that provides exact references, which can be used as benchmarks for numerical results.

The above researches were based on Kirchhoff plate theory that is also known as classical plate theory and is applicable for thin plates with a large length/ width to depth ratio usually larger than at least 20. Neglecting transverse shear deformation and rotatory inertia can lead to overestimated frequency values for higher modes or plates with a small transverse shear modulus. Therefore, the Mindlin plate theory, also knows as first order plate theory, is often applied for moderately thick plates. However, it requires an appropriate shear correction factor due to the assumption of a constant shear stress distribution throughout the thickness. Thus, higher order plate theories were also proposed for moderate thick plates especially like laminated composite and sandwich panels. A start-of-art literature review on computational models for laminated composite and sandwich panels was conducted by Kreja (2011). Similar to solving vibration problems of thin plates, Rayleigh-Ritz and FEM are the most often used methods. Several typical studies are reviewed below.

Liew et al. (1995) conducted a literature review about the research on thick plate vibration before 1993. It was found that most studies were based on Mindlin plate theory and its modifications. Liew et al. (1998) also published a monograph dealing with vibration of Mindlin plates, in which the Ritz method with programming codes (p-Ritz method) were developed for obtaining the approximate solutions. Qatu (2004) published a monograph about vibration of laminated shells and plates, which paid special attentions to shell theory and linear analysis using the Ritz, Galerkin and FEM for plate and shell vibration problems.

On the exact solution of free vibrations of moderate thick orthotropic rectangular plates, it was often believed the exact solution only existed with the boundary condition of SSSS before Liu and Xing (2011). Liu and Xing (2011) obtained the exact closed-form solutions for free vibration of orthotropic rectangular Mindlin plates by using the separation of variables method. The exact solutions were given for boundary conditions with a pair of two opposite edges simply supported and the other two being the combination of free, simple support and/ or clamp. The results were validated through both mathematical proof and numerical comparisons with available *p*-Ritz solutions and FEM solutions.

Sayyad and Ghugal (2015) conducted a literature review on the studies of free vibration analysis of laminated composite and sandwich plates reported between 2000 and 2013. Many displacement fields of various displacement based shear deformation theories were summarized and compared. It was pointed out that their application to laminated composite and sandwich plates is still in rudimentary stage. These theories were limited to solve free vibration of all edges simply supported (SSSS) laminated composite and sandwich plates. Reddy's higher order theory for laminated composite plates (Reddy, 1984) might be the only higher order plate theory with exact solutions for boundary conditions with a pair of two opposite edges simply supported and the other two being the combination of free, simply supported and/ or clamped. Khdeir (1988) developed an exact mathematical tool to analyze the free vibration and buckling of symmetric cross-ply laminated plates based on a generalized Levy-type solution based on Reddy's higher order plate theory.

The forward solutions for free transverse vibration of thin and moderately thick rectangular orthotropic plates are briefly reviewed, which are often used for the inverse determination of elastic constants of orthotropic plates by modal testing. In-depth and detailed discussion about the aforementioned theories and methods can be found in the reviewed references and monographs. More advanced plate theories and 3D plates are not covered here.

2.3 Inverse Determination of Elastic Constants of Composite Materials by Modal Testing

The use of laminated composite, sandwich plates and shells such as fiber-reinforced composites in many engineering applications has been expanding rapidly in the past decades. The knowledge of the elastic properties of composite materials is crucial for the design of structural applications subject to static or dynamic loading as well as material design. Vibration-based methods have been proven to be efficient to characterize the elastic properties of orthotropic materials (Ayorinde and Yu, 2005; De Wilde, 2001; Gibson, 2000; Tam et al., 2016). This type of inverse problem is aimed at determining the elastic constants by minimizing the differences between experimental and calculated natural frequencies of a plate specimen. The aforementioned forward solutions of free vibration of rectangular plates by different solving techniques are often used to formulate the inverse problem. Experimental modal tests and analysis are conducted to obtain the experimental natural frequencies, mode shapes and other modal parameters if needed. According to a few literature review articles (Ayorinde and Yu, 2005; De Wilde, 2001; Gibson, 2000; Tam et al., 2016), most of such research works were based on classical plate theory for the

21

determination of in-plane elastic constants, and a small part of studies were based on moderate thick plate theory for additional out-of-plane shear moduli. Due to the extensive studies conducted in this field, only a few classical studies were reviewed as follows.

Sol (1986) was the first to adopt Kirchhoff thin plate theory for the identification of four in-plane elastic constants of anisotropic plates using natural frequency data measured under boundary condition of FFFF with a Bayesian parameter estimation procedure. The forward solution was solved by Rayleigh-Ritz method with Lagrange polynomials. Thereafter, the mixed numerical-experimental techniques (MNETs) for material identification has been proposed and developed not only for elastic constants but also other mechanical properties at Free University of Brussels (VUB) by Sol and De Wilde (De Wilde and Sol, 1987; H. Sol and Oomens, 1997). A review on MNETs for the characterization of anisotropic composites through their vibrational behavior was conducted by De Wilde (2001). MNETs were employed by their graduate students, collaborators and other researchers for the identification of elastic properties of different orthotropic materials. Hua (1993) extended the method of Sol (1986) with a sandwich model, a moderate thick Mindlin plate model and circular orthotropic disks. De Visscher (De Visscher, 1995) applied the MNET method for the identification of complex stiffness matrix of orthotropic materials. The material damping properties of fibre reinforced polymers were obtained by using a numerical model of the specimen in combination with the modal strain energy method (De Visscher et al., 1997). Lauwagie determined the elastic properties of the constituent layers of layered materials using MNET method (Lauwagie, 2005; Lauwagie et al., 2004). The layer properties were derived from natural frequencies of rectangular beam- or plate-shaped

22

specimens for both isotropic and orthotropic materials. Lauwagie et al. (2010) also extended the developed method for the identification of the Poisson's ratio of orthotropic materials. It is worth noting that in the identification of both damping ratios and Poisson's ratio, the so-called Poisson's plate of a specific aspect ratio was prepared for modal testing. Due to the non-destructive nature of this method, Sol and Bottiglieri (2010) applied the MNET method for the identification of temperature dependent elastic properties of a thermoplastic composite material. In the studies by Lauwagie (2005), Lauwagie et al. (2010) and Sol and Bottiglieri (2010), FEM was employed for solving the forward solution.

Deobald and Gibson (1988) reported a study on determination of the elastic constants of a square aluminum and three graphite/ epoxy plates by modal analysis, which was conducted about the same time of Sol's study (1986). The forward problem was solved by the Rayleigh-Ritz method using characteristic functions of vibrational beams, and a program was proposed for obtaining natural frequencies and mode shapes. A second program was proposed to determine the four apparent elastic constants with an iterative technique. The modal tests were conducted under three boundary conditions, namely FFFF, CFFF and CCFC. The major problem was found that the experimental natural frequencies did not match the predicted values well, which was thought to be caused by the non-ideal experimental boundary conditions and inaccurate Rayleigh-Ritz model. The completely free boundary condition was suggested for practical tests, because it was proven to be easier to replicate in practice than simply supported or clamped boundary conditions. Since then, the boundary condition of FFFF becomes the most popular boundary condition for this type study. The vibrational method proposed by Deobald and Gibson (1988) was further

developed with the classical lamination theory and potential-energy-optimized few-modes representation of the transverse displacement of a completely free plate (Ayorinde and Gibson, 1993). A suitably formed least-squares objective function was used in the inverse analysis. Their subsequent research works were mainly aimed at improving the proposed method with trimodal and hexamodal Rayleigh formulations (Ayorinde and Gibson, 1995), applying the proposed method for thick orthotropic composite plates (Ayorinde, 1995), using diagonal modes for the identification process (Ayorinde and Yu, 1999), and specimen design for identification of through-thickness shear properties (Gagneja et al., 2001). Gibson and their collaborators' work on the use of modal vibration response measurements to characterize the mechanical properties of fiber-reinforced composite materials and structures were introduced by (Gibson, 2000). Ayorinde and Yu (2005) reviewed the proposed method with a global look regarding many aspects which would influence the accuracy, ease of use and computational economy. The most recent study in this series on measuring five elastic constants of orthotropic plates by the existing optimized Rayleigh's method was preformed by Yu (2006). This series of work devoted to the application of Rayleigh-Ritz method and its improvements for solving forward solution due to its great computational efficiency compared with FEM.

Pedersen and Fredericksen at Technical University of Denmark were also among the pioneers who conducted the studies on the identification techniques for composites with a pilot project initiated in 1987. Pedersen and Fredericksen (1992) reported the identification of in-plane orthotropic material moduli by a combined experimental/ numerical method. The classical Rayleigh-Ritz method based on global expansion functions was used for

solving the forward problem. The proposed method was used for the identification of four in-plane elastic constants for a rolled aluminium plate, a glass/epoxy plate and a carbon/epoxy plate as well as temperature dependence for elastic constants of the glass/epoxy plate. Frederiksen extended the work for thick plates first based on Reddy's higher-order shear deformation theory (Frederiksen, 1997b) and then improved with another higher-order shear deformation theory by Lo et al. (1977) (Frederiksen, 1997a). He also investigated the parameter uncertainty in the identification process, and proposed the design of optimal experiments for the estimation of elastic constants based on uncertainty analysis (Frederiksen, 1998). An overview of the state of the art on their works was reported by Pedersen (1999).

Soares et al. (1993) probably made the first attempt to develop a finite element model as the forward solution for the identification of six material parameters of composite plate specimens based on Mindlin plate theory. They pointed out that their model was very dependent on aspect ratio of the specimen and good experimental natural frequencies. Araújo et al. (1996) extended their study with more results of composite materials being presented.

Besides the aforementioned studies, a significant of similar work with FFFF boundary condition has been done to improve the accuracy and simplify the optimization procedure since the early 1990s. Lai and Lau (1993) extended the work by Deobald and Gibson (1988) for a generally orthotropic plate and found that choosing the right combinations of natural modes together with a set of reasonable initial estimates for the constants to start the

iteration was crucial in achieving convergence. Moussu and Nivoit (1993) used the method of superposition developed by Gorman (1982) as the forward solution for the identification of elastic constants for a glass plate, a laminated steel plate and a glass/ epoxy plate. Hwang and Chang (2000) proposed a method of combining finite element analysis and optimum design in order to simplify the modeling processes and to reduce complicated derivation in the numerical method for the inverse determination of the elastic constants. Daghia et al. (2007) proposed a complex method based on Bayesian framework in the optimization process for the estimation of elastic constants of thick laminated plates by taking into account the priori information on the elastic constants. A combined low/ high frequency dynamic identification approach was presented by Bartoli and Marzani (2012). They combined the frequency identification approach with finite element modeling in order to solve the identification difficulty caused by the small sensitivity of the natural frequencies to transverse elastic shear constants and Poisson's ratios. Ismail et al. (2013) presented the determination of material properties of orthotropic plates with general elastic boundary supports using the inverse method and Fourier series. The results of a graphite epoxy plate with FFFF, CFFF and CCFC boundary conditions were simulated and compared with the material properties reported by Deobald and Gibson (1988), and they found that the average material properties error was less than 10%.

Most of the studies employed conventional derivative-based optimization technique for the inverse identification, which required initial guesses and sometimes had convergence problems. Cunha et al. (1999) first applied genetic algorithm (GA) for the identification of elastic constants of composite materials from dynamic tests based on the first-order shear

deformation theory. Their results showed that GA was very effective and robust in the inverse estimation of elastic constants. Silva et al. (2004) also adopted the GA for identifying the four in-plane elastic parameters of composite material. It was proved that GA was able to handle the usual drawbacks of conventional optimization techniques including the presence of several local minima and ill-conditioning. Hwang et al. (2009) proposed a hybrid genetic algorithm for the identification of the five effective elastic constants of transversely isotropic composite material, which showed great advantage in repeatability and accuracy. The selection and comparison of different optimization techniques for non-destructive evaluation of composite materials using computational inverse techniques can be referred to the monograph by Liu and Han (2003).

The ultimate goal of the aforementioned studies was to apply vibration-based testing method for on-line evaluation of full-scale composite components during the manufacturing process. However, the major difficulty in testing full-scale specimens appears to be in the development of the analytical model for the solution of the inverse problem in the case where *in-situ* properties are desired (Gibson, 2000). For those boundary conditions such as the mostly investigated FFFF where no close-formed solution exists, numerical simulation that may require significant computation time cannot be avoided, which is not practical for on-line testing. While for boundary condition like SSSS which has an exact analytical frequency equation, the boundary condition is not easy to be achieved in practice. Therefore, the development of such techniques needs the contribution from plate theory development with user-friendly forward solutions.

Moreover, modal information such as mode sequence is important for elastic properties characterization procedures because they basically rely on comparison of measured and computed frequency parameters (Ayorinde and Yu, 2005). The mode shape indices essentially represent the number of flexure half sine waves in the orthogonal directions of the plate geometry, which would define each mode explicitly by substituting the mode indices to the closed-form frequency equation. The common practice of identifying the mode sequence is to compare the experimental mode shape with the predicted one, which requires an experimental modal analysis consisting of impacts on a grid of points and mode shape plotting. Even though a direct method of identification of elastic constants of anisotropic plates by modal analysis without the need to identify the mode shapes was proposed (Grediac and Paris, 1996; Grédiac et al., 1998), the method was only applicable for small specimens due to the limitations of the optical technique. The key of such methods was to apply optical technique to measure the mode shape and derive deflection functions for solving the governing equation, which made the method exact rather than through an approximation algorithm based on Rayleigh-Ritz or numerical simulation method.

As discussed by De Wilde (2001) and Ayorinde and Yu (2005), there were many aspects of this method that had important bearing on accuracy, ease of use and computational economy. The issues that arise include vibration representation functions, selection of experimental mode shapes and frequencies for analysis, goodness of experimental data, frequency sensitivity of the elastic constants, influence of diagonal modes where relevant, plate thickness, plate aspect ratio, material orthotropic ratio and orientation of reinforcing fibers in laminate composites. Tam et al. (2016) conducted a review on the identification

28

of material properties of composite materials using non-destructive vibrational evaluation approaches. Though not all related researches were reviewed, some new trends and development in this field were analyzed. They concluded that the future research could focus on hybrid use of the Fourier method and particle swarm optimization method via combined use of natural frequencies, mode shapes, nodal lines, and damping as a global error function, applied on composite plates with arbitrary shapes and mixed boundary conditions for improving accuracy, rate of convergence, cost, as well as versatility and flexibility.

2.4 Vibrational Methods for Measuring Elastic Properties of Wood-based Materials

Solid wood and wood-based composites are often used as structural components in wood construction. Engineered wood-based panels such as oriented strand board (OSB) are even more widely used in modern wood constructions, especially in light frame wood construction. Elastic constants are critical mechanical properties for structural design, which are also the key quality control parameters. Wood as a natural composite material has also received much attention for the development of vibration-based NDT to measure its elastic constants similar to other composite materials as reviewed above. Among all the vibrational methods for wood material, most of the studies were based on beam vibration theory, and the rest were based on plate vibration theory.

The vibration testing of wood has been studied for a long time for a variety of purposes such as stress grading of lumber products. Some early research work was reviewed and the

theoretical derivations were also given by Hearmon (1966). The measurements of the elastic modulus (E) and shear modulus (G) of beam-like solid wood and wood-based materials can be based on longitudinal vibration, torsional vibration and transverse vibration methods.

Sobue (1986, 1988) proposed a tapping method using complex vibrations of bending and twisting of free-free beams for measuring the E and G values of structural lumber simultaneously. Chui (1991) also reported a simultaneous testing method based on Timoshenko beam theory for determining the E and G values of Canadian white spruce as well as the influence of knots on E to G ratio. The influence of rotatory inertia, shear deformation and support condition on the natural frequencies of wooden beams was discussed before the development of vibration-based test method for evaluating the bending and shear moduli of wood (Chui and Smith, 1990) using a free-free beam test arrangement. The method was also used for non-destructive testing of laminated and unlaminated, reconstituted wood panels used for furniture manufacture (Ilic and Ozarska, 1996). The non-destructive dynamic E corrected for shear and rotatory inertia effects, was positively correlated with E and modulus of rupture (MOR) from static tests, but the uncorrected E showed a better correlation. Hu and Hsu found that span-to-depth ratios were a critical factor for the application of the transverse free-free beam vibration technique (Hu and Hsu, 1996).

The different theoretical models and their approximate solutions of free vibration of clear wooden beams were reviewed by Brancheriau and Baillères (2002) that allowed them to

determine with sufficient accuracy the longitudinal E and G values in transverse vibrations. More recently, the specimen configuration and analysis methods in the flexural and longitudinal vibration tests of solid wood and wood-based materials were investigated by Yoshihara (2011, 2012a, 2012b, 2012c, 2012d). It was found that the shear modulus was significantly dependent on the specimen configuration, namely depth/ length ratio, as well as Poisson's ratio. Three analysis methods: a) the method based on the rigorous solution of Timoshenko's beam equation b) the iteration procedure proposed by Hearmon and c) the method in which modulus of elasticity measured by the longitudinal vibration test is substituted into the equation proposed by Goens (1931), were compared for calculation of elastic constants (Yoshihara, 2012a). Higher modes were recommended for using the third method, which was simpler than the other two and can reduce the influence of depth/ length ratio.

As it can be seen, the testing of beam-like solid wood and wood-based materials using vibration techniques has been a subject of many research studies. These techniques have been also proven effective in practical use in both the laboratory and factory such as stress grading of structural lumber.

Similar to the reviewed studies for composite plates, research studies evaluating the elastic constants of wood-based panels by use of modal testing could be traced back to the late 1980s. Different boundary conditions (BCs) with corresponding calculation methods have been adopted for measuring the elastic constants of panel type products such as solid wood panels, particleboard, OSB, plywood and medium density fibreboard (MDF) and cross

31

laminated timber (CLT). Due to the successes of vibrational methods for beam-like wood products, the studies on plate-like wood composites aimed at not only developing a test method for elastic constants measurement but also a NDT for quality control of full-size panel products. This is found to be obviously different from the aforementioned studies on other composite materials. In addition, the dimension of wood composite plate specimens investigated was also much larger than that of the composite plate specimens in aforementioned studies.

Since all four sides free (FFFF) has proved to the most suitable BC for modal testing by the reviewed studies for orthotropic plates, it was also mostly used among the studies done for plate-like wood products. As there is no exact solution for FFFF boundary condition, the one-term Rayleigh frequency solution was frequently employed as forward solution due to its simple and straight-forward formula (Bos and Casagrande, 2003; Carfagni and Mannucci, 1996; Coppens, 1988; Nakao and Okano, 1987; Sobue and Kitazumi, 1991). The natural frequency of the torsional mode was used for measuring the in-plane shear modulus of wood-based panels by Nakao and Okano (1987). The method appeared to be much simpler than static plate-twist shear tests. Coppens (1988) tested particleboard specimens to measure their elastic constants in the laboratory of individual company for quality control purposes. Sobue and Kitazumi (1991) measured the elastic constants (E_x and E_y) of wood panels (western red cedar, hemlock, buna and keyaki) with FFFF BC using a vibration technique. The results were verified with static test results of beam specimens. A simplified dynamic method based on experimental modal analysis for estimating the in-plane elastic properties of solid wood panels was presented by (Carfagni and Mannucci

1996), which was based on assessing whether the response and excitation were in or out of phase. The number of impact points was reduced to six for rectangular wood panels with FFFF BC. An on-line non-destructive evaluation system called VibraPann for quality control of wood-based panels was introduced in (Bos and Casagrande, 2003). The in-plane moduli of elasticity in the two orthogonal directions of selected eight OSB panels, 260 plywood panels, and one MDF panels were tested from the measurement of two vibration modes of bending, $f_{(2,0)}$ and $f_{(0,2)}$, using the system. The results showed an absolute difference within 15% of E_x and E_y values for plywood. They also pointed out the spatial variability of elastic properties within a panel by testing of small panels cut from the full-size panel.

Besides the Rayleigh frequency solution, FEM was also used for the determination of elastic constants combined with modal testing (Larsson, 1996, 1997; Martínez et al., 2011). The elastic constants were estimated by minimizing the difference between the experimental frequencies and FEM values using an iterative process. Full-size MDF and OSB panels, modeled as thin orthotropic plates under FFFF BC, were tested by Larsson (1996, 1997) using modal testing. The proposed dynamic method was proved to be accurate because of the good agreement between measured and calculated natural frequencies (up to the 7th mode) within 1-5%, though the average differences between dynamic and static bending data of E_x and E_y were 14.1% and 31.0%, respectively. A similar method was adopted to study the effects of moisture content on the in-plane elastic constants of wooden boards used in musical instruments (Martínez et al., 2011). It was found that the vibrational behavior of wood varied considerably with changes in moisture content. With the moisture

33

content ranging from 0% to 25%, the E values in radial and longitudinal directions and G of longitudinal and radial plane changed approximately 88%, 51% and 47%, respectively. Recently, Gsell et al. (2007) measured the natural frequencies and mode shapes of a rectangular CLT specimen. An analytical model based on Reddy's higher order plate theory (Reddy, 1984) was applied to calculate natural frequencies and mode shapes numerically. All three shear moduli and the two in-plane moduli of elasticity were identified by minimizing the difference between measured and estimated natural frequencies based on the least-squares method. Gülzow (2008) further studied the modal testing method proposed in (Gsell et al., 2007) to evaluate the elastic properties of CLT panels with different layups.

FFFF, however, is not the best BC for large size panels and for production environment. Other boundary conditions such as one edge simply supported and the other three edges free (SFFF) and one edge clamped and the other three edges free (CFFF) were also used for the determination of elastic constants of full-size structural panels for the purpose of quality control in production. A simultaneous determination of orthotropic elastic constants of standard full-size plywood by vibration method was conducted with SFFF boundary condition (Sobue and Katoh, 1992). The results showed an agreement to within 10% of E and G values measured using static bending and plate torsional tests respectively. Particleboard and MDF panels of full-size dimensions were tested using a vibration technique in both vertical and horizontal cantilever (CFFF) arrangements (Schulte et al., 1996). It was found that there was no significant difference between measured frequencies from the vertical and horizontal position, which indicated that the deflection caused by self-

weight under horizontal position had no effect on measured frequencies. The absolute values of the dynamic E values were about 20-25 % higher than the static values, while MDF had a better correlation and smaller difference between dynamic and static results than particleboard.

Though the studies on vibrational methods for wood composite plates were not as common as those for other composite plates, the research for wood composites was more related to practical application for wood-based panel products. However, the above reported vibrational methods have so far not been implemented for on-line evaluation of full-size wood-based panel products. SFFF and CFFF boundary conditions cannot be realized in a production line as the panel are either in a vertical or in a cantilever position, which can be easily affected by the clamping system. Wood is too soft for a reliable full clamping in practice, which was already discussed by Hearmon (1946). Theoretically, FFFF could be more easily realized for plates with small sizes, but it is not suitable for large full-size CLT panels with the size up to 20 m × 3 m. The one-term Rayleigh frequency solution is not accurate enough, while the FE iteration method and frequency solution based on Reddy's higher order plate theory require significant computation resources and operator intervention.

2.5 Summary

To sum up, non-destructive measurement of elastic constants of composite plate materials by modal testing has been researched for several decades. Many achievements were made,

but most of them were still in the academic stage. The same situation happened in the research on vibration testing of panel-shaped wood materials. The forward and inverse problems both become more complicated for two-dimension or even three-dimension plate than single one-dimension beam. The key problems that limit the industrial application of this non-destructive method are: a) lack of suitable forward solutions for free transverse vibration of different kinds of plate-like composites; b) no studies on practical boundary conditions except completely free that are robust and can be replicated in laboratories and factories and c) difficulties in identifying the sensitive natural frequencies from a few frequency spectra for extracting elastic constants. In order to better implement the vibrational methods for orthotropic plates including wood-based panels and potentially for on-line testing, a deeper investigation on the development of a suitable boundary condition, direct frequency identification method and related calculation algorithms is desired.

References

Araújo, A. L., Mota Soares, C. M., and Moreira De Freitas, M. J. (1996).
Characterization of material parameters of composite plate specimens using
optimization and experimental vibrational data. *Composites Part B: Engineering*,
27(2), 185–191.

Ayorinde, E. O. (1995). Elastic constants of thick orthotropic composite plates. *Journal
of Composite Materials*, *29*(8), 1025–1039.

Ayorinde, E. O., and Gibson, R. F. (1993). Elastic constants of orthotropic composite
materials using plate resonance frequencies, classical lamination theory and an
optimized three-mode rayleigh formulation. *Composites Engineering*, *3*(5), 395–
407.

Ayorinde, E. O., and Gibson, R. F. (1995). Improved method for in-situ elastic constants
of isotropic and orthotropic composite materials using plate modal data with
trimodal and hexamodal Rayleigh formulations. *Journal of Vibration and Acoustics*,
117(2), 180–186.

Ayorinde, E. O., and Yu, L. (1999). On the use of diagonal modes in the elastic
identification of thin composite plates. *Journal of Vibration and Acoustics*, *121*(1),
33–40.

Ayorinde, E. O., and Yu, L. (2005). On the elastic characterization of composite plates
with vibration data. *Journal of Sound and Vibration*, *283*(1–2), 243–262.

Bartoli, I., and Marzani, A. (2012). A low/high frequency combined approach for the
identification of mechanical properties of composite structural elements. *Theoretical
and Applied Mechanics*, *39*(1), 1–25.

Bos, F., and Casagrande, S. B. (2003). On-line non-destructive evaluation and control of wood-based panels by vibration analysis. *Journal of Sound and Vibration*, *268*(2), 403–412.

Brancheriau, L., and Baillères, H. (2002). Natural vibration analysis of clear wooden beams: a theoretical review. *Wood Science and Technology*, *268*(2), 403–412.

Carfagni, M., and Mannucci, M. (1996). A simplified dynamic method based on experimental modal analysis for estimating the in-plane elastic properties of solid wood panels. In J. L. Sandoz (Ed.), *International symposium on nondestructive testing of wood* (pp. 247–258). Lausanne: Presses polytechniques et universitaires romandes.

Chui, Y. H. (1991). Simultaneous evaluation of bending and shear moduli of wood and the influence of knots on these parameters. *Wood Science and Technology*, *25*(2), 125–134.

Chui, Y. H., and Smith, I. (1990). Influence of rotatory inertia, shear deformation and support condition on natural frequencies of wooden beams. *Wood Science and Technology*, *24*(3), 233–245.

Coppens, H. (1988). Quality control of particleboards by means of their oscillation behavior. In *FESYP Technical Conference* (pp. 143–165). Munich.

Cunha, J., Cogan, S., and Berthod, C. (1999). Application of genetic algorithms for the identification of elastic constants of composite materials from dynamic tests. *International Journal for Numerical Methods in Engineering*, *45*(7), 891–900.

Daghia, F., de Miranda, S., Ubertini, F., and Viola, E. (2007). Estimation of elastic constants of thick laminated plates within a Bayesian framework. *Composite*

Structures, *80*(3), 461–473.

De Visscher, J. (1995). *Identification of the complex stiffness matrix of orthotropic materials by a mixed numerical/ experimental method*. Free University of Brussels (VUB).

De Visscher, J., Sol, H., De Wilde, W. P., and Vantomme, J. (1997). Identification of the damping properties of orthotropic composite materials using a mixed numerical experimental method. *Applied Composite Materials*, *4*(1), 13–33.

De Wilde, W. P. (2001). Mixed numerical-experimental techniques for the characterisation of anisotropic solids through their vibrational behaviour: a review. *WIT Transactions on Modelling and Simulation*, *30*, 723–733.

De Wilde, W. P., and Sol, H. (1987). Anisotropic material identification using measured resonant frequencies of rectangular composite plates. In I. H. Marshall (Ed.), *Composite Structures 4* (pp. 317–324). Springer Netherlands.

Deobald, R. F., and Gibson, R. L. (1988). Determination of Elastic Constants of Orthotropic Plated by a Model Analysis/Rayleigh-Ritz Technique. *Journal of Sound and Vibration*, *124*(2), 269–283.

Frederiksen, P. (1997a). Application of an improved model for the identification of material parameters. *Mechanics of Composite Materials and Structures*, *4*(4), 297–316.

Frederiksen, P. (1997b). Experimental Procedure and Results for the Identification of Elastic Constants of Thick Orthotropic Plates. *Journal of Composite Materials*, *31*(4), 360–381.

Frederiksen, P. S. (1998). Parameter uncertainty and design of optimal experiments for

the estimation of elastic constants. *International Journal of Solids and Structures*, *35*(12), 1241–1260.

Gagneja, S., Gibson, R. F., and Ayorinde, E. O. (2001). Design of test specimens for the determination of elastic through-thickness shear properties of thick composites from measured modal vibration frequencies. *Composites Science and Technology*, *61*(5), 679–687.

Gibson, R. F. (2000). Modal vibration response measurements for characterization of composite materials and structures. *Composites Science and Technology*, *60*(15), 2769–2780.

Goens, E. (1931). Über die Bestimmung des Elastizitätsmoduls von Stäben mit Hilfe von Biegungsschwingungen. *Annalen Der Physik*, *403*(6), 649–678.

Gorman, D. J. (1978). Free vibration analysis of the completely free rectangular plate by the method of superposition. *Journal of Sound and Vibration*, *57*(3), 437–447.

Gorman, D. J. (1982). *Free Vibration Analysis of Rectangular Plates*. North Holland: Elsevier Ltd.

Gorman, D. J. (1993). Accurate Free Vibration Analysis of the Completely Free Orthotropic Rectangular Plate by the Method of Superposition. *Journal of Sound and Vibration*, *165*(3), 409–420.

Gorman, D. J. (1999). *Vibration analysis of plates by the superposition method*. Singapore: World Scientific.

Gorman, D. J., and Ding, W. (1996). Accurate free vibration analysis of clamped antisymmetric angle-ply laminated rectangular plates by the Superposition-Galerkin method. *Composite Structures*, *34*(4), 387–395.

Gorman, D. J., and Ding, W. (2003). Accurate free vibration analysis of completely free

symmetric cross-ply rectangular laminated plates. *Composite Structures*, *60*(3), 359–

365.

Grédiac, M., Fournier, N., Paris, P.-A., and Surrel, Y. (1998). Direct identification of

elastic constants of anisotropic plates by modal analysis: experimental results.

Journal of Sound and Vibration, *210*(5), 643–659.

Grediac, M., and Paris, P. A. (1996). Direct identification of elastic constants of

anisotropic plates by modal analysis: theoretical and numerical aspects. *Journal of

Sound and Vibration*, *195*(3), 401–415.

Gsell, D., Feltrin, G., Schubert, S., … Motavalli, M. (2007). Cross-Laminated Timber

Plates: Evaluation and Verification of Homogenized Elastic Properties. *Journal of

Structural Engineering*, *133*(1), 132–138.

Gülzow, A. (2008). *Zerstörungsfreie Bestimmung der Biegesteifigkeiten, von

Brettsperrholzplatten*. ETH Zürich.

Hearmon, R. F. S. (1946). The fundamental frequency of vibration of rectangular wood

and plywood plates. *Proceedings of the Physical Society*, *58*(1), 78–92.

Hearmon, R. F. S. (1959). The frequency of flexural vibration of rectangular orthotropic

plates with clamped or supported edges. *Journal of Applied Mechanics*, *26*(23),

537–540.

Hearmon, R. F. S. (1961). *An introduction to applied anisotropic elasticity*. London:

Oxford University Press.

Hearmon, R. F. S. (1966). Vibration testing of wood. *Forest Products Journal*, *16*(8), 29–

39.

Hu, L. J., and Hsu, W. E. (1996). Implementation of transverse simple beam vibration
    technique to determine MOE for wood based materials: accuracy, comparability,
    and limitations. In J. Sandoz (Ed.), *International symposium on nondestructive
    testing of wood* (pp. 247–258). Lausanne: Presses polytechniques et universitaires
    romandes.

Hua, H. (1993). *Identification of plate rigidities of anisotropic rectangular plates,
    sandwich panels and orthotropic circular disks using vibration data*. Free
    University of Brussels (VUB).

Huffington, N. J., and Hoppmann, W. H. (1958). On the transverse vibrations of
    rectangular orthotropic plates. *Journal of Applied Mechanics*, *25*(3), 389–395.

Hwang, S.-F., and Chang, C.-S. (2000). Determination of elastic constants of materials by
    vibration testing. *Composite Structures*, *49*(2), 183–190.

Hwang, S.-F., Wu, J.-C., and He, R.-S. (2009). Identification of effective elastic constants
    of composite plates based on a hybrid genetic algorithm. *Composite Structures*,
    90(2), 217–224.

Ilic, J., and Ozarska, B. (1996). Nondestructive evaluation of properties of reconstituted
    wood products used in Australia. In J. Sandoz (Ed.), *International symposium on
    nondestructive testing of wood* (pp. 269–278). Lausanne: Presses polytechniques et
    universitaires romandes.

Ismail, Z., Khov, H., and Li, W. L. (2013). Determination of material properties of
    orthotropic plates with general boundary conditions using Inverse method and
    Fourier series. *Measurement*, *46*(3), 1169–1177.

Jayaraman, G., Chen, P., and Snyder, V. W. (1990). Free vibrations of rectangular

orthotropic plates with a pair of parallel edges simply supported. *Computers and Structures*, *34*(2), 203–214.

Khdeir, A. A. (1988). Free vibration and buckling of symmetric cross-ply laminated plates by an exact method. *Journal of Sound and Vibration*, *126*(3), 447–461.

Kim, C. S., and Dickinson, S. M. (1985). Improved approximate expressions for the natural frequencies of isotropic and orthotropic rectangular plates. *Journal of Sound and Vibration*, *103*(1), 142–149.

Kreja, I. (2011). A literature review on computational models for laminated composite and sandwich panels. *Central European Journal of Engineering*, *1*(1), 1–39.

Lai, T. C., and Lau, T. C. (1993). Determination of elastic constants of a generally orthotropic plate by modal analysis. *Modal Analysis*, *8*(1), 15–33.

Larsson, D. (1996). Stiffness characterization of wood based panels by modal testing. In J. Sandoz (Ed.), *International symposium on nondestructive testing of wood* (pp. 237–246). Lausanne: Presses polytechniques et universitaires romandes.

Larsson, D. (1997). Using modal analysis for estimation of anisotropic material constants. *Journal of Engineering Mechanics*, *222–229*(123), 3.

Lauwagie, T. (2005). *Vibration-based methods for the identification of the elastic properties of layered materials*. Katholieke Universiteit Leuven.

Lauwagie, T., Lambrinou, K., Sol, H., and Heylen, W. (2010). Resonant-based identification of the Poisson's ratio of orthotropic materials. *Experimental Mechanics*, *50*(4), 437–447.

Lauwagie, T., Sol, H., Heylen, W., and Roebben, G. (2004). Determination of the in-plane elastic properties of the different layers of laminated plates by means of

vibration testing and model updating. *Journal of Sound and Vibration*, *274*(3–5), 529–546.

Leissa, A. W. (1969). Anisotropic Plates. In A. W. Lesissa (Ed.), *Vibration of plates* (pp. 250–260). Washington D. C.: National Aeronautics Space Administration.

Leissa, A. W. (1973). The free vibration of rectangular plates. *Journal of Sound and Vibration*, *31*(3), 257–293.

Leissa, A. W. (1977). Recent research in plate vibrations, 1973–1976: classical theory. *Shock and Vibration Digest*, *9*(10), 13–24.

Leissa, A. W. (1978). Recent research in plate vibrations, 1973–1976: complicating effects. *Shock and Vibration Digest*, *10*(12), 21–35.

Leissa, A. W. (1981). Plate vibration research, 1976–1980: complicating effects. *Shock and Vibration Digest*, *13*(10), 19–36.

Leissa, A. W. (1987). Recent studies in plate vibration, 1981–1985: complicating effects. *Shock and Vibration Digest*, *19*(3), 10–24.

Liew, K. M., Xiang, Y., and Kitipornchai, S. (1995). Research on thick plate vibration: a literature survey. *Journal Of Sound And Vibration*, *180*(1), 163–176.

Liew, K. M., Xiang, Y., Kitipornchai, S., and Wang, C. M. (1998). *Vibration of Mindlin Plates: Programming the p-Version Ritz Method*. Oxford: Elsevier Science Ltd.

Liu, B., and Xing, Y. (2011). Exact solutions for free vibrations of orthotropic rectangular Mindlin plates. *Composite Structures*, *93*(7), 1664–1672.

Liu, G. R., and Han, X. (2003). *Computational inverse techniques in nondestructive evaluation*. CRC Press LLC.

Lo, K. H., Christensen, R. M., and Wu, E. M. (1977). A High-Order Theory of Plate

Deformation Part 1: Homogeneous Plates. *Journal of Applied Mechanics*, *44*(4), 663–668.

Martínez, M. P., Poletti, P., and Espert, L. G. (2011). Vibration Testing for the Evaluation of the Effects of Moisture Content on the In-Plane Elastic Constants of Wood Used in Musical Instruments. In C. M. A. Vasques & J. Dias Rodrigues (Eds.), *Vibration and Structural Acoustics Analysis* (pp. 21–57). Springer Netherlands.

Moussu, F., and Nivoit, M. (1993). Determination of Elastic Constants of Orthotropic Plates By A Modal Analysis/Method of Superposition. *Journal of Sound and Vibration*, *165*(1), 149–163.

Nakao, T., and Okano, T. (1987). Evaluation of modulus of rigidity by dynamic plate shear testing. *Wood and Fiber Science*, *19*(4), 332–338.

Ng, S. F., and Kulkarni, G. G. (1972). On the transverse free vibrations of beam-slab type highway bridges. *Journal of Sound and Vibration*, *21*(3), 249–261.

Pedersen, P. (1999). Identification techniques in composite laminates. In C. A. Mota Soares, C. M. Mota Soares, & M. J. M. Freitas (Eds.), *Mechanics of Composite Materials and Structures* (pp. 443–452). Springer Netherlands.

Pedersen, P., and Frederiksen, P. S. (1992). Identification of orthotropic material moduli by a combined experimental/numerical method. *Measurement*, *10*(3), 113–118.

Qatu, M. S. (2004). *Vibration of laminated shells and plates*. Oxford: Elsevier Ltd.

Reddy, J. N. (1984). A simple higher-order theory for laminated composite plates. *Journal of Applied Mechanics*, *51*(4), 745–752.

Sayyad, A. S., and Ghugal, Y. M. (2015). On the free vibration analysis of laminated

composite and sandwich plates: A review of recent literature with some numerical results. *Composite Structures*.

Schulte, M., Frühwald, A., and Bröker, F. W. (1996). Non-destructive testing of panel products by vibration technique. In J. Sandoz (Ed.), *International symposium on nondestructive testing of wood* (pp. 259–268). Lausanne: Presses polytechniques et universitaires romandes.

Silva, M. F. T., Borges, L. M. S. A., Fernando, A. R., and De Carvalho, L. A. V. (2004). A genetic algorithm applied to composite elastic parameters identification. *Inverse Problems in Science and Engineering*, *12*(1), 17–28.

Singal, R. K., Gorman, D. J., and Forgues, S. A. (1992). *A comprehensive analytical solution for free vibration of rectangular plates with classical edge coditions: Experimental verification*.

Soares, C. M. M., de Freitas, M. M., Araújo, A. L., and Pedersen, P. (1993). Identification of material properties of composite plate specimens. *Composite Structures*, *25*(1–4), 277–285.

Sobue, N. (1986). Instantaneous measurement of elastic constants by analysis of the tap tone of wood: application to flexural vibration of beams. *Mokuzai Gakkaishi*, *32*(4), 274–279.

Sobue, N. (1988). Simultaneous determination of Young's modulus and shear modulus of structural lumber by complex vibrations of bending and twisting. *Mokuzai Gakkaishi*, *34*(8), 652–657.

Sobue, N., and Katoh, A. (1992). Simultaneous determination of orthotropic elastic constants of standard full-size plywoods by vibration method. *Mokuzai Gakkaishi*,

38(10), 895–902.

Sobue, N., and Kitazumi, M. (1991). Identification of power spectrum peaks of vibrating

completely-free wood plates and moduli of elasticity measurements. *Mokuzai*

Gakkaishi, *37*(1), 9–15.

Sol, H. (1986). *Identification of anisotropic plate rigidities using free vibration data*. Free

University of Brussels (VUB).

Sol, H., and Bottiglieri, M. (2010). Identification of the elastic properties on composite

materials as a function of temperature. In *Proceedings of PACAM XI* (pp. 1–6). Foz

do Iguaçu.

Sol, H., and Oomens, C. W. J. (Eds.). (1997). Material Identification Using Mixed

Numerical Experimental Methods. In *Material Identification Using Mixed*

Numerical Experimental Methods. Kerkrade: Kluwer Academic Publishers.

Tam, J. H., Ong, Z. C., Ismail, Z., … Khoo, S. Y. (2016). Identification of material

properties of composite materials using non-destructive vibrational evaluation

approaches: A review. *Mechanics of Advanced Materials and Structures*, 1–16.

Warburton, G. B. (1954). The vibration of rectangular plates. *Proceedings of the*

Institution of Mechanical Engineers, *168*(1), 371–384.

Xing, Y. F., and Liu, B. (2009). New exact solutions for free vibrations of thin

orthotropic rectangular plates. *Composite Structures*, *89*(4), 567–574.

Yoshihara, H. (2011). Measurement of the Young's modulus and shear modulus of in-

plane quasi-isotropic medium-density fiberboard by flexural vibration.

BioResources, *6*(4), 4871–4885.

Yoshihara, H. (2012a). Examination of the specimen configuration and analysis method

in the flexural and longitudinal vibration tests of solid wood and wood-based

materials. *Forest Products Journal*, *62*(3), 191–200.

Yoshihara, H. (2012b). Influence of specimen configuration on the measurement of the

off-axis Young's modulus of wood by vibration tests. *Holzforschung*, *66*(4), 485–

492.

Yoshihara, H. (2012c). Influence of the specimens depth to length ratio and lamination

construction on Young's modulus and in-plane shear modulus of plywood measured

by flexural vibration. *BioResources*, *7*(1), 1337–1351.

Yoshihara, H. (2012d). Off-axis Young's modulus and off-axis shear modulus of wood

measured by flexural vibration tests. *Holzforschung*, *66*(2), 207–213.

Yu, L. (2006). *Identification of elastic constants of composite materials from vibration

data of thick plates*. Wayne State University.

CHAPTER 3 SIMULTANEOUS MEASUREMENT OF ELASTIC CONSTANTS OF FULL-SIZE ENGINEERED WOOD-BASED PANELS BY MODAL TESTING

Abstract: Engineered wood-based panels are widely used in structural applications. Accurate measurement of their elastic properties is of great importance for predicting their mechanical behaviour during structural design. In this study, an efficient non-destructive test method for measurement of effective elastic constants of orthotropic wood-based panel products was proposed based on a modal testing technique. An algorithm was developed based on an improved approximate frequency equation of transverse vibration of orthotropic plates under the boundary condition, in which two opposite sides were simply supported and the other two were free (SFSF). The method was able to predict the frequency ranges and mode indices as well as corresponding normalized sensitivity to elastic constants based on initial estimates of orthotropic ratios with uncertainties and measured fundamental natural frequency. Full-size engineered wood-based panels including cross laminated timber (CLT), oriented strand board (OSB) and medium density fiberboard (MDF) were tested with the proposed method. In general, the measured elastic constants of the three types of panel based on modal test agreed well with those corresponding values measured from static tests. Future work will expand on the range of panel sizes and types to further validate the proposed test method.

3.1 Introduction

Traditional engineered wood-based panels such as plywood and oriented strand board (OSB) are frequently used in light frame wood construction as walls, roofs and floor sheathings. The latest and popular massive timber panels such as cross laminated timber (CLT) is an innovative wood product and included into this study due to its potential application in high-rise buildings worldwide (Gagnon and Pirvu, 2011). Elastic constants of such materials are usually evaluated by conventional static methods including bending and shear tests. These tests are, however, tedious and costly, and the results are not necessarily valid for full-size panels (Bos and Casagrande, 2003).

The determination of the elastic constants by modal testing is an efficient non-destructive approach (Ayorinde and Gibson, 1993; Ayorinde and Yu, 2005). The application of modal testing for property evaluation of beam-like wood materials was investigated thoroughly (Biechle et al., 2011; Brashaw et al., 2009; Bucur, 2006; Ponneth et al., 2014; Yoshihara, 2011a, 2011b, 2013), while the method was not widely used for wood-based panel products. The vibrational behavior of a layered product is controlled by the overall stiffness of the elements rather than by the additive stiffness of its individual element (Lauwagie, 2005). The in-plane elastic constants are frequently determined, namely the moduli of elasticity in major and minor strength directions loaded in bending (E_x and E_y) and in-plane shear modulus (G_{xy}), of solid wood plate, OSB, medium density fiberboard (MDF), plywood, and CLT. The most frequently adopted modal testing (nondestructive testing, NDT) is, in this context, the completely free (FFFF) boundary condition with one-term

Rayleigh frequency solution (Bos and Casagrande, 2003; Carfagni and Mannucci, 1996; Coppens, 1988; Schulte et al., 1996; Sobue and Kitazumi, 1991). Coppens (1988) applied first NDT to measure the elastic constants of particleboard (PB) elastic constants. Sobue and Kitazumi (1991) measured the orthotropic elastic constants of wood plate (western red cedar, hemlock et al.) under FFFF boundary condition by means of a vibration technique and verified the results with static tests on beam-like specimens cut from these plates. The impact tests were conducted on several locations with a grid on the panel for identifying the frequency modes. A simplified dynamic method is based on the observation of imaginary part of frequency spectra whether they are in- or out-of-phase (Carfagni and Mannucci, 1996). The number of impact locations was reduced to six at two adjacent edges for rectangular wood panels under completely free support condition. An on-line NDT system, called VibraPann, for quality control of wood-based panels was presented by Bos and Casagrande (2003). The in-plane moduli of elasticity in the two orthogonal directions of selected OSB, plywood, and MDF were tested from the measurement of two vibration modes of bending, $f_{(2,0)}$ and $f_{(0,2)}$, under FFFF support condition. Besides Rayleigh frequency solution, finite element (FE) modelling was also used for the determination of elastic constants combined with NDT (Grimsel, 1999; Larsson, 1996, 1997; Martínez et al., 2011). The elastic constants were estimated by minimizing the difference between the experimental frequency and FE modeled values by an iteration process. Full-sized PB and OSB were tested and modeled as thin orthotropic plates under FFFF support condition by Larsson (1996, 1997). The proposed dynamic method was proved to be accurate because of the good agreement between measured and calculated natural frequencies (up to the 7th mode) within 1-5%, though the average difference between NDT and static bending data

of E_x and E_y were 14.1 and 31.0%, respectively. Grimsel (1999) applied the FE method based on 3D solid element and 2D shell element in the iteration process for determination of elastic properties of beech wood. The obtained data were compared with those obtained by coordinate-transformation and by calculation according to the Rayleigh-Ritz method. 2D modeling had closer results to Rayleigh-Ritz method, while 3D modeling results were closer to transformed values, which were also smaller than the 2D results. The sensitivity analysis in both 3D and 2D FE modeling indicated that Poisson's ratios were not very sensitive to frequency modes. A similar method was adopted to study the effects of moisture content (MC) on the in-plane elastic constants of wood for musical instruments (Martínez et al., 2011). Recently, experimental modal analysis was applied to determine natural frequencies and mode shapes of rectangular cross laminated timber specimens (Gsell et al., 2007). An analytical model based on Reddy's higher order plate theory (Reddy, 1984) under FFFF boundary condition was used to numerical calculation of natural frequencies and mode shapes. All three shear moduli and the two in-plane moduli of elasticity were identified by minimizing the difference between measured and estimated natural frequencies obtained by the least-squares method. The modal testing approach of Gsell et al. (2007) was adopted to evaluate the elastic properties of CLT and the results were validated by static bending experiments on whole panels and panel stripes except in-plane shear modulus (Gülzow et al., 2008; Gülzow, 2008; Steiger et al., 2012).

The one edge simply supported and three edges free boundary condition (SFFF), one edge clamped and three edges free boundary condition (CFFF) as illustrated in Figure 3.1 were also employed for modal testing of wood-based panels. A simultaneous determination of

orthotropic elastic constants of standard full-size plywood by vibration method was conducted under SFFF boundary condition (Sobue and Katoh, 1992). The results, E_x, E_y, and G_{xy}, were compared with static bending and torsional tests, which showed a relative measuring error of less than 15%. Particleboard (PB) and MDF panels of full-size dimensions were tested by a vibration technique in a vertical cantilever position (CFFF) with a laser head (Schulte et al., 1996).
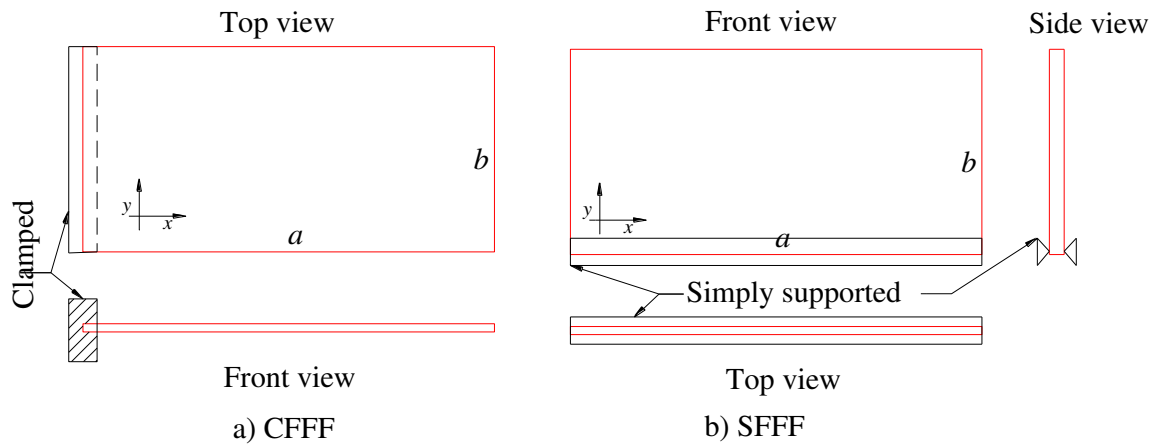
Figure 3.1 Schematic illustration of CFFF and SFFF boundary conditions

The above reported methods have so far not been implemented for on-line evaluation of full-size composite panel products. SFFF and CFFF boundary conditions cannot be realized in a production line as the panel are either in a vertical or in a cantilever position, which can be easily affected by the clamping system. Wood is too soft for a reliable full clamping in practice. Theoretically, FFFF could be more easily realized, but it is not suitable for large full-size CLT panels with the size up to 20 m × 3 m. The one-term Rayleigh frequency solution is not accurate enough, while the FE iteration method and

frequency solution based on Reddy's higher order plate theory require considerable computation resources and operator intervention.

This study is aiming at tackling the difficulties in measuring elastic constants by modal testing. The aim is to develop a NDT approach for engineered wood-based panels with a boundary condition, in which two opposite sides are simply supported and the other two sides are free (SFSF). A test method will be proposed with a user-friendly elastic constants calculation algorithm and NDT procedure for OSB, MDF, and CLT panels. The NDT results should be verified with standard static tests.

3.2 Material and Methods

3.2.1 Algorithm Development for Simultaneous Measurement of Elastic Constants

The governing differential equation for the transverse vibration of a rectangular orthotropic plate, which neglects the effects of shear deformation and rotatory inertia, is (Leissa, 1969):

$$D_x \frac{\partial^4 w}{\partial x^4} + D_y \frac{\partial^4 w}{\partial y^4} + 2(D_1 + 2D_{xy}) \frac{\partial^4 w}{\partial x^2 y^2} + \rho h \frac{\partial^2 w}{\partial t^2} = 0 \tag{3.1}$$

where D's are the flexural and torsional rigidities: $D_x = \dfrac{E_x h^3}{12(1 - v_{xy} v_{yx})}$, $D_y = \dfrac{E_y h^3}{12(1 - v_{xy} v_{yx})}$

, $D_1 = D_x v_{yx} = D_y v_{xy}$, $D_{xy} = \dfrac{G_{xy} h^3}{12}$. E_x, E_y and G_{xy} are the elastic moduli in the major and minor strength directions and in-plane shear modulus, respectively. In the present study, the elastic constants of CLT panels are treated as the effective elastic constants. v_{xy} and v_{yx}

54

are the major and minor Poisson's ratios, and *a, b, h* are the length, width, and thickness of the plate, respectively, and ρ is the density.

In this study, the SFSF boundary condition is chosen as it has the greatest potential for on-line testing. Even though an analytical solution was offered for this boundary condition (Huffington and Hoppmann, 1958), it is still very difficult to solve the equations for transcendental frequency characteristics. Therefore, a closed-form approximate frequency expression was adopted from Kim and Dickinson (1985) based on the three-term Rayleigh frequency solution:

$$
f_{mn} = \frac{ab}{\pi^2} \sqrt{\frac{\rho h}{H}} \sqrt{\frac{C_{ij} + c^2 C_{i\dot{n}} + d^2 C_{\dot{m}j} - 2cE_{ij} - 2dE_{ji} + 2cdF}{1 + c^2 + d^2}}
$$
(3.2)

where f_{mn} is the natural frequency of mode (m, n), m and n are the number of node lines including the simply supported sides in y and x direction, respectively. Here, (m, n) are equivalent to (i, j) as in the work of Kim and Dickinson (1985), $\dot{m}$ and $\dot{n}$ are equal to m and n in the reference, respectively. For the ease of calculation, the other constants are expressed according to Kim and Dickinson (1985):

$$
H = D_1 + 2D_{xy} ;
$$

$$
C_{ij} = (D_x / H)G_x^4 r^2 + (D_y / H)G_y^4 (1/r)^2 + 2(H_x H_y + 2(D_{xy} / H)(J_x J_y - H_x H_y)) ;
$$

$$
E_{ij} = H_x (K_y + L_y)(2(Dx_y / H) - 1) + 4(D_{xy} / H)J_x M_y ;
$$

$$
E_{ji} = H_y (K_x + L_x)(2(D_{xy} / H) - 1) + 4(D_{xy} / H)J_y M_x ;
$$

$$
F = -(K_x K_y + L_x L_y)(2(D_{xy} / H) - 1) + 4(D_{xy} / H)M_x M_y ;
$$

$$c = (C_{\dot{m}j} E_{ij} - E_{ji} F) / (C_{\dot{m}} C_{\dot{m}j} - F^2) \, ;$$

$$d = (C_{\dot{m}} E_{ji} - E_{ij} F) / (C_{\dot{m}} C_{\dot{m}j} - F^2) \, .$$

The relationship between frequencies, elastic constants and geometric parameters can be summarized as:

$$f_{mn} \propto (m, n, k, h, \rho, \sigma_1, \sigma_2) \tag{3.3}$$

where k is the aspect ratio $k = a/b$; σ_1 and σ_2 are the orthotropic ratios, $\sigma_1 = E_y/E_x$ and $\sigma_2 = G_{xy}/E_x$, respectively.

In general, h, ρ, and k are constant for a given panel, σ_1 and σ_2 values are within a certain range for a specific product. For a CLT panel, σ_1 is usually in the range of 0.03 - 0.50 depending on lay-up configuration, σ_2 is usually about 0.02-0.08, which can be predicted by different models such as modified analogy to plywood method (Sylvain and Marjan, 2011; APA, 2012). For wood materials, σ_1, σ_2, and v_{xy} can be obtained from (Forest Products Laboratory, 2010). The initial E_x value can be calculated by the fundamental natural frequency equation, which is always a bending mode sensitive to E_x (Leissa, 1969):

$$E_{x0} = \frac{48(1 - v_{xy} v_{yx}) a^2 f_{20}^2 \rho}{\pi^2 h^2} \tag{3.4}$$

where E_{x0} is the calculated initial value of E_x, f_{20} is the fundamental natural frequency. $(1 - v_{xy} v_{yx})$ is about 0.99 for wood materials (Hearmon, 1946).

With the input of initial orthotropic ratios and geometric parameters and density, the simultaneous determination of E_x, E_y, G_{xy} and v_{xy} is achieved by minimizing the difference

between measured and calculated frequencies to less than 0.01 Hz individually and a total

relative frequency difference of less than 5.0% through an iteration procedure as shown in

Figure 3.2.

It is also possible to predict the relationship between frequency order and mode shape,

namely the value f_{mn} and mode indices (m, n). A frequency identification procedure with

normalized sensitivity analysis was developed based on the above theoretical analysis. The

sensitive frequencies can be easily located by means of the imaginary parts of a few

selected impact locations (Zhou and Chui, 2014). An integrated elastic constant calculation

algorithm with frequency identification procedure is illustrated in Figure 3.2.

Vibration test	**Input**
Frequency spectra	a, b, h, ρ and orthotropic ratios

Initial values

Initial E_x is calculated using f_{20};

Initial E_y and G_{xy} are based on orthotropic ratios, and v_{xy}.

Sensitivity analysis

Sensitive modes & Frequencies *vs* Mode orders

Frequency identification

Select 3-4 experimental sensitive frequencies $\boldsymbol{f_{mne}}$

Iteration procedure

If $|\boldsymbol{f_{mne}} - \boldsymbol{f_{mnc}}| > 0.01$ Hz, then E_x, E_y, G_{xy} and v_{xy} will decrease or increase 0.1 to 0.2 percent individually. Iteration will stop when the total frequency difference less than 1-5 percent.

Output

E_x, E_y, G_{xy} and v_{xy}

Figure 3.2 Flow chart for algorithm for frequency identification and elastic constant calculation

3.2.2 Sensitivity Analysis

Theoretically, any four natural frequencies can be used for calculating the four elastic constants (E_x, E_y, G_{xy} and v_{xy}). For specific boundary conditions, however, the identification of the most sensitive modes for calculation is helpful. Thus a sensitivity analysis is needed, which should be integrated into the algorithm for elastic constant calculation (Ayorinde, 1995). Lai and Ip (1996) introduced a sensitivity matrix to improve the accuracy of final results. One approach is to change each elastic constant by 10% in a finite element model (FEM) and to check the relative frequency differences (Antunes et al., 2008; Larsson, 1997). In the present study, a closed-form frequency equation was established, and thus the sensitivity can be defined as the frequency change as a function of the specific elastic constant change (Ayorinde and Yu, 2005):

$$S_{f_{mn}/X} = \frac{\partial f_{mn}}{\partial X} \cdot \frac{X}{f_{mn}} \tag{3.5}$$

where f_{mn} is the frequency of mode (m, n), X is the elastic constant to be analyzed, $\frac{\partial f_{mn}}{\partial X}$ is the partial derivative of f_{mn} to X.

The sensitivities of all four elastic constants to a natural frequency at mode (m, n) can be expressed in a matrix form:

$$S_{f_{mn}/Xs} = \begin{bmatrix} \dfrac{\partial f_{mn}}{\partial E_x} \cdot \dfrac{E_x}{f_{mn}} \\[2ex] \dfrac{\partial f_{mn}}{\partial E_y} \cdot \dfrac{E_y}{f_{mn}} \\[2ex] \dfrac{\partial f_{mn}}{\partial G_{xy}} \cdot \dfrac{G_{xy}}{f_{mn}} \\[2ex] \dfrac{\partial f_{mn}}{\partial v_{xy}} \cdot \dfrac{v_{xy}}{f_{mn}} \end{bmatrix} \qquad (3.6)$$

The normalized sensitivity is introduced and defined with orthotropic ratios, which are normalized to E_x. Therefore $S_{f_{mn}/Xs}$ can be evaluated at $E_x{=}1$, $E_y{=}\sigma_1 E_x$, $G_{xy}{=}\sigma_2 E_x$ and v_{xy}.

Table 3.1 Elastic constants input for sensitivity analysis

Material	Elastic constants							
	E_x	uncert.*	σ_1	uncert.*	σ_2	uncert.*	v_{xy}	uncert.*
CLT	1	±10%	0.045	±20%	0.030	±20%	0.35[1]	±10%
OSB	1	±10%	0.500	±20%	0.300	±20%	0.23[2]	±10%
MDF	1	±10%	0.900	±10%	0.500	±20%	0.33[3]	±10%

Note: E_x is regarded as a unit. [1](Sylvain and Marjan, 2011); [2](Thomas, 2003); [3](Ganev et al., 2005). *uncertainty

3.2.3 Materials

Two full-size 103.0-mm-thick commercial Canadian E1 grade three-ply spruce-pine-fir (SPF) CLT panels were tested. Each layer in a CLT panel was 35 mm thick. Each CLT panel was 5.50 m in length and 2.15 m in width. Each layer in a CLT panel had non-edge-gluing and exhibited a gap between two neighboring lumber elements of around 2.0 mm in the same layer. Five full-size 11.1-mm-thick commercial APA-rated sheathing OSB panels were studied, which were 2.44 m long and 1.22 m wide. Five full-size 15.7-mm-thick commercial industrial grade MDF panels were also investigated, which were 2.46 m long and 1.24 m wide. The OSB panels were made of southern yellow pine (*Pinus spp.*) with phenol formaldehyde copolymer adhesive. The MDF panels were made of a mix of hardwood species with urea-formaldehyde. The average MCs of CLT, OSB, MDF panels measured were about 12.0, 4.3, and 4.6%, respectively. Modal tests were conducted on all the panels to obtain the sensitive frequencies as input for the calculation algorithm first. Then the panels were cut for static tests according to the dimensions presented in Table 3.2.

Table 3.2 Specimen information for modal and static tests

Material	Density (kg/m^3)	Thickness (mm)	Modal tests (m^2)	Bending tests				Shear tests (mm)
				Major (mm^2)	Span (mm)	Minor (mm^2)	Span (mm)	
CLT	520	103.0	5.50×2.15	2100×890	2070	2100×890	2070	1500×500
OSB	614	11.1	2.44×1.22	600×50	540	450×50	270	600×600
MDF	697	15.7	2.46×1.24	600×50	570	450×50	380	600×600

Note: The areas in the table refer to the size of the specimen (length × width).

3.2.4 Modal Test

The impact vibration tests were conducted on the specimen under SFSF boundary condition. The specimen was simply resting on steel pipes which were in turn seating on top of wood supports to achieve a continuous simply supported condition at the edges as illustrated in Figure 3.3. The position for attaching accelerometer was selected at 7/12 length of one free edge, which was not on the perpendicular nodal lines of first several modes up to the first 15 modes. The positions at free edges will only be nodal points when the perpendicular nodal lines meet the free edges. The impact and acceleration time signals were recorded by a data acquisition device (LDS Dactron, Brüel & Kjær) and the frequency response function (FRF) was calculated from the time signals by a data analysis software (RT Pro 6.33, Brüel & Kjær). The frequency spectrum was post-processed by MATLAB software for frequency identification and calculation of the elastic constants. Since the 1st and 2nd natural frequencies of a plate under SFSF are modes (2, 0) and (2, 1), respectively, only vibration mode (2, 2) or (2, 3) has to be identified. The detailed procedure of identifying sensitive frequencies of imaginary patterns from optimal impact locations was discussed by Zhou and Chui (2014). The typical frequency spectra for free transverse vibration of selected panels under simply-supported boundary condition are presented in Figure 3.4.
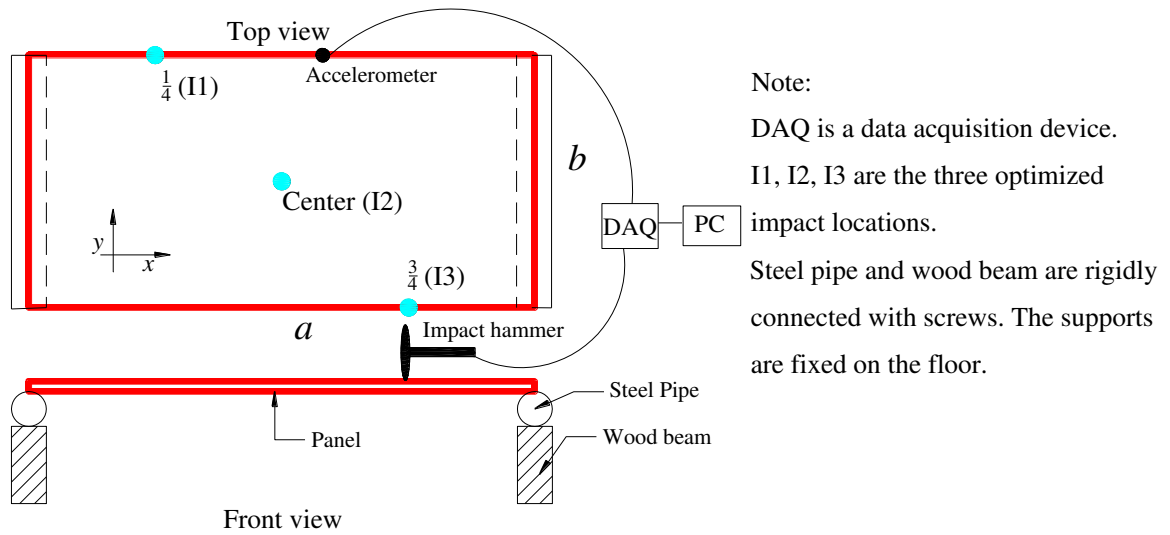
Figure 3.3 Illustration of modal tests and details of simply support of EWPs

a) CLT
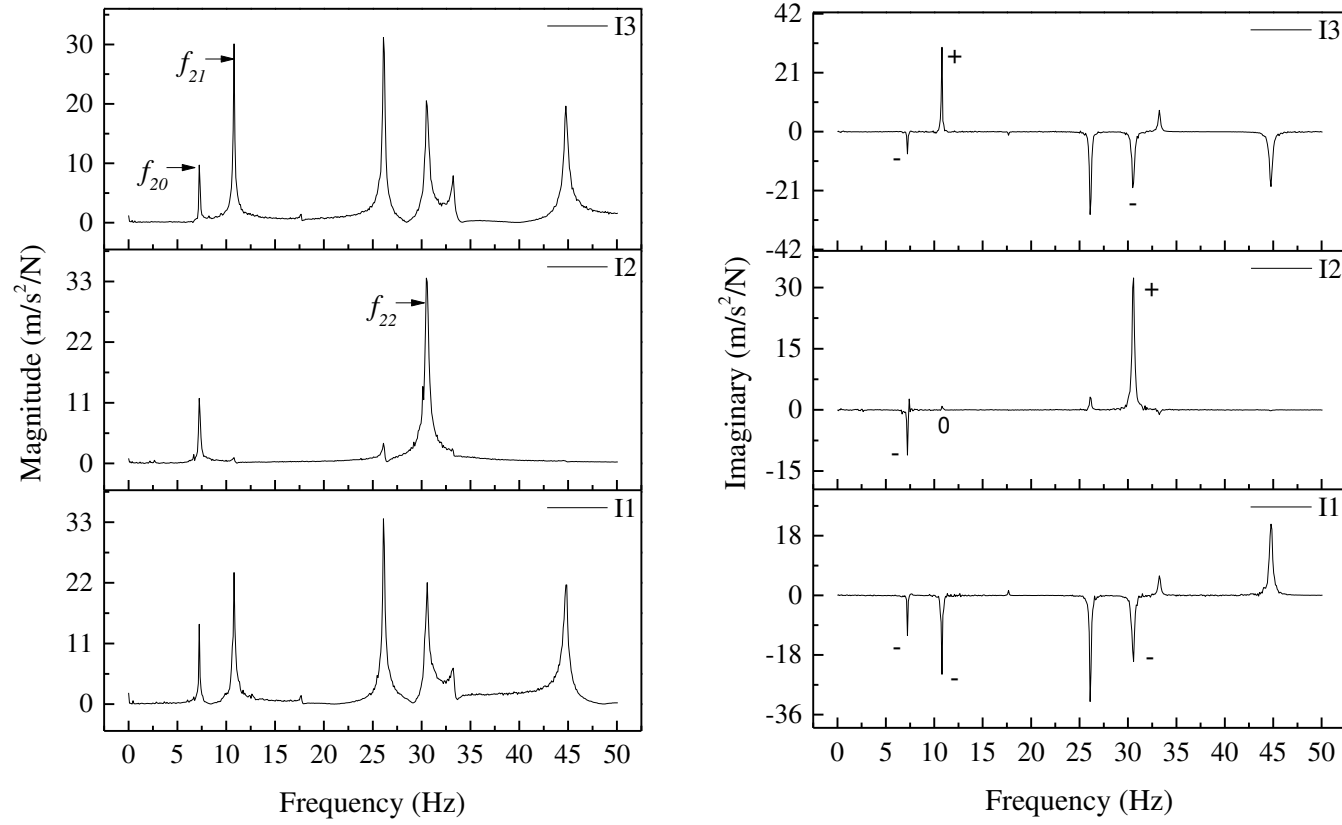
b) OSB
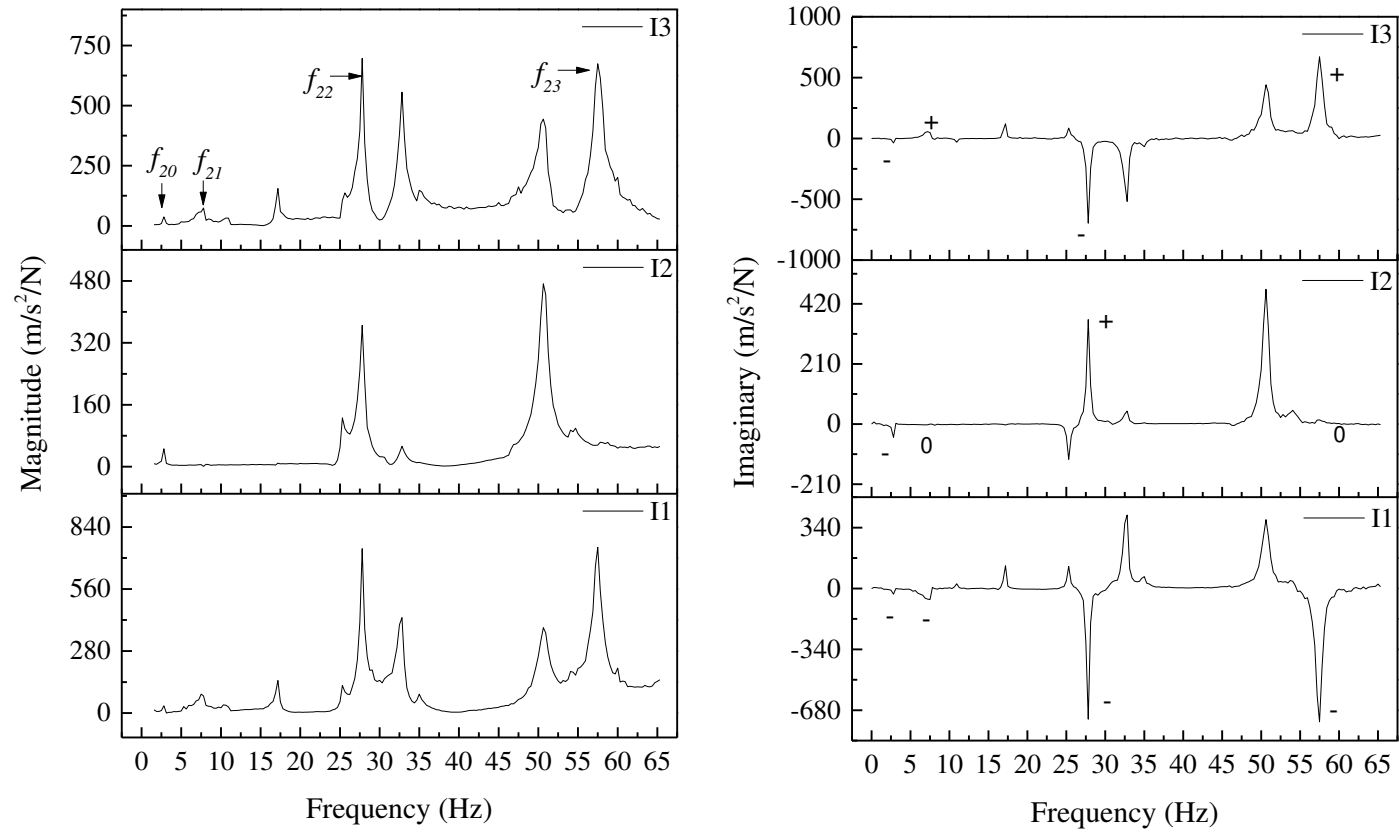
c) MDF
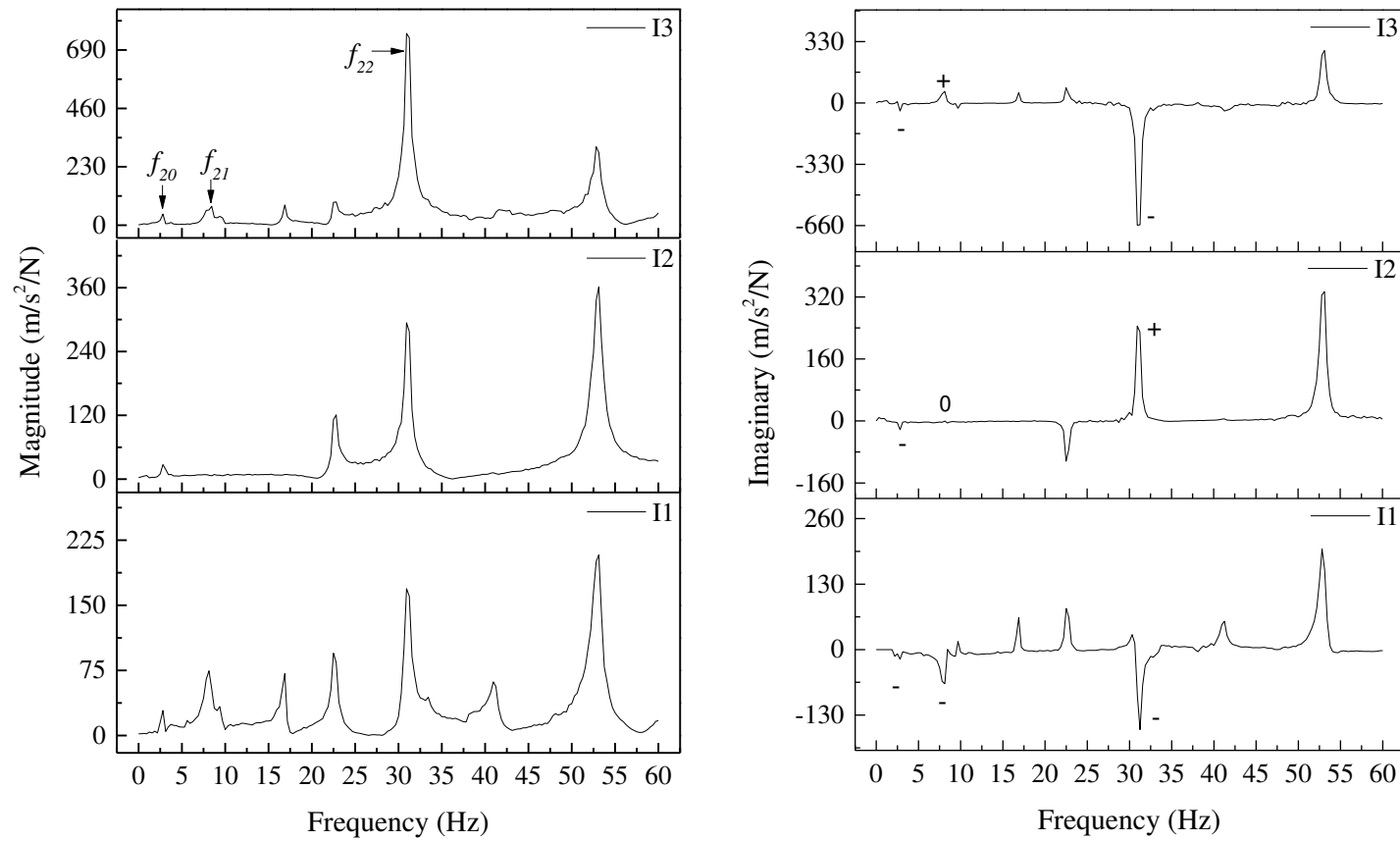
Figure 3.4 Typical frequency spectra from three optimal impact locations (I1, I2, I3) for a) CLT, b) OSB and c) MDF panel

3.2.5 Static Tests

The E_x, E_y and G_{xy} of OSB and MDF panels were obtained from static centre-point flexure tests according to Method A in ASTM D3043 (ASTM 2011a) and shear tests according to ASTM D3044 (ASTM 2011b), respectively. A total of 12 strips along each strength direction cut from each panel were tested for E values. A total of four square panels cut from each panel were tested for G_{xy} values. The E values of CLT were measured by third-point flexure tests with the strips cut from the panel according to ASTM D4761 (ASTM 2013). Two CLT strips along each strength direction were cut from each CLT panel for third-point bending test. The static G_{xy} value of CLT panel could not be performed because of an instrumental problem.

3.3 Results and Discussion

3.3.1 Results of Sensitivity Analysis

In this study, the sensitivity analysis incorporated with Monte Carlo simulation was performed for selected CLT, OSB, and MDF panels based on the orthotropic ratios with different uncertainties shown in Table 3.1. The uncertainties of each parameter are selected based on reference ranges (Forest Products Laboratory, 2010; Sylvain and Marjan, 2011; APA 2012). The density, thickness, and dimensions were measured as listed in Table 3.2. The sensitivities of elastic constants to different frequency modes for CLT, OSB, and MDF panels are presented in Figure 3.5, where the error bars indicate the range of sensitivity values within the ranges of orthotropic ratios.

For all three products, the sensitivity of E_x to mode (m, 0) is the highest among four elastic constants. It decreases very slightly with increasing m, and (2, 0) mode is the most sensitive one to E_x. The sensitivity of E_y to mode (2, n) (n≥2) is the highest among four elastic constants and increases with increasing n. The sensitivity of G_{xy} to mode (m, 1) (m≥2) is the highest among four elastic constants. Mode (2, 1) is found to be the most sensitive one to G_{xy} for selected panels in this study. Modes (2, 0) and (2, 1) are the most sensitive for calculating E_x and G_{xy}, respectively. In addition, these two frequencies are always the first two natural frequencies of a panel with SFSF boundary condition. Frequency of mode (2, 2) or (2, 3) can be used for calculating E_y depending on its sensitivity. The frequency mode with sensitivity higher than 0.35 is recommended for calculation. For those modes with the highest sensitivity to an elastic constant but still lower than 0.35, a coupled effect should be considered in the iterative calculation process. For instance, the highest sensitivity of G_{xy} for the CLT panel can be found in mode (2, 1). It ranges from 0.19 to 0.26 with the uncertainties considered in the simulation, which is still lower than the sensitivity of E_x. For panels with large aspect ratio (*a/b*) and small orthotropic ratio σ_2, the sensitivity of G_{xy} will be low for all the vibration modes. The same mechanism applies to the sensitivity of E_y. Therefore, for a given panel product with fixed dimensions, sensitivity analysis is helpful as a means of determining the most sensitive frequencies for calculation and of incorporating a coupled effect when necessary. On the other hand, sensitivity analysis can also be used to find the optimal specimen dimension for modal testing with appropriate orthotropic ratios when developing standard test method. Antunes et al. (2008) found that sensitivity of natural frequencies to geometry and elastic properties was relatively low and varied quite considerably with geometry by FE modeling. Moreover, for all three types of

69

products in this study, it has been found that no sensitive vibration mode can be found for the calculation of v_{xy}, but sensitivity level increases as mode number increases. To summarize, the sensitive frequency modes for calculation of E_x, E_y and G_{xy} of selected products are (2, 0), (2, 2 or 3) and (2, 1), respectively, and these are applied in the following.
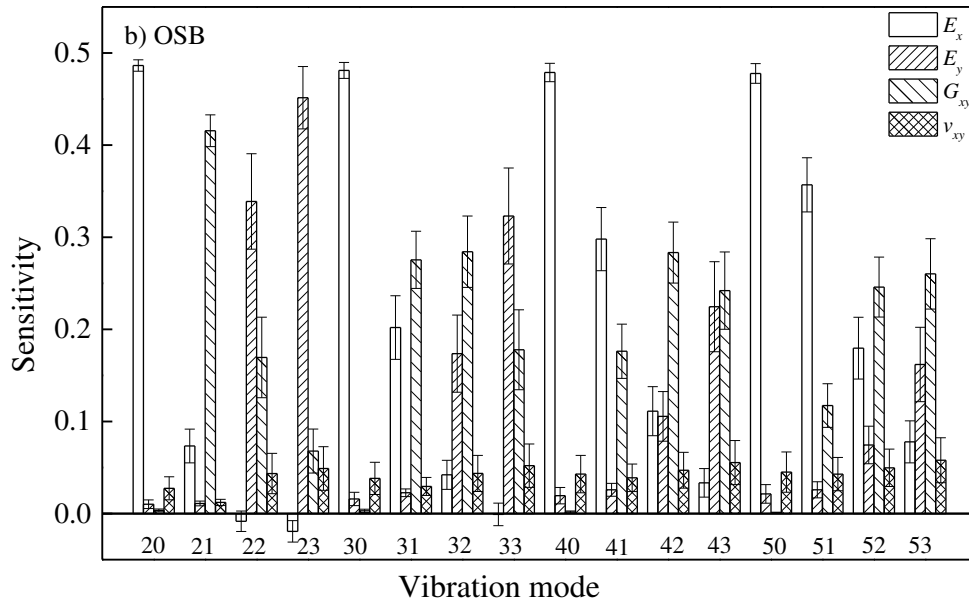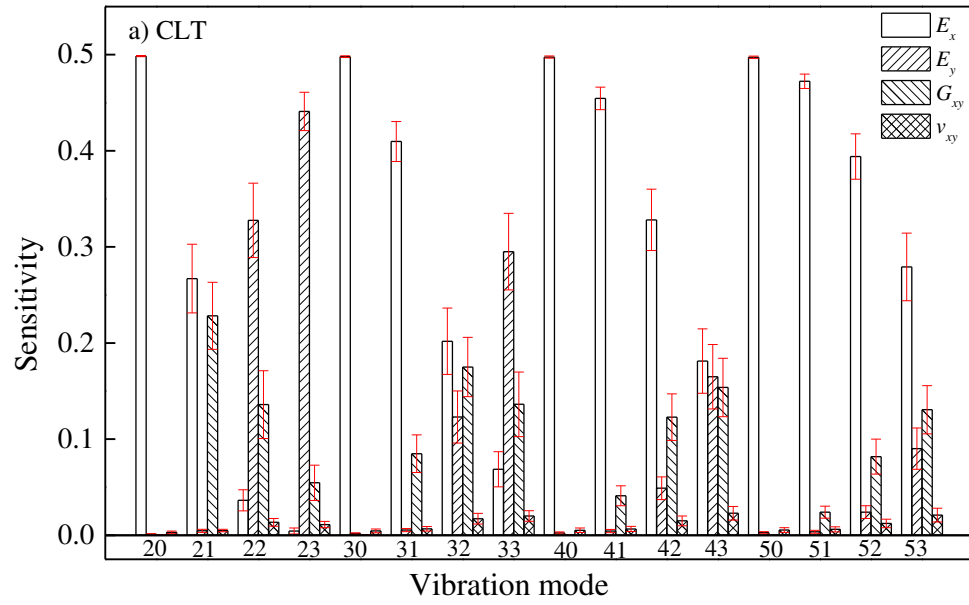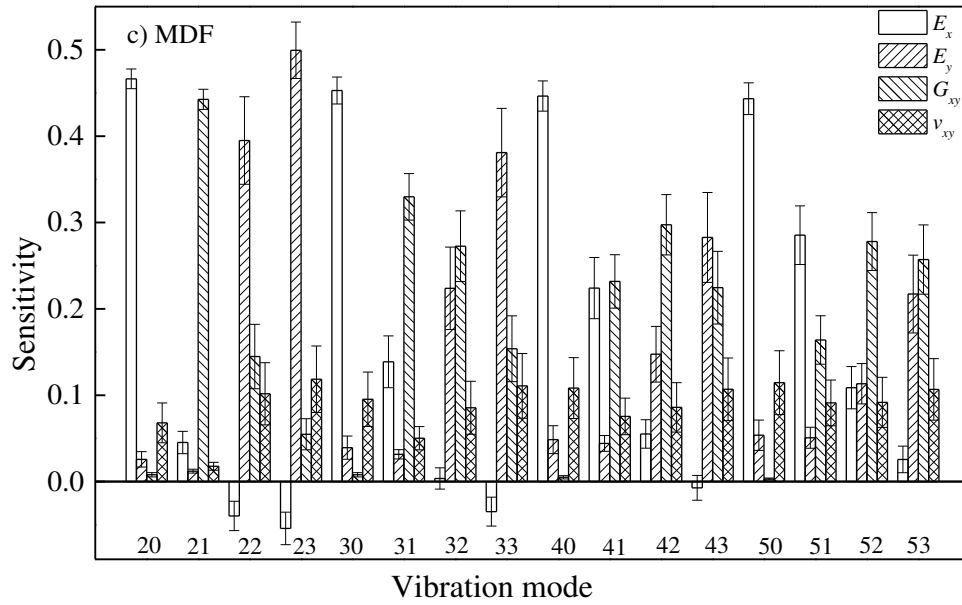
Figure 3.5 Sensitivities of selected a) CLT, b) OSB and c) MDF elastic constants to

different vibration modes

3.3.2 Comparison of Modal (NDT) and Static tests

In Table 3.3, the mean values of modal and static test results of CLT, OSB and MDF panels are summarized and compared. Generally, the data of modal and static tests are in agreement, while the differences are around 10%, except E_y values of OSB panels.

Table 3.3 Mean values of measured elastic constants of selected EWPs

Material	Modal test (MPa)			Static test (MPa)		
	E_x	E_y	G_{xy}	E_x	E_y	G_{xy}
CLT	11306 ($\Delta 6.4\%$)	519 ($\Delta 3.8\%$)	292 (Δ-4.6%)	10630	500	306[*]
OSB	6524 ($\Delta 1.6\%$)	3482 ($\Delta 28.7\%$)	2242 (Δ-9.8%)	6420	2705	2484
MDF	3488 ($\Delta 11.9\%$)	3245 (Δ-0.8%)	1480 (Δ-4.3%)	3115	3272	1547

Note: The ($\Delta\%$) data are the difference between modal and static test. *according to Dröscher (2014).

For CLT panels, the elastic data are close to each other with an average difference of 6.4 and 3.8% for E_x and E_y, respectively. Even though the static in-plane shear test on CLT could not be conducted, it can be stated that the modal test value is in the range of the expectable. Dröscher (2014) measured the in-plane shear strength and shear modulus of CLT panels with different lay-ups and characteristics by a static method. The average G_{xy} of CLT panels made of grade C24 spruce with a gap of 5 mm and lay-up 30 (mm) /30 (mm) /30 (mm) was 306 MPa (270_{min} MPa and 340_{max} MPa). The Canadian SPF E1 grade CLT panels tested here have a similar lay-up, gap distance and mechanical properties. The NDT-G_{xy} values are only about 4.6% lower than the quoted static mean value. The real orthotropic ratios σ_1 and σ_2 are smaller than the initial ones due to the non-edge glue and existing gaps for CLT panels.
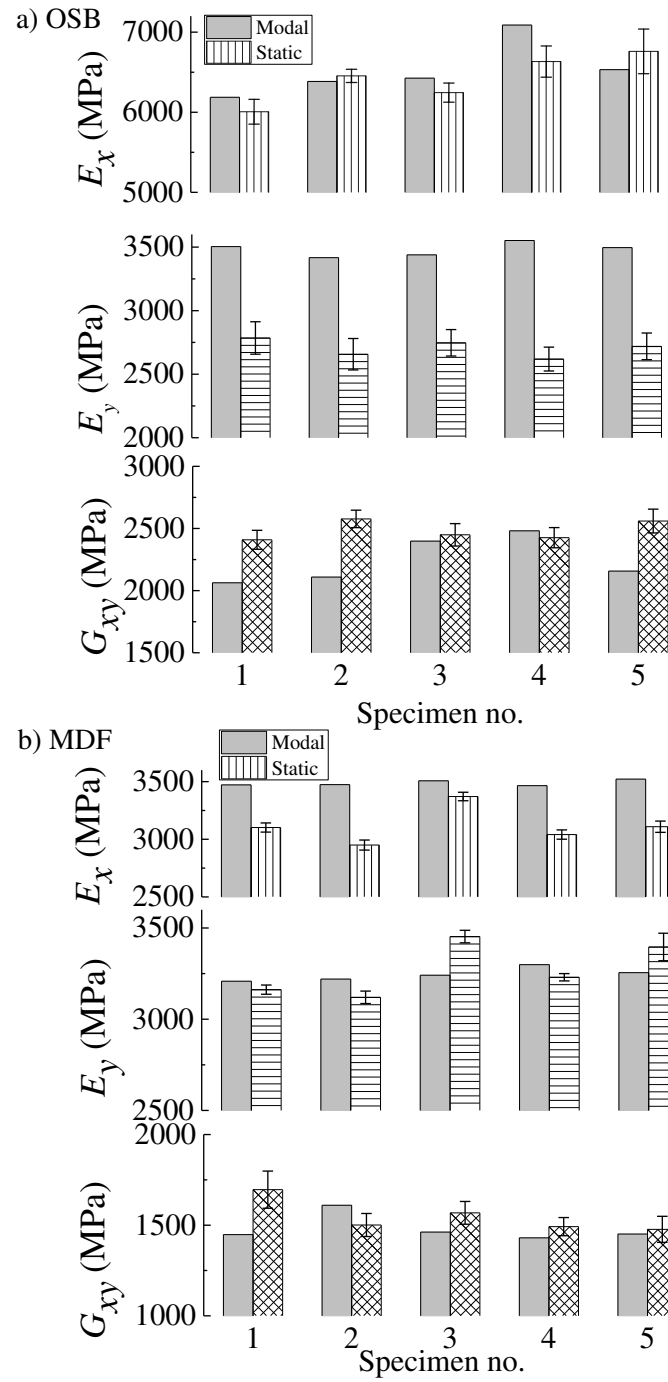
Figure 3.6 Measured elastic constants of a) OSB and b) MDF panels by modal and static

tests

As shown in Figure 3.6 and Table 3.3, the E_x values of OSB panels agree very well with an average difference of 1.6%. NDT-G_{xy} values are about 9.8% smaller than static test values. However, NDT-E_y values are about 28.7% greater than static test values. Similar differences between NDT-E_y and static E_y values of OSB panels were reported by Larsson (1997) being 14.9 to 57.7%. The surface strand characteristics and alignment analysis of commercial OSB panels showed that only 43% of the measured strands were oriented within 20° from the major strength axis (Chen et al., 2008) and thus small size tests are not representative for the whole panel. Considering a 50-mm-wide strip specimen and an up to 150-mm-long single strand (CWC, 2015), the static data are lower than those obtained by NDT of full size panels. Moreover, spatial variability within an OSB panel contributes to the non-homogeneity of stiffness. The density along with an OSB panel width varied from 500 to 850 kg m^{-3} (average 670 kg m^{-3}) (Kruse et al., 2000), and even from 460 to 980 kg m^{-3} (average 690 kg m^{-3}) as obtained by digital X-ray analysis with a fine grid cell size (Chen et al., 2010). Regarding the combined effects of strand angle, density, and stiffness (Liu et al., 2010), it is obvious why the static test results of strips are scattering and are different to NDT results of the full size panel.

Though the NDT-E_x values of MDF panels are about 11.9% greater than the static ones, MDF panel is more isotropic than the other panels (Figure 3.6 and Table 3.3). E_y and G_{xy} from NDT are only 0.8 and 4.3% smaller than those from the static tests, respectively. The difference between E_x values obtained by the two approaches could be caused by warping in the length direction due to self-weight and low stiffness during testing. This reduces the

effective length and results in higher experimental natural frequency and in an overestimation of E_x.

Obviously, the data of CLT and MDF panels obtained by the two methods are in better agreement than those of OSB panels, especially in terms on E_y values. The differences between NDT and static E_y values for CLT, MDF and OSB are 3.8, 28.7, and -0.8%, respectively. The CLT process is well controlled from the selection of lamina to finger jointing to panel pressing (Brandner, 2013). For fiber- and strand- based wood composites, the larger the elements in a panel are, the larger is the variation of the horizontal density distributions in the panels (Chen et al., 2010). The smaller elements also have smaller overlapping areas and include finer voids between them and therefore the material is more uniform (Kruse et al., 2000).

3.4 Conclusions

The proposed method and algorithm in the course of modal testing under SFSF boundary condition is able to measure the three elastic constants simultaneously of CLT, OSB and MDF panels. This technique is sensitive and simple, and the determination of the elastic constants is efficient and reflects the total (average) mechanical properties of full size panels. Even though the difference between modal and static tests varies for different types of engineered wood-based panels, it is obvious that the proposed method is applicable for on-line non-destructive testing and quick evaluation of elastic constants. Further research should focus on the applicability for CLT panels of industrial sizes with different layups

and characteristics. The effect of material structure, namely fiber-, particle-, strand- and veneer-based, on the difference between modal and static test methods needs to be investigated as well.

Acknowledgements

References

APA. (2012). *ANSI/ APA PRG 320 Standard for performance-rated cross-laminated timber*. APA - The Engineered Wood Association.

ASTM International. (2011a). *ASTM D3043-00 Standard Test Methods for Structural Panels in Flexure*. Retrieved from https://doi.org/10.1520/D3043-00R11

ASTM International. (2011b). *ASTM D3044-94 Standard Test Method for Shear Modulus of Wood-Based Structural Panels*. Retrieved from https://doi.org/10.1520/D3044-16

ASTM International. (2011b). *ASTM D4761-13 Standard Test Methods for Mechanical Properties of Lumber and Wood-Base Structural Material.* Retrieved from https://doi.org/10.1520/D4761-13

Antunes, F., Ramalho, A., Ferreira, J. A. M., … Reis, P. (2008). Determination of elastic properties by resonant technique: a sensitivity analysis. *Journal of Testing and Evaluation*, *36*(1), 1–11.

Ayorinde, E. O. (1995). On the sensitivity of derived elastic constants to the utilized modes in the vibration testing of composite plates. In W. Ng (Ed.), *ASME International Mechanical Engineering Congress and Exposition* (pp. 55–64). San Francisco: ASME.

Ayorinde, E. O., and Gibson, R. F. (1993). Elastic constants of orthotropic composite materials using plate resonance frequencies, classical lamination theory and an optimized three-mode rayleigh formulation. *Composites Engineering*, *3*(5), 395–407.

Ayorinde, E. O., and Yu, L. (2005). On the elastic characterization of composite plates with vibration data. *Journal of Sound and Vibration*, *283*(1–2), 243–262.

Biechle, T., Chui, Y. H., and Gong, M. (2011). Comparison of NDE techniques for assessing mechanical properties of unjointed and finger-jointed lumber. *Holzforschung*, *65*(3), 397–401.

Bos, F., and Casagrande, S. B. (2003). On-line non-destructive evaluation and control of wood-based panels by vibration analysis. *Journal of Sound and Vibration*, *268*(2), 403–412.

Brandner, R. (2013). Production and Technology of Cross Laminated Timber (CLT): A State-of-the-art Report. In *Focus Solid Timber Solutions - European Conference on CLT* (pp. 3–36). Graz.

Brashaw, B. K., Bucur, V., Divos, F., … Yin, Y. (2009). Nondestructive testing and evaluation of wood: a worldwide research update. *Forest Products Journal*, *59*(3), 7–14.

Bucur, V. (2006). *Acoustics of Wood*. Boca Raton: CRC Press.

Carfagni, M., and Mannucci, M. (1996). A simplified dynamic method based on experimental modal analysis for estimating the in-plane elastic properties of solid wood panels. In J. L. Sandoz (Ed.), *International symposium on nondestructive testing of wood* (pp. 247–258). Lausanne: Presses polytechniques et universitaires romandes.

Chen, S., Du, C., and Wellwood, R. (2008). Analysis of strand characteristics and alignment of commercial OSB panels. *Forest Products Journal*, *58*(6), 94–98.

Chen, S., Liu, X., Fang, L., and Wellwood, R. (2010). Digital X-ray analysis of density distribution characteristics of wood-based panels. *Wood Science and Technology*, *44*(1), 85–93.

Coppens, H. (1988). Quality control of particleboards by means of their oscillation

    behavior. In *FESYP Technical Conference* (pp. 143–165). Munich.

CWC. (2015). OSB. Retrieved October 12, 2015, from http://cwc.ca/wood-

    products/panel-products/osb/

Dröscher, J. (2014). *Prüftechnische Ermittlung der Schubkenngrößen von*

    BSPScheibenelementen und Studie ausgewählter Parameter. Graz University of

    Technology.

Forest Products Laboratory. (2010). *Wood Handbook - Wood as an Engineering*

    Material. (R. J. Ross, Ed.) (Centennial). Madison: United States Department of

    Agriculture Forest Service.

Gagnon, S., and Pirvu, C. (2011). *CLT Handbook*. (S. Gagnon & C. Pirvu, Eds.). Quebec

    City: FPInnovations.

Ganev, S., Gendron, G., Cloutier, A., and Beauregard, R. (2005). Mechanical properties

    of MDF as a function of density and moisture content. *Wood and Fiber Science*,

    37(2), 314–326.

Grimsel, M. (1999). *Mechanisches Verhalten von Holz: Struktur und*

    Parameteridentikation eines anisotropen Werkstoes. Technische Universität

    Dresden.

Gsell, D., Feltrin, G., Schubert, S., … Motavalli, M. (2007). Cross-Laminated Timber

    Plates: Evaluation and Verification of Homogenized Elastic Properties. *Journal of*

    Structural Engineering, *133*(1), 132–138.

Gülzow, A. (2008). *Zerstörungsfreie Bestimmung der Biegesteifigkeiten, von*

    Brettsperrholzplatten. ETH Zürich.

Gülzow, A., Gsell, D., and Steiger, R. (2008). Non-destructive evaluation of elastic

parameters of square-shaped cross-laminated solid wood panels, built up

symmetrically with 3 layers. *Holz Als Roh-Und Werkstoff*, *66*(1), 19–37.

Hearmon, R. F. S. (1946). The fundamental frequency of vibration of rectangular wood

and plywood plates. *Proceedings of the Physical Society*, *58*(1), 78–92.

Huffington, N. J., and Hoppmann, W. H. (1958). On the transverse vibrations of

rectangular orthotropic plates. *Journal of Applied Mechanics*, *25*(3), 389–395.

Kim, C. S., and Dickinson, S. M. (1985). Improved approximate expressions for the

natural frequencies of isotropic and orthotropic rectangular plates. *Journal of Sound

and Vibration*, *103*(1), 142–149.

Kruse, K., Dai, C., and Pielasch, A. (2000). An analysis of strand and horizontal density

distributions in oriented strand board (OSB). *European Journal of Wood and Wood

Products*, *58*(4), 270–277.

Lai, T. C., and Ip, K. H. (1996). Parameter estimation of orthotropic plates by Bayesian

sensitivity analysis. *Composite Structures*, *34*(1), 29–42.

Larsson, D. (1996). Stiffness characterization of wood based panels by modal testing. In

J. Sandoz (Ed.), *International symposium on nondestructive testing of wood* (pp.

237–246). Lausanne: Presses polytechniques et universitaires romandes.

Larsson, D. (1997). Using modal analysis for estimation of anisotropic material

constants. *Journal of Engineering Mechanics*, *222–229*(123), 3.

Lauwagie, T. (2005). *Vibration-based methods for the identification of the elastic

properties of layered materials*. Katholieke Universiteit Leuven.

Leissa, A. W. (1969). Anisotropic Plates. In A. W. Lesissa (Ed.), *Vibration of plates* (pp.

250–260). Washington D. C.: National Aeronautics Space Administration.

Liu, X., Chen, S., and Wellwood, R. (2010). Synergistic effect of strand angle and panel density on bending properties of strand-based wood composites. *Forest Products Journal*, *60*(4), 390–394.

Martínez, M. P., Poletti, P., and Espert, L. G. (2011). Vibration Testing for the Evaluation of the Effects of Moisture Content on the In-Plane Elastic Constants of Wood Used in Musical Instruments. In C. M. A. Vasques & J. Dias Rodrigues (Eds.), *Vibration and Structural Acoustics Analysis* (pp. 21–57). Springer Netherlands.

Ponneth, D., Vasu, A. E., J.C., E., … S., C. S. (2014). Destructive and non-destructive evaluation of seven hardwoods and analysis of data correlation. *Holzforschung*, *68*(8), 951–956.

Reddy, J. N. (1984). A simple higher-order theory for laminated composite plates. *Journal of Applied Mechanics*, *51*(4), 745–752.

Schulte, M., Frühwald, A., and Bröker, F. W. (1996). Non-destructive testing of panel products by vibration technique. In J. Sandoz (Ed.), *International symposium on nondestructive testing of wood* (pp. 259–268). Lausanne: Presses polytechniques et universitaires romandes.

Sobue, N., and Katoh, A. (1992). Simultaneous determination of orthotropic elastic constants of standard full-size plywoods by vibration method. *Mokuzai Gakkaishi*, *38*(10), 895–902.

Sobue, N., and Kitazumi, M. (1991). Identification of power spectrum peaks of vibrating completely-free wood plates and moduli of elasticity measurements. *Mokuzai*

Gakkaishi, *37*(1), 9–15.

Steiger, R., Gülzow, A., Czaderski, C., … Niemz, P. (2012). Comparison of bending

stiffness of cross-laminated solid timber derived by modal analysis of full panels and

by bending tests of strip-shaped specimens. *European Journal of Wood and Wood

Products*, *70*(1–3), 141–153.

Sylvain, G., and Marjan, P. (2011). Structure design of cross-laminated timber elements.

In G. Sylvain & P. Ciprian (Eds.), *CLT Handbook* (1st ed., pp. 114–185).

FPInnovations.

Thomas, W. H. (2003). Poisson's ratios of an oriented strand board. *Wood Science and

Technology*, *37*(3), 259–268.

Yoshihara, H. (2011a). Influence of specimen configuration on the measurement of the

off-axis Young's modulus of wood by vibration tests. *Holzforschung*, *66*(4), 485–

492.

Yoshihara, H. (2011b). Off-axis Young's modulus and off-axis shear modulus of wood

measured by flexural vibration tests. *Holzforschung*, *66*(2), 207–213.

Yoshihara, H. (2013). Comparison of results obtained by static 3- and 4-point bending

and flexural vibration tests on solid wood, MDF, and 5-plywood. *Holzforschung*,

67(8), 941–948.

Zhou, J., and Chui, Y. H. (2014). Efficient measurement of elastic constants of cross

laminated timber using modal testing. In A. Salenikovich (Ed.), *World Conference

on Timber Engineering*. Quebec City.

CHAPTER 4 COMPARATIVE STUDY ON MEASUREMENT OF ELASTIC CONSTANTS OF WOOD-BASED PANELS UISING MODAL TESTING: CHOICE OF BOUNDARY CONDITIONS AND CALCULATION METHODS

Abstract: Modal testing based on the theory of transverse vibration of orthotropic plate has shown great potentials in measuring elastic constants of panel products. Boundary condition (BC) and corresponding calculation method are key in affecting its practical application in terms of setup implementation, frequency identification, accuracy and calculation efforts. In order to evaluate different BCs for non-destructive testing of wood-based panels, three BCs with corresponding calculation methods were investigated for measuring their elastic constants, namely in-plane elastic moduli (E_x, E_y) and shear modulus (G_{xy}). As a demonstration of the concept, the products used in this study were oriented strand board (OSB) and medium density fiberboard (MDF). The BCs and corresponding calculated methods investigated were, a) all sides free (FFFF) with one-term Rayleigh frequency equation and finite element modeling, b) one side simply supported and the other three free (SFFF) with one-term Rayleigh frequency equation, c) a pair of opposite sides along minor strength direction simply supported and the other pair along major strength direction free (SFSF) with improved three-term Rayleigh frequency equation. Differences between modal and static results for different BCs were analyzed for each case. Results showed that all three modal testing approaches could be applied for evaluation of the elastic constants of wood-based panels with different accuracy levels compared with standard static test methods. Modal testing on full-size panels is

recommended for developing design properties of structural panels as it can provide global properties.

Keywords: elastic properties, wood panels, non-destructive technique, modal testing

4.1 Introduction

Wood-based panel products are used for both structural and non-structural applications. Engineered wood-based panels such as oriented strand board (OSB) are even more widely used in modern wood constructions, especially in light frame wood construction. Elastic constants are critical mechanical properties for structural design, which are also the key quality control parameters. Research studies of evaluating the elastic constants of wood-based panels by use of modal testing could be traced back to the 1980s. Different BCs with corresponding calculation methods have been adopted for measuring the elastic constants, namely the modulus of elasticity (E) and shear modulus (G), of panel type products such as solid wood panels, particleboard, OSB, plywood and medium density fibreboard (MDF) and cross laminated timber (CLT).

Boundary condition with all four sides free (FFFF) has been mostly used among the studies done for modal testing of panel-shaped wood products because it requires the least efforts for implementation. However, there is no exact solution for FFFF BC. The one-term Rayleigh frequency solution was frequently applied for the calculation of elastic constants due to its simple and straight-forward formula (Bos and Casagrande, 2003; Carfagni and Mannucci, 1996; Coppens, 1988; Nakao and Okano, 1987; Sobue and Kitazumi, 1991). The natural frequency of torsional mode was used for measuring the in-plane shear

85

modulus of wood-based panels by Nakao and Okano (1987). The method appeared to be much simpler than static plate-twist shear tests. Coppens (1988) measured the elastic constants (E_x, E_y and G_{xy}) of particleboard by modal testing in the laboratory of individual company for quality control purposes. Sobue and Kitazumi (1991) applied the same vibration technique for measuring elastic constants of wood panels (western red cedar, hemlock, buna and keyaki). The results were verified with static test results of beam specimens. Carfagni and Mannucci (1996), simplified the method in identifying modal shapes based on assessing whether the response and excitation were in or out of phase. The number of impact points was reduced to six for rectangular wood panels. Bos and Casagrande (2003) presented the E_x and E_y values of selected eight OSB panels, 260 plywood panels, one MDF panels tested by an on-line non-destructive evaluation system called VibraPann, which utilized the measurement of the first bending modes in two strength directions. The results showed an absolute difference within 15% of E_x and E_y values for plywood compared with static test values. The spatial variability of elastic properties within a panel was also reported by testing of small panels cutting from a full-size panel.

Besides Rayleigh frequency solution, finite element modelling (FEM) was often used for the determination of elastic constants combined with modal testing (Larsson, 1996, 1997; Martínez et al., 2011). The elastic constants were estimated by minimizing the difference between the experimental frequencies and FE modeled values using an iterative process. Full-size MDF and OSB panels, modeled as thin orthotropic plates under FFFF BC, were tested by Larsson (1996, 1997) using modal testing. The proposed method was proved to

be accurate because of the good agreement between measured and calculated natural frequencies (up to the 7th mode) within 1-5%, though the average differences between dynamic and static bending data of E_x and E_y were 14.1% and 31.0%, respectively. A similar method was adopted to study the effects of moisture content on the in-plane elastic constants of wooden boards used in musical instruments (Martínez et al., 2011). It was found that, with the moisture content ranging from 0% to 25%, the E values in radial and longitudinal directions and G of longitudinal and radial plane changed approximately 88%, 51% and 47%, respectively. Gsell et al. (2007) measured the natural frequencies and mode shapes of a rectangular CLT specimen. An analytical model based on Reddy's higher order plate theory (Reddy, 1984) was applied to calculate natural frequencies and mode shapes numerically. All three G and the two in-plane E values were identified by minimizing the difference between measured and estimated natural frequencies based on the least-squares method. Gülzow (2008) further studied the modal testing method to evaluate the elastic properties of CLT panels with different layups and characteristics.

FFFF, however, is not the best BC for large size panels, especially in the production environment. Other BCs such as one edge simply supported and the other three edges free (SFFF) and one edge clamped and the other three edges free (CFFF) were also used for the determination of elastic constants of full-size structural panels for the purpose of quality control in production. A simultaneous determination of orthotropic elastic constants of standard full-size plywood by vibration method was conducted with SFFF BC (Sobue and Katoh, 1992). The results showed an agreement to within 10% of E and G values measured using static bending and plate torsional tests respectively. Particleboard and MDF panels

of full-size dimensions were tested using a vibration technique in both vertical and horizontal cantilever (CFFF) arrangements (Schulte et al., 1996). It was found that there was no significant difference between measured frequencies from the vertical and horizontal position, which indicated that the deflection caused by self-weight under horizontal position had no effect on measured frequencies. The absolute values of the dynamic E values were about 20-25 % higher than the static values, while MDF had a better correlation and smaller difference between dynamic and static results than particleboard.

Currently, boundary condition of a pair of opposite sides along minor strength direction simply supported and the other pair free (SFSF) was adopted with improved approximate natural frequency expressions for measuring elastic constants for full-size wood-based panels including CLT, OSB and MDF panels (Zhou et al., 2016). The difference between dynamic and static test results were about 10% or less except for E_y of OSB. The reason was thought to be the inappropriate strip specimen size for static bending test, which could not well represent the E_y of full-size OSB panels. The method with SFSF BC has great potential for further implementation in on-line evaluation of full-size wood-based panels.

The study described in this paper was conducted to compare three methods of measuring elastic constants of wood-based panel products with different BCs (FFFF, SFFF and SFSF) with corresponding calculation procedures. Standard static tests were performed to provide reference values for comparison. The objective of the study was to develop a better understanding on how the accuracy of measured elastic constants are affected by the BC

chosen for modal testing and data analysis procedure. The ultimate goal is to contribute to the development of standard modal testing method for measuring the elastic constants of wood-based panels as well as potential development of on-line quality control techniques.

4.2 Theoretical Background

In the application of the three methods, the following assumptions were made:

a) the material has a uniform mass and in-plane elastic property distribution;

b) the effects of transverse shear deformation and rotatory inertia are negligible.

4.2.1 Forward Problem

The governing differential equation for the transverse vibration of a thin rectangular orthotropic plate based on the above assumptions is expressed as follows (Leissa, 1969),

$$D_x \frac{\partial^4 w}{\partial x^4} + D_y \frac{\partial^4 w}{\partial y^4} + 2(D_1 + 2D_{xy}) \frac{\partial^4 w}{\partial x^2 y^2} + \rho h \frac{\partial^4 w}{\partial t^2} = 0 \qquad (4.1)$$

where:

$$D_x = \frac{E_x h^3}{12(1 - v_{xy} v_{yx})},$$

$$D_y = \frac{E_y h^3}{12(1 - v_{xy} v_{yx})},$$

$$D_1 = D_x v_{xy} = D_y v_{yx},$$

$$D_{xy} = \frac{G_{xy} h^3}{12},$$

E_x = modulus of elasticity in length (x)/ major strength direction,

E_y = modulus of elasticity in width (y)/ minor strength direction,

G_{xy} = in-plane shear modulus,

v_{xy} and v_{yx} = Poisson's ratios,

$(1 - v_{xy}v_{yx}) \approx 0.99$ for most wood materials (Hearmon, 1946),

a = length of the plate,

b = width of the plate,

h = thickness of the plate, and

ρ = mass density.

For the cases considered in this study, the aspect ratio (a/b) of the test specimens were greater than 1.

With the input of four elastic constants, dimensional information and density, all the natural frequencies and corresponding mode shapes can be calculated under different BCs as a forward problem. However, due to the complexity of boundary condition, the analytical solution of the forward problem cannot be simply generated from the governing differential equation. Therefore, numerical methods such as Rayleigh method and FEM have been applied for solving the forward problem. In this study, the forward problem solutions for FFFF and SFFF BCs were both generated by Rayleigh method with one-term deformation expression (Bos and Casagrande, 2003; Sobue and Kitazumi, 1991). These frequency equations are explicit and in closed form, which need less computation efforts compared with analytical method and finite element modeling. The frequency equation can be expressed as,

$$f_{(m,n)} = \frac{1}{2\pi}\sqrt{\frac{1}{\rho h}}\sqrt{D_x\frac{\alpha_{1(m,n)}}{a^4} + D_y\frac{\alpha_{2(m,n)}}{b^4} + 2D_1\frac{\alpha_{3(m,n)}}{a^2b^2} + 4D_{xy}\frac{\alpha_{4(m,n)}}{a^2b^2}} \qquad (4.2)$$

For SFSF BC, a closed-form approximate frequency equation by Rayleigh method with three-term deformation expression was adopted from (Kim and Dickinson, 1985),

$$f_{(m,n)} = \frac{ab}{\pi^2}\sqrt{\frac{\rho h}{H}}\sqrt{\frac{C_{ij} + c^2C_{in} + d^2C_{\dot{m}j} - 2cE_{ij} - 2dE_{ji} + 2cdF}{1 + c^2 + d^2}} \qquad (4.3)$$

where:

$f_{(m,\,n)}$ = natural frequency of mode (m, n), and

m and n = mode indices, the number of node lines including the simply supported sides in y and x directions, respectively, and

$H = D_1 + 2D_{xy}$.

In Eq. 4.2, $\alpha_{1(m,\,n)}$, $\alpha_{2(m,\,n)}$, $\alpha_{3(m,\,n)}$ and $\alpha_{4(m,\,n)}$ = the coefficients for mode (m, n), which can be pre-determined for different boundary conditions (Bos and Casagrande, 2003; Sobue and Kitazumi, 1991). In Eq. 4.3, (m, n) is equivalent to (i, j) as in (Kim and Dickinson, 1985), $\dot{m}$ and $\dot{n}$ are equal to m and n in the reference, respectively. The expressions and values of other constants can be found in the same reference as well.

4.2.2 Inverse Problem

Theoretically, with a proper forward solution, density, dimensions and any four measured frequencies, the four elastic constants (E_x, E_y, G_{xy} and v_{xy}) can be calculated through an inverse process, known as an inverse problem. However, the sensitivity of each natural frequency to elastic constants is different. Only the sensitive frequencies result in accurate determination of the appropriate elastic constants. Sensitivity analysis is always required

in order to identify the most sensitive natural frequencies for calculation of each elastic constant (Ayorinde, 1995).

To exclude the difference among different Rayleigh frequency solutions for different BCs, FEM was employed for sensitivity analysis by changing with ±10% of the mean of each elastic constant. FEM was performed in ABAQUS finite element software ver. 6.12-3 with initial elastic constants and geometry information listed in Table 4.1 (Ganev et al., 2005; Thomas, 2003; Zhou et al., 2016). OSB and MDF panels were modeled as a 3D deformable shell using shell element S4R (Abaqus, 2013) with a global mesh size of 0.02. For FFFF BC, no constraints were added to the plate, and for SFFF and SFSF BCs, the simply supported edge or edges were constrained in three translational directions. The natural frequencies of up to 20 modes were computed with embedded 'Lanczos eigensolver'. The ratio of frequency difference of each mode to corresponding frequency obtained from initial elastic constants is defined as the sensitivity of each mode to the elastic constants.

Table 4.1 Material properties for FEM sensitivity analysis

Material	E_x, (MPa)	E_y, (MPa)	v_{xy}	G_{xy}, (MPa)	G_{xz}, (MPa)	G_{yz}, (MPa)	Density (kg/m^3)	Dimension (a×b×h, mm)
OSB	6400	2700	0.23	2500	770	750	614	1210×610×11.1
MDF	3100	3300	0.33	1500	120	120	697	1220×620×15.7

FEM sensitivity analysis results of an OSB and a MDF panel are shown in Figure 4.1. It can be seen that for all three BCs, Poisson's ratio is almost not sensitive to any frequency

modes, therefore Poisson's ratio cannot be properly determined. As reported in previous research (Coppens, 1988), Poisson's ratio might be determined unless the plate has a certain aspect ratio of $\sqrt[4]{E_x/E_y}$. The sensitive modes for E_x, E_y and G_{xy} are (2, 0), (0, 2) and (1, 1) with FFFF BC, respectively, and are ($m \geq 2$, 1), (0, 2) and (1, 1) with SFFF BC, respectively. The sensitivity of mode ($m \geq 2$, 1) to E_x increases with the increase of m. A desirable sensitivity can be found with m equals to 3 or 4 depending on the aspect ratio (a/b) and elastic constant ratio (E_x/E_y) of the panel. Natural frequency of mode (3, 1) was used in this study. For SFSF BC, the sensitive frequency modes for E_x, E_y and G_{xy} are (2, 0), (2, $n \geq 2$) and (2, 1), respectively. The sensitivity of mode (2, $n \geq 2$) to E_x increases with the increase of n. In most cases, the frequency of mode (2, 2) or (2, 3) is sensitive enough for calculating E_y. For all three BCs, the sensitive modes for E_x and E_y are those bending modes in x and y axis, and sensitive mode for G_{xy} is the first torsional mode shown in Figure 2. If there is no constraint at the edge along the minor stiffness axis, the sensitivity of low bending mode with only one half sine wave is sufficient for E_x or E_y. Otherwise, the sensitivity of higher bending mode with two or three half sine waves is required. For highly coupled modes with comparable equal m and n, each elastic constant contributes more evenly to the frequency value than modes with $m >> n$ or $m << n$. If such mode is used for calculation, the coupled effect of all elastic constants should be included in the calculation.
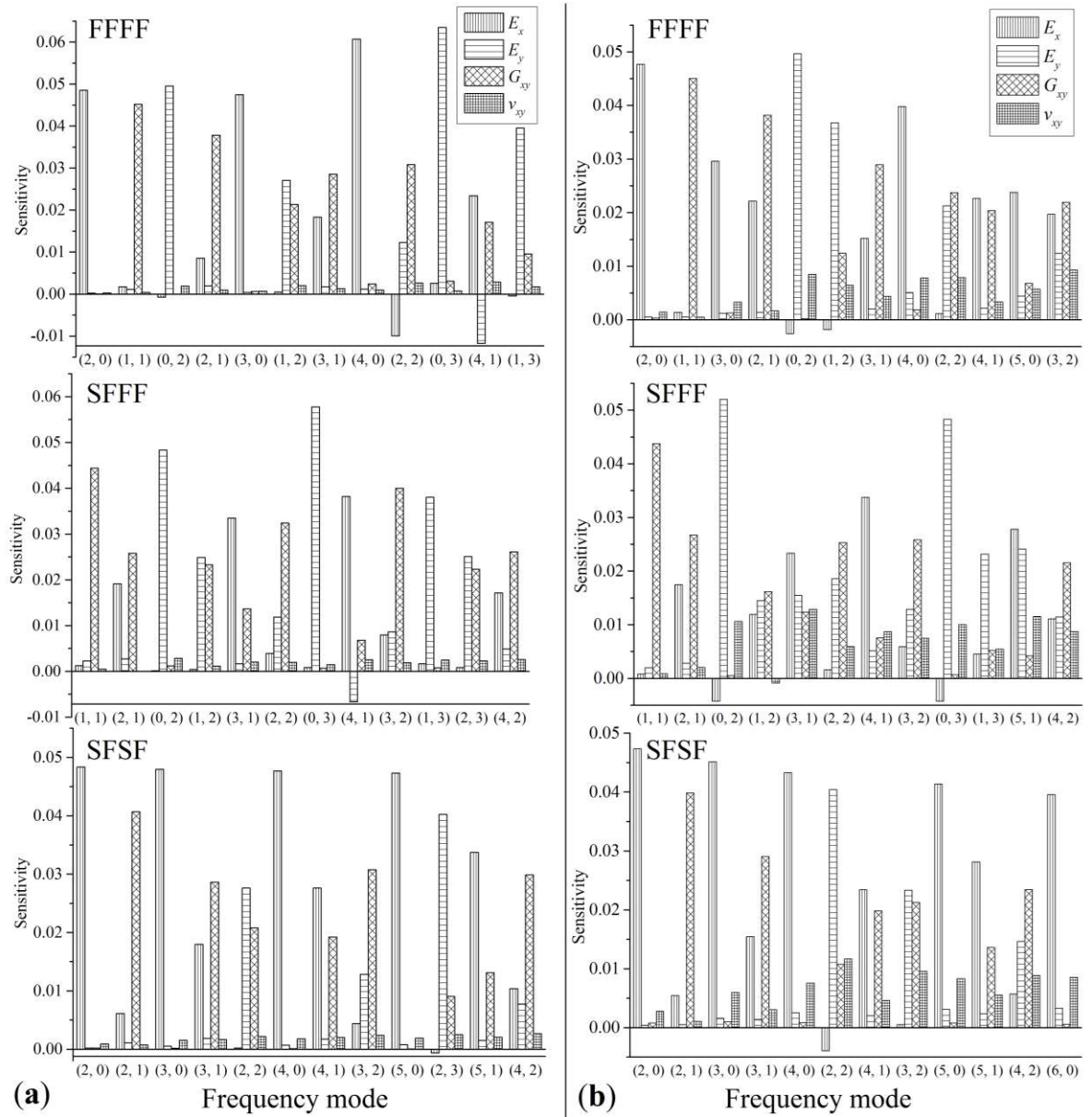
Figure 4.1 Sensitivies of each frequency mode to elastic constants under different BCs for

a) a OSB panel and b) a MDF panel
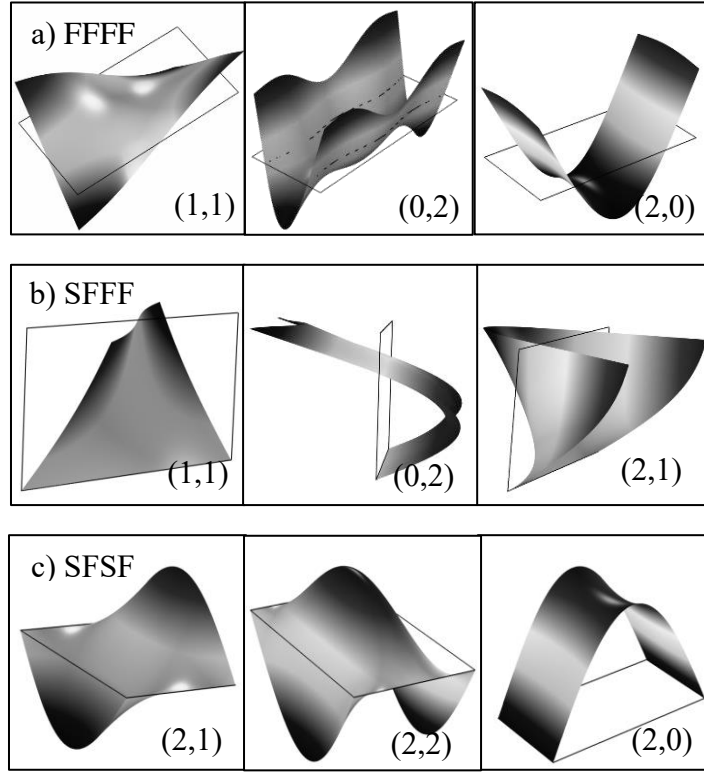
Figure 4.2 Illustration of mode shapes of sensitive frequency modes under different BCs

From Eq. 4.2, for FFFF BC, the elastic constants can be calculated using the following

formulas (Bos and Casagrande, 2003; Nakao and Okano, 1987),

$$E_x = \frac{48\pi^2 \rho a^4 f_{(2,0)}^2 (1 - v_{xy} v_{yx})}{500.6 h^2} \tag{4.4}$$

$$E_y = \frac{48\pi^2 \rho b^4 f_{(0,2)}^2 (1 - v_{xy} v_{yx})}{500.6 h^2} \tag{4.5}$$

$$G_{xy} = 0.9 \rho (\frac{ab}{h} f_{(1,1)})^2 \tag{4.6}$$

Furthermore, the calculated values can be used as initial input values for FEM updating. First the difference Δf_i between sensitive FEM frequencies (f_{FEMi}) and experimental frequencies (f_{expi}) will be calculated.

$$\Delta f_i = (f_{FEM\,i} - f_{expi}) / f_{expi} \tag{4.7}$$

where:

$i =$ to 1, 2, 3, and corresponds to (2, 0) (0, 2) (1, 1).

If any relative frequency difference $|\Delta f_i|$ is larger than 0.01, then

$$X = X_0 \times (1 - \Delta f_i)^2 \tag{4.8}$$

where:

$X =$ elastic constant (E_x, E_y, G_{xy}) to be updated and

$X_0 =$ the corresponding initial value from Eqs. 4, 5 or 6.

The iteration process stops when all $|\Delta f_i|$ are smaller than 0.01 and outputs from the last iteration will be the calculated elastic constants. Experience has shown that less than five iterations are required to achieve convergence.

For SFFF BC, the elastic constants can be calculated using the following formulas (Sobue and Katoh, 1992),

$$E_x = \frac{12\pi^2 \rho a^4 (1 - v_{xy} v_{yx})(4 f_{(3,1)}^2 - 36.27 f_{(1,1)}^2)}{3805.04 h^2} \tag{4.9}$$

$$\text{or } E_x = \frac{12\pi^2 \rho a^4 (1 - v_{xy} v_{yx})(4 f_{(2,1)}^2 - 16.49 f_{(1,1)}^2)}{500.6 h^2} \tag{4.10}$$

$$E_y = \frac{48\pi^2 \rho b^4 f_{(0,2)}^2 (1 - v_{xy} v_{yx})}{237.86 h^2} \qquad (4.11)$$

$$G_{xy} = \frac{\pi^2 \rho a^2 b^2 f_{(1,1)}^2}{3h^2} \qquad (4.12)$$

For SFSF BC, a calculation method was developed using the improved frequency equation, Eq. 4.3, based on an iteration process. The initial value of E_x is first calculated using the fundamental frequency, $f_{(2,0)}$. The other initial values are set as the ratios with E_x based on reported reference value or theoretical prediction. The iteration stops when the total difference between measured and calculated frequencies is less than 1%. Details about the calculation method can be found in (Zhou et al., 2016).

To summarize, the BCs and corresponding calculation methods to be investigated are listed in Table 4.2.

Table 4.2 Selected BCs and calculation method

BC	Calculation method	Sensitive modes	Note
FFFF	Closed-form frequency equation by Rayleigh method with one-term deformation expression	(2, 0), (1, 1), (0, 2)	Can be used as initial values for FEM.
	FEM updating by ABAQUS with S4R shell element		S4R shell element includes the effect of transverse shear deformation.
SFFF	Closed-form frequency equation by Rayleigh method with one-term deformation expression	(m≥2, 1), (1, 1), (0, 2)	$f_{(3,1)}$ is used for calculating E_x.
SFSF	Improved frequency equation by Rayleigh method with three-term deformation expression	(2, 0), (2, 1), (2, n≥2)	MATLAB based iteration process.

4.3 Materials and Methods

4.3.1 Materials

Five full-size 11.1 mm thick OSB panels of dimensions 2.44 m × 1.22 m and five full-size 15.7 mm thick MDF panels of dimensions 2.46 m × 1.24 m were purchased from a building supplies store. The average moisture contents and densities of OSB and MDF panels were about 4% and 5%, 614 kg/m^3 and 697 kg/m^3, respectively. Each full-size panel was cut into four panels of dimensions 1.21 m × 0.60 m. In total, twenty panels were obtained from each type of panel for modal testing. Then two panels with the closest masses were selected from four panels of the same full-size panel to glue a double-thick panel using a two-component structural polyurethane adhesive. Five panels were prepared from each type of panel respectively for investigating the effect of thickness on the accuracy of modal tests. The average thicknesses of double-thick OSB (DOSB) and MDF (DMDF) panels were 22.1 mm and 31.2 mm, respectively. The remaining ten panels of each type were cut into square panels of dimension 0.60 m × 0.60 m for in-plane shear tests. Then three strips were cut from each strength direction from a square panel for bending tests. For the double-thick panels, they were cut into square panels for in-plane shear tests and panel bending tests as well. The cutting scheme is shown in Figure 4.3.
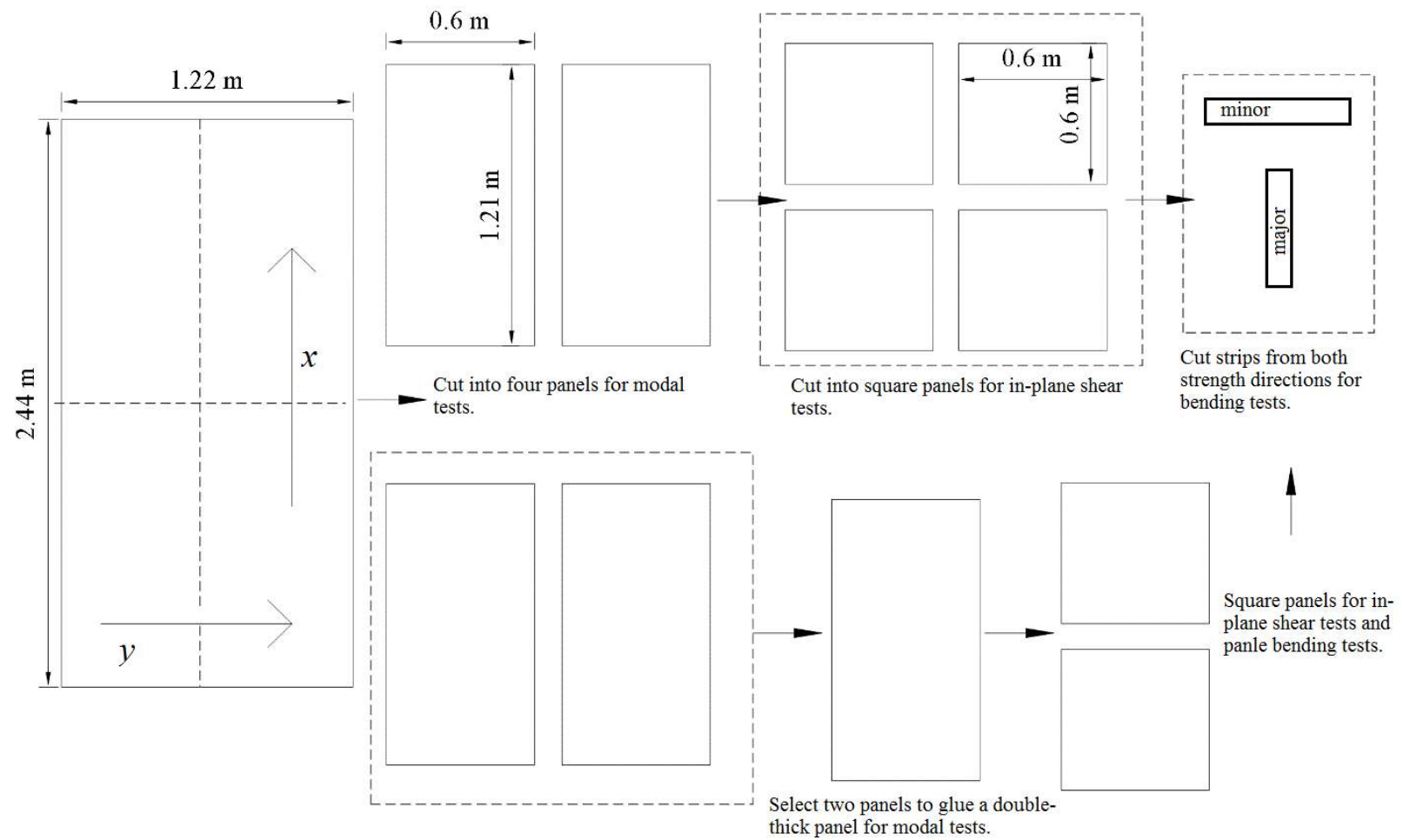
Figure 4.3 Cutting Scheme for different tests

100

4.3.2 Modal Tests

The impact vibration tests were conducted on the specimens with three different BCs for both OSB and MDF panels. Only modal tests with FFFF and SFSF BCs were conducted for DOSB and DMDF panels, because SFFF BC could not be achieved easily in practice as the other two BCs for thick panels. The BCs were realized using ropes and steel pipes in the lab. The panel was suspended with a pair of ropes on a steel frame as shown in Figure 4.4a to simulate FFFF BC. A pair of steel pipes were used to clamp one side of the panel to simulate simple support. As shown in Figure 4.4b and c, the panels were clamped with proper pressure at one side parallel to major strength direction or a pair of two opposite sides parallel to minor strength direction to achieve SFFF or SFSF BC, respectively. For SFFF BC, one edge along the length direction of the panel was supported, which should not touch the base.

For FFFF and SFFF BCs, the accelerometer was attached at the top left corner of the panel, while for SFFF it was attached at 7/12 length of one free edge. The locations selected were not on the nodal lines of first several modes up to the first 15 modes including the sensitive natural frequencies. The impact and acceleration time signals were recorded by a data acquisition device (LDS Dactron, Brüel & Kjær) and the frequency response function (FRF) was calculated from the time signals using a data analysis software (RT Pro 6.33, Brüel & Kjær). The frequency spectra were post-processed by MATLAB software for frequency identification and calculation of the elastic constants.
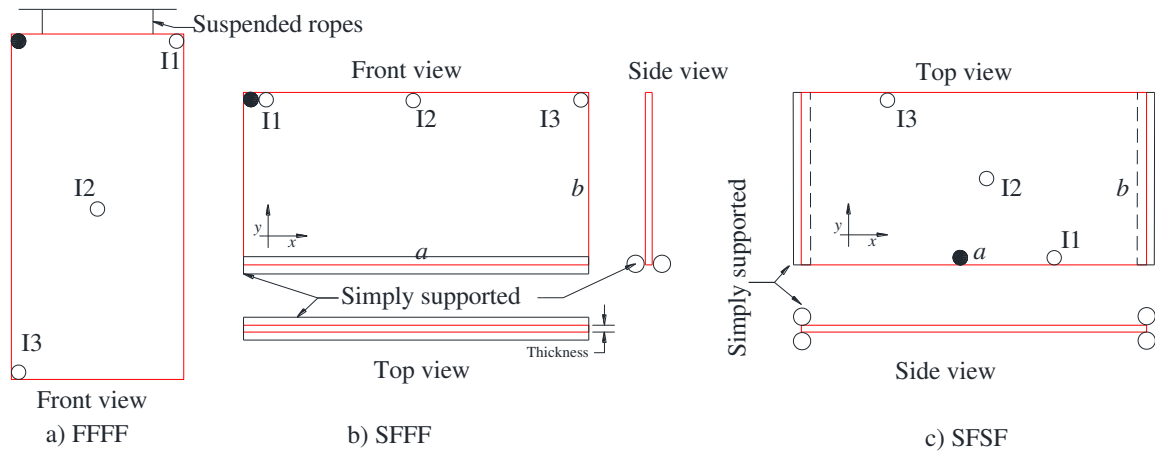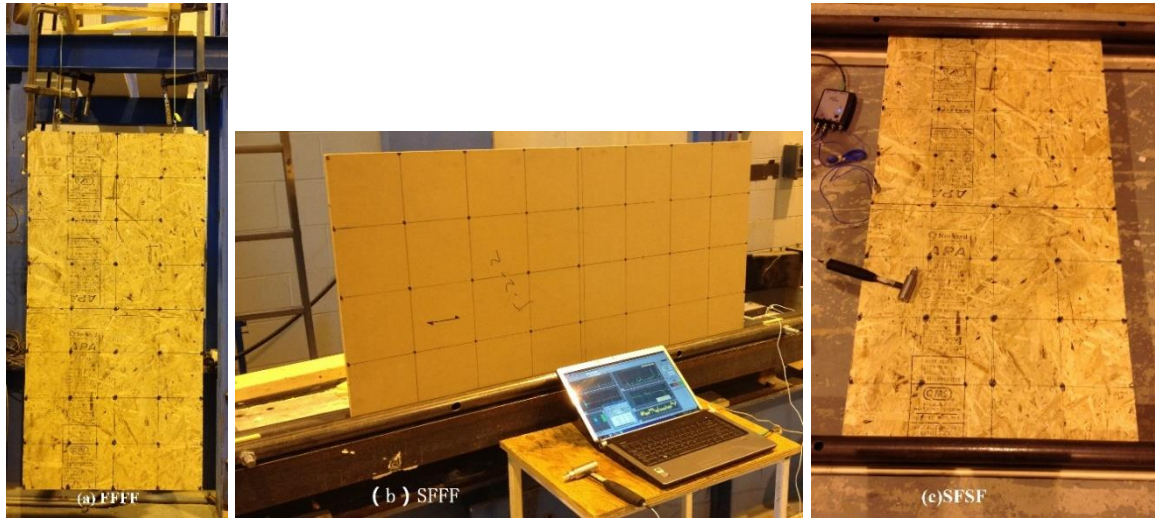
Figure 4.4 Test setups for modal tests under different boundary conditions (solid circle refers to the location of accelerometer and blank circle (I1-3) refers to the impact location)

4.3.3 Identification of Sensitive Frequencies

Mathematically, for a given plate, the natural frequency increases nonlinearly with an increase of mode indices (m, n). From the sensitivity analysis, it can be seen that for all three BCs the sensitive frequencies have small mode indices with either m or n less than 3 for the material considered in this study. Low mode frequencies are easier to be detected than high mode frequencies. Normally, for 2D and 3D structures, it is necessary to conduct modal test on the whole surface of a structure with a grid to obtain the experimental mode shapes for frequency identification. However, for simple structures such as plates with given BCs and approximate material properties, it is possible to identify the frequency modes with a few impacts at specific locations, based on modal displacements at those locations. Modal displacements are generally estimated from the imaginary part of the FRF as shown in Figure 4.5.
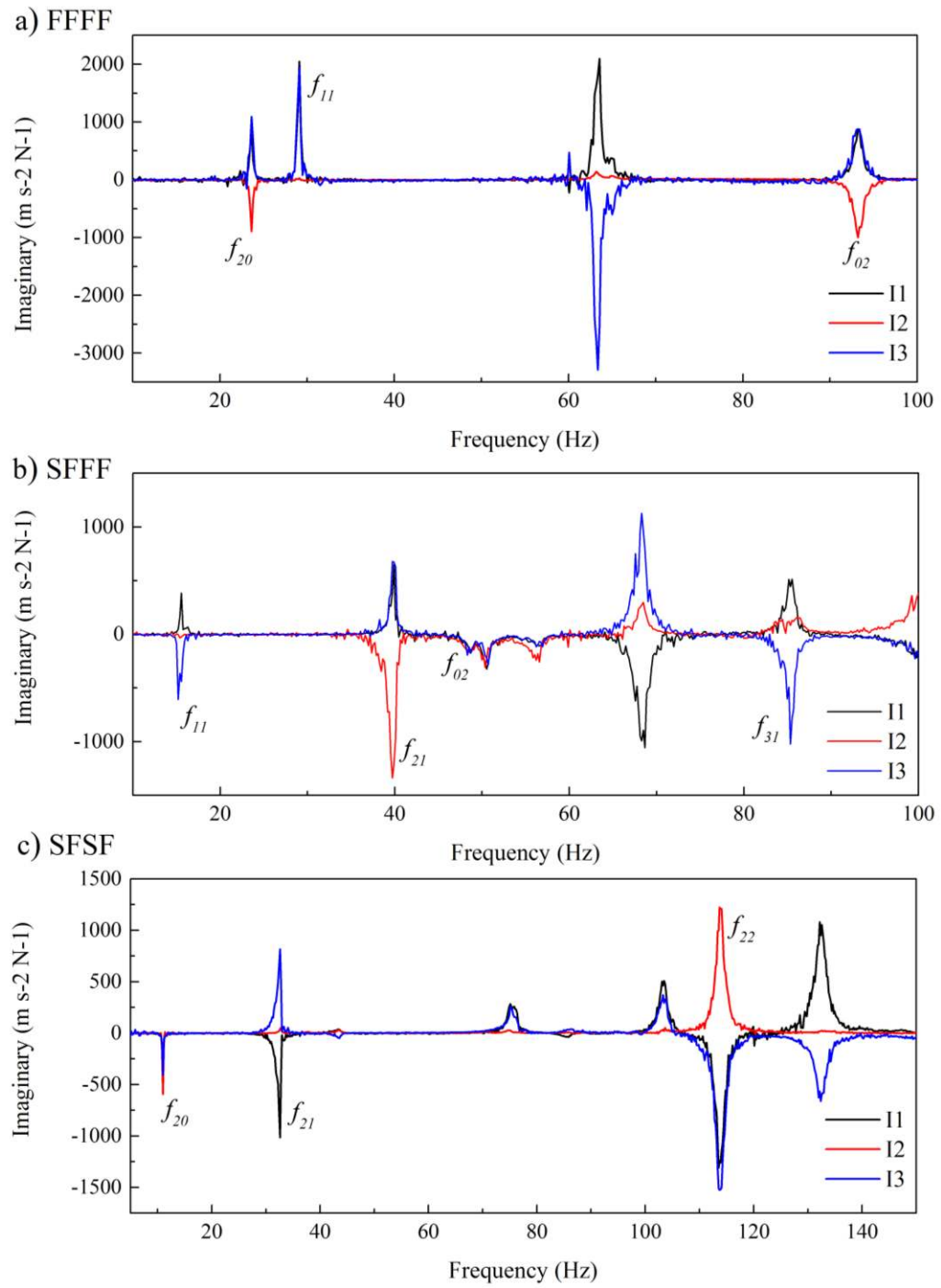
Figure 4.5 Selected plots of imaginary part of FRF for sensitive frequency identification at three impact locations under the three BCs

For FFFF BC, the frequencies of modes (2, 0) and (1, 1) are the first two in a frequency spectrum because (2, 0) or (1, 1) is the mode indices giving the starting frequency value. Modes (m, n) with either m or n being an odd number have a node at the centre of a plate. Therefore, modes (2, 0) and (0, 2) are the first two modes that would appear and mode (1, 1) is the first mode that would vanish when impacted at the centre of the plate. Thus, with the accelerometer located at the left right corner, only three spectra with impacts at the centre (I2) and a pair of diagonal corners (I1 and I3) are sufficient for sensitive frequency identification as shown in Figure 5a. Mathematically, frequency of mode (0, 2) or any (0, n) bending mode in y direction decreases with any increase of E_x/E_y and decrease of a/b. Slender plates with similar E_x and E_y (i.e., that approaching an isotropic plate) would result in a very high mode (0, 2), which is difficult to detect. However, for isotropic material, there is no need to identify mode (0, 2), as modes (2, 0) and (1, 1) are sufficient for calculating E and G. For nearly isotropic material like MDF, plate of aspect ratio a/b greater than 3 is not recommended.

For SFFF BC, modes (1, 1) and (1, 2) are the first two modes in a frequency spectrum for the material considered in this study. Frequency of mode (0, 2) decreases with the increase of E_x/E_y and the decrease of a/b, which behaves similarly with mode (0, 2) with FFFF BC. With the accelerometer located at the left right corner, frequency spectra from three impacts at the middle (I2) and two ends (I1 and I3) of the top edge are helpful for frequency identification as is shown in Figure 5b. Modes (m, n) with m being an odd number have out-of-phase modal displacements (i.e., movement is in opposite direction) when being impacted at the two ends and vanish when being impacted in the middle. Mode (1, 1) is the

105

first of such modes and mode (3, 1) is the second one. While modes (m, n) with m being an even number have in-phase modal displacement (i.e. movement is in the same direction) when impacted at the two ends but out-of-phase modal displacement when impacted in the middle. Mode (2, 1) is the first of such modes. Modes (0, n) have in-phase modal displacements when impacted at all three locations (I1, I2 and I3), and mode (0, 2) is the first of such modes.

For SFSF BC, as was discussed in previous research (Zhou and Chui, 2014; Zhou et al., 2016), three spectra with impacts at the centre (I2) and two locations from the two opposite free edges (I1 and I3) can assist with identifying the sensitive frequency modes needed for calculation. Modes (2, 0) and (2, 1) are the first two modes that appear in the frequency spectra. Mode (2, 2) is the first mode that has out-of-phase modal displacement to mode (2, 0) while mode (2, 1) vanishes when impacted at the center, Figure 5c. Similar to mode (0, 2) in FFFF BC, frequency of mode (2, 2) decreases with the increase of E_x/E_y and the decrease of a/b. For some wood-based products, E_x/E_y can be close to 1 for MDF, 1 to 10 for OSB or laminated wood products, and about 20 for solid wood. The effort for identifying mode (2, 2) depends on the material property and specimen aspect ratio.

4.3.4 Static Tests

Static tests were conducted as a reference for comparison with dynamic tests. The elastic moduli and shear modulus of OSB and MDF panels were obtained from static centre-point flexure tests according to (ASTM, 2011) and shear tests according to (ASTM, 2016), respectively. Twelve strips along each strength direction were cut from full-size panel and

they were tested for E values. A total of four square panels were cut from each panel and tested for G_{xy} values. For the double-thick panels (DOSB and DMDF), two square panels from one DOSB or DMDF specimen are used for both in-plane shear tests and panel bending tests. Then six strips along each strength direction of DOSB and DMDF panels were cut for centre-point flexure tests as well. The dimensions for static test specimens are given in Table 4.3.

Table 4.3 Dimensions of specimens for static tests

| Material | Strip bending test | | | | In-plane shear test or/ and panel bending test |
	Major (mm^2)	Span (mm)	Minor (mm^2)	Span (mm)	(mm^2)
OSB	600×50	540	450×50	270	600×600
MDF	600×50	570	450×50	380	600×600
DOSB	600×50	540	450×50	400	600×600
DMDF	600×50	570	450×50	400	600×600

4.5 Results and Discussion

4.5.1 Mean Value Comparison

The mean elastic constants of OSB and MDF panels measured by dynamic methods with different BCs and static methods are listed in Table 4.4. It can be seen that, for all three BCs, dynamic E values of OSB panels are larger than their static counterparts, while dynamic G_{xy} values are smaller than static G_{xy} value. The differences between dynamic and

static E_x values of OSB panels are 16.9%, 2.5% and 9.4% for FFFF, SFFF and SFSF BCs, respectively. The differences between dynamic and static E_y values of OSB panels are 39.9%, 29.0% and 22.5% for FFFF, SFFF and SFSF BCs, respectively. The differences between dynamic and static G_{xy} values of OSB panels are -27.5%, -22.6% and -16.6% for FFFF, SFFF and SFSF BCs, respectively. Among the three BCs, the three elastic constants of OSB panels obtained from FFFF BC exhibited the largest difference from the corresponding static values. The difference between dynamic and static E_y values of OSB has been explained in previous research (Zhou et al., 2016). For commercial OSB panels, around 50% of the strands are oriented within 20° from the major strength axis and thus stiffness distribution showed significant variations spatially (Chen et al., 2008, 2010). However, the width of the strips for bending tests was 50 mm, which is much smaller than the length of a single strand, 150 mm. Therefore, the static data are lower than those obtained by modal tests of full size panels.

Table 4.4 Elastic constants of OSB and MDF measured by dynamic methods with different BCs and static methods

Panel #	Elastic constants measured by dynamic methods (MPa)									Elastic constants measured by static methods (MPa)		
	FFFF[*]			SFFF			SFSF					
	E_x	E_y	G_{xy}	E_x	E_y	G_{xy}	E_x	E_y	G_{xy}	E_x	E_y	G_{xy}
OSB1	7769	3534	1790	6533	3168	2092	7496	3177	2045	6424	2654	2504
OSB2	7740	3530	1820	6818	3060	1929	7334	3071	2162	6732	2520	2589
OSB3	8231	3848	1935	6994	3434	2119	7542	3319	2243	6376	2627	2450
OSB4	7678	3483	1768	6820	3225	1897	6921	3049	1959	6808	2574	2488
OSB5	7782	3700	1872	7223	3789	1763	7386	3222	2155	6694	2555	2637
Mean	7840	3619	1837	6878	3335	1960	7336	3167	2113	6607	2586	2534
COV	6.4%	6.5%	7.1%	6.5%	9.7%	9.9%	6.3%	8.1%	8.8%	10.7%	14.9%	7.5%
Diff.	16.9%	39.9%	-27.5%	2.5%	29.0%	-22.6%	9.4%	22.5%	-16.6%	/	/	/
MDF1	3323	3282	1394	3273	2818	1324	3297	3216	1341	3073	3162	1626
MDF2	3290	3188	1377	3233	2938	1319	3210	2906	1411	2929	3078	1450
MDF3	3460	3423	1459	3276	3072	1406	3473	3185	1492	3371	3453	1568
MDF4	3221	3182	1353	3050	2848	1359	3055	3017	1280	3041	3231	1492
MDF5	3440	3310	1446	3280	3031	1434	3403	3200	1526	3078	3251	1477
Mean	3347	3277	1406	3222	2942	1368	3288	3105	1410	3098	3235	1522
COV	4.0%	3.6%	3.9%	5.3%	4.5%	4.9%	5.4%	7.3%	7.3%	6.7%	6.0%	8.1%
Diff.	8.0%	1.3%	-7.6%	4.0%	-9.1%	-10.1%	6.1%	-4.0%	-7.7%	/	/	/

Note: * refers to the results of FEM updating. COV was the coefficient of variation.

For MDF panels, the differences between dynamic and static values are much smaller than those for OSB panels. The differences between dynamic and static E_x values of MDF panels are 8.0%, 4.0% and 6.1% for FFFF, SFFF and SFSF BCs, respectively. The differences between dynamic and static E_y values of MDF panels are 1.3%, -9.1% and -4.0% for FFFF, SFFF and SFSF BCs, respectively. The differences between dynamic and static G_{xy} values of MDF panels are -7.6%, -10.1% and -7.7% for FFFF, SFFF and SFSF BCs, respectively. There are no significant differences between the values measured using the three BCs for a specific elastic constant.

Generally, dynamic E_x values from all three BCs are larger than static values, and dynamic G_{xy} values from all three BCs are smaller than static values. Dynamic E_y values of MDF from SFFF and SFSF BCs are slightly smaller than static E_y values, while dynamic E_y values of MDF from FFFF BC is slightly larger than static E_y values. From the comparisons between mean values by dynamic and static methods, it can be seen that all three dynamic methods show the same trends of measured values, though the differences with static values varied.

4.5.2 Correlation between Dynamic and Static Results

In order to better compare the dynamic methods with static methods, the dynamic values from each BC were compared with static values through paired-sample t-tests. As shown in Table 4.5, most of the paired groups have a p value less than 0.05 at the 95% confidence level except paired group 'SFFF & Static' of E_x for OSB panels and paired groups 'FFFF & Static' and 'SFSF & Static' of E_y for MDF panels. Generally, the elastic values by

dynamic methods exhibit a significant difference with the elastic values by static methods at the 95% confidence level. Thus the linear correlation of each elastic constant between dynamic and static method are not as good as most reported correlation between dynamic and static values of beam-like specimens (Brancheriau and Baillères, 2002).

Figures 4.6 and 4.7 illustrate the differences in percentage (Diff.) between each dynamic and static elastic constant of all panel specimens with different BCs. It can be seen that in Figure 4.6, the difference between dynamic and static E_x of each individual OSB panel ranges from -1 to 37% with most of them around -16% for FFFF BC, from -11 to 16% with most of them around -3% for SFFF BC, from -6 to 31% with most of them around -9% for SFSF BC, respectively. The difference between dynamic and static E_y and G_{xy} values of each individual OSB panel is within 60% (except for one panel) and -40%, respectively. Most of the differences are distributed around their averaged differences for each BC. The exceptions happen when the static values are either too large or too small. However, corresponding dynamic values from the three BCs are consistent with each other, indicating their reliability. Compared with OSB panel results, MDF panel results show better uniformity in differences distributions for three elastic constants within an absolute difference of 20%.

Table 4.5 Paired-Samples t-test results of each elastic constant between dynamic and static test values

Material	Elastic constants	Paired group	Correlation	t	df	Sig. (2-tailed)
OSB	E_x	FFFF & Static	.174	7.879	19	.000
		SFFF & Static	.459	1.559	19	**.136**
		SFSF & Static	.099	4.371	19	.000
	E_y	FFFF & Static	-.428	11.242	19	.000
		SFFF & Static	-.280	7.220	19	.000
		SFSF & Static	-.332	6.284	19	.000
	G_{xy}	FFFF & Static	.220	-14.722	19	.000
		SFFF & Static	-.097	-8.744	19	.000
		SFSF & Static	.220	-14.722	19	.000
MDF	E_x	FFFF & Static	.351	5.482	19	.000
		SFFF & Static	.059	2.107	19	.049
		SFSF & Static	.467	4.196	19	.000
	E_y	FFFF & Static	**.520**	1.147	19	**.266**
		SFFF & Static	.431	-7.245	19	.000
		SFSF & Static	.132	-2.068	19	**.053**
	G_{xy}	FFFF & Static	-.065	-3.664	19	.002
		SFFF & Static	-.050	-4.678	19	.000
		SFSF & Static	-.128	-3.003	19	.007

Note: df is short for degree of freedom. Sig. refers to the significance of paired-samples t test of each group. If sig.<0.05, there is significant difference between paired group at the 95% confidence level. The tests were performed using software SPSS 19.0.
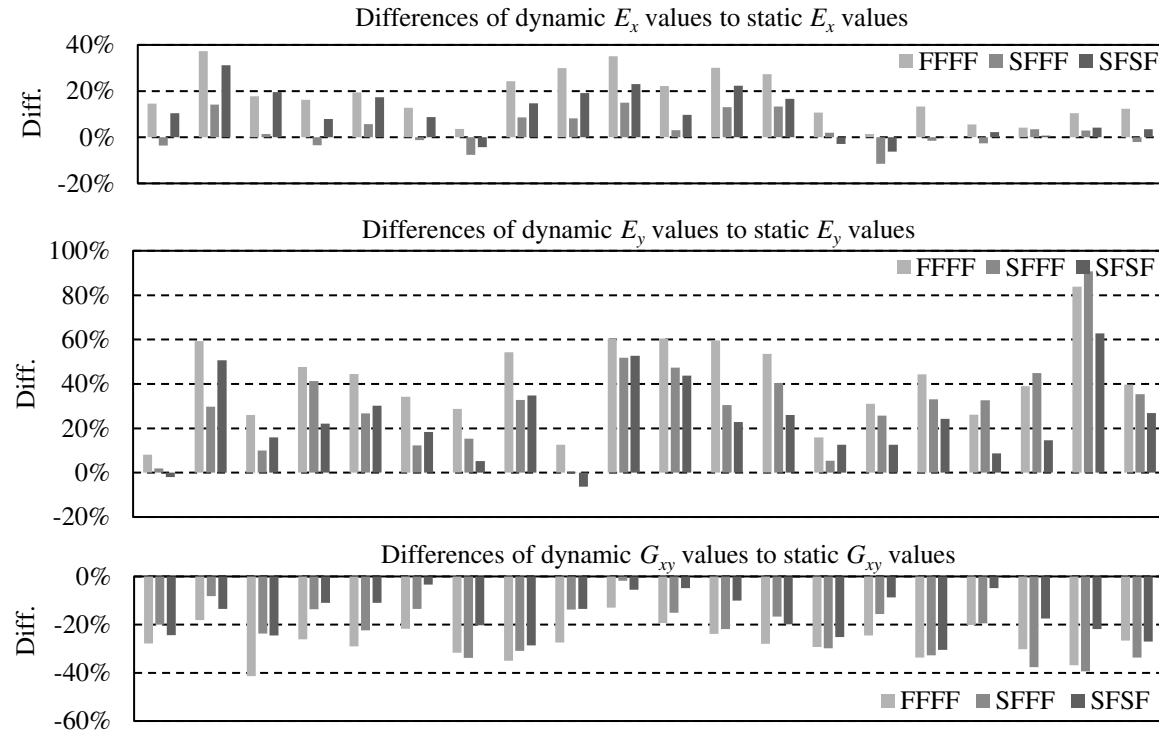
Figure 4.6 Differences of dynamic elastic constants from different BCs to corresponding static values of OSB
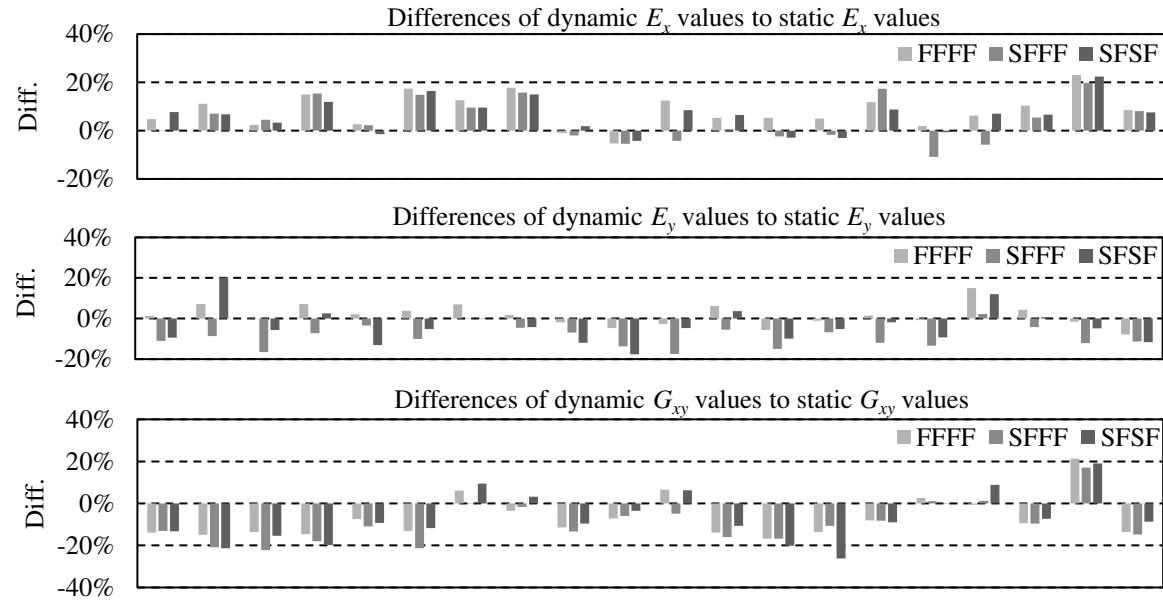
Figure 4.7 Differences of dynamic elastic constants from different BCs to corresponding static values of MDF

The differences between dynamic and static values can be mainly explained by the material structure of the panels and the nature of the test methods. Dynamic values by modal tests of panels are always considered to be the general elastic constants as representative of the whole panel, while the static values are the localized elastic constants. Nakao and Okano (1987) reported differences between dynamic and static G_{xy} values for particleboard and fiberboard such as hardboard and MDF panels of -35 to 18%, while the difference for plywood was -8 to 14%. Larson (1996, 1997) also reported an average difference between dynamic and static E_x and E_y of 14% and 31% for OSB panels, respectively. The results from static test on small strip specimens are questionable for some particle-based wood panel products because the relative size of the specimen and wood elements in the panel (McNatt, 1984).

4.5.3 Accuracy Analysis of Dynamic Test Methods

The differences between each BC are primarily caused by the influence of BCs in practice, the accuracy of chosen forward problem solutions and sensitivity level of selected vibration modes. The influence of implementing BC in practice is not easy to be assessed. FFFF BC is the one requiring the least efforts and free from added constraints among three BCs. SFFF and SFSF BCs require partial clamping to stabilize the test panel. Aside from the influences of implementation of BC, the chosen forward solutions affect the results to different extents for OSB and MDF panels. As shown in Figure 4.8, the differences between values obtained from Eqs 4.4-4.6 and FEM updating are different for different elastic constants and materials. There is virtually no difference for E_x and E_y of OSB panels from both calculations, while there is an average difference of about 5% for G_{xy}. Similarly,

115

no difference was found for E_x value of MDF from both calculations, but there are differences of about 5% and 10% for E_y and G_{xy} value of MDF from both calculations, respectively. For both MDF and OSB panels, E_y was obtained from $f_{(0, 2)}$, where the effect of transverse shear may contribute if the transverse shear moduli are small or the wavelength to depth ratio become small for high modes. MDF has a much smaller transverse shear modulus than OSB. FEM updating in this study employed a shell element that included this effect, while Eqs 4.4-4.6 do not. In Eq. 4.6, a factor of 0.9 is used based on previous research (Nakao and Okano, 1987), but current results shown here suggest a 5% and 10% increase for OSB and MDF panels, respectively.
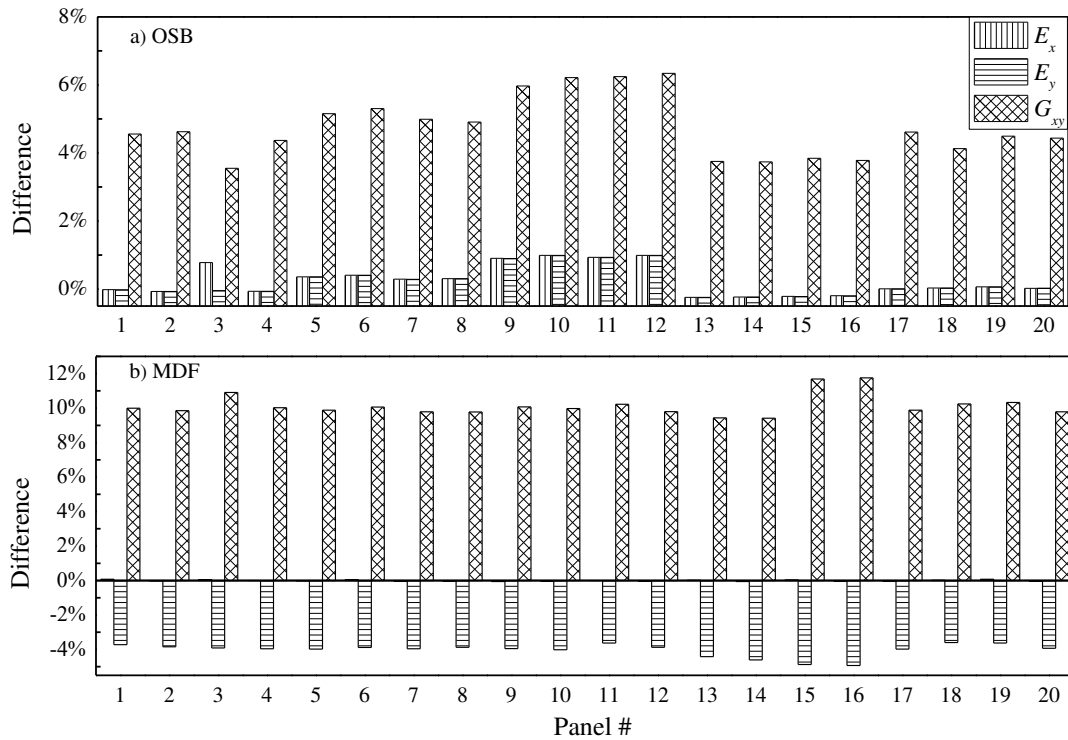
Figure 4.8 Influence of forward solution on elastic constants by dynamic method under FFFF BC for a) OSB and b) MDF panels

Sensitivity level of selected frequencies has an effect on calculated values. For instance, the E_x value can be obtained from Eq. 4.9 or 4.10 for SFFF BC. However, selected frequencies with different sensitivity will result in different calculated values. As shown in Figure 4.9, the differences of E_x values of OSB and MDF panels from the two equations can vary from 10% to 40% because of the lower sensitivity to mode (2,1) than to mode (3, 1). Sobue and Katoh (1992), who first adopted SFFF BC for modal testing of wood-based panel material, used different combinations of frequency equations to calculate the elastic constants. It is an alternative method but ignored the effect of nonlinear distribution of sensitivity. Also, in the case of calculating E_y value of MDF using frequency of mode (2, 2) under SFSF BC, the coupled effect of E_y and G_{xy} was included in the iteration of frequency of mode (2, 2) as both elastic constants contribute evenly.

Other influences may include width to thickness ratio and transverse shear rigidity. FEM was performed using material properties in Table 4.1 and two types of shell elements, S4R and STRI3. STRI3 ignores the effect of transverse shear deformation, while S4R considers it (Abaqus, 2013). MDF has much lower transverse shear modulus than OSB. The theoretical effect of transverse shear deformation on natural frequency increases with an increase in thickness is shown in Table 4.6. As expected, the effects are different under FFFF and SFSF BCs. The differences are almost doubled under SFSF BC compared with FFFF BC, for natural frequencies related to E_y and G_{xy}.
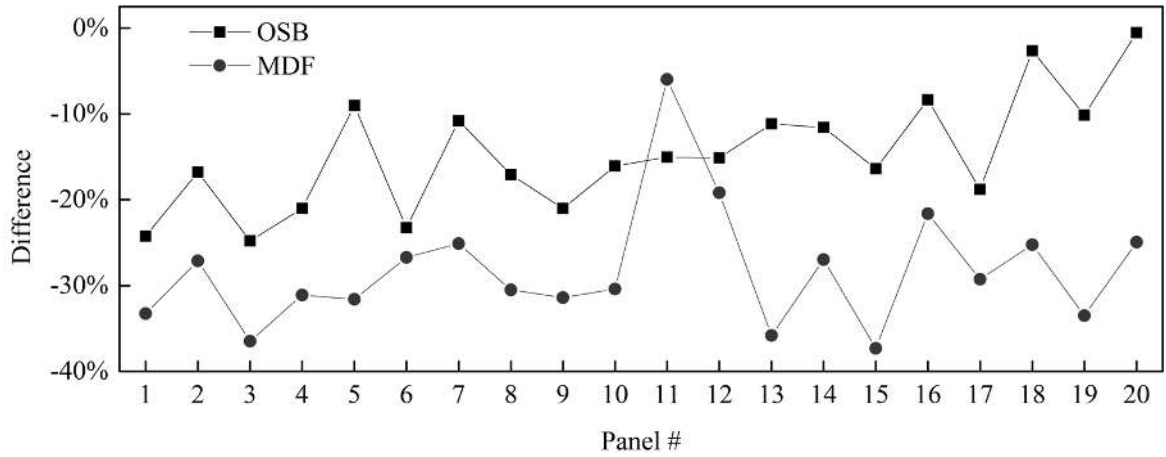
Figure 4.9 Differences of calculated E_x values using frequencies of different sensitivities under SFFF BC

Table 4.6 Theoretical effects of thickness and transverse shear deformation on selected sensitive natural frequencies

Material	FFFF			SFSF		
	$f_{(2,0)}$	$f_{(1,1)}$	$f_{(0,2)}$	$f_{(2,0)}$	$f_{(2,1)}$	$f_{(2,2)}$
OSB	0.08%	-0.74%	0.39%	-0.02%	-1.47%	-0.83%
DOSB	-0.06%	-1.81%	0.16%	-0.15%	-3.43%	-2.55%
MDF	-0.32%	-3.01%	-1.06%	-0.47%	-5.45%	-3.45%
DMDF	-1.17%	-6.52%	-4.28%	-1.33%	-11.44%	-9.07%

Note: FEM was performed using material properties presented in Table 1, for DOSB and DMDF.

Commercial OSB and MDF panels, due to the saddle-shaped vertical density profile, can be regarded as three-layer composites. DOSB and DMDF panels become five-layer composites after gluing, which are expected to have slightly different elastic properties to the component OSB and MDF due to lamination. As shown in Table 4.7, compared with panel static test results, dynamic results of both DOSB and DMDF panels from SFSF BC seems to be much closer to panel static test results than those from FFFF BC. This may be explained by the same degree of effect of transverse shear deformation on vibration and deflection under static load of the panel for SFSF BC with the increase of thickness. For DOSB panels, the differences between dynamic results from FFFF BC and panel static test results are 8.3%, 7.7% and 4.9% for E_x, E_y and G_{xy}, respectively, which are just a little higher than the differences between dynamic results from SFSF BC and panel static test results. However, the corresponding differences between dynamic and static tests for DMDF panels are much higher with FFFF BC than those with SFSF BC. As shown in Table 4.6, with the increase of thickness, the effect of transverse shear on the selective frequencies are two times smaller with FFFF BC than with SFSF BC. In addition, the transverse shear modulus of MDF are much smaller than OSB. Thus, the dynamic results of DMDF from FFFF BC are least affected with the increase of thickness and are much larger than those with SFSF BC.

Table 4.7 Elastic constants of DOSB and DMDF measured by modal methods with different BCs and static methods

| Panel # | Elastic constants measured by dynamic method (MPa) | | | | | | Elastic constants measured by static methods (MPa) | | | | |
| | FFFF | | | SFSF | | | Panel bending | | Strip bending | | G_{xy} |
	E_x	E_y	G_{xy}	E_x	E_y	G_{xy}	E_x	E_y	E_x	E_y	
DOSB1	6438	4200	1760	6194	3909	1638	6141	4099	4785	2970	1716
DOSB2	6664	4701	1867	6325	4066	1557	6151	4430	4681	2867	1804
DOSB3	6768	4562	1843	6291	3734	1522	5908	3960	5253	3111	1672
DOSB4	6269	4158	1739	5514	4147	1782	5618	3877	4499	2646	1530
DOSB5	6418	4312	1743	6520	3715	1779	6231	4008	5073	2897	1814
Mean	6511	4387	1790	6169	3914	1656	6010	4075	4858	2898	1707
Diff.	8.3%	7.7%	4.9%	2.6%	-3.9%	-3.0%	/	/	-19.2%	-28.9%	/
DMDF1	3207	3282	1343	2750	2812	1148	2772	2670	2599	2297	1128
DMDF2	2854	2790	1188	2611	2321	1046	2434	2440	2331	2022	1062
DMDF3	2715	2766	1180	2252	2305	1040	2392	2468	2259	2072	1050
DMDF4	2636	2564	1100	2420	2662	970	2208	2430	2170	1862	1107
DMDF5	2865	2796	1171	2456	2663	969	2394	2405	2279	2112	1069
Mean	2855	2840	1196	2498	2553	1035	2440	2483	2328	2073	1083
Diff.	17.0%	14.4%	10.5%	2.4%	2.8%	-4.5%	/	/	-4.6%	-16.5%	/

In addition, the increase in thickness has a decreasing effect on measured G_{xy} values due to increasing transverse shear deflection. Yoshihara and Sawamura (2006) found that in-plane shear modulus of western hemlock solid wood plates measured by static square-plate twist method increased from 0.5 to 1.0 GPa with an increase in length or width to thickness ratio from 14 to 60.

4.5.4 Panel versus Beam Bending Tests

In Table 4.7, it can be observed that the differences in E_x and E_y values measured using panel and strip bending tests are -19.2% and -28.9% for DOSB, and -4.6% and -16.5% for DMDF, respectively. For DOSB, the difference is due to the inappropriate size (width) of strip specimens from two strength directions. McNatt (1984) once tested bending properties of structural wood-based panels of large panel size (2.44 (length) × 1.22 (width) m^2) and small strip size specified in ASTM D1037. The results indicated that for OSB, waferboard and flakeboard panels, the E values were not affected much by reducing panel size from 2.44×1.22 to 0.61×0.30 m^2. The panel bending test values of E_x and E_y were about 23% and 15% larger than corresponding strip bending test values for OSB, respectively. This was likely caused by the reduction in the strand length when strip specimens were cut which reduced the lap lengths of the adhesive bond between strands. It was suggested that large-panel test should be used when developing design properties for structural panels.

For DMDF, a fiber-based material, which is an almost isotropic material and more uniform than DOSB, the difference between panel and strip bending test E_x values is small. The

difference between E_x and E_y by strip bending test is likely caused by a shorter span-to-depth of the strips along the width direction (18.3 for strips in the length direction and 12.8 for strips in the width direction). The smaller span-to-depth ratio and transverse shear modulus of the material are the reasons for the smaller E_x and E_y values of DMDF panel and strip specimens than the corresponding MDF specimens. It can be concluded that static panel test results are closer to dynamic test results than strip bending test results.

4.6 Conclusions

Through this study it has been shown that different accuracy levels are achieved with the three modal testing approaches, which incorporate different boundary conditions and calculation procedures. The influences of different aspects on accuracy have been also discussed. Modal test methods can be an option for measuring elastic constants of engineered wood-based panels due to its non-destructive nature and fast testing time. For orthotropic wood-based panel products, modal testing is recommended as it can account for the influence of coupling between elastic constants and is less tedious to conduct compared with static testing approaches. The elastic constants obtained are the general properties of the panel products, which are comparable to the static test of the whole panel. It is recommended for property evaluation of panel products, especially those intended for structural application.

All three BCs with corresponding calculation methods can be applied in the laboratory environment. FFFF is the easiest BC to be replicated in a testing environment and can be

applied for panels of small to moderate dimensions, but advanced forward problem solution such as FEM is needed. Simple frequency solutions can give an appropriate initial guess of elastic constants. SFFF is not recommended for large and thick panels as the support condition is practically unstable which requires some efforts in restraining the specimen in a vertical position. SFSF BC with the proposed calculation method shows great potential for laboratory and on-line application, especially for massive panels with large dimensions. Proper selection of BC and corresponding calculation method is important for characterizing the material of interest.

Acknowledgements

References

ABAQUS. (2013). *ABAQUS version 6.13 Documentation*. Providence, RI, USA: Dassault Systèmes Simulia Corp.

ASTM International. (2011). *ASTM D3043-00 Standard Test Methods for Structural Panels in Flexure*. Retrieved from https://doi.org/10.1520/D3043-00R11

ASTM International. (2016). *ASTM D3044-16 Standard Test Method for Shear Modulus of Wood-Based Structural Panels*. Retrieved from https://doi.org/10.1520/D3044-16

Ayorinde, E. O. (1995). On the sensitivity of derived elastic constants to the utilized modes in the vibration testing of composite plates. In W. Ng (Ed.), *ASME International Mechanical Engineering Congress and Exposition* (pp. 55–64). San Francisco: ASME.

Bos, F., and Casagrande, S. B. (2003). On-line non-destructive evaluation and control of wood-based panels by vibration analysis. *Journal of Sound and Vibration*, *268*(2), 403–412.

Brancheriau, L., and Baillères, H. (2002). Natural vibration analysis of clear wooden beams: a theoretical review. *Wood Science and Technology*, *268*(2), 403–412.

Carfagni, M., and Mannucci, M. (1996). A simplified dynamic method based on experimental modal analysis for estimating the in-plane elastic properties of solid wood panels. In J. L. Sandoz (Ed.), *International symposium on nondestructive testing of wood* (pp. 247–258). Lausanne: Presses polytechniques et universitaires romandes.

Chen, S., Du, C., and Wellwood, R. (2008). Analysis of strand characteristics and alignment of commercial OSB panels. *Forest Products Journal*, *58*(6), 94–98.

124

Chen, S., Liu, X., Fang, L., and Wellwood, R. (2010). Digital X-ray analysis of density distribution characteristics of wood-based panels. *Wood Science and Technology*, *44*(1), 85–93.

Coppens, H. (1988). Quality control of particleboards by means of their oscillation behavior. In *FESYP Technical Conference* (pp. 143–165). Munich.

Ganev, S., Gendron, G., Cloutier, A., and Beauregard, R. (2005). Mechanical properties of MDF as a function of density and moisture content. *Wood and Fiber Science*, *37*(2), 314–326.

Gsell, D., Feltrin, G., Schubert, S., … Motavalli, M. (2007). Cross-Laminated Timber Plates: Evaluation and Verification of Homogenized Elastic Properties. *Journal of Structural Engineering*, *133*(1), 132–138.

Gülzow, A. (2008). *Zerstörungsfreie Bestimmung der Biegesteifigkeiten, von Brettsperrholzplatten*. ETH Zürich.

Hearmon, R. F. S. (1946). The fundamental frequency of vibration of rectangular wood and plywood plates. *Proceedings of the Physical Society*, *58*(1), 78–92.

Kim, C. S., and Dickinson, S. M. (1985). Improved approximate expressions for the natural frequencies of isotropic and orthotropic rectangular plates. *Journal of Sound and Vibration*, *103*(1), 142–149.

Larsson, D. (1996). Stiffness characterization of wood based panels by modal testing. In J. Sandoz (Ed.), *International symposium on nondestructive testing of wood* (pp. 237–246). Lausanne: Presses polytechniques et universitaires romandes.

Larsson, D. (1997). Using modal analysis for estimation of anisotropic material constants. *Journal of Engineering Mechanics*, *222–229*(123), 3.

Leissa, A. W. (1969). Anisotropic Plates. In A. W. Lesissa (Ed.), *Vibration of plates* (pp. 250–260). Washington D. C.: National Aeronautics Space Administration.

Martínez, M. P., Poletti, P., and Espert, L. G. (2011). Vibration Testing for the Evaluation of the Effects of Moisture Content on the In-Plane Elastic Constants of Wood Used in Musical Instruments. In C. M. A. Vasques & J. Dias Rodrigues (Eds.), *Vibration and Structural Acoustics Analysis* (pp. 21–57). Springer Netherlands.

McNatt, J. D. (1984). Static bending properties of structural wood-base panels: large-panel versus small-specimen tests. *Forest Products Journal*, *34*(4), 50–54.

Nakao, T., and Okano, T. (1987). Evaluation of modulus of rigidity by dynamic plate shear testing. *Wood and Fiber Science*, *19*(4), 332–338.

Reddy, J. N. (1984). A simple higher-order theory for laminated composite plates. *Journal of Applied Mechanics*, *51*(4), 745–752.

Schulte, M., Frühwald, A., and Bröker, F. W. (1996). Non-destructive testing of panel products by vibration technique. In J. Sandoz (Ed.), *International symposium on nondestructive testing of wood* (pp. 259–268). Lausanne: Presses polytechniques et universitaires romandes.

Sobue, N., and Katoh, A. (1992). Simultaneous determination of orthotropic elastic constants of standard full-size plywoods by vibration method. *Mokuzai Gakkaishi*, *38*(10), 895–902.

Sobue, N., and Kitazumi, M. (1991). Identification of power spectrum peaks of vibrating completely-free wood plates and moduli of elasticity measurements. *Mokuzai Gakkaishi*, *37*(1), 9–15.

Thomas, W. H. (2003). Poisson's ratios of an oriented strand board. *Wood Science and Technology*, *37*(3), 259–268.

Yoshihara, H., and Sawamura, Y. (2006). Measurement of the shear modulus of wood by the square-plate twist method. *Holzforschung*, *60*(5), 543–548.

Zhou, J., and Chui, Y. H. (2014). Efficient measurement of elastic constants of cross laminated timber using modal testing. In A. Salenikovich (Ed.), *World Conference on Timber Engineering*. Quebec City.

Zhou, J., Chui, Y. H., Gong, M., and Hu, L. (2016). Simultaneous measurement of elastic constants of full-size engineered wood-based panels by modal testing. *Holzforschung*, *70*(7), 673–682.

CHAPTER 5 ELASTIC PROPERTIES OF FULL-SIZE MASS TIMBER PANELS: CHARACTERIZATION USING MODAL TESTING AND COMPARISON WITH MODEL PREDICTIONS

Abstract: Mass timber panel products are leading the evolution of wood construction throughout the world. In-plane elastic properties of mass timber panels are critical in serviceability design, especially when two-dimensional mechanical behaviour is considered. In this study, the moduli of elasticity (MOE) in major and minor strength directions (E_x and E_y), and in-plane shear modulus (G_{xy}) of 51 industrial size cross laminated timber (CLT) panels, 4 multi-ply solid wood panels (MSWP) were measured by a modal testing method. It was found that the modal testing method was capable of characterizing the elastic constants of mass timber panels with at least 90% agreement with the results via conventional static tests. The modal test measured values were used to examine the effective stiffness prediction models of CLT and MSWP, including k-Method, Gamma Method and Shear Analogy Method. The k-Method could be used for predicting E_x and E_y values of full-size CLT and MSWP panels with a large length/width to thickness ratio. G_{xy} could not be well predicted by k-Method, which is greatly affected by edge bonding and gaps between laminas. The Gamma Method and Shear Analogy Method could account for the effect of transverse shear to different extents in the prediction of apparent E_x and showed close results with a large length to thickness ratio. However, the effect of transverse shear on apparent E_y could not be properly accounted for by the Shear Analogy Method for CLT panels with typical width between 1 to 3 meters.

5. 1 Introduction

With the advent of mass timber panels, the trend of mass timber construction is spreading throughout the world in recent years. Mass timber construction is a category of framing styles using heavy timber products including cross laminated timber (CLT), nailed laminated timber (NLT), structural composite lumber (SCL) or glued-laminated timber (GLT) panels. Panel-type products such as CLT, NLT, SCL and GLT are example of mass timber panels. Due to the outstanding machinability of wood, mass timber panels intended for floor, wall and roof construction could be prefabricated with precise dimensions and openings in a factory, thereby allowing for a faster construction process and minimal construction waste. Of all the mass timber panels, CLT is currently the most popular product. It is composed of crosswise layers of structural lumber laminates usually glued together by a structural adhesive (Brandner et al., 2016). The edge surfaces of adjacent lumber in one layer can be bonded, known as edge bonding, or left without bonding or even with very small gaps. CLT has been used or proposed to be used in several tall wood buildings such as the 14-storey TREET project in Norway (Malo et al., 2016) and the 18-storey Brock Commons building in Canada. A similar product to CLT is called the multi-ply (typically three- or five-ply) solid wood panel (MSWP) (Blass and Fellmoser, 2004), which is made of smaller lumber laminas with edge bonding. Besides lumber-based panels, structural composite lumber (SCL), including laminated strand lumber (LSL), oriented

strand lumber (OSL), parallel strand lumber (PSL), and laminated veneer lumber (LVL), is an another important series of mass timber panels, which are created by layering dried and graded wood strands, flakes or veneers with moisture resistant adhesive into a block of material known as a billet. Mass timber panels are engineered to have high strength and dimensional stability, which can be used as an alternative to concrete, masonry and steel in many building types and make wood skyscrapers possible.

In structural design, serviceability limit states, including deflection and vibration, are important considerations. It is known that the design of structural assemblies built with mass timber panels can be governed by serviceability limit states. Serviceability limit states design checks require elastic properties as input parameters. Therefore, it is necessary to accurately characterize the elastic properties of mass timber panels for their structural applications. Even though different prediction models were proposed for calculation of effective stiffness of, MSWP (Blass and Fellmoser, 2004), CLT (Sylvain and Marjan, 2011), LVL and LSL (Moses et al., 2003) panels, verification is still required using test measurements. In addition, elastic properties of each full-size panel should be measured for quality control purposes as the large panels serve as a whole wall, floor or roof component in a building. Conventional static test methods according to relevant standards (APA, 2012; CEN, 2015) can provide fundamental mechanical properties of different mass timber panels, usually by testing small specimens cutting from the full-size panels. These static tests are tedious and costly, and the results are not necessarily reflective of those of the full-size panels. Steiger et al. (2012) has recommended that bending test of CLT should be conducted with panel or strip specimens with a large width. Moreover, not all the elastic

constants can be tested according to relevant standard test methods. For instance, there is currently no standard static method for measuring the in-plane shear properties of a full-size mass timber panel. Brandner et al. (2015) and Andreolli et al. (2014) have proposed shear test methods based on compressive loading to study the in-plane shear properties of CLT with different panel characteristics. They both found that edge bonding and gaps affected the in-plane shear modulus while layup had a minor effect on in-plane shear modulus. However, the shear stress field present in the test specimens of these two methods deviated from the assumptions that underpin the calculation models for shear modulus in both methods.

An alternative to static tests for characterizing the elastic constants of mass timber panels is modal testing based on the transverse vibration of an orthotropic plate. Gsell et al. (2007) applied experimental modal analysis to measure natural frequencies and mode shapes of one rectangular CLT specimen with completely free (FFFF) boundary condition. Three shear moduli and the two in-plane MOE were determined by minimizing the difference between measured and estimated natural frequencies based on the least-squares method. Gülzow (2008) further studied the vibration-based testing method proposed by Gsell et al. (2007) to evaluate the elastic properties of CLT panels of up to 4 meters in length and 2.5 meters in width. Recently, a non-destructive method based on modal testing has been proposed by Zhou et al. (2016) for measuring in-plane elastic constants of full-size CLT panels and other wood-based composites. The support condition adopted for the method was two opposite edges simply supported and the other two free (SFSF). The modal test results agreed well with those by static tests. Using this method, MOE in both major and

minor strength directions (E_x and E_y) and in-plane shear modulus (G_{xy}) of plate-like specimen can be obtained.

This study was aimed to further evaluate the method proposed by Zhou et al. (2016) by applying it for measuring the elastic constants (E_x, E_y and G_{xy}) of full-size CLT and MSWP panels in a mill environment, with a special focus on CLT. In addition to provide the elastic constants of mass timber panels, different effective stiffness prediction models of CLT and MSWP were also examined by comparing the model predictions with the measured elastic constants. The effect of layup and edge bonding on elastic properties was investigated for CLT panels produced by a few producers.

5.2 Materials and Methods

5.2.1 Materials

Three series of CLT panels (namely CLT-A, CLT-B and CLT-C) with different dimensions and layups from three producers as well as one series of MSWP panels were tested in this study. The layup, dimensions and number of specimens of all specimens are given in Table 5.1. All specimens were labelled in terms of "Producer (A/B/C/D)-number of layers (#s)-total thickness (in mm)", and all the specimens had strong axis parallel-to-grain direction of the outmost top and bottom layers. CLT-A and CLT-B panels were made of European Norway spruce (*Picea abies*) of visual grade C24 with a mean density of 420 kg/m³. CLT-A panels were fabricated without edge bonding nor obvious gaps, while laminas in CLT-B panels were edge-bonded as shown in Figure 1. CLT-C panels were made of Canadian

black spruce (*Picea mariana*) of machine stress rated grade 1950f-1.7E in parallel layers and visual grade No. 3 in perpendicular layers with a mean density of 520 kg/m^3. All CLT-C panel specimens had no edge bonding but non-uniform gaps throughout the panel as shown in Figure 5.1. The width of the laminas for the three series of CLT panels was 180 mm, 105 mm and 89 mm, respectively. Most of the panels had orthogonal adjacent layers except groups of B-7s-220 and B-8s-300. Groups B-7s-220 and B-8s-300 had double longitudinal layers in outmost two top and bottom layers and B-8s-300 also had additional double longitudinal layer in core. This kind of CLT panel is typically used for long-span floor system and can be regarded as five-layer CLT panels in the theoretical calculation of elastic constants. Another four three-layer MSWP panels produced with the similar raw material of CLT-A and CLT-B panels and a lamina width of 35 mm were tested as well. According to producers' technical approval documents and assumptions in reference standards (APA, 2012; CEN, 2009), the elastic constants of the laminas are summarized in Table 5.2, which were used to calculate the effective stiffness of CLT and MSWP panels.

CLT with edge bonding   CLT without edge bonding   CLT with gaps   MSWP
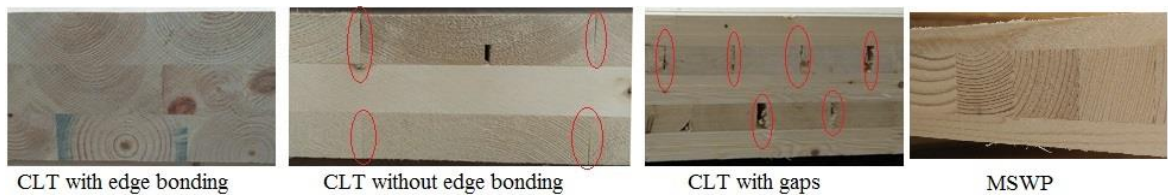
Figure 5.1 Cross sections of mass timber panels with/ without edge bonding and with gaps

Table 5.1 Mass timber panel information

Material	Panel Type	Layup (mm)	Length (m)×width (m) with No. of specimens in parentheses	Length-to-depth ratio[*]
CLT-A	A-3s-120	**40**/40/**40**	6.50×0.90 (6)	54
CLT-B	B-3s-100	**30**/40/**30**	10.55×2.30 (1)	105
	B-3s-120	**40**/40/**40**	10.35×3.00 (1)	86
	B-5s-100	**20**/20/**20**/20/**20**	11.05×3.00 (2), 12.65×2.80 (3), 11.05×2.80 (1), 12.65×2.50 (1)	110, 126
	B-5s-120	**30**/20/**20**/20/**30**	13.25×2.30 (1)	110
	B-5s-150	**40**/20/**30**/20/**40**	9.40×2.44 (1)	62
	B-5s-160	**40**/20/**40**/20/**40**	9.35×2.50 (1), 10.15×2.30 (1), 10.35×2.80 (1), 8.05×3.00 (1)	50, 58, 63, 64
	B-5s-200	**40**/40/**40**/40/**40**	13.75×2.50 (1)	68
	B-7s-220	**30**/30/**30**/40/**30**/30/**30**	12.00×2.95 (1), 5.57×1.98 (1)	25, 54
	B-8s-300	**40**/40/30/**40**/**40**/30/**40**/40	7.40×2.50 (1)	24
CLT-C	C-3s-78	**26**/27/**26**	4.86×2.48 (1)	62
	C-3s-97	**35**/27/**35**	5.02×2.48 (1)	51
	C-3s-105	**35**/35/**35**	[2.95 (1), 3.21 (1), 5.45 (1), 6.45 (1), 6.85 (1), 9.95 (1), 11.10 (1)] ×2.48	28, 30, 51, 61, 65, 94, 105
	C-5s-131	**26**/27/**26**/27/**26**	4.87×1.02 (3)	37
	C-5s-175	**35**/35/**35**/35/**35**	[15.98 (1), 16.40 (1), 17.70 (9)] ×2.48, 4.00 × 1.57 (1)	22, 91, 93, 101
	C-7s-220	**35**/27/**35**/27/**35**/27/**35**	8.30×1.00 (3)	37
MSWP	D-3s-40	**12.5**/15/**12.5**	6.02×2.13 (3)	150
	D-3s-55	**12.5**/30/**12.5**	4.00×2.13 (1)	72

[*]: Values were rounded to the single digits.

Table 5.2 Elastic properties of laminas in CLT and MSWP panels assumed in design

calculations

Material	Strength direction	E_0 (MPa)	E_{90} (MPa)	G_{090} (MPa)	G_r (MPa)
CLT-A & B	Major & Minor	11000	370	690	69
CLT-C	Major	11700	390	731	73
	Minor	9000	300	562	56
MSWP	Major & Minor	11500	383	600	90

Note: E_0 and E_{90} are the MOE of lumber parallel to grain and perpendicular to grain, respectively. G_{090} is the mean shear modulus and G_r is the rolling shear modulus.

5.2.2 Methods

A simplified modal test procedure and an algorithm for calculating the elastic constants (E_x, E_y and G_{xy}) of an engineered wood-based panel were presented in (Zhou et al., 2016). The dimensions and mass of each panel should be measured before modal tests. The impact vibration tests were conducted on the specimen under SFSF boundary condition as shown in Figure 5.2 & 5.3, where the test specimen was supported on two wooden blocks. The impact and acceleration time signals were recorded by a data acquisition device (LDS Dactron, Brüel & Kjær) and the frequency response function (FRF) was calculated from the time signals by a data analysis software (RT Pro 6.33, Brüel & Kjær). The sensitive frequencies, f_{20}, f_{21} and f_{22}, were identified from frequency spectra at three selected impact locations based on a frequency identification method presented in (Zhou et al., 2016), which took the advantages of the sign characteristics, e.g. positive, zero and negative, of

imaginary values as shown in Figure 5.4. f_{20}, f_{21} and f_{22} are the natural frequencies of the first bending mode in major strength direction, the first torsional mode and the first bending mode in the minor strength direction, respectively. With an iterative algorithm and the input information of dimension, density and frequency, the elastic constants of the test specimens can be determined by minimizing the differences between experimental and calculated frequencies.
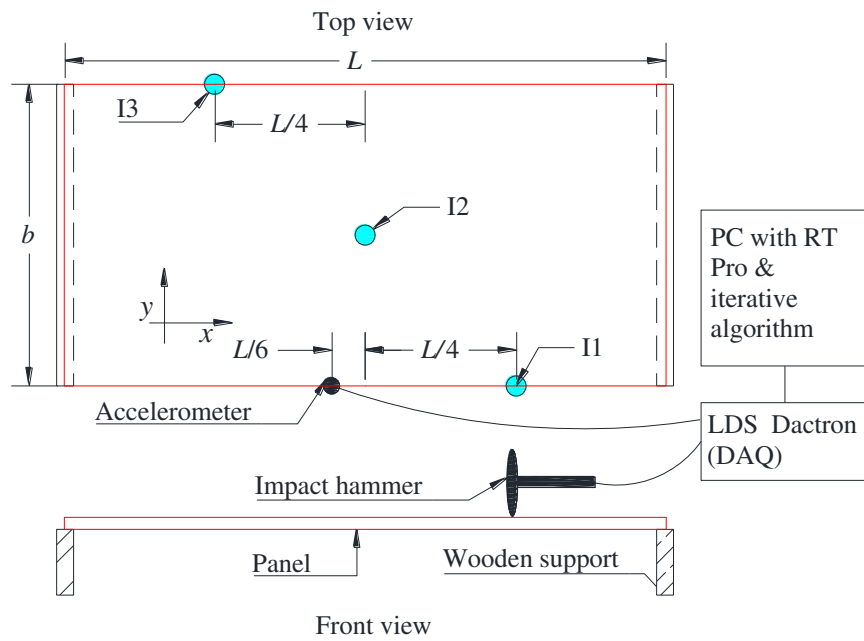
Figure 5.2 Schematic drawing of modal test setup with selected impact locations (I1, I2, I3)

Figure 5.3 Support condition of a CLT panel
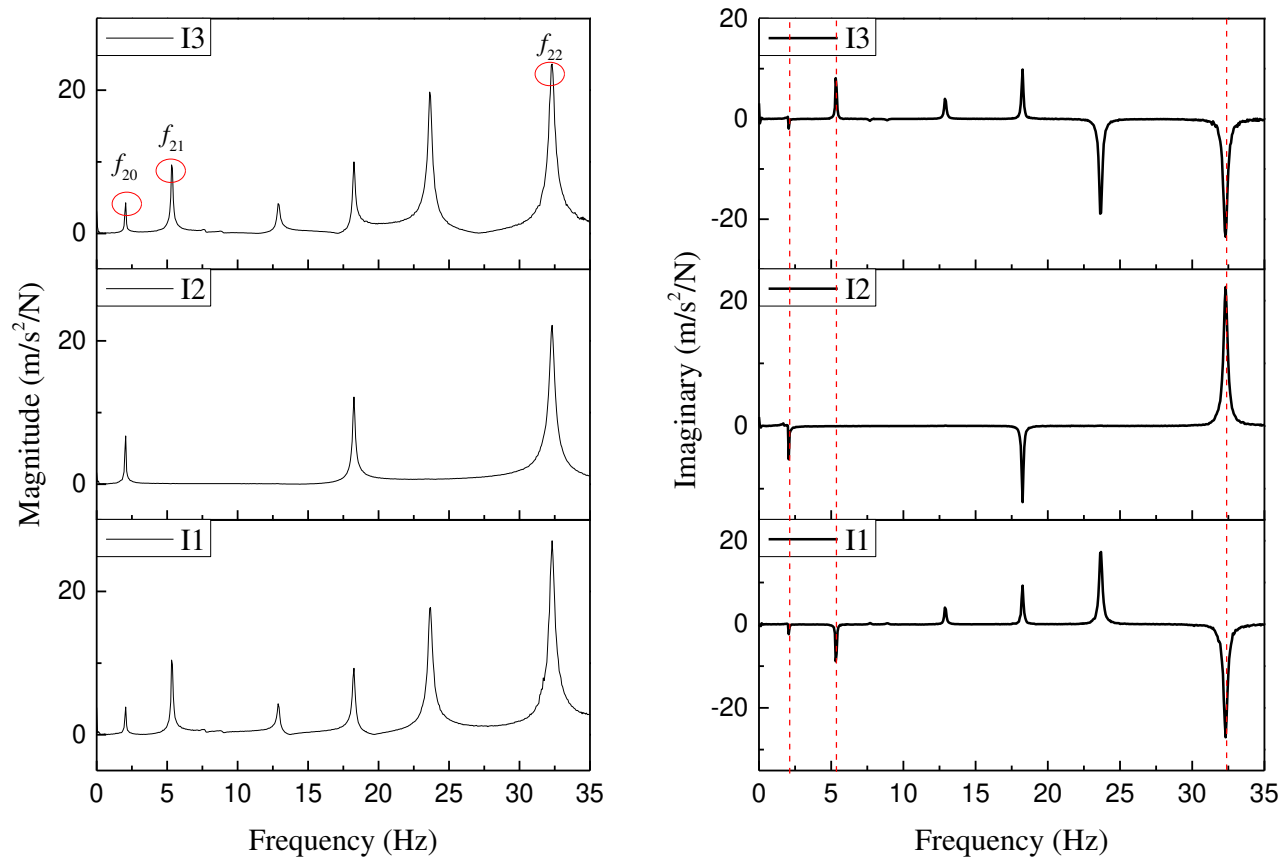
Figure 5.4 Typical frequency spectra from three selected impact locations of a CLT panel

138

Besides modal tests, each of the CLT-A panel specimen was tested under four-point bending tests in the major strength direction to obtain E_x value according to section 9 in EN 408 (CEN, 2004) with a test setup shown in Figure 5. The span between two supports, l, of the tested specimens was 6000 mm. The static E values can be calculated using the following expression:

$$E = \frac{(\frac{1}{3})(\frac{5l}{18})^2}{16I} \times \frac{\Delta F}{\Delta w} \qquad (5.1)$$

where I is the second moment of area of the specimen, $\frac{\Delta F}{\Delta w}$ is the slope of the load-deflection curve in the elastic range.

For MSWP panels of groups D-3s-40 and D-3s-55, six beam specimens with a width of 300 mm and a length of 31 times its thickness from each strength directions were cut from each groups for four-point bending tests using the same method. The span of each specimen at test was 30 times its thickness. The static E_x and E_y values were obtained for both groups D-3s-40 and D-3s-55 using Eq. 5.1.
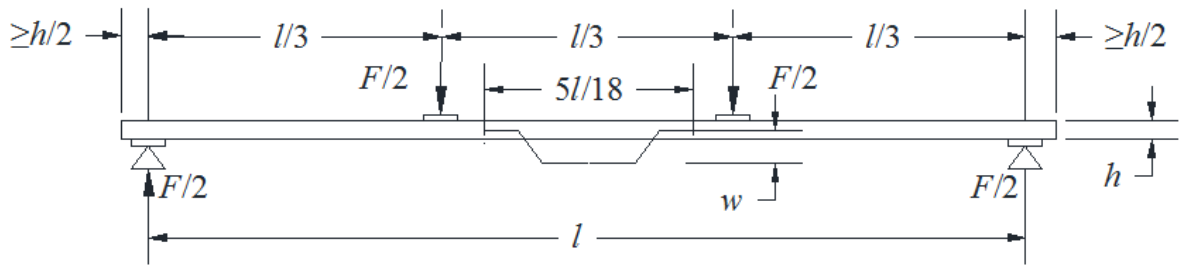
Figure 5.5 Schematic drawing of four-point bending test setup

5.2.3 Modal Tests in Laboratories and Mills

All CLT-A and MSWP panels were tested at the laboratory of Graz University of Technology (TUGraz) in Austria. The average densities of CLT-A panels and MSWP panels were measured to be 433 and 441 kg/m^3, with a coefficient of variation (COV) of 1.5% and 0.6%, respectively. All the CLT panels of groups C-5s-131 and C-7s-220 were tested in the same way at the laboratory of the University of New Brunswick (UNB) in Canada. The average density of the CLT panels was measured to be 522 kg/m^3 with a COV of 2.0%. Besides the panels tested at two laboratories, the rest of the CLT panels were tested off the production line in the mills before CNC machine processing. It should be noted that all mill tests were conducted in condition that the manufactures' production couldn't be interrupted. Only panels were not urgent for CNC processing can be tested. Due to these restrictions, the panels were tested in the same way as in the laboratory without weighing. Average densities from previous measurements of the same manufacturers' products in laboratories were used for calculation, which was reasonable considering the low COVs of measured densities of CLT panels in laboratories.

5.3 Prediction Models

One of the greatest advantages of engineered wood products is that they have highly predictable mechanical properties. Based on the elastic properties of raw materials used, layups and orientations of elements, it is possible to predict the elastic properties of the finished composite products (Fang et al., 2015; Franzoni et al., 2016; Gliniorz et al., 2002). Since CLT and MSWP have similar structure and were both invented in the same area in

Europe, the elastic property prediction models can be applied to both products. Even though CLT and MSWP panels are designed to act like two-dimensional plates, their design under transverse load is currently based on beam theory (Stürzenbecher et al., 2010). The most straight-forward prediction model is the so-called *k*-Method based on the "Composite Theory" (Bodig and Jayne, 1982). The other two commonly used models are Gamma Method (GM) based on the "Mechanically Jointed Beams Theory" adopted from (CEN, 2006) and Shear Analogy Method (SAM) (Kreuzinger, 1999). Both GM and SAM account for transverse shear deformation to different extents. Details of these methods can be found in (Sylvain and Marjan, 2011). A summary of the three methods is presented here with cross section information shown in Figure 5.6.

Figure 5.6 Cross section of a five-layer CLT (*m* is the total number of layers, *i*=1, 2, …*m*)

5.3.1 *k*-Method

According to the assumptions in (Bodig and Jayne, 1982), the following equations can be used for calculating the effective global elastic constants of CLT and MSWP panels. First, the composite factors should be calculated.

$$k_1 = 1 - \left(1 - \frac{E_{90,\perp}}{E_{0,//}}\right) \cdot \frac{h_{m-2}^3 - h_{m-4}^3 + L \pm h_1^3}{h_{tot}^3} \tag{5.2}$$

$$k_2 = \frac{E_{90,//}}{E_{0,\perp}} + \left(1 - \frac{E_{90,//}}{E_{0,\perp}}\right) \cdot \frac{h_{m-2}^3 - h_{m-4}^3 + L \pm h_1^3}{h_{tot}^3} \tag{5.3}$$

where k_1 and k_2 are the composite factors for major and minor strength directions under transverse load, respectively. $E_{0,//}$ and $E_{90,//}$, $E_{0,\perp}$ and $E_{90,\perp}$ are the MOE of the lumber parallel to grain and perpendicular to grain in longitudinal and cross layers in CLT/ MSWP, respectively. For CLT of series A and B and MSWP, in which the laminas of all layers are the same, E_{90}/E_0 equals to 30 based on the assumption in (APA, 2012; CEN, 2009). m is the total number of layers and h_i is the thickness of the ith layer, h_{tot} is the total thickness of the CLT/ MSWP panel.

Thus, the effective MOE ($E_{x,eff,k}$ and $E_{y,eff,k}$) and G ($G_{xy,eff,k}$) based on *k*-Method can be computed as,

$$E_{x,eff,k} = E_{0,//} \cdot k_1 \tag{5.4}$$

$$E_{y,eff,k} = E_{0,\perp} \cdot k_2 \tag{5.5}$$

$$G_{xy,eff,k} = \frac{G_{090,//} \cdot \sum\limits_{i=1,3...}^{(m+1)/2} h_i + G_{090,\perp} \cdot \sum\limits_{i=2,4...}^{(m-1)/2} h_i}{h_{tot}}$$ (5.6)

where $G_{090,//}$ and $G_{090,\perp}$ are the shear moduli of the laminas in parallel and perpendicular layers in CLT, respectively. For CLT-A and B and MSWP, in which the laminas of all layers are the same, $G_{090,//}$ equals to $G_{090,\perp}$. $G_{xy,eff,k}$ is called the weighted mean value of all layers based on the thickness of each layer and it is recommended for CLT with edge bonding and MSWP panels. A further study (Bogensperger et al., 2010) showed the in-plane shear modulus of CLT without edge bonding should be estimated by

$$G_{xy,CLT,est} = \frac{G_{xy,eff,k}}{1 + 6 \times p \times \left(\dfrac{h_{l,mean}}{w_l}\right)^{1.21}}$$ (5.7)

where w_l is the width of a lamina, $h_{l,mean} = \dfrac{h_{tot}}{m}$, $p = (0.53, 0.43, 0.39)$ for $m = (3, 5, 7)$.

5.3.2 Gamma Method

Gamma method (GM) includes the effect of transverse shear deformation by treating the cross layers as 'fasteners' that connect the parallel layers. The effective bending stiffness including transverse shear effect can be expressed as,

$$EI_{eff,GM} = \sum\limits_{j=1}^{(m+1)/2} \left(E_j I_j + \gamma_j E_j A_j a_j^2 \right)$$ (5.8)

where E_j is MOE of the jth layer in the strength direction considered, $j=2i-1$, I_j is the moment of inertia of the jth layer, a_j is the distance between the center line of the jth layer and the center line for a symmetric CLT/ MSWP, and γ_j is the coefficient related to rolling shear modulus and is calculated using Eq. 5.8.

$$\gamma_j = \left\{ 1 + \left(\pi^2 \cdot \frac{E_j \cdot A_j}{L^2} \cdot \frac{h_{j+1}}{G_{r,j+1} \cdot b} \right) \right\} \qquad (5.9)$$

where L is the span or length of a panel and h_{j+1} is the thickness. $G_{r,j+1}$ is the rolling shear modulus of the $(j+1)^{\text{th}}$ cross layer next to the jth layer ($j=1, 3$), and for $j=2$, $\gamma_2=1$. Therefore, the apparent MOE based on gamma method can be formulated as

$$E_{app,GM} = EI_{eff,GM} / I_{gross} \qquad (5.10)$$

where $I_{gross} = bh_{tot}^3 / 12$, b is the width of the panel, which is often treated as 1 meter for calculation.

GM cannot give proper effective stiffness in the minor strength direction by simply applying the same mechanism that treats the cross layer as a 'fastener'. The lumbers in the cross layer are the main contribution to its stiffness in the minor strength direction. If the cross layer was treated as a 'fastener' that connects the parallel layers with MOE perpendicular to grain, the effective stiffness of CLT/MSWP panels would be governed by the MOE perpendicular to grain of the parallel layers, which will result in unreasonable apparent stiffness of CLT/MSWP panels in the minor strength direction. Therefore, GM is only used for predicting the effective bending stiffness of CLT/ MSWP in the major strength direction.

5.3.3 Shear Analogy Method

Shear analogy (SA) method includes the transverse shear effect and has been proven to be the best model for calculating bending stiffness of CLT/ MSWP (Fellmoser and Blass, 2004; Sylvain and Marjan, 2011). First, the effective bending stiffness is defined as,

$$EI_{eff,SA} = \sum_{i=1}^{m} E_i \cdot b_i \cdot \frac{h_i^3}{12} + \sum_{i=1}^{m} E_i \cdot A_i \cdot z_i^2 \tag{5.11}$$

where E_i is the MOE parallel to major or minor strength direction of the ith layer depending on the strength direction considered, b_i is the width of the ith layer and equals to 1 m for CLT/ MSWP, h_i is the height of the ith layer and A_i is the sectional area of the ith layer, z_i is the distance between the center of the ith layer and the neutral axis of CLT/ MSWP, which can be computed by,

$$z_i = z - Y_i \tag{5.12}$$

where z is the location of the neutral axis of cross section which can be determined by Eq. 5.13, Y_i is the distance from the center of the ith layer to the outmost surface layer of CLT/ MSWP. z can be calculated by

$$z = \frac{\sum_{i=1}^{n} (E_i A_i) \cdot Y_i}{\sum_{i=1}^{n} E_i A_i} \tag{5.13}$$

Second, the effective shear stiffness $GA_{eff,SA}$ can be calculated as,

$$GA_{eff,SA} = a^2 \cdot \left[\frac{h_1}{2 \cdot G_1 \cdot b_1} + \sum_{i=2}^{m-1} \frac{h_i}{G_i \cdot b_i} + \frac{h_m}{2 \cdot G_m \cdot b_m} \right]^{-1} \tag{5.14}$$

where G_i is the shear modulus of the ith layer, a is the distance between the centroid of the surface and bottom layers.

The effective bending stiffness will be used together with effective shear stiffness for calculation of deflection of CLT under out-of-plane loading. By applying SAM, apparent

145

MOE ($E_{app,SA}$) values of a CLT/ MSWP beam under center point loading can be obtained. The apparent bending stiffness, $EI_{app,SA}$, is introduced for different boundary conditions,

$$EI_{app,SA} = \frac{EI_{eff,SA}}{1 + \dfrac{K_s EI_{eff,SA}}{GA_{eff,SA} L^2}} \quad (5.15)$$

where K_s is 14.4 for a concentrated load at mid-span with pinned supports at the two ends (Sylvain and Marjan, 2011), L is the span of the specimen.

Eq. 5.14 can be simplified to,

$$E_{app,SA} = \alpha / \left(1 + \frac{\beta}{L^2}\right) \quad (5.16)$$

where $\alpha = EI_{eff,SA} / I_{gross}$, which is, in fact, equal to $E_{eff,k}$, $\beta = K_s EI_{eff,SA} / GA_{eff,SA}$.

$E_{app,SA}$ will approach α with increasing L, and β is the parameter that quantifies the effect of effective shear stiffness through the shear factor, K_s, and E/G ratio.

5.4 Results and Discussion

5.4.1 Summary of the Elastic Constants Measured

The mean values of elastic constants of all CLT and MSWP panels measured by modal testing are listed in Table 5.3. From Table 5.2, it is known that the elastic properties of the laminas for all three series of CLT panels are similar. Generally, the layup is the most important factor for the global E_x and E_y of CLT and MSWP panels, while G_{xy} is not greatly affected by layup, especially for CLT-B panels with edge bonding and MSWP panels. The ratio between the total thickness of parallel-to-grain layers to the total thickness of cross layers is the dominant factor governing the values of E_x and E_y. A higher portion of parallel-

146

to-grain layer thickness in one strength direction will increase the global MOE in that direction. For instance, B-3s-100 vs B-5s-100 and B-3s-120 vs B-5s-120, with the same total thickness for each paired CLT groups, CLT panels with five layers have higher E_y value than those with three layers, and a lower E_x value correspondingly. Also, it can be found that the COVs of E_x, E_y and G_{xy} of panels of C-5s-175 panels are 2.6%, 8.1% and 5.8%, respectively, while the corresponding COVs for C-3s-105 panels are 4.2%, 12.0% and 27.6% respectively. This suggests that the variation of measured properties of the panels decreases with the increase of the number of layers.

The G_{xy} values fall into the range between 248 and 701 MPa for all types of CLT panels measured in this study. The G_{xy} values of three-layer CLT-A panels, with a mean of 411 MPa (range 381 - 433 MPa), fall in the range of G_{xy} values listed in Table 5.4 (Dröscher, 2014) of three-layer CLT made of grade C24 spruce wood without edge bonding and gaps. In the case of CLT-B panels with edge bonding, the average G_{xy} of 672 MPa for three-layer CLT-B panels (B-3s-100 & B-3s-120) is close to the G_{xy} value (637 MPa) reported by Dröscher (Dröscher, 2014) for three-layer CLT with edge bonding. Similar to three-layer CLT-B, the average G_{xy} values of MSWP panels are 721 MPa and 658 MPa for D-3s-40 and D-3s-55, respectively. It seems that the G_{xy} values of CLT-B and MSWP panels decease with the increase of layer and total thickness. Though there was a limited number of specimens (one or two) tested for some groups, the trend discovered agrees with what was reported in (Andreolli et al., 2014; Dröscher, 2014; Brandner et al., 2015), where the five-layer CLT panels possess a higher G_{xy} values than seven-layer CLT. Within the groups of five-layer CLT-B, thicker panels have similar or a slightly smaller G_{xy} values. For CLT-

C without edge bonding and with non-uniform gaps (0-10 mm), the average G_{xy} value of group C-3s-105 is 518 MPa (range 333 - 658 MPa) and the mean G_{xy} value of group C-5s-175 is 543 MPa (range 497 - 611 MPa). The mean G_{xy} value of group C-7s-220 is 338 MPa with two specimens tested. In (Dröscher, 2014; Brandner et al., 2015), the specimens were manufactured in the laboratory for a scientific study, the gaps or no gaps were very well controlled, while those CLT-C panels without edge bonding were produced in the factory without special care given to gaps. It can be concluded that the G_{xy} values of CLT-C are similar to those in (Dröscher, 2014; Brandner et al., 2015) without edge bonding. G_{xy} value increases slightly from three-layer to five-layer and then decreases with the number of layers as shown in Tables 5.3 and 5.4.

Table 5.3 Mean values of measured elastic constants and corresponding predicted values by three methods of all CLT and MSWP groups

Panel Type	Measured elastic constants (MPa)			Predicted elastic constants (MPa)						
				k-Method			GM	SAM		Eq. 5.7
	E_x	E_y	G_{xy}	$E_{x, eff, k}$	$E_{y, eff, k}$	$G_{xy, eff, k}$	$E_{x, app, GM}$	$E_{x, app, SA}$	$E_{y, app, SA}$	$G_{xy, CLT, est}$
A-3s-120	12173 (7.5%)[*]	511 (3.7%)	411 (4.9%)	10606	764	690	10041	10081	637/ 747[**]	455
B-3s-100	10761	1074	644	10320	1050	690	10134	10175	1023	
B-3s-120	10010	786	701	10606	764	690	10367	10393	747	
B-5s-100	8470 (3.6%)	2724 (3.0%)	620 (5.0%)	8789	2581	690	8679	8724	2481	
B-5s-120	9369	1611	593	9720	1650	690	9626	9631	1550	
B-5s-150	10556	1197	607	10005	1365	690	9837	9752	1259	/
B-5s-160	10242	1370	621	9837	1533	690	9689	9587	1402	
B-5s-200	8379	2459	564	8789	2581	690	8601	8596	2152	
B-7s-220	10200	1235	495	10066	1304	690	9849	9720	1171	
B-8s-300	10171	939	452	10121	1249	690	9478	8903	942	
C-3s-78	11174	1090	405	11245	734	674	10635	10692	726	392
C-3s-97	10341	277	248	11454	576	684	10708	10721	568	354
C-3s-105	10393 (7.1%)	711 (12.0%)	518 (27.6%)	11278	709	675	10741	10363	697	333
C-5s-131	9657	2293	542	9249	2241	662	8674	8418	1570/ 2135[**]	417
C-5s-175	9268 (2.6%)	2201 (8.1%)	543 (5.8%)	9329	2181	664	9195	9204	1937	362
C-7s-220	9873	2488	338	9007	2462	669	8708	8359	996/ 2331[**]	402
D-3s-40	10829	826	721	10914	970	600	10827	10860	966	/
D-3s-55	9220	2112	658	9696	2187	600	9365	9471	2163	

[*]: Values in the brackets refer to the COV if sample size is larger than 5. Only the results of CLT panels with a length to thickness ratio of more than 30 were averaged and presented for groups C-3s-105 and C-5s-175.

[**]: the values were calculated using an imaginary width of 3 meters to reveal the effect of width.

Table 5.4 In-plane shear modulus values of CLT panels reported in (Dröscher, 2014)

Layup (mm)	Edge bonding	G_{xy} (MPa)		
		min.	mean	max.
30/30/**30**	Yes	568	637	706
29/29/**29**	No	388	469	536
30/30/**30**	No[*]	273	311	341
17/32/**19**/32/**19**	No	462	515	589
28/30/**30**/30/**30**	No	485	524	599
40/19/**30**/19/**40**	No	423	449	482
31/19/**20**/19/**31**	No	464	532	613
40/19/**40**/19/**40**	No	357	432	516
30/30/**30**/30/**30**/30/**30**	No	416	469	501

[*]: With a gap of 6mm.

The comparison of dynamic and static E_x and/ or E_y values of selected mass timber panels is shown in Table 5.5. It can be seen that the measured dynamic E_x values of CLT-A panels are on average 4.6 % higher than those obtained by four-point bending tests. The differences between dynamic and static E_x and E_y values of D-3s-40, D-3s-55 panels are about 7.4 % and -2.0 %, -9.2 % and 0.5 %, respectively. The results further proved the accuracy of the proposed modal testing method.

Table 5.5 Mean elastic constant values of selected specimens by dynamic and static test methods

Panel Type	E_x (MPa)		E_y (MPa)	
	Dynamic	Static	Dynamic	Static
A-3s-120	12173 (7.5%)[*]	11633 (10.1%)	/	/
D-3s-40	11829	11012 (4.2%)	826	843 (8.5%)
D-3s-55	9220	10157 (5.5%)	2112	2113 (7.7%)

[*]: Values in the bracket refer to the coefficient of variance (COV) if the sample size is larger than 6.

5.4.2 Effect of Edge Bonding on Elastic Constants of CLT Panels

In current CLT product standards (APA, 2012; CEN, 2015), edge bonding is not required for CLT production. However, a few CLT producers have started to apply edge bonding for the reason of air-tightness, smoke resistance and better in-plane shear performance (Brandner, 2013). According to the results presented above, edge bonding has little effect on E_x, but it may affect E_y and certainly increases G_{xy}. For example, B-3s-120 with edge bonding has higher E_y and G_{xy} values than A-3s-120 without edge bonding, but both types have a same layup and similar lamina properties. With the same number of layers, the G_{xy} values of CLT-B panels are generally higher than those of CLT-A and CLT-C panels. This finding agrees well with that from other studies using static test methods (Andreolli et al., 2014; Dröscher, 2014; Brandner et al., 2015). Without edge bonding and with gaps, the COVs of the measured elastic constants values are high, such as 12.8% and 29.2% of E_y and G_{xy} values in group C-3s-105, whereas for group A-3s-120 without gaps, the

corresponding COVs are 3.7% and 4.9% of the measured E_y and G_{xy} values, respectively. CLT-B panels have even lower COVs of the measured elastic constants than those of CLT-A. Thus edge bonding can reduce the variation in CLT properties.

5.4.3 Modal Testing Results vs. Model Predictions

The above-described prediction models have been adopted for the structural design of CLT/ MSWP under transverse load, using lamina properties in design standards or technical approval documents. It should be noted that the actual properties of the laminas used in production may differ from the published design values, and there is currently no explicit requirement to measure lamina elastic properties in production of commercial CLT if the laminas are already visually or stress graded. Moreover, processing parameters, such as edge bonding, gaps and stress relief cuts, and workmanship will affect the global elastic constants of CLT/ MSWP panels. Therefore, online non-destructive quality control testing for full-size mass timber panels would be beneficial to ensure that commercial mass timber panels consistently meet their design specifications.

The measured elastic constants of each group of CLT and MSWP panels are compared with the predictions by the k-Method, which is capable of computing all three corresponding elastic constants. The predicted values are given in Table 5.3 and the differences to measured values ((Prediction-Test)/Test × 100%) are plotted in Figure 5.7. For most of the panels with a length-to-thickness ratio larger than 30, the measured mean E_x and E_y values agree well with corresponding values predicted by the k-Method, especially for CLT-B and MSWP panels. The predicted E_x can be up to 13% lower and

11% higher than the measured E_x, and the difference in value between predicted and measured E_y values can vary from -33% to 49% if group C-3s-97 is ignored, which had large gaps on top and bottom surface layers and cracks in the cross layer. It is thought that the large gaps caused exceptionally low E_y and G_{xy} values of group C-3s-97. Apart from E_y of groups A-3s-120, B-8s-300 and C-3s-78, for other groups of CLT panels with large length/width to thickness ratio, the k-Method predicts E_x and E_y with reasonable accuracy with a relative difference of less than 10% and 15%, respectively. It can be observed that edge bonding and the presence of gaps can affect the accuracy of k-Method in Figure 5.7, in which CLT-B and MSWP panels with edge bonding had better agreement with predicted E_x and E_y values than other groups without edge bonding. However, the k-Method is not capable of predicting G_{xy} of CLT panels with a reasonable accuracy, with only type CLT-B with three and five layers and MSWP panels show a difference of less than 20%. The other groups of CLT panels have much smaller measured G_{xy} values than predicted. It appears that neither the k-Method nor the static bending test method is capable of accounting for the effect of edge bonding and gaps. Bogensperger et al. (2010) have proposed a method of calculating the in-plane shear modulus of CLT that is capable of considering the effect of gap and thickness to width ratio of lamina. If that model was used, the differences between measured and predicted G_{xy} of the CLT groups without edge bonding are summarized in Figure 5.8. For CLT groups of A-3s-120, C-3s-78 and C-7s-220, the differences were less than 20%, which is similar to what was reported in (Brandner et al., 2015). However, for CLT groups of C-3s-105, C-5s-131 and C-5s-175, the G_{xy} values were up to 35% under-estimated compared with modal test measurements. The reason is thought to be the mean thickness to width ratios of laminas in these panels was about double

153

of those used for proposing and verifying the formula in (Bogensperger et al., 2010; Brandner et al., 2015). The influence of thickness to width ratio of laminas on the G_{xy} values was over-estimated in (Bogensperger et al., 2010) after a certain ratio value. Therefore, plate modal test method applied to full-size CLT panels has shown promise to be adopted as the most appropriate test method to characterize G_{xy}.
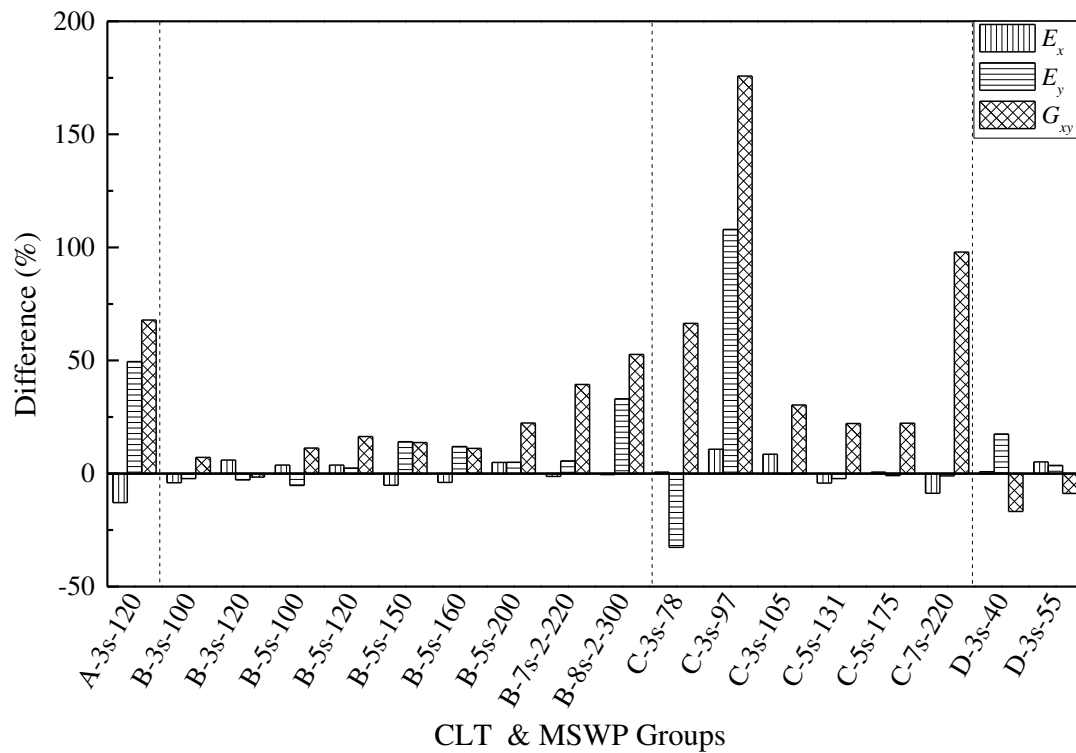
Figure 5.7 Difference between values of each elastic constant of CLT and MSWP panels from *k*-Method calculation and modal testing
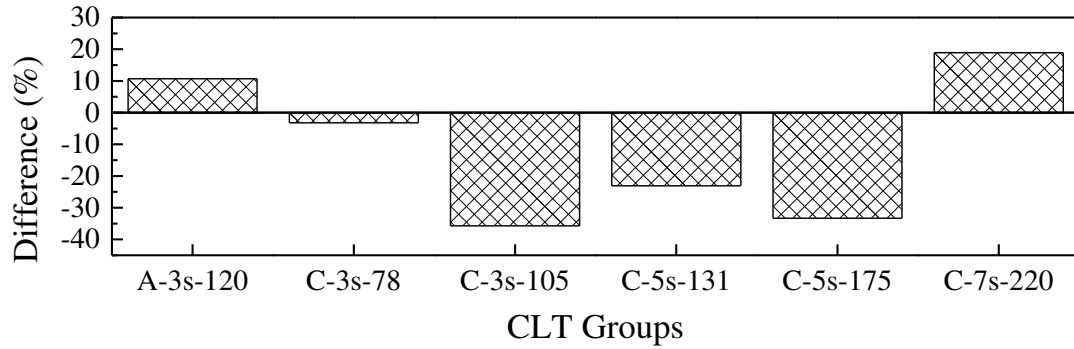
Figure 5.8 Difference between values of G_{xy} of CLT panels without edge bonding predicted by Eq. 5.6 and modal testing performed in this study

As concluded in section 3, both GM and SAM can include the transverse shear effect for predicting the effective bending stiffness of CLT and MSWP in the major strength direction. Compared with k-Method results, GM and SAM predictions of E_x are lower than the measured values for most of the CLT and MSWP panels. Both GM and SAM results are quite close to each other for most of the CLT and MSWP panels with a large length to thickness ratio. For CLT groups B-8s-2-300, C-5s-131 and C-7s-220, whose length-to-thickness ratios are 25, 36 and 38, the GM-predicted E_x values are 7%, 10% and 12% lower than those modal test measured, respectively, and the SAM-predicted E_x values are 12%, 13% and 15% lower than those modal test measured, respectively. The SAM accounts more for the effect of transverse shear than GM when length to thickness ratio is small. CLT panels in group C-3s-105 covered a wide range of length to thickness ratio from 28 to 105, and they were used in studying the effect of transverse shear on the elastic properties of CLT panels. As it can be observed in Figure 5.9, the measured apparent E_x ranges from

155

6757 to 11135 MPa because the modal test method is based on the transverse vibration of thin orthotropic plate theory which ignores the transverse shear effect. The predictions based on GM and SAM can describe the trend but cannot predict the actual values. Both GM and SAM curves show a rapid decrease of $E_{x, app}$ when the length is smaller than 4 meters (length/ thickness $\approx$ 40) for C-3s-105.

Compared with CLT panels of C-3s-105, those of C-5s-175 have three parallel-to-grain layers in the major strength direction with one of them as the middle layer. Therefore, the transverse shear modulus of C-5s-175 is higher than that of C-3s-105 (Gülzow, 2008). In addition, as more parallel-to-grain layers are used in the major strength direction, the effect of transverse shear on the E_x values measured is not as obvious as those predicted by GM and SAM such as in the case of B-8s-2-300 with a length to thickness ratio of 25. B-8s-2-300 can be treated as five-layer CLT with a large portion of parallel layers. The results indicate that using double parallel layers has a strengthening role in the major strength direction, however, can reduce the transverse shear deformation, especially with a parallel layer in the middle layer where the shear stress reaches the maximum.
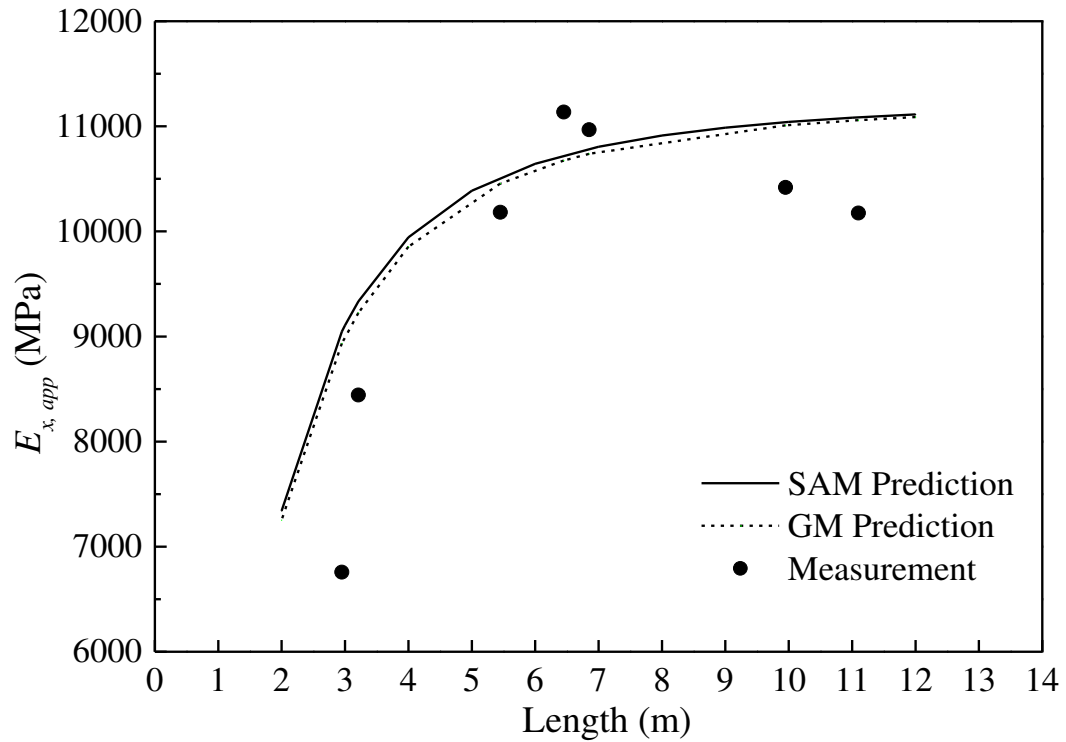
Figure 5.9 Apparent E_x of CLT panels in group C-3s-105 measured by modal tests and predicted by gamma method and shear analogy method

As shown in Table 5.3, SAM results in lower E_y values for CLT and MSWP than k-Method because of their different approaches used for accounting the effect of transverse shear in their equations. The effect of transverse shear is different for CLT panels with different layups and widths as shown in Figure 5.10. The width of CLT panels tested in this study varies from 0.9 to 3.0 meters, correspondingly the width to thickness ratio varies from 4 to 32. For A-3s-120, B-5s-200, B-8s-300, C-5s-131 and C-7s-220 CLT panels, the SAM results are more than 20% lower than modal test results. However, the modal test measured values of each group do not change significantly within the common range of width of CLT

products, although properties of five-layer and seven-layer CLT panels predicted by SAM are influenced by panel width. It is known that transverse shear modulus in the width-thickness plane (G_{yz}) is not as low as that in the length-thickness plane (G_{xz}), and the frequency mode chosen for calculating E_y is not sensitive to G_{yz} for the modal test method. It is questionable to use SAM for predicting the effective stiffness of CLT in the minor strength direction with short spans, though it is not the case for current application of CLT panels. If CLT panel is designed to have a two-way behaviour, then more in-depth investigations on the properties in the minor strength direction are needed.
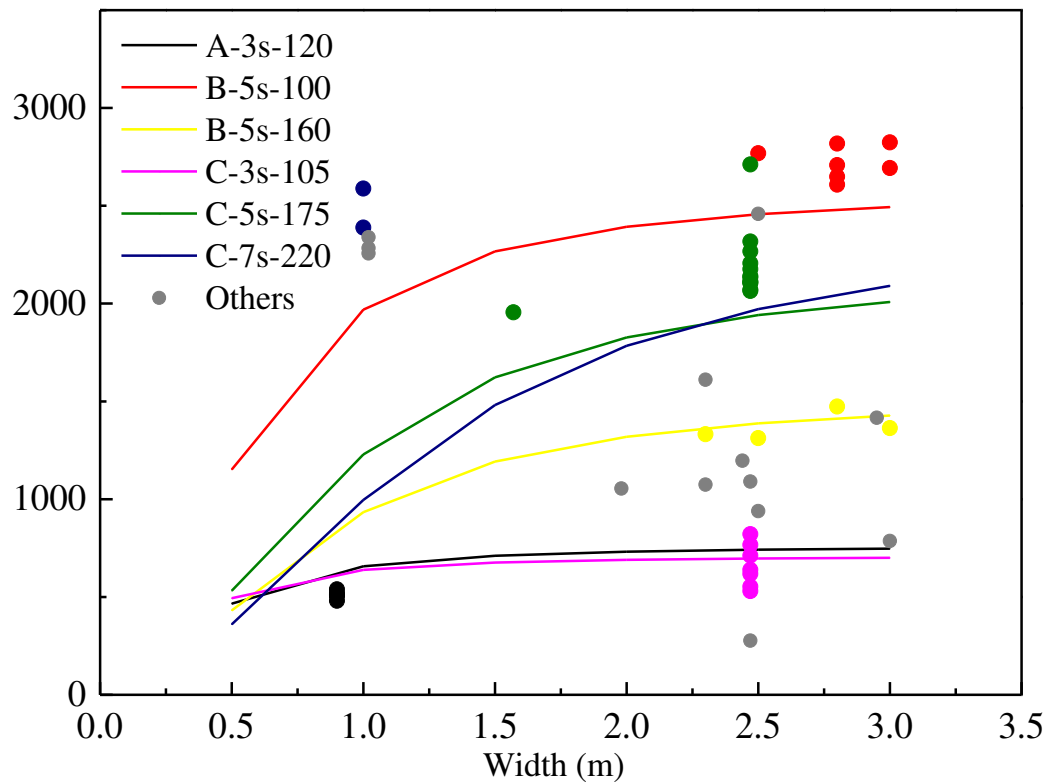
Figure 5.10 Apparent E_y of CLT panels measured by modal tests (solid circles) and some selected groups predicted by shear analogy method (solid lines with corresponding color)

5.5 Conclusions

The modal test method developed by the first author has provided an efficient method of directly measuring in-plane elastic properties of a full-size mass timber panel, namely modulus of elasticity in the major (E_x) and minor (E_y) strength direction and the in-plane shear modulus (G_{xy}). This test method is non-destructive since it avoids the need to cut the mass timber panel into smaller specimens that are required for static test methods. Using the developed modal test method, this study compares elastic properties of CLT and MSWP panels measured using the modal testing method, and predictions from a number of analytical models, including k-Method, gamma method and shear analogy method. It can be concluded that all three prediction methods are valid for calculating effective bending stiffness of CLT panels with a large length-to-thickness ratio in the major strength direction. The k-Method could also provide effective bending stiffness in the minor strength direction that was close to the value measured by modal test method. However, the accuracy of k-Method in prediction of effective bending stiffness in the minor strength direction was influenced by layup and edge bonding. SAM could be a better choice in comparison to other two methods when CLT had a small length-to-depth ratio. However, SAM could include an over-estimated transverse shear effect for CLT with a small width-to-thickness ratio and leads to a much smaller prediction of E_y value. In-plane shear modulus was greatly influenced by edge bonding and gaps, and could not be well predicted by k-Method. The formula proposed in (Bogensperger et al., 2010) could be further modified for better prediction of in-plane shear modulus of CLT panels.

For panels with a small transverse shear modulus such as CLT, the elastic properties are dependent on layup to some degree. The minimum length-to-thickness ratios for appropriate measurement of elastic properties are suggested to be 40, 35 and 30 for three-, five- and seven-layer CLT, respectively. For panels with a small length-to-thickness ratio, a modified method that considers the effect of transverse shear modulus is required.

References

APA. (2012). *ANSI/ APA PRG 320 Standard for performance-rated cross-laminated timber*. APA - The Engineered Wood Association.

Andreolli, M., Rigamonti, M., and Tomasi, R. (2014). Diagonal Compresion Test on Cross Laminated Timber Panels. In A. Salenikovich (Ed.), *World Conference on Timber Engineering* (p. 9). Quebec City.

Blass, H. J., and Fellmoser, D. P. (2004). Design of solid wood panels with cross layers. In *World Conference on Timber Engineering*. Lahti.

Bodig, J., and Jayne, B. A. (1982). *Mechanics of Wood and Wood Composites*. Florida: Krieger Publishing Company.

Bogensperger, T., Moosbrugger, T., and Silly, G. (2010). Verification of CLT-plates under loads in plane. In *World Conference on Timber Engineering*. Riva del Garda.

Brandner, R. (2013). Production and Technology of Cross Laminated Timber (CLT): A State-of-the-art Report. In *Focus Solid Timber Solutions - European Conference on CLT* (pp. 3–36). Graz.

Brandner, R., Dietsch, P., Schulte-wrede, M., and Sieder, M. (2015). Scheibenschub von Brettsperrholz : Verifizierung einer Prüfkonfiguration und Parameterstudie. *Bautechnik*, *92*, 759–769.

Brandner, R., Flatscher, G., Ringhofer, A., … Thiel, A. (2016). Cross laminated timber (CLT): overview and development. *European Journal of Wood and Wood Products*, *74*(3), 331–351.

CEN. (2004). *Timber structures - Structural timber and glued laminated timber. Determination of some physical and mechanical properties (EN408:2004)*. Brussels:

European Committee for Standardization CEN/TC 124.

CEN. (2006). *Eurocode 5 Design of timber structures. Part 1-1: General Common rules and rules for buildings (EN 1995-1-1)*. Brussels: European Committee for Standardization CEN/TC 250.

CEN. (2009). *Structural timber - Strength classes (EN 338:2009)*. Brussels: European Committee for Standardization CEN/TC 124.

CEN. (2015). *Timber structures - Cross laminated timber – Requirements (EN 16351:2015)*. Brussels: European Committee for Standardization CEN/TC 124.

Dröscher, J. (2014). *Prüftechnische Ermittlung der Schubkenngrößen von BSPScheibenelementen und Studie ausgewählter Parameter*. Graz University of Technology.

Fang, H., Sun, H., Liu, W., … Hui, D. (2015). Mechanical performance of innovative GFRP-bamboo-wood sandwich beams: Experimental and modelling investigation. *Composites Part B: Engineering*, *79*, 182–196. Retrieved from http://dx.doi.org/10.1016/j.compositesb.2015.04.035

Fellmoser, P., and Blass, H. J. (2004). Influence of rolling shear modulus on strength and stiffness of structural bonded timber elements. In *CIB-W18 Meeting*.

Franzoni, L., Lebée, A., Lyon, F., and Foret, G. (2016). Influence of orientation and number of layers on the elastic response and failure modes on CLT floors: modeling and parameter studies. *European Journal of Wood and Wood Products*, *74*(5), 671–684.

Gliniorz, K. U., Mosalam, K. M., and Natterer, J. (2002). Modeling of layered timber beams and ribbed shell frameworks. *Composites Part B: Engineering*, *33*(5), 367–

381.

Gsell, D., Feltrin, G., Schubert, S., … Motavalli, M. (2007). Cross-Laminated Timber
Plates: Evaluation and Verification of Homogenized Elastic Properties. *Journal of
Structural Engineering*, *133*(1), 132–138.

Gülzow, A. (2008). *Zerstörungsfreie Bestimmung der Biegesteifigkeiten, von
Brettsperrholzplatten*. ETH Zürich.

Kreuzinger, H. (1999). Platten, Scheiben und Schalen - ein Berechnungsmodell für
gängige Statikprogramme. *Bauen Mit Holz*, (1), 34–39.

Malo, K. A., Abrahamsen, R. B., and Bjertnæs, M. A. (2016). Some structural design
issues of the 14-storey timber framed building "Treet" in Norway. *European
Journal of Wood and Wood Products*, *74*(3), 407–424.

Moses, D. M., Prion, H. G. L., Li, H., and Boehner, W. (2003). Composite behavior of
laminated strand lumber. *Wood Science and Technology*, *37*(1), 59–77.

Steiger, R., Gülzow, A., Czaderski, C., … Niemz, P. (2012). Comparison of bending
stiffness of cross-laminated solid timber derived by modal analysis of full panels and
by bending tests of strip-shaped specimens. *European Journal of Wood and Wood
Products*, *70*(1–3), 141–153.

Stürzenbecher, R., Hofstetter, K., and Eberhardsteiner, J. (2010). Structural design of
Cross Laminated Timber (CLT) by advanced plate theories. *Composites Science and
Technology*, *70*(9), 1368–1379.

Sylvain, G., and Marjan, P. (2011). Structure design of cross-laminated timber elements.
In G. Sylvain & P. Ciprian (Eds.), *CLT Handbook* (1st ed., pp. 114–185).
FPInnovations.

Zhou, J., Chui, Y. H., Gong, M., and Hu, L. (2016). Simultaneous measurement of elastic

constants of full-size engineered wood-based panels by modal testing.

Holzforschung, *70*(7), 673–682.

CHAPTER 6 EFFECTIVE BENDING AND SHEAR STIFFNESS OF CROSS LAMINATED TIMBER BY MODAL TESTING: METHOD DEVELOPMENT AND APPLICATION

Abstract: Mass timber panels, especially cross laminated timber (CLT), are gaining popularity worldwide with the development of mid- to high-rise wood construction. The elastic properties of CLT panels are fundamental for their structural applications. A non-destructive testing (NDT) technique employing modal testing for the measurement of natural frequencies, and a genetic algorithm for minimizing the difference between calculated and measured natural frequencies has been proposed for the inverse determination of in-plane and out-of-plane elastic constants of orthotropic Mindlin plates. Based on the exact solution of free transverse vibration of orthotropic Mindlin plates under a pair of opposite edges simply supported and the other pair free (SFSF), the effective bending and shear stiffness of two three-layer and one five-layer symmetric CLT panels were inversely determined for structural design purposes. Moreover, the results showed that to include five sensitive vibration modes was more efficient than having a large number of frequencies for the inverse determination. This study demonstrated the efficiency and potential of the proposed method for determining the effective bending and shear stiffness of mass timber panels.

Keywords: cross laminated timber, bending and shear stiffness, modal testing, genetic algorithm

6.1 Introduction

Wood is an environmental-friendly and sustainable building material. It has different mechanical and physical properties between the parallel to the grain and perpendicular to grain directions. In current structural wood design codes, such as Canadian CSA O86 (CSA, 2016) and Eurocode 5 (CEN, 2006), it is often assumed that the modulus of elasticity (MOE) of softwood parallel to grain is twenty times that of its MOE perpendicular to grain and sixteen times that of the shear modulus (G) in the longitudinal-radial or longitudinal-tangential plane. The shear modulus in the radial-tangential plane, also called rolling shear modulus, can be as low as one-tenth of the shear modulus in the longitudinal-transverse planes. Structural wood-based panel products such as plywood made of rotary-cut veneers and cross laminated timber (CLT) panels made of dimensional lumber pieces would have relatively low transverse shear modulus due to the layers with radial-tangential planes in the cross sections. Chui and Gong (2015) reported that the rolling shear modulus of black spruce (*Picea mariana*) varied from 125 to 141 MPa measured by planar shear tests with block specimens cut directly from CLT panels. Ehrhart et al. (2015) also found that the rolling shear modulus of Norway spruce (*Picea abies*) was 100 MPa on average. The low transverse shear stiffness to bending stiffness ratio requires attention to be paid in structural design of CLT panels in out-of-plane bending applications where the span is short or there are openings, where transverse shear deformation or stress becomes dominant (Gagnon and Popovski, 2011) .

Non-destructive testing (NDT) techniques such as vibration tests based on the Mindlin plate theory are good alternatives to static methods. Soares et al. (1993) made the first

attempt to develop a finite element model as the forward solution for the identification of six material parameters of composite plate specimens based on Mindlin plate theory. It was pointed out that their model was dependent on aspect ratio of the specimen and accurate experimental natural frequencies. Araújo et al. (1996) extended their study with more results of composite materials presented. Ayorinde (1995) also developed a method for obtaining the elastic constants of a completely free thick orthotropic composite plate from experimental plate vibration data using an optimized three-mode Rayleigh formulation that incorporated transverse shear and rotatory inertia. His work was further developed for determining five elastic constants of thick plates with specially orthotropic and transversely isotropic materials by Yu (2006). Frederiksen (1997a) proposed a method to identify the four in-plane elastic constants and two transverse shear moduli using the higher mode natural frequencies of a completely free thick plate solved by an accurate numerical model based on a higher-order shear deformation theory (Reddy, 1984). The transverse shear moduli were claimed to be overestimated and improved by using another higher-order shear deformation theory by Lo et al. (1977) in a later study by Frederiksen (1997b). Gsell et al. (2007) conducted the experimental modal analysis to determine the natural frequencies and mode shapes of a rectangular CLT specimen for the purpose of measuring three shear and two in-plane bending stiffness of CLT panels. It can be seen as an extended application of the method proposed by Frederiksen (1997a) in characterizing the elastic properties of wood composites. The method was then applied to evaluate the elastic properties of CLT panels (Gülzow, 2008; Steiger et al., 2012).

All above studies were aimed at minimizing the nonlinear objective function in the form of least squares of the difference between measured and numerical frequencies. A reasonably close initial guess of each elastic constant is required for optimization. This is because such conventional optimization techniques may have difficulties in producing convergent results when a large number of frequencies are involved or inappropriate initial guesses are used. To overcome these difficulties, Cunha et al. (1999) first applied genetic algorithm (GA) for the identification of elastic constants of composite materials from dynamic tests based on the first-order shear deformation theory. Their results showed that GA was very effective and robust in the inverse estimation of elastic constants. Silva et al. (2004) also adopted the GA for identifying the four in-plane elastic parameters of composite material. It was proved that GA was able to handle the usual drawbacks of conventional optimization techniques including the presence of several local minima and ill-conditioning. Hwang et al. (2009) proposed a hybrid genetic algorithm for the identification of the five effective elastic constants of transversely isotropic composite materials, which showed great advantage in repeatability and accuracy. It is also worth mentioning that most such studies either applied Rayleigh-Ritz method or finite element method (FEM) to solve the eigenvalue problem of the transverse vibration of a completely free orthotropic Mindlin plate. The reasons are, first, there is no exact solution for the eigenvalue problem under the boundary condition of completely free (FFFF), and second, the FFFF boundary condition is not easy to be implemented in practice. However, due to the problem of high nonlinearity, those numerical models are either not very computation effective nor accurate enough for the development of an inverse technique for characterizing the elastic properties of thick composite materials.

168

In the previous studies (Zhou et al., 2016 & 2017), two apparent MOE values in major and minor strength directions and one in-plane G values of full-size CLT panels with different characteristics were measured using a vibration-based NDT by treating the panel as a homogenous thin orthotropic plate. The developed method utilized the modal testing of a CLT panel under the boundary condition of a pair of opposite edges in the width direction simply supported and the other pair free (SFSF), making the modal tests of full-size panels easier and more efficient than under the boundary condition of FFFF. It was found that the measured MOE decreased with the decrease in length-to-thickness ratio, especially when it is less than 50.

Therefore, this study further developed the proposed method of combining the exact solution for free transverse vibration of orthotropic rectangular Mindlin plates under SFSF boundary condition by Liu and Xing (2011) with genetic algorithm as the optimization technique for the inverse determination of effective bending and shear stiffness of CLT panels using their natural frequencies from modal testing.

6.2 Theoretical Basis and Method Development

6.2.1 Exact Solution of Free Transverse Vibration of a Rectangular Orthotropic Mindlin Plate

The CLT panel in this study is considered as a moderate-thick rectangular plate of length a, width b and uniform thickness h with a defined Cartesian coordinates as shown in

169

Figure 6.1. The displacements along x, y and z directions of a rectangular orthotropic Mindlin plate are

$$w = w(x, y, z, t), \quad u = -z\psi_x(x, y, z, t), \quad v = -z\psi_y(x, y, z, t) \tag{6.1}$$

where t is time, w is the transverse deflection, ψ_x and ψ_y are the angles of rotation of a normal line due to plate bending with respect to y and x coordinates, respectively. The relations between the internal forces and displacements for orthotropic Mindlin plates can be expressed by

$$M_x = -(D_{11}\frac{\partial \psi_x}{\partial x} + D_{12}\frac{\partial \psi_y}{\partial y}) \tag{6.2a}$$

$$M_y = -(D_{22}\frac{\partial \psi_y}{\partial y} + D_{21}\frac{\partial \psi_x}{\partial x}) \tag{6.2b}$$

$$M_{xy} = -D_{66}(\frac{\partial \psi_x}{\partial y} + \frac{\partial \psi_y}{\partial x}) \tag{6.2c}$$

$$Q_y = -C_{44}(\frac{\partial w}{\partial y} - \psi_y) \tag{6.2d}$$

$$Q_x = -C_{55}(\frac{\partial w}{\partial x} - \psi_x) \tag{6.2e}$$

where $D_{11} = \dfrac{E_x h^3}{12(1 - v_{xy}v_{yx})}$, $D_{12} = \dfrac{v_{xy}E_x h^3}{12(1 - v_{xy}v_{yx})}$, $D_{22} = \dfrac{E_y h^3}{12(1 - v_{xy}v_{yx})}$, $D_{21} = \dfrac{v_{yx}E_y h^3}{12(1 - v_{xy}v_{yx})}$,

$D_{66} = \dfrac{G_{xy}h^3}{12}$; $C_{44} = \kappa_{yz}G_{yz}h$ and $C_{55} = \kappa_{xz}G_{xz}h$ are the bending and shear rigidities, respectively; and k_{yz} and k_{xz} are the shear correction factors with respect to two individual transverse planes, which are usually equal to $\pi^2/12$ (≈ 0.822) or 5/6 (≈ 0.833) for continuous Mindlin or Reissner plates. E_x and E_y are the in-plane MOE in the x and y directions,

170

respectively. G_{xy} is the in-plane shear modulus. G_{xz} and G_{yz} are the transverse shear moduli in the xz and yz planes, respectively. v_{xy} and v_{yx} are the in-plane major and minor Poisson's ratios, respectively. The governing differential equations for free transverse vibration of a rectangular orthotropic Mindlin plate are given by

$$-\frac{\partial M_x}{\partial x} - \frac{\partial M_{xy}}{\partial y} + Q_x - \rho J \frac{\partial^2 \psi_x}{\partial t^2} = 0 \tag{6.3a}$$

$$-\frac{\partial M_{xy}}{\partial x} - \frac{\partial M_y}{\partial y} + Q_y - \rho J \frac{\partial^2 \psi_y}{\partial t^2} = 0 \tag{6.3b}$$

$$\frac{\partial Q_x}{\partial x} + \frac{\partial Q_y}{\partial y} - \rho h \frac{\partial^2 w}{\partial t^2} = 0 \tag{6.3c}$$

where $J = h^3 / 12$ is area axial moment of inertia of cross section per unit length, ρ is the density of the plate material.
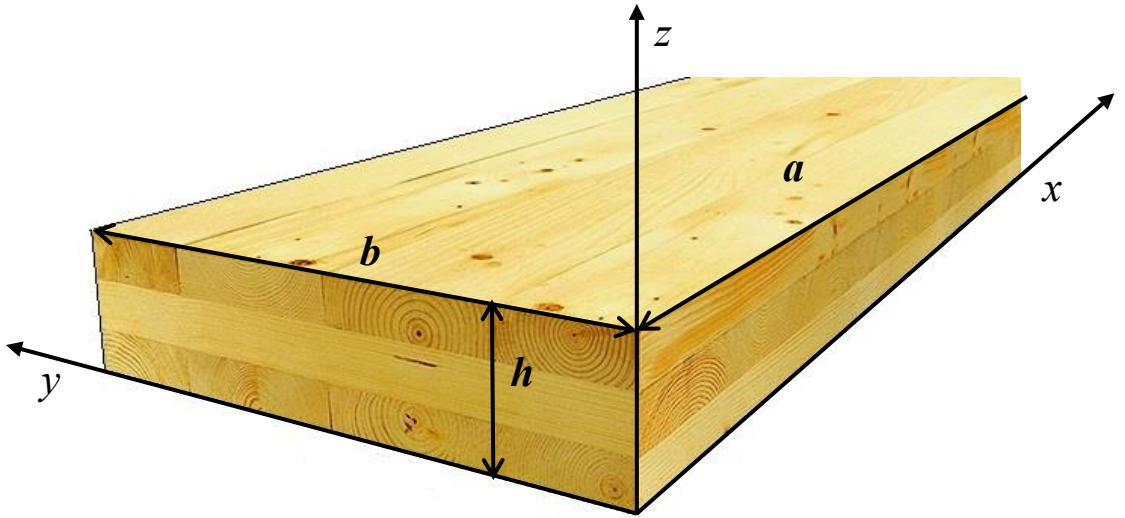
Figure 6.1 A three-layer CLT panel with assigned coordinates

171

The exact closed-form solutions for the above governing equations were obtained using the separation of variables method for boundary condition of one pair of opposite edges simply supported and all possible combinations of simple support, free and clamp at the other two edges by Liu and Xing (2011). For the boundary condition of SFSF, the characteristic frequency equations were presented and solved with Newton-Raphson method by Liu et al. (2014). The results of frequency parameters of square three-ply laminated plates and single-ply orthotropic Mindlin plates showed great agreement with results by FEM. The MATLAB codes provided by Xing and Liu (2015) have been adopted and modified as the forward solution in this study.

6.2.2 Verification of Forward Solution by FEM

Finite element modelling was conducted to verify the forward solution using commercial finite element analysis software ABAQUS. CLT panels were modeled as a 3D deformable shell with thick conventional shell element types S8R, which include the effect of transverse shear in the calculation for every vibration mode (ABAQUS, 2013). A three-layer CLT plate model of dimensions 3.15 m in length, 1.05 m in width and 105 mm in thickness and density of 520 kg/m^3 was created for the numerical verification. The input elastic constants were: $E_x = 10,400$ MPa, $E_y = 711$ MPa, $G_{xy} = 518$ MPa, $G_{xz} = 130$ MPa, $G_{yz} = 350$ MPa, $v_{xy}=0.02$, which were approximated from previous measurements (Gülzow, 2008; Zhou et al., 2016). The plate model was meshed with a global size of 0.02 mm with a sufficient accuracy. The simply supported edges were constrained in the three translational directions. To be noted, the shear correction factor in ABAQUS is set to be 5/6 by default, thus, a same value was used in the forward solution as well. The natural

frequencies of up to twenty modes were computed with embedded 'Lanczos eigensolver'. Then ten natural frequencies of interests were selected for comparison with their corresponding values calculated from the exact solution as listed in Table 6.1. It can be seen that the differences are very small for most of the modes, only mode (2, 1) has a significant difference between exact solution and FEM results. Since exact solution is often set as benchmarks for numerical method, it is reasonable to conclude that the exact solution and its corresponding MATLAB code are valid for calculating the natural frequencies of CLT panels.

Table 6.1 Natural frequencies of numerical case obtained by exact solution and FEM

Vibration mode [a]	Frequency value (Hz)		f_{diff} [b]
	f_{exact}	f_{FEM}	
(2, 0)	20.6	20.6	-0.02%
(2, 1)	35.8	34.3	4.19%
(2, 2)	125.1	123.7	1.14%
(2, 3)	299.7	298.8	0.29%
(2, 4)	540.8	540.4	0.08%
(3, 0)	73.8	73.8	0.00%
(3, 1)	90.8	88.8	2.14%
(3, 2)	165.6	162.0	2.18%
(4, 0)	144.2	144.2	-0.01%
(5, 0)	222.1	221.2	0.41%

[a] Vibration mode is expressed using the mode indices (m, n), where m and n are the number of nodal lines including the simply supported sides in y and x direction, respectively.

[b] f_{diff} is the difference in percent between f_{exact} and f_{FEM} which is calculated using the equation $f_{diff} = (f_{exact} - f_{FEM})/ f_{exact} \times 100\%$.

6.2.3 Sensitivity Analysis and Design of Specimen

In aforementioned studies, the first several natural frequencies in the mode sequences without knowing their mode shapes were often used in the inverse identification of elastic constants. However, the order of natural frequencies is not only dependent on the elastic constants but also the aspect ratio of the plates. Though the number of frequencies used for inverse determination were usually more than the number of elastic constants to be determined, it cannot ensure that every elastic constant can be accurately determined. The contribution of each elastic constant to each vibration mode, known as sensitivity, differs with the orthotropic ratios, i.e. E_x/E_y, E_x/G_{xy}, E_x/G_{xz} and E_y/G_{yz}, and aspect ratio. Also, no vibration modes are sensitive to Poisson's ratio unless the plate has a certain modulus ratio of $\sqrt[4]{E_x/E_y}$ (Coppens, 1988). Therefore, in order to improve the accuracy of the determination, it is of great importance to conduct the sensitivity analysis and choose the appropriate vibration modes for the inverse determination.

With the MATLAB code of exact solution, the sensitivity analysis can be conducted simply by changing each initial elastic constant by ±10% and calculating the relative frequency difference for each mode. Two numerical cases were analyzed to demonstrate the sensitivity analysis of two plates, which were representatives of a three-layer CLT panel and a five-layer CLT panel. Both panels had a length-to-thickness ratio of 30, a width to thickness ratio of 10 and an aspect ratio of 3. Thus, the effect of orthotropic ratios on the sensitivity levels could be investigated. The three-layer CLT was the same one used for FEM verification. The five-layer CLT had a length of 3.93 m, a width of 1.31 m and

174

thickness of 131 mm and a density of 520 kg/m^3. The input elastic constants for the five-layer CLT were E_x = 9,657 MPa, E_y = 2,290 MPa, G_{xy} = 542 MPa, G_{xz} = 458 MPa, G_{yz} = 512 MPa, v_{xy}=0.02, which were approximated based on reported values (Steiger et al., 2012; Zhou et al., 2017).

The sensitivity analysis results of the three-layer CLT panel and five-layer CLT panel are presented in Figure 6.2 and 6.3, respectively. Similar to previous study based on the thin orthotropic plate theory (Zhou et al., 2016), the sensitive modes to E_x, E_y and G_{xy} are mode (2, 0), (2, 2) and (2,1), respectively. Due to the effect of transverse shear, for pure bending modes (m, 0) in the length direction or (2, n) in the width direction, the sensitivities of these bending modes to E_x or E_y decrease with the increase of mode number. In contrast, their sensitivity to G_{xz} or G_{yz} which increases with the increase of mode number since the wavelength of such bending mode decreases with the increase of mode indices m or n. Due to the different layups of the two panels, which result in different elastic constants, the sensitivity results reflect the effect of orthotropic ratios. As can be seen from Figure 6.1 and 6.2, since the three-layer CLT has a slightly larger E_x/ G_{xz} and a much smaller E_y/ G_{yz} values than those of the five-layer CLT, the sensitivity of mode (m, 0) to G_{xz} for three-layer CLT is slightly higher than corresponding values for five-layer CLT. The sensitivity of mode (2, n) to G_{yz} for five-layer CLT is much higher than corresponding values for three-layer CLT. Therefore, in order to measure G_{xz} and G_{yz}, either frequencies of high bending mode or panel specimens with small length/ width to thickness ratio should be used. In practice however it is difficult to excite high vibration modes of CLT panels through impact

tests even with hammer tips with high hardness due to the relatively low hardness of wood surface.
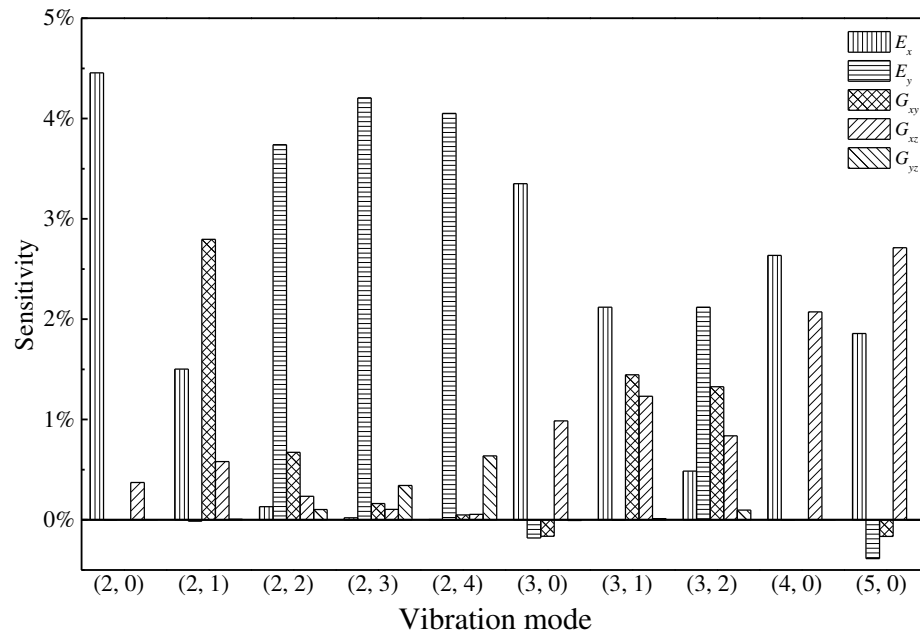
Figure 6.2 Sensitivity of selected vibration modes to elastic constants of a three-layer CLT panel
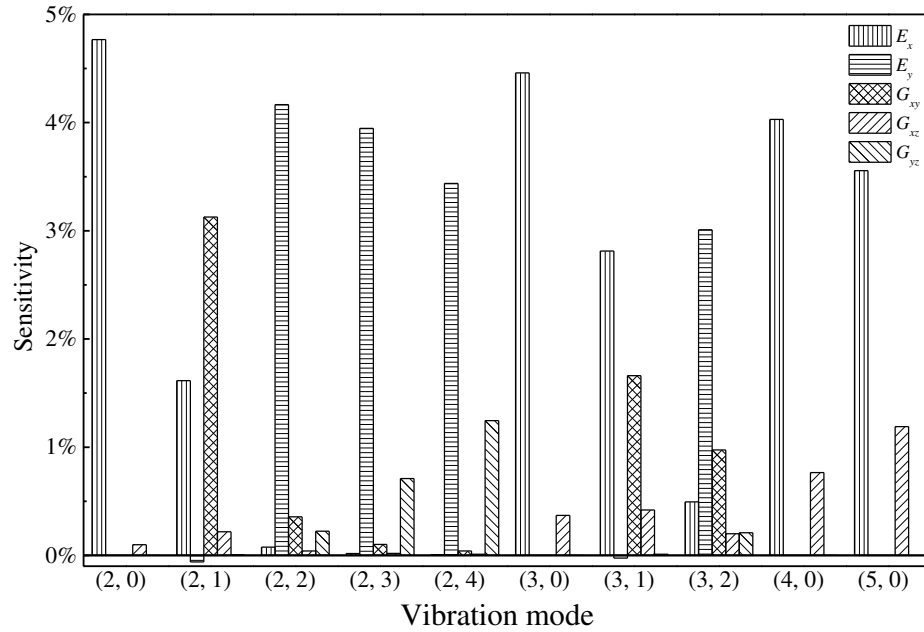
Figure 6.3 Sensitivity of selected vibration modes to elastic constants of a five-layer CLT panel

Besides the idea of including more frequencies in the inverse optimization, it is helpful to improve the precision of measuring transverse shear stiffness by reducing the length/ width to thickness ratio. Frederiksen (1998) concluded that the aspect ratio had great impact on the vibration mode shapes which in turn are decisive for the frequency sensitivity. Therefore, specimen design, namely the aspect ratio of specimen, is very important to the estimation of elastic constants. Gagneja et al. (2001) also made such attempts to design test specimens for the determination of transverse shear moduli of thick composites from measured natural frequencies. They recommended a length to thickness ratio of not less than 8 and not greater than 13 for the materials of square plate in their study. Though the importance of aspect ratio and the sensitivity of certain frequency mode to transverse

moduli were recognized by researchers, only the first five or more frequencies in the frequency order were often used in their studies, which might not be extensive enough to cover all the sensitive vibration modes. Therefore, more numerical cases with different aspect ratios were analyzed for an optimal specimen dimension to increase the reliability in this study. The three-layer CLT numerical case was used to investigate the effect of aspect ratio on the sensitivity of each vibration mode to each elastic constant. Four different aspect ratios of 3, 2, 1.5 and 1.05 were achieved by keeping its length constant at 3.15 m and changing the width to 1.05, 1.575, 2.1 and 3 m accordingly.

The sensitivity of the selected modes to each elastic constant E_x, G_{xz}, E_y, G_{yz} and G_{xy} with different aspect ratios is plotted separately in Figure 6.4. With the unchanged length, the sensitivity of bending modes $(m, 0)$ to E_x and G_{xz} is not significantly affected by the aspect ratio. However, the sensitivity of bending modes $(2, n)$ to E_x decreases with the increase of aspect ratio. With aspect ratio of 3, the sensitivity of bending modes $(2, n)$ to E_x is the lowest among the four aspect ratios, the sensitivity to E_x is nearly negligible for modes $(2, 3)$ and $(2, 4)$. With the aspect ratio increased from 1.05 to 3, the sensitivity of mode $(2, n$ $(n \geq 2))$ to E_y deceases while the sensitivity of the same mode to G_{yz} increases. This is attributed to the changing of width, which leads to the increase in width-to-thickness ratio. However, since the E_y / G_{yz} value is relatively small for the three-layer CLT in this study, even for a small width-to-thickness ratio and high frequency mode $(2, 4)$, the sensitivity level is still not significant. Therefore, in this case, the aspect ratio of 3 and higher mode such as $(2, 4)$ are recommended for the experimental design. It is also interesting to note that the sensitivity of mode $(2, 1)$ to G_{xy} increases with an increase in aspect ratio, which

178

in turn would reduce its sensitivity to E_x. There seems to be a coupled effect of G_{xy} and E_x on mode (2, 1), while the other three elastic constants have no influence on it. Mode (2, 1) was also found to be the second mode after mode (2, 0) in the frequency order (Zhou et al 2016), which makes them easy to be identified. To ensure its high sensitivity to G_{xy}, a large aspect ratio should be considered in the experimental design.

To summarize, sensitivity analysis plays an important role in selecting the sensitive frequencies for the inverse determination of all five elastic constants. The sensitivity level of a certain mode to different elastic constants depends on not only the orthotropic ratios and aspect ratio but also the mode shape. Due to the nature of some materials, for example, the E_y/ G_{yz} is in the range of 1 to 3 for the CLT panels in this study, it is very difficult to find the optimal aspect ratio for all the elastic constants of interest. A balanced experimental design and selection of vibration modes is required for a successful measurement of all five elastic constants by modal testing. Therefore, aspect ratio of 3 and vibration modes including (2, 0), (2, 1), (2, 2), (3, 0), (2, 3) or with additional (4, 0) and (2, 4) are recommended for the CLT panels in this study.

(c) E_y
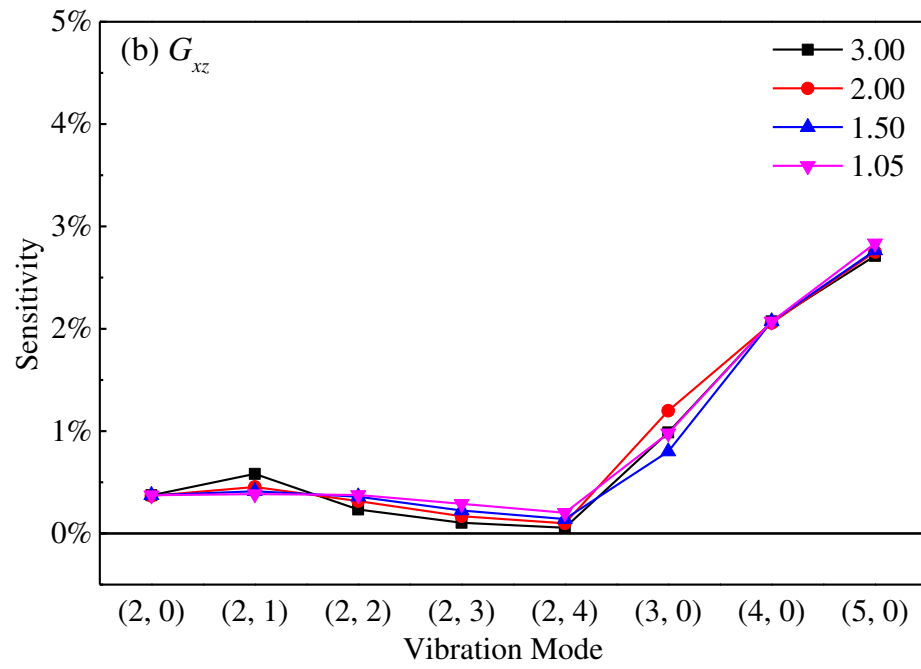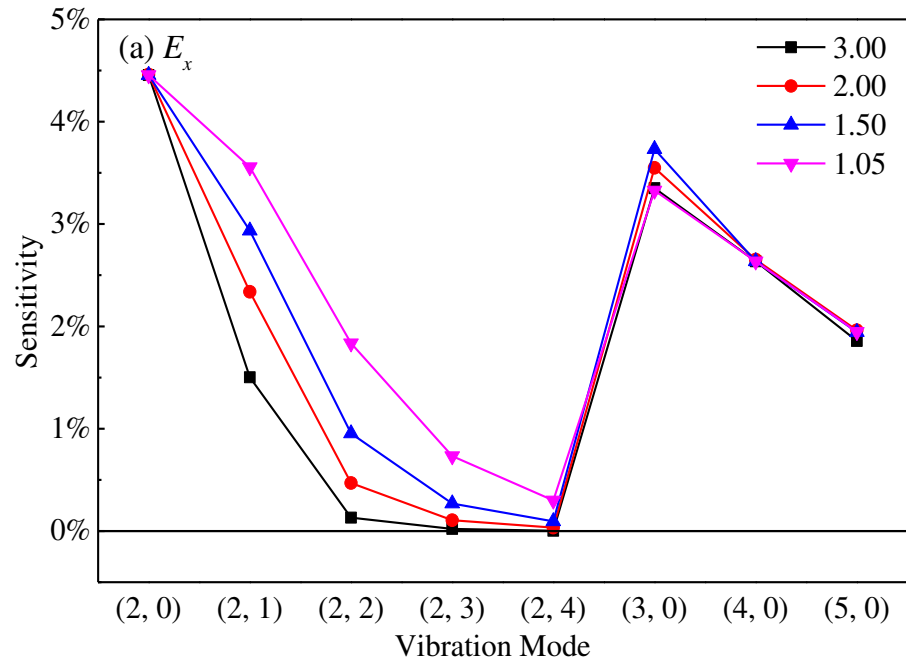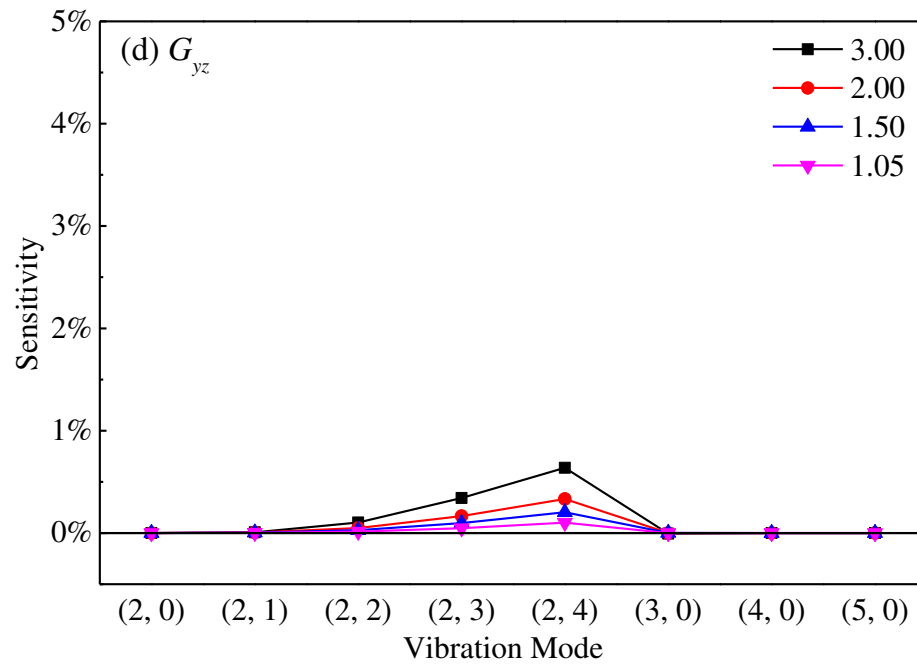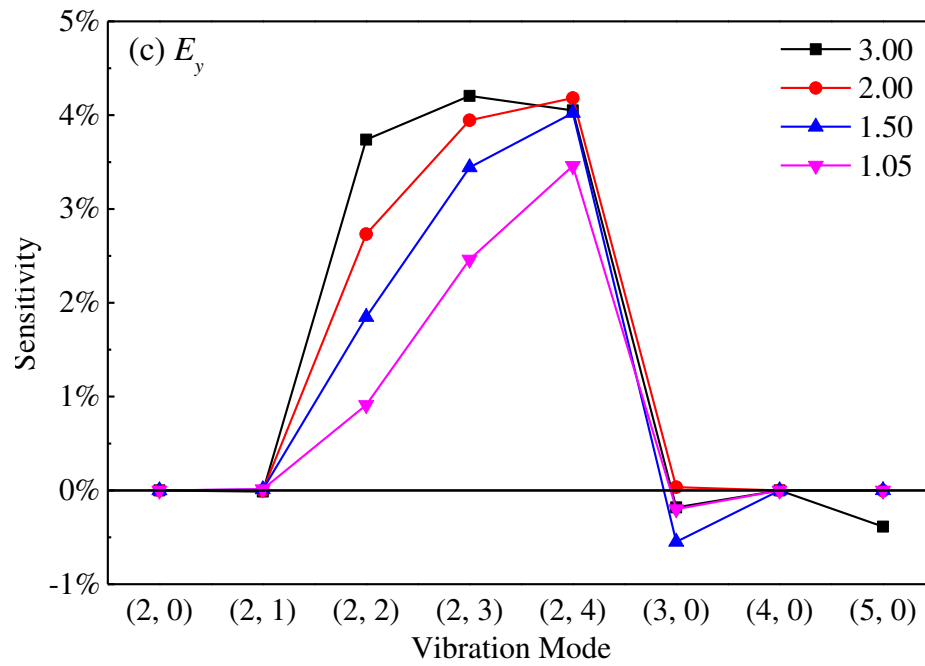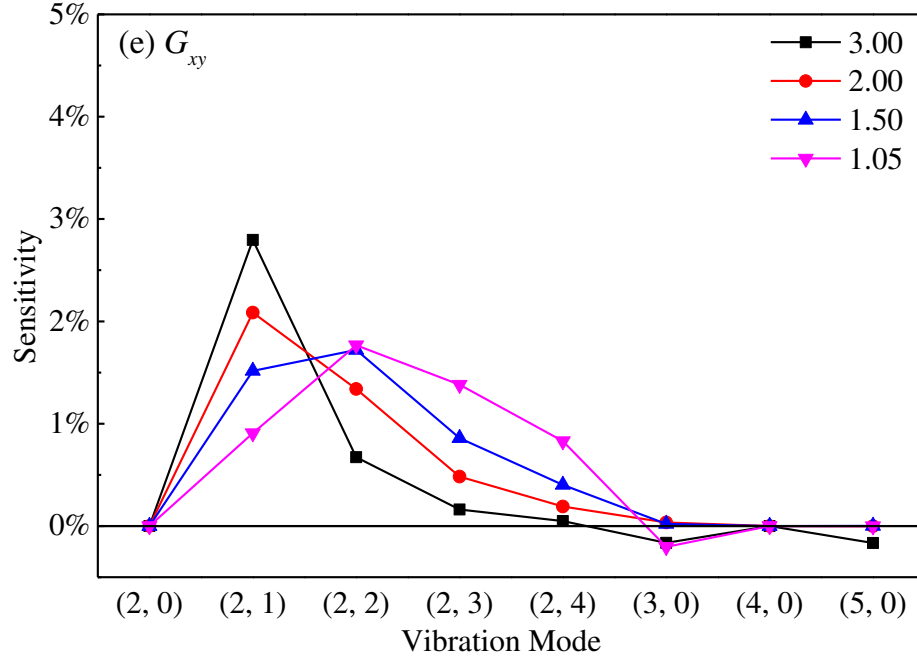
(d) G_{yz}

Figure 6.4 Sensitivity of selected vibration modes to each elastic constant: (a) E_x, (b) G_{xz}, (c) E_y, (d) G_{yz} and (e) G_{xy} for a three-layer CLT panel with different aspect ratios

6.2.4 Genetic Algorithm for Inverse Determination of Elastic Constants

Due to the complexity of the inverse problem, namely the high nonlinearity of the exact solution adopted in this study, genetic algorithm (GA) was chosen as the optimization technique for the inverse determination of the elastic constants of CLT panels using natural frequencies obtained from modal testing. GA has already shown its strong capability in the inverse determination of elastic constants of both thin and thick composite plates in aforementioned studies and many other engineering fields (Liu and Han, 2003; Dasgupta and Michalewicz, 2013).

In this study, the objective function $F(X)$, known as fitness function for GA, is defined as the sum of the absolute relative difference between each experimental and calculated frequency of all selected modes.

$$F(X) = \sum_{i=1}^{n} \left| \frac{f_{\text{exp}i} - f_{\text{cal}i}}{f_{\text{exp}i}} \right| \qquad (6.4)$$

where n is the total number of natural frequencies used; $f_{\text{exp}i}$ and $f_{\text{cal}i}$ are the ith pair of experimental and calculated natural frequencies; and X is a set of elastic constants, i.e. $[E_x, E_y, G_{xy}, G_{xz}, G_{yz}]$. Theoretically, n equals to five as only five elastic constants need to be estimated. However, a greater number of natural frequencies may be used to improve the accuracy.

The fitness function is subjected to the following bound constraints,

$$X_{min} \leq X \leq X_{max} \qquad (6.5)$$

where $X_{min} = [E_{x,min}, E_{y,min}, G_{xy,min}, G_{xz,min}, G_{yz,min}]$ and $X_{max} = [E_{x,max}, E_{y,max}, G_{xy,max}, G_{xz,max}, G_{yz,max}]$. The lower and upper bounds of each elastic constant can be estimated based on prediction models and reported values in the literature.

By minimizing the fitness function, an optimal set of elastic constants would be obtained as the determined elastic constants of a tested CLT panel. The GA solver in MATLAB (MathWorks, 2014) is adopted in this study. The procedure is illustrated in Figure 6.5. The population size is set to 100 after several trials of different sizes. The initial population is created using the default function 'constraint dependent' in the solver. The fitness of each chromosome in one generation is evaluated in the fitness function, which would recall the forward solution function for calculating the natural frequencies. The experimental natural

183

frequencies are used as the initial guesses for the Newton-Raphson iteration in the forward solution, which can greatly improve its computing efficiency and accuracy. Then all the fitness values are ranked and if the best one meets the fitness limit stopping criterion, the corresponding chromosome (a set of values) will be the elastic constants of the tested CLT panel. Otherwise, a set of parent values with high standings in the fitness ranking are chosen for the next generation followed by crossover and mutation to create a new population for the fitness evaluation until the stopping criterion is met. To be noted, the fitness limit should be as close as possible to zero theoretically, however, it depends on the quality of the measured experimental frequencies as well as the accuracy of prediction model. The fitness limit should be determined with several initial GA executions according to different requirements of accuracy and computing time. The best fitness can usually be achieved within twenty generations. Since GA is a stochastic method, slightly different results may be obtained from different runs. Therefore, in this study, the optimal solutions from five individual GA executions will be averaged as the determined elastic constants of the tested CLT panels.
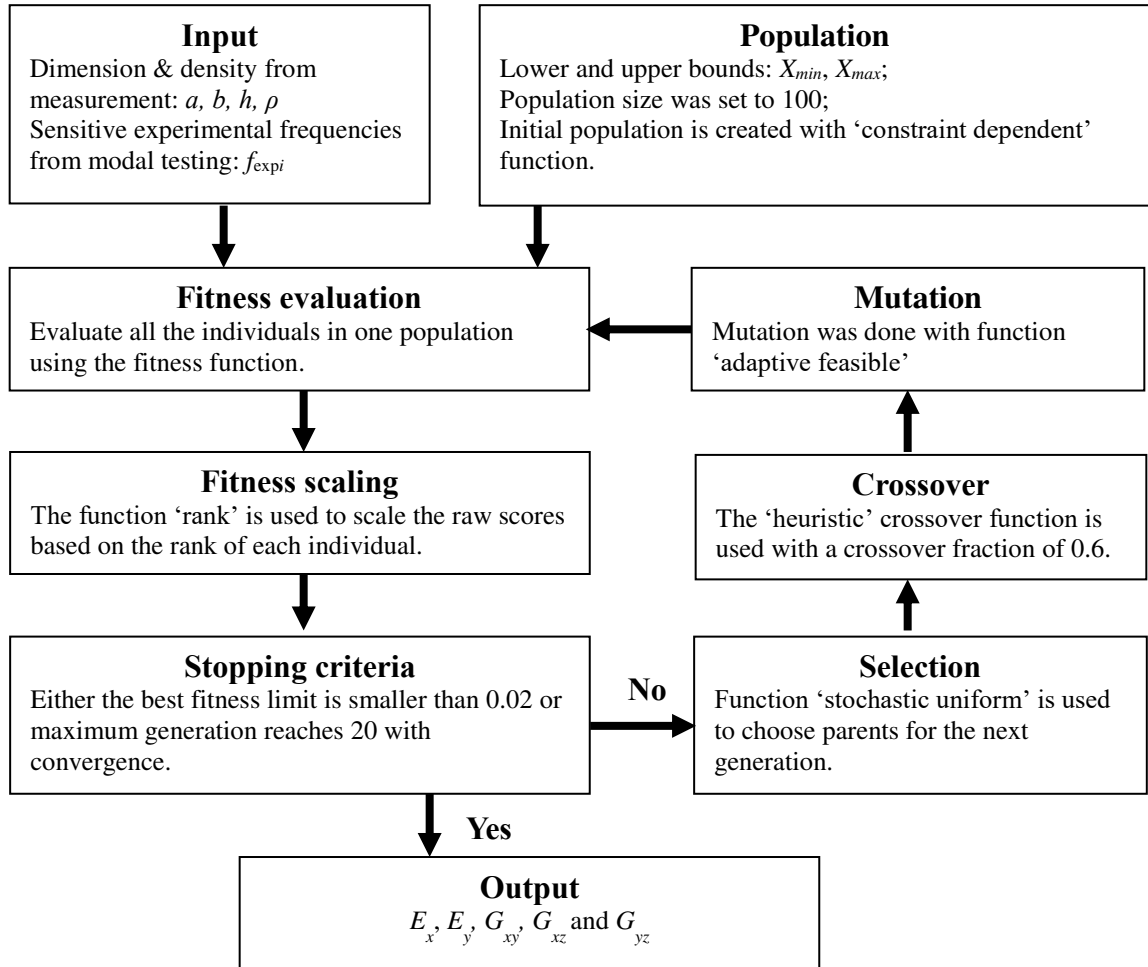
Figure 6.5 Flowchart of genetic algorithm and corresponding functions used in MATLAB

To verify the proposed algorithm, the three-layer CLT numerical model for FEM verification is used for numerical case study. The natural frequencies from exact solution in Table 1 are used as the input experimental natural frequencies. With a lower bound of [10000, 600, 400, 50, 250] MPa and an upper bound of [12000, 800, 600, 150, 450] MPa, five GA executions with first combination labeled 'Lower-5-Freqs' of frequency modes

(2, 0), (2, 1), (2, 2), (2, 3) and (3, 0) have been executed. The effective elastic constants for the numerical case have been determined as listed in Table 6.2. Each of the determined elastic constants is close to its corresponding exact value and the results from different executions are very consistent. The relative differences between the average and exact elastic constants are less than 3% and all five executions have fitness values of less than 2%. In addition, two more combinations of frequency modes have been applied for the inverse optimization. The second combination labeled as 'Higher-5-Freqs' includes modes (3, 0), (2, 1), (2, 3), (2, 4) and (4, 0), which has two higher bending modes, and the third combination labeled as '7-Freqs' includes all seven frequency modes (2, 0), (2, 1), (2, 2), (2, 3), (2, 4), (3, 0) and (4, 0). The average value and coefficient of variation (CV) for each elastic constant obtained from five GA executions are presented in Table 3. It can be seen that the differences between the average and exact elastic constants are about at the same level for all three combinations of vibration modes. However, the results of G_{xz} and G_{yz} from 'Higher-5-Freqs' and '7-Freqs' have smaller CV values than those from 'Lower-5-Freqs'. This can be explained by the low sensitivity of the selected bending modes to transverse shear moduli. It also seems that employing more frequencies such as '7-Freqs' does not provide better efficiency than employing enough sensitive frequencies such as 'Higher-5-Freqs'.

The above results have shown that the proposed method can be used for the measurement of elastic constants of thick orthotropic plates such as CLT panels using experimental natural frequencies. If a high level of accuracy is required, a number of approaches can be used, a) to execute more GA runs and take the average of all executions; b) to narrow the

range of the lower and upper bounds after several initial GA executions; and c) to include natural frequencies with high sensitivity levels.

Table 6.2 Effective elastic constants determined for the numerical case

	Run 1	Run 2	Run 3	Run 4	Run 5	Average	Exact	Δ^a
E_x (MPa)	10460	10315	10631	10515	10898	10564	10400	1.6%
E_y (MPa)	705	719	706	718	713	712	711	0.2%
G_{xy} (MPa)	521	528	524	512	521	521	518	0.6%
G_{xz} (MPa)	135	133	123	129	115	127	130	-2.4%
G_{yz} (MPa)	387	297	373	368	358	357	350	1.9%
$F(X)$	1.73%	1.39%	1.41%	1.84%	1.94%	1.66%	0	

[a] $\Delta = (x_{average}- x_{exact}) / x_{exact} \times 100\%$.

Table 6.3 Effective elastic constants determined for numerical case with different

combinations of natural frequencies

	Lower-5-Freqs			Higher-5-Freqs			7-Freqs		
	Average	CV	Δ	Average	CV	Δ	Average	CV	Δ
E_x (MPa)	10564	2.1%	1.6%	10450	2.5%	0.5%	10435	1.2%	0.3%
E_y (MPa)	712	0.9%	0.6%	711	0.4%	0.0%	713	0.5%	0.2%
G_{xy} (MPa)	521	1.1%	0.2%	514	2.9%	-0.7%	517	2.1%	-0.2%
G_{xz} (MPa)	127	6.3%	1.9%	129	4.1%	-0.7%	127	2.1%	-2.1%
G_{yz} (MPa)	357	9.9%	-2.4%	355	3.8%	1.4%	347	4.2%	-0.9%

6.3 Application to Determination of Effective Bending and Shear Stiffness of CLT

6.3.1 Materials

According to the sensitivity analysis and specimen design, the CLT panel specimens were supposed to have a length-to-thickness ratio of about thirty and width-to-thickness ratio of about ten for possible measurement of the transverse shear moduli. Therefore, two 3.24 m long and 1.07 m wide three-layer CLT panels with a lay-up of 35 mm/ 35 mm/ 35 mm were cut from one of the two full-size commercial Canadian E1 grade CLT panels reported in the previous study (Zhou and Chui, 2014). Each layer in a CLT panel was not edge-glued and exhibited a gap between two adjacent lumber elements of average 3 mm in the same layer. The gaps became much larger due to shrinkage than previously measured about two years prior to the current study and delamination could be observed in the cross sections as shown in Figure 6.6. Another 4.06 m long and 1.02 m wide five-layer SPF CLT panel with a lay-up of 26 mm/ 27 mm/ 26 mm/ 27 mm /26 mm was also prepared for modal testing. The five-layer CLT panel specimen was manufactured in year 2015 and had gaps of around 2 mm and no observed delamination. All three CLT panels had an average density of 520 kg/m^3 and a moisture content of about 12%.
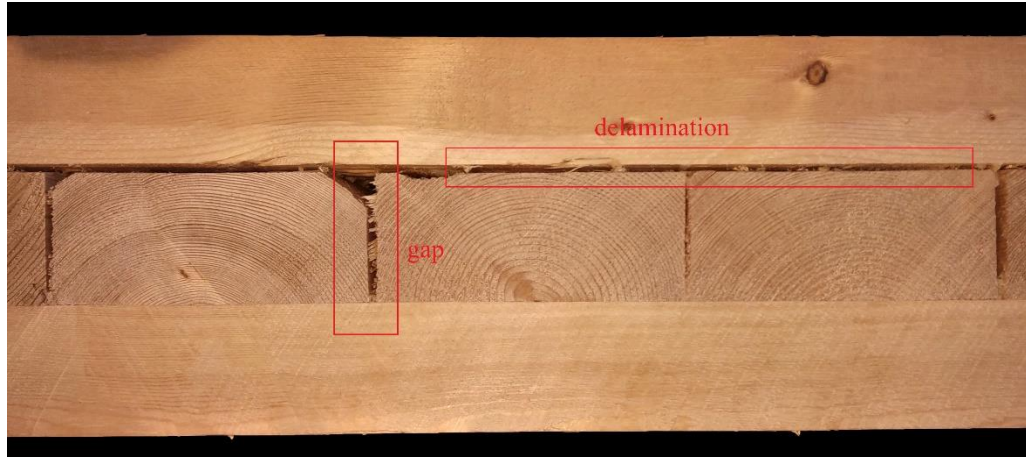
Figure 6.6 A CLT cross section with gaps and delamination

6.3.2 Experimental Modal testing and Analysis

Using the same modal test setup by Zhou et al. (2017), impact vibration tests were conducted on the specimen under SFSF boundary condition as shown in Figures 6.7 and 6.8, where the test specimen was supported on two CLT beams resting on the floor in the laboratory. The width of the contact area between the CLT specimen and the beam support was 50 mm at each end. The position for attaching accelerometer was selected at 7/12 length of one free edge, which was not on the perpendicular nodal lines of the selected sensitive frequency modes. The impact force and acceleration time signals were recorded by a data acquisition device (LDS Dactron, Brüel & Kjær) and the frequency response function (FRF) was calculated from the time signals by a data analysis software (RT Pro 6.33, Brüel & Kjær).

189
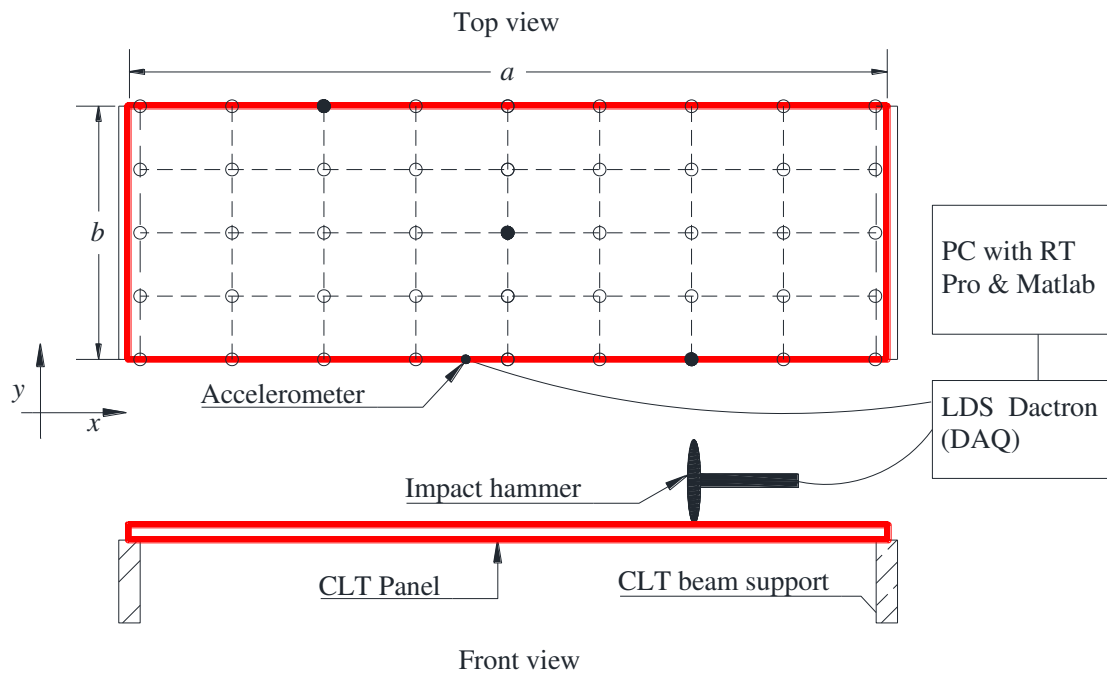
Figure 6.7 Schematic drawing of modal test setup for CLT panel specimens

Figure 6.8 A CLT panel specimen under modal testing

As discussed in the previous study (Zhou et al., 2016), the 1st and 2nd natural frequencies of a plate under SFSF were modes (2, 0) and (2, 1), respectively, which could be easily identified together with the natural frequency of mode (2, 2) from the frequency spectra of three impact positions marked as the solid circle in Figure 6.7. The other sensitive vibration modes such as (3, 0), (4, 0), (2, 3) and (2, 4) were identified by roving impact locations on all the grid nodes shown in Figure 6.7. Each of the modes was impacted three times and its average FRF was recorded. All the frequency spectra were collected and post-processed by the code written in MATLAB software for experimental modal analysis, namely mode shape plotting using imaginary patterns of the FRFs at a certain natural frequency, to identify the selected sensitive natural frequencies. The typical experimental mode shapes of the selected sensitive frequency modes are presented in Figure 6.9.
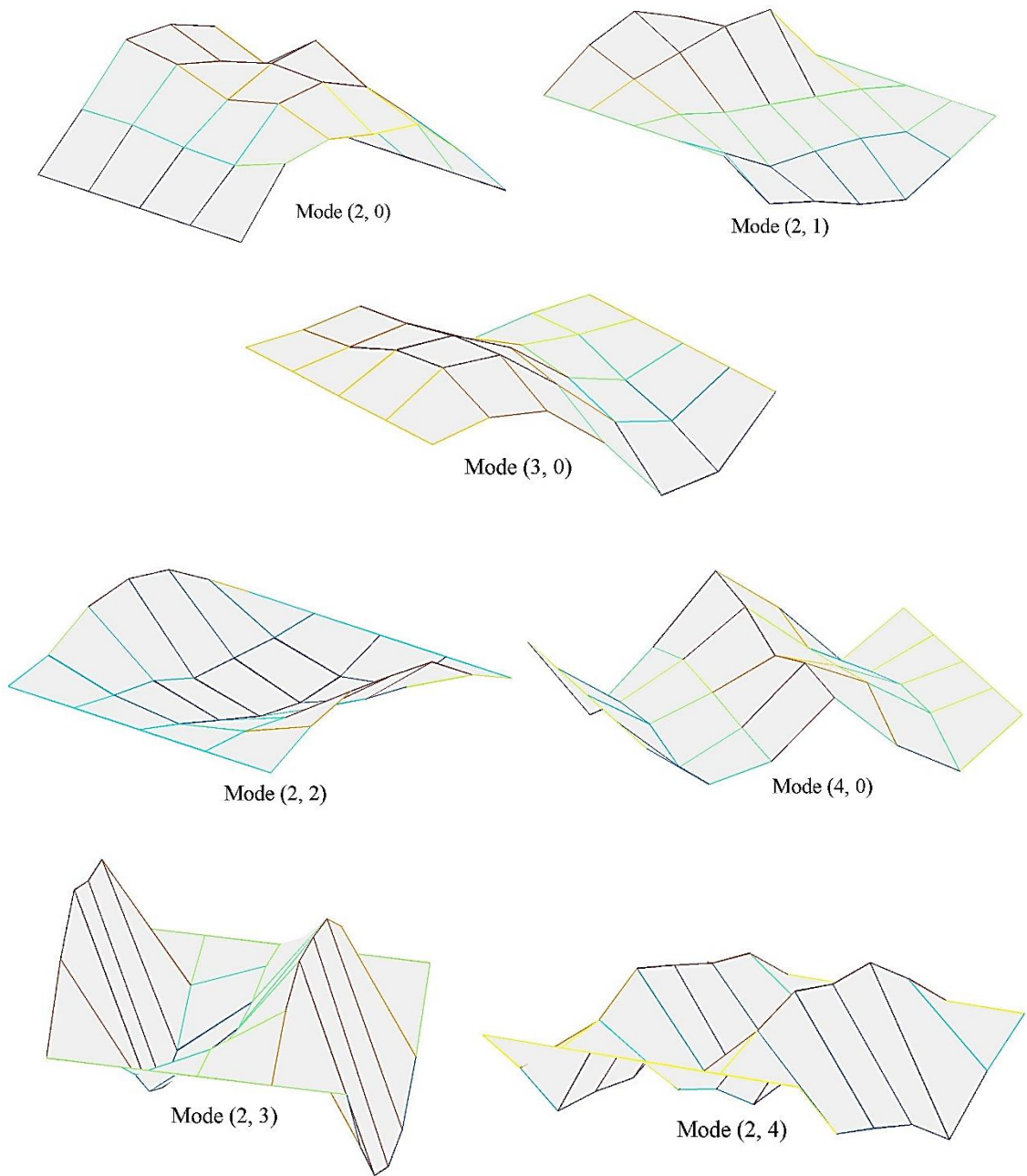
Figure 6.9 Selected mode shapes of a CLT panel specimen by experimental modal

analysis

6.3.3 Effective Bending and Shear Stiffness

Since all five elastic constants can be determined by the proposed method, either the effective bending and shear stiffness values can be obtained for the structural design of CLT such as calculation of deflections and frequency. In this study, the effective bending and shear stiffness are defined as $EI_{eff,0} = E_x I_{gross}$, $EI_{eff,90} = E_y I_{gross}$, $GA_{eff,0} = k_{xz} G_{xz} A_{gross}$ and $GA_{eff,90} = k_{yz} G_{yz} A_{gross}$. The subscripts 0 and 90 indicate the major and minor strength directions of a CLT panel, respectively. I_{gross} and A_{gross} are the gross moment of inertia and cross sectional area respectively based on the nominal thickness of the panel and a width of 1.0 m. $k_{xz} G_{xz}$ and $k_{yz} G_{yz}$ are treated as a combined term respectively in the algorithm for the determination of effective shear stiffness.

6.4 Results and Discussion

6.4.1 Fitness Evaluation of GA Executions

The effective elastic stiffness values of all three CLT panels were determined following the same procedure demonstrated in the numerical case. The selected natural frequencies measured from modal testing are listed in Table 6.4. Even though the two three-layer CLT panels were cut from the same full-size CLT panels, the frequencies of the same modes differed slightly. This was caused by the reduced homogenized elastic properties due to the existence of gaps, cracks and delamination within a full-size panel.

Table 6.4 Selected measured natural frequencies of two three-layer (CLT #1 and 2) and

one five-layer (CLT #3) CLT panels

Vibration mode	Frequency value (Hz)		
	CLT #1	CLT #2	CLT #3
(2, 0)	20.0	20.4	15.3
(2, 1)	27.7	27.9	31.1
(3, 0)	65.8	65.7	100.2
(2, 2)	96.8	100.4	289.2
(4, 0)	124.9	113.4	217.4
(2, 3)	246.3	254.5	611.2
(2, 4)	447.6	467.5	1019.0

The measured natural frequencies together with dimensions and density were input into the proposed GA for inverse determination of the effective elastic stiffness values for each CLT panel. A lower bound of [10000, 500, 200, 100, 100] MPa and an upper bound of [13000, 650, 350, 350, 350] MPa were set for the three-layer CLT panels, and lower bound of [9000, 2000, 450, 100, 100] MPa and an upper bound of [10000, 3000, 650, 350, 350] MPa were set for the five-layer CLT panel according to previous studies (Niederwestberg et al., 2016; Zhou et al., 2016). For all GA executions, the mean and best fitness values can converge within twenty generations such as that shown in Figure 6.10.
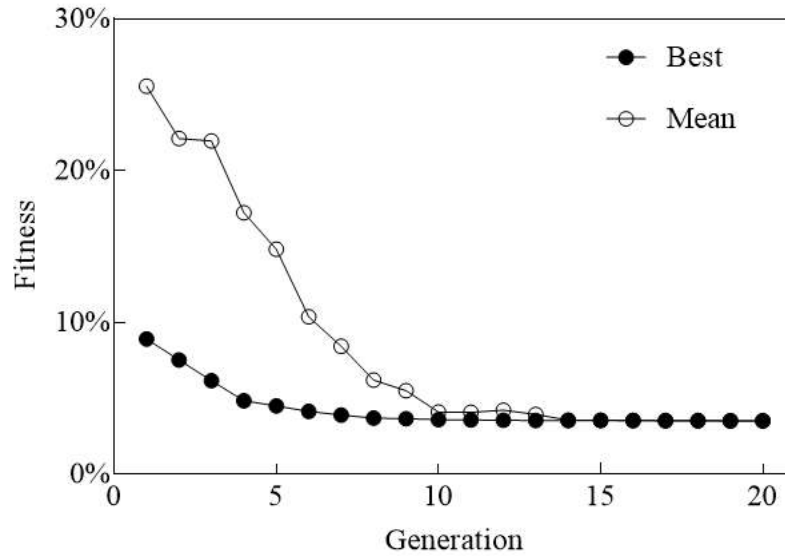
Figure 6.10 Representative mean and best fitness obtained with the increase of generation

It was found that the best fitness values for all CLT panels cannot meet the pre-defined criterion of 2% such as in the numerical case, which is mainly due to the fact that the CLT panels are not perfectly homogenous orthotropic Mindlin plates as assumed. Therefore, the second stopping criteria applied in all GA executions and the optimal results were recorded if the convergences were achieved within twenty generations. The best fitness values of all GA executions for all three CLT panels are plotted in Figure 6.11. It can be seen that with five input measured frequencies, the best fitness is about 3-5%, with seven input measured frequencies, the best fitness is about 6-8% for three-layer CLT panels and around 10% for the five-layer CLT panel. However, this does not mean that each calculated natural frequency is on average about 1% off its corresponding measured one.
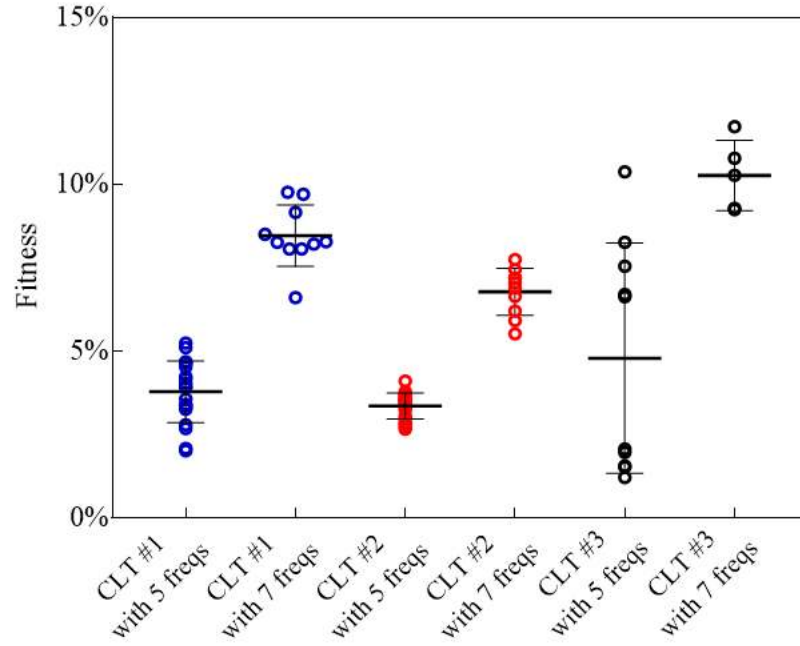
Figure 6.11 Best fitness values distribution for three CLT panels

With a further investigation of the difference between calculated and measured frequencies of each mode shown in Figure 6.12, the calculated frequencies of mode (2, 0), (2, 1), (3, 0) and (2, 4) for both three-layer CLT panels have very small discrepancies from their corresponding measured ones, while the calculated frequencies of other modes may have more possibility to be about 2-3% away from their corresponding measured ones, such as modes (2, 2) and (4, 0) for CLT #1, mode (2, 3) for CLT #2. These frequency modes are critical for the determination of $k_{yz}G_{yz}$, and the differences reveal that the low sensitivity of G_{yz} to the chosen frequency modes may increase the uncertainty of the shear stiffness determined for the CLT panels. For the five-layer CLT panel (CLT #3), the calculated frequencies of modes (2, 1) and (2, 2), especially (2, 2) which is not very sensitive to G_{yz},

were a bit off their measured values in some GA executions due to the nearly zero differences between calculated and measured frequencies of the other four modes.
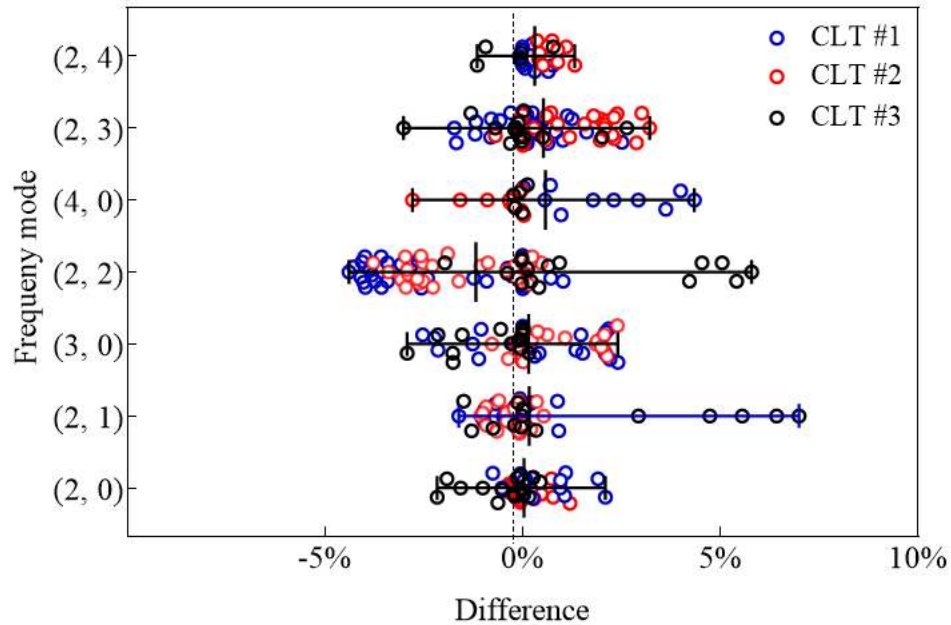
Figure 6.12 Differences between calculated and measured frequencies

6.4.2 Summary of Effective Bending and Shear Stiffness

The effective bending and shear stiffness values of all three CLT panels determined by the proposed method are listed in Table 6.5. Compared with reference values calculated based on shear analogy method using the lamination properties and assumptions for E1 grade CLT in ANSI/ APA PRG 320 (APA, 2017), to which the CLT panels in this study belong, the average $EI_{eff,0}$ values of all three panels from experiments are slightly higher. The average $EI_{eff,90}$ and $GA_{eff,0}$ values of the three-layer CLT panels is about 20% and 25% lower than their predicted reference values, respectively, due to gaps and delamination between

laminations, while the averaged $EI_{eff,90}$ value of the five-layer CLT panel is about 18% higher than its predicted reference value and its averaged $GA_{eff,0}$ value is about 15% lower than its predicted reference value. These reported differences are acceptable considering that there are inevitable variations of the assumed lamination properties from the actual properties. However, the average $GA_{eff,90}$ values of the three-layer and five-layer CLT panels are both about 163% higher than their corresponding predicted reference values. It is thought that the predicted reference $GA_{eff,90}$ values by shear analogy method are underestimated. Experimental verifications are needed.

Moreover, it is found that, CLT #2 has higher measured effective bending stiffness in both strength directions than CLT #1, because the measured natural frequencies of modes (2, 0), (2, 1) and (2, 2) of CLT #2 are higher as seen in Table 6.4. CLT #2 was also found to have less delamination than CLT #1, which may explain the differences found in their natural frequencies and stiffness values. It can also be found in Table 6.5 that the CVs of bending stiffness values are generally smaller than those of shear stiffness values, especially in the minor strength direction. The trend here is similar with what was found for the numerical case because of the different sensitivity of each elastic constant to the selected vibration modes. However, the coefficient of variations (CVs) in the brackets in Table 6.5 for the actual CLT panels are larger than those in Table 6.3 for the numerical case because of the differences between experimental and calculated frequencies as discussed above.

Table 6.5 Mean effective bending and shear stiffness values of all three CLT panels

Material	Frequency combination	$EI_{eff,0}$ (10^9 N·mm^2/m)		$EI_{eff,90}$ (10^9 N·mm^2/m)		$GA_{eff,0}$ (10^6 N/m)		$GA_{eff,90}$ (10^6 N/m)	
	Lower-5-Freqs	1129	(2.9%)	51	(2.5%)	5.6	(1.5%)	22.3	(11.4%)
CLT #1	Higher-5-Freqs	1058	(5.2%)	52	(1.6%)	6.6	(6.6%)	21.7	(13.2%)
	7-Freqs	1108	(2.5%)	52	(1.5%)	6.2	(6.2%)	23.0	(9.9%)
	Lower-5-Freqs	1216	(1.0%)	54	(2.5%)	5.2	(1.8%)	23.7	(11.3%)
CLT #2	Higher-5-Freqs	1231	(2.3%)	56	(2.0%)	4.7	(1.1%)	27.4	(13.0%)
	7-Freqs	1240	(1.2%)	56	(1.3%)	4.7	(2.9%)	25.5	(9.2%)
Average		1164		54		5.5		23.9	
Ref[1]		1088		68		7.3		9.1	
	Lower-5-Freqs	1789	(3.4%)	524	(6.0%)	10.1	(19.1%)	34.4	(15.3%)
CLT #3	Higher-5-Freqs	1837	(3.0%)	476	(2.5%)	8.9	(2.7%)	39.4	(2.7%)
	7-Freqs	1823	(2.1%)	524	(5.4%)	9.0	(2.2%)	35.7	(8.5%)
Average		1816		508		9.3		36.5	
Ref[2]		1773		430		10.9		13.9	

Note: [1,2] Reference values were calculated based on shear analogy method using the properties and assumptions for E1 grade CLT in ANSI/ APA PRG 320 (APA, 2017). The number in the bracket refers to the coefficient of variation (CV) of the elastic parameter in five genetic algorithm executions.

6.5 Conclusions

In this study a non-destructive technique employing modal testing and genetic algorithm has been proposed for the inverse determination of effective in-plane and out-of-plane elastic constants of thick orthotropic plates such as CLT panels. As verified in the numerical case, the proposed method is reliable and accurate in determining the elastic constants of orthotropic Mindlin plates using natural frequencies of selected sensitive

natural frequencies. Sensitivity analysis, specimen design and GA execution strategies are also provided for reliable measurements. Based on that, the effective bending and shear stiffness values of three symmetric CLT panels have been successfully determined. The effect bending and shear stiffness values in the major strength determined from the proposed method agree well with the reference values based on shear analogy method. A discrepancy was observed between determined and predicted effective shear stiffness values in the minor strength direction. Future research will focus on the verification of the proposed method with more experimental data, especially for transverse shear moduli.

Acknowledgements

References

ABAQUS. (2013). *ABAQUS version 6.13 Documentation*. Dassault Systèmes Simulia Corp., Providence, RI.

APA (The Engineered Wood Association). (2017). *Standard for performance-rated cross-laminated timber*. ANSI/ APA PRG 320. APA - The Engineered Wood Association, Tacoma, WA, USA.

Araújo, A. L., Mota Soares, C. M., & Moreira De Freitas, M. J. (1996). Characterization of material parameters of composite plate specimens using optimization and experimental vibrational data. *Composites Part B: Engineering*, *27*(2), 185–191.

Ayorinde, E. (1995). Elastic constants of thick orthotropic composite plates. *Journal of Composite Materials*, *29*(8), 1025–1039.

CEN. (2006). *Eurocode 5 Design of timber structures. Part 1-1: General Common rules and rules for buildings*. EN 1995-1-1. European Committee for Standardization, Brussels.

Chui, Y. H., Gong, M. (2015). *Evaluation of planar shear properties of cross layer in massive timber panel*. Final Report #: WSTC2013-015, Wood Science and Technology Centre, the University of New Brunswick, Fredericton, NB, Canada.

Coppens, H. (1988). Quality control of particleboards by means of their oscillation behavior. In *FESYP Technical Conference* (pp. 143–165). Munich.

CSA. (2016). *Engineering design in wood*. CSA O86.14. Canadian Standards Association, Mississauga, ON, Canada.

Cunha, J., Cogan, S., & Berthod, C. (1999). Application of genetic algorithms for the identification of elastic constants of composite materials from dynamic tests.

International Journal for Numerical Methods in Engineering, *45*(7), 891–900.

Dasgupta, D., & Michalewicz, Z. (Eds.). (2013). *Evolutionary Algorithms in Engineering Applications*. Springer Science & Business Media.

Ehrhart, T., Brandner, R., Schickhofer, G., & Frangi, A. (2015). European Timber Species with Focus on Cross Laminated Timber (CLT): Test Configuration and Parameter Study. In R. Görlacher (Ed.), *Proceedings of 2nd International Network on Timber Engineering Research* (pp. 61–75). Sibenik: Timber Scientific Publishing.

Frederiksen, P. (1997a). Experimental Procedure and Results for the Identification of Elastic Constants of Thick Orthotropic Plates. *Journal of Composite Materials*, *31*(4), 360–381.

Frederiksen, P. (1997b). Application of an improved model for the identification of material parameters. *Mechanics of Composite Materials and Structures*, *4*(4), 297–316.

Frederiksen, P. S. (1998). Parameter uncertainty and design of optimal experiments for the estimation of elastic constants. *International Journal of Solids and Structures*, *35*(12), 1241–1260.

Gagneja, S., Gibson, R. F., & Ayorinde, E. O. (2001). Design of test specimens for the determination of elastic through-thickness shear properties of thick composites from measured modal vibration frequencies. *Composites Science and Technology*, *61*(5), 679–687.

Gsell, D., Feltrin, G., Schubert, S., Steiger, R., & Motavalli, M. (2007). Cross-Laminated Timber Plates: Evaluation and Verification of Homogenized Elastic Properties.

Journal of Structural Engineering, *133*(1), 132–138.

Gülzow, A. (2008). *Zerstörungsfreie Bestimmung der Biegesteifigkeiten, von Brettsperrholzplatten*. ETH Zürich.

Hwang, S.-F., Wu, J.-C., & He, R.-S. (2009). Identification of effective elastic constants of composite plates based on a hybrid genetic algorithm. *Composite Structures*, *90*(2), 217–224.

Liu, B., & Xing, Y. (2011). Exact solutions for free vibrations of orthotropic rectangular Mindlin plates. *Composite Structures*, *93*(7), 1664–1672.

Liu, B., Xing, Y. F., & Reddy, J. N. (2014). Exact compact characteristic equations and new results for free vibrations of orthotropic rectangular Mindlin plates. *Composite Structures*, *118*(1), 316–321.

Liu, G. R., & Han, X. (2003). *Computational inverse techniques in nondestructive evaluation*. CRC Press LLC.

Lo, K. H., Christensen, R. M., & Wu, E. M. (1977). A High-Order Theory of Plate Deformation Part 1: Homogeneous Plates. *Journal of Applied Mechanics*, *44*(4), 663–668.

MathWorks. (2014). *Optimization Toolbox™ User's Guide (r2014a)*. Natick, MA: The MathWorks, Inc.

Niederwestberg, J., Chui, Y. H., & Gong, M. (2016). Influence of layer and laminate characteristics on shear properties of cross laminated timber and hybrids. In E. Josef, W. Wolfgang, F. Alireza, & P. Martina (Eds.), *World Conference on Timber Engineering* (pp. 1081–1090). Vienna: TU-MV Media Verlag GmbH.

Reddy, J. N. (1984). A simple higher-order theory for laminated composite plates.

Journal of Applied Mechanics, *51*(4), 745–752.

Silva, M. F. T., Borges, L. M. S. A., Fernando, A. R., & De Carvalho, L. A. V. (2004). A genetic algorithm applied to composite elastic parameters identification. *Inverse Problems in Science and Engineering*, *12*(1), 17–28.

Soares, C. M. M., de Freitas, M. M., Araújo, A. L., & Pedersen, P. (1993). Identification of material properties of composite plate specimens. *Composite Structures*, *25*(1–4), 277–285.

Steiger, R., Gülzow, A., Czaderski, C., Howald, M. T., & Niemz, P. (2012). Comparison of bending stiffness of cross-laminated solid timber derived by modal analysis of full panels and by bending tests of strip-shaped specimens. *European Journal of Wood and Wood Products*, *70*(1–3), 141–153.

Gagnon, S. & Popovski, M.. (2011). Structure design of cross-laminated timber elements. In G. Sylvain & P. Ciprian (Eds.), *CLT Handbook* (1st ed., pp. 114–185). FPInnovations.

Xing, Y., & Liu, B. (2015). *Exact Sloutions of Free Vibrations of Plates and Shells* (1st ed.). Beijing: Science Press Ltd.

Yu, L. (2006). *Identification of elastic constants of composite materials from vibration data of thick plates*. Wayne State University.

Zhou, J., & Chui, Y. H. (2014). Efficient measurement of elastic constants of cross laminated timber using modal testing. In A. Salenikovich (Ed.), *World Conference on Timber Engineering*. Quebec City.

Zhou, J., Chui, Y. H., Gong, M., & Hu, L. (2016). Simultaneous measurement of elastic constants of full-size engineered wood-based panels by modal testing.

Holzforschung, *70*(7), 673–682.

Zhou, J., Chui, Y. H., Gong, M., & Hu, L. (2017). Elastic properties of full-size mass timber panels: Characterization using modal testing and comparison with model predictions. *Composites Part B: Engineering*, *112*, 203–212.

CHAPTER 7 EFFECTIVE BENDING AND SHEAR STIFFNESS OF CROSS LAMINATED TIMBER BY MODAL TESTING: EXPERIMENTAL VERIFICATION

Abstract: A non-destructive method employing modal testing and genetic algorithm has been proposed to determine the elastic constants of cross laminated timber (CLT) by the first author. The elastic constants measured by static methods were used to verify the effective bending and shear stiffness values of two 3-layer CLT panels obtained by the proposed method in this study. The results showed that the in-plane elastic constants including E_x, E_y and G_{xy} agreed well with static test results. The values of transverse shear moduli, namely G_{xz} and G_{yz}, were determined using effective shear stiffness values with proper shear correction factors (SCFs). The transverse shear moduli by modal tests together with the calculated SCFs were verified with reference values by a modified planar shear tests of CLT blocks. Timoshenko beam theory with modified SCFs method was shown to be more appropriate for predicting effective shear stiffness of the 3-layer CLT than shear analogy method based on the measured transverse shear stiffness values.

Keywords: cross laminated timber, transverse shear modulus, shear correction factor, planar shear tests

7.1 Introduction

In the previous study (Zhou et al., 2018), the effective bending and shear stiffness of cross laminated timber (CLT) panels were determined by modal testing for structural design purposes. It was found that CLT as a non-homogenous laminated composite material made of highly orthotropic lumber pieces has relatively small shear stiffness values compared with its bending stiffness values. Though five elastic constants can be obtained by the proposed method with five selected experimental frequencies, it is difficult to present the transverse shear moduli of CLT since common shear correction factors (SCFs) such as $\pi^2/12$ and 5/6 are not appropriate. Stürzenbecher et al. (2010) demonstrated that, only with suitable SCFs, orthotropic Mindlin plate theory can be used for the structural design of CLT as a plate element with adequate accuracy compared with high-order shear theory using predicted transverse shear moduli. Shear analogy method by Kreuzinger (1999) and Timoshenko beam theory with modified SCFs by Schickhofer et al. (2009) are the two main structural design methods of CLT as a beam element that account for the transverse shear effect by calculating the effective bending and shear stiffness values separately. Bogensperger et al. (2012) demonstrated that, the difference between Timoshenko beam theory with modified SCFs and shear analogy method was nearly negligible for the structural design of CLT beams by various case studies, especially in terms of deflection calculation in the major strength directions. However, little experimental data can be found to verify the accuracy of both models in predicting effective transverse shear stiffness in both strength directions. Thus, it is of great interest to determine the transverse shear moduli of CLT panels obtained from the proposed method (Zhou et al., 2018) based on orthotropic Mindlin plate theory with proper SCFs.

It is known that the shear effect increases with the decrease of length-to-depth ratio or wavelength as well as the increase of elastic modulus-to-transverse shear modulus ratio (E/G). Shear correction factors (SCFs) were introduced to compensate for the assumption of first-order shear theory that the shear strain is uniform through the depth of the cross section. SCFs can be determined by energy principle for laminated composite materials (Vlachoutsis, 1992; Whitney, 1973). Stürzenbecher et al. (2010) calculated the SCFs of three- to seven-layer CLT panels using Whitney's equations. The SCFs in two transverse planes, namely k_{xz} and k_{yz}, were determined to be 0.154 and 0.752, respectively, for a 3-layer symmetric CLT panel made of grade C24 lumber (CEN, 2004) with an assumed rolling shear modulus (G_r) of 50 MPa. Bogensperger et al. (2012) presented the SCFs in the transverse plane along major strength direction (k_{xz}) for symmetric 3-layer, 5-layer and 7-layer CLT panels. k_{xz} ranges from 0.149 to 0.206 for symmetric 3-layer CLT panels with the shear modulus-to-rolling shear modulus ratio (G/G_r) of lumber from 14.4 to 10.0. A formula was provided to determine k_{xz} with other G/G_r ratios by interpolation. Both methods showed the SFCs of CLT were significantly affected by the shear moduli of face and core layers, especially the low shear modulus of core layer.

On measuring the transverse shear modulus of wood-based materials, there are mainly two static methods. The first static method is to conduct center point bending test on a beam specimen with variable span-to-depth ratios to measure different apparent modulus of elasticity (MOE) values as described in ASTM D198 (ASTM, 2015). Then the true MOE and shear modulus (G) can be determined by fitting the apparent MOE and span-to-depth ratios based on Timoshenko beam theory. The variable-span bending test method is

208

applicable for homogenous solid beams. However, its accuracy is highly dependent on the precision of load and displacement measurements as well as the goodness of curve fitting. In addition, the SCF of $\pi^2/12$ or $5/6$ may result in inappropriate transverse shear modulus of CLT. The second static method is to conduct planar shear test for direct measurement of shear force and deformation, such as Method A in ASTM D2718 (ASTM, 2011). It was developed for testing the transverse (through thickness) shear properties of thin structural wood-based panels such as plywood and oriented strand board (OSB). If thick massive timber panels such as structural composite lumber (SCL) and CLT panels are to be tested, modification of the test method is needed to minimize the influence of secondary stresses.

The aim of this study was to verify the elastic constants of the 3-layer CLT panels obtained from modal tests, especially transverse shear moduli, by static tests. The modified planar shear test method according to Niederwestberg et al. (2016) was chosen for measuring the transverse shear moduli in both strength directions as reference values for the 3-layer CLT panels tested in the previous study (Zhou et al. 2018). The test results were compared with predicted effective transverse shear stiffness by shear analogy method by Kreuzinger (1999) and Timoshenko beam theory with modified SCFs by Schickhofer et al. (2009).

7.2 Materials and Method

7.2.1 Materials

The 3-layer CLT panels in the previous study (Zhou et al., 2018) were used for preparing the test specimens in this study. Six CLT shear block specimens of 400 mm long and 152

mm wide were cut from the major and minor strength directions of the CLT panel, respectively. The shear blocks were selected with gaps of not larger than 2 mm and without visible delamination. Then the top and bottom surfaces of a block specimen were glued to two aluminium plates using a two-component epoxy adhesive. All the specimens were pressed with a pressure of 0.8 MPa under the environmental temperature around 20 °C for at least 24 hours for curing before tests. The CLT shear block specimens were prepared for planar shear tests.

7.2.2 Planar Shear Tests

Since the static results of the other three elastic constants (E_x, E_y and G_{xy}) can be found in a previous study (Zhou and Chui, 2014), only transverse shear moduli were measured by static tests in this study. Planar shear tests were conducted for transverse shear moduli according to ASTM D2718 (ASTM, 2011) with a modified setup and formula by Niederwestberg et al. (2016). The specimen was assembled on the universal testing machine similar to a compression test as shown in Figure 7.1. A compressive load was applied to the top edge of the aluminium shear plate with displacement rate of 0.5 mm/ min. Other than the test setup in ASTM D2718 (ASTM, 2011), the CLT shear block specimens were loaded at an angle to keep the thick specimen stable during the test. The relative displacements between the plates were measured using two linear variable differential transformers (LVDTs) attached on the aluminium plates both front and back. The slopes of both load-displacement curves were averaged for the calculation of global transverse shear moduli, G_{xz} and G_{yz}, using the following formula.

$$G_{transverse} = \frac{Ph}{\Delta lw} \cos \theta \tag{7.1}$$

210

where $G_{transverse}$ is the transverse shear modulus, G_{xz} or G_{yz}, P/Δ is the slope of the load-displacement in the elastic range, l, w and h are the length, width and thickness of a CLT block specimen, respectively, and θ is the angle between the load direction and the center line of CLT block specimen shown in Figure 6.1, which is about 14 degrees in this study.
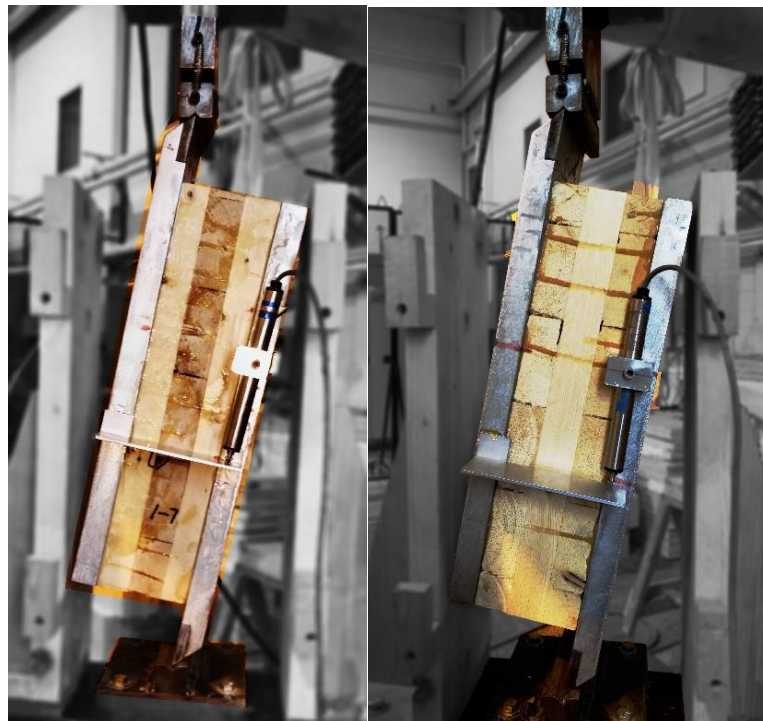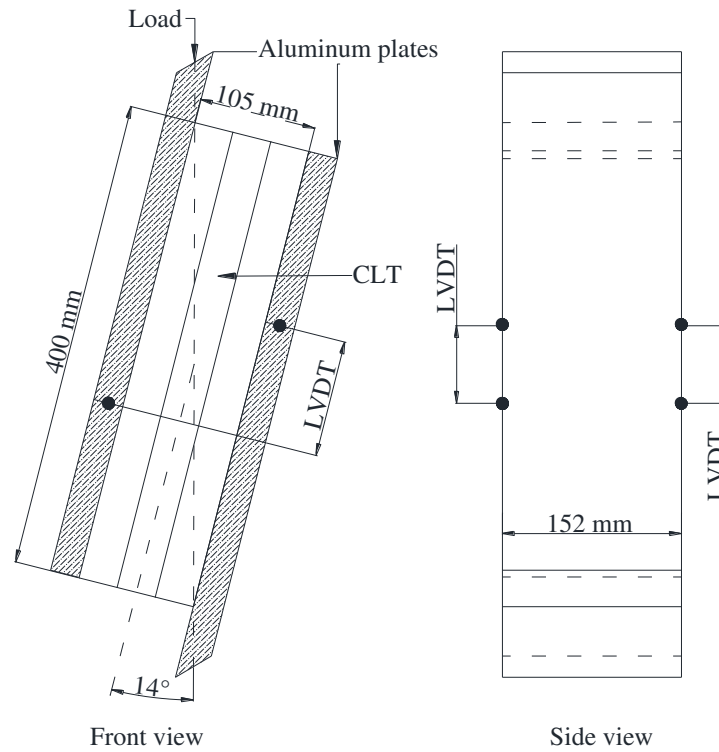
Figure 7.1 Schematic drawing of planar shear test setup (top) and CLT blocks under testing in the major (bottom-right) and minor (bottom-left) strength directions

7.2.3 Shear Correction Factors of CLT

The shear correction factor (k) of CLT can by calculated by the following equation (Bogensperger et al., 2012)

$$k = \frac{EI_{eff}^2}{\sum G_i A_i \cdot \int\limits_{-t/2}^{t/2} \frac{[E(z) \cdot S(z)]^2}{G(z) \cdot b(z)} dz} \tag{7.2}$$

$$EI_{eff} = \sum_{i=1}^{n} E_i \cdot b_i \cdot \frac{h_i^3}{12} + \sum_{i=1}^{n} E_i \cdot A_i \cdot z_i^2 \tag{7.3}$$

where EI_{eff} is the effective bending stiffness; E_i, G_i, b_i, h_i, A_i and z_i are the elastic modulus, shear modulus, width, thickness, cross sectional area and the distance from the center of the ith layer to the neutral axis of the ith layer, respectively; t is the total thickness; $E(z)$, $G(z)$, $S(z)$, $b(z)$ are the elastic modulus, shear modulus, the first moment of inertia of the integrated section and width of the cross section as a function of z; z is the axis along the thickness ranging from $-t/2$ to $t/2$ with its origin at the neutral axis of the cross section. The calculation of k can be simplified in a tabular manner presented by Wallner-Novak et al. (2014).

7.2.4 Prediction Models of Effective Transverse Shear Stiffness

According to shear analogy method (Kreuzinger 1999), the effective shear stiffness ($GA_{eff,SA}$) of CLT in two strength directions can be calculated as,

$$GA_{eff,SA} = a^2 \cdot \left[\frac{h_1}{2 \cdot G_1 \cdot b_1} + \sum_{i=2}^{m-1} \frac{h_i}{G_i \cdot b_i} + \frac{h_m}{2 \cdot G_m \cdot b_m} \right]^{-1} \tag{7.4}$$

and according to Timoshenko beam theory with modified SCFs (Schickhofer et al., 2009), the effective shear stiffness ($GA_{eff,Timo}$) is calculated as,

$$GA_{eff,Timo} = k \cdot GA = k \cdot \sum_{i=1}^{m}(G_i \cdot b_i \cdot h_i) \tag{7.5}$$

where G_i, b_i and h_i are the shear modulus, width and thickness of the ith layer; a is the distance between the centroid of the surface and bottom layers; m is total number of layers; k is the shear correction factor calculated by Eq. 7.2.

7.3 Results and Discussion

7.3.1 Verification of In-plane Elastic Constants

The validity of E_x, E_y and G_{xy} determined by modal tests in the previous study (Zhou et al., 2018) can be checked with the static values of the full-size CLT panel from which the CLT panels in this study were cut presented in our previous study (Zhou and Chui, 2014; Zhou et al., 2016). As shown in Table 6.1, the mean values of E_x and E_y by static methods are 10887 MPa and 516 MPa, respectively, which are about 10% and 7% lower than the mean values of E_x and E_y obtained in this study. The static G_{xy} values were reported to range from 270 to 340 MPa with a mean about 300 MPa (Zhou et al., 2016), while the modal test G_{xy} values range from 230 to 256 MPa with a mean about 244 MPa due to the gaps and delamination discussed in the previous study (Zhou et al., 2018).

Table 7.1 In-plane elastic constants of the 3-layer CLT panels measured by different

methods

Methods	Frequency combination	E_x (MPa)	E_y (MPa)	G_{xy} (MPa)
Mindlin plate vibration[1]	$f_{20}, f_{21}, f_{22}, f_{23}, f_{30}$	12151	547	239
	$f_{30}, f_{21}, f_{23}, f_{24}, f_{40}$	11866	564	248
	$f_{20}, f_{21}, f_{22}, f_{23}, f_{30}, f_{24}, f_{40}$	12168	559	244
	Mean	12062	557	244
Thin plate vibration[2]	f_{20}, f_{21}, f_{22}	11606	508	268
Static methods[3]	/	10887	516	300

Note: [1] (Zhou et al., 2018), [2] (Zhou and Chui, 2014), [3] (Zhou et al., 2016).

Generally, E_x, E_y and G_{xy} are not significantly affected by the combination of frequencies, since their sensitive vibration modes are included in all three frequency combinations. The mean values of E_x, E_y and G_{xy} for both CLT panels are inversely determined to be 12062 MPa, 557 MPa, and 244 MPa, respectively, regardless of frequency combinations. Their corresponding values of the full-size CLT panel, from which the two CLT panels were cut, were previously measured to be 11606 MPa, 508 MPa and 268 MPa respectively, by modal testing based on the theory of orthotropic thin plate vibration (Zhou and Chui, 2014). A small increase of E_x and E_y and a small decrease of G_{xy} are observed in this study. The increase of E_x and E_y was not surprising because the Mindlin plate theory considers the effect of transverse shear. Even though the length/ width to thickness ratio of the full-size CLT panel tested in (Zhou and Chui, 2014) is much larger than that for the two CLT panels tested in (Zhou et al., 2018), the effect of transverse shear is still not negligible. However, the decrease of G_{xy} is mainly due to the increasing gap between lumber laminates in the

same layer, delamination between layers observed on the cross sectional surfaces and cracks developed at the ends of the lumber.

7.3.2 Verification of Transverse Shear Moduli

The G_{xz} and G_{yz} values of CLT block specimens measured by planar shear tests are presented in Figure 7.2 with a mean value of 255 and 253 MPa, respectively. One of the block shear specimens was excluded from the analysis as its G_{xz} was measured to be 60 MPa. An initial delamination between cross layers was observed after it quickly failed. The G_{xz} and G_{yz} values measured by Niederwestberg et al. (2016) using the same static method range from 100 to 330 MPa, and 75 to 350 MPa, respectively, for three-layer symmetric spruce CLT panels with 19-mm-thick spruce lumber laminates and different saw patterns. The static results obtained in this study fall into the ranges reported by Niederwestberg et al. (2016).
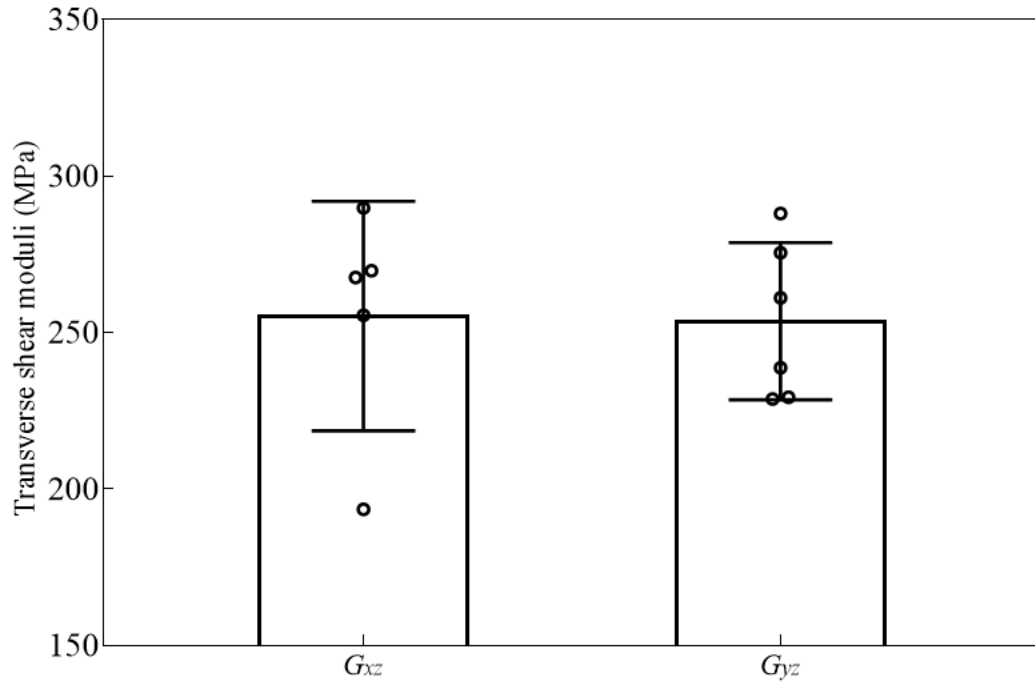
Figure 7.2 Transverse shear moduli of CLT by planar shear tests

Recall the effective shear stiffness determined in the previous study (Zhou et al., 2018), they were presented in terms of the product of shear modulus, area and shear correction factor. Therefore, the effect transverse shear modulus can be calculated using the effective shear stiffness values obtained from modal tests if SCF can be determined based on Eq. 7.2. However, it is impossible to calculate the exact SCF value of each individual CLT specimens tested, since the lumber pieces within a CLT panel vary in terms of density, growth ring orientation, grain angle and local defects. Chui and Gong (2015) reported that the rolling shear modulus of Canadian black spruce, which was the raw material of the CLT specimens tested in this study, were measured to be 130 MPa on average, with a maximum and minimum of 180 MPa and 80 MPa, respectively. Given that the shear modulus of spruce-pine-fir (SPF) is between 560 and 730 MPa (APA, 2017), the G/G_r ratio

of the three-layer CLT panels in this study is assumed to range from 3 to 10. The SCFs in two strength directions of 3- and 5-layer symmetric CLT panels were calculated using the elastic properties of lumber laminates assumed for E1 grade CLT (APA, 2017) with a G/G_r ratio from 3 to 10 as shown in Figure 7.3. It can be seen that the SCFs decrease with increase of G/G_r ratio except the k_{yz} of the 3-layer CLT, which increases slightly with the G/G_r ratio increases from 3 to 6 and then decreases thereafter.
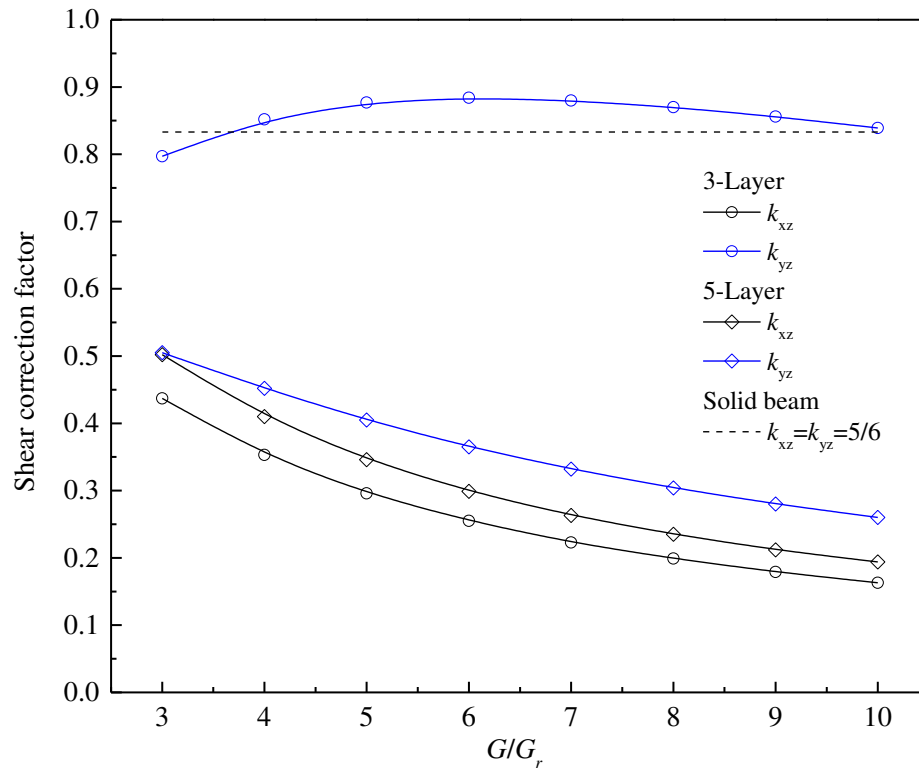
Figure 7.3 Shear correction factors of 3- and 5-layer symmetric CLT in two strength directions

With the relationship between SCFs and G/G_r ratios, the mean effective shear stiffness values in two strength directions determined in the previous study (Zhou et al., 2018) were

transformed to effective transverse shear moduli values as shown in Figure 7.4 and 7.5. It can be seen that with G/G_r ratios increasing from 3 to 10, the effective transverse shear modulus in the major strength direction increase from 120 to 320 MPa, while the one in the minor strength direction slightly changes between 250 and 286 MPa. With the mean planar shear test values as references, a G/G_r ratio of around 7 results in the most appropriate effective transverse shear moduli for the 3-layer CLT panels tested in this study. This is in line with the mean G/G_r ratio of around 6 based on the reported rolling shear modulus values reported by Chui and Gong (2015). Therefore, the proposed method in the previous study (Zhou et al., 2018) is proved to be able to determine transverse shear moduli using effective shear stiffness values obtained from the modal tests, but appropriate SCFs should be determined for both strength directions based on its layup and lamination properties.
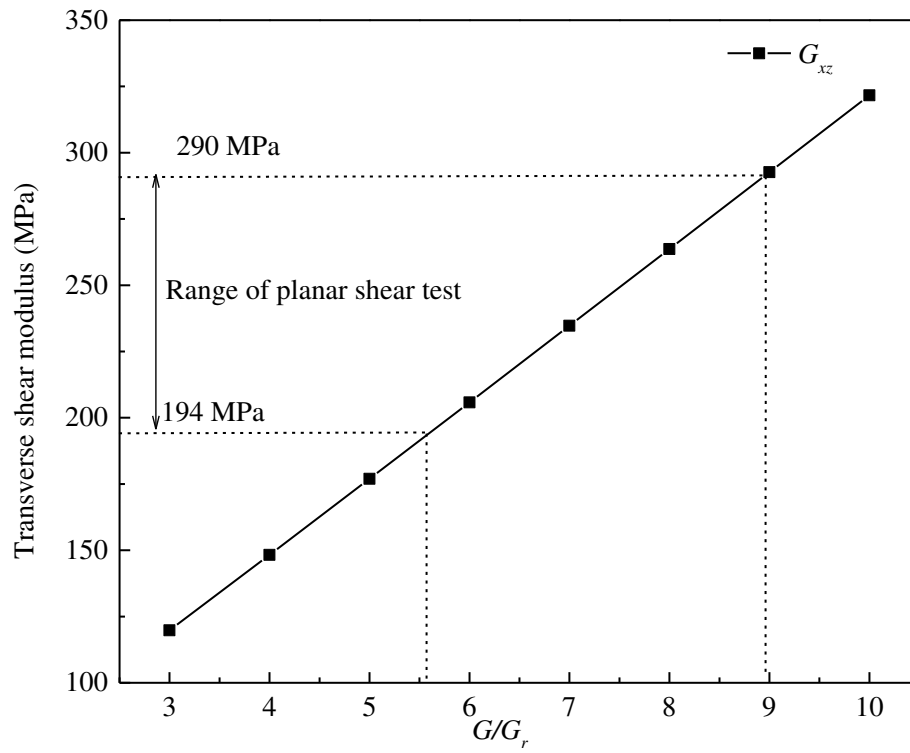
Figure 7.4 Effective transverse shear modulus in the major strength directions with

different G/G_r ratios
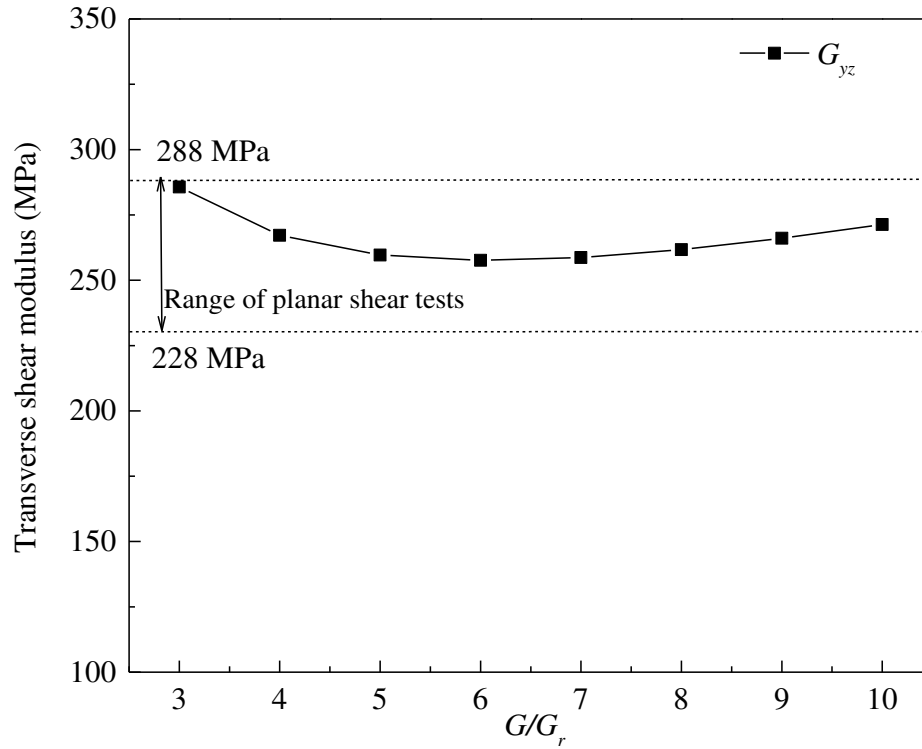
Figure 7.5 Effective transverse shear modulus in the minor strength directions with

different G/G_r ratios

7.3.3 Comparison with Predicted Effective Transverse Shear Stiffness

The effective transverse shear stiffness values of the 3-layer CLT panel were calculated

using the laminate properties assumed for E1 grade CLT by the shear analogy method and

Timoshenko beam theory with modified SCFs method. The comparison between measured

values by modal tests in the previous study (Zhou et al., 2018) and the predicted values in

two strength directions are illustrated in Figures 7.6 and 7.7. It can been from Figure 7.6

that the measured effective transverse shear stiffness values are smaller than the predicted

values with the G/G_r ratio ranging from 3 to 10 by both models. The difference is thought

to cause by two reasons. First, the 3-layer CLT were not edge-glued and had gaps, which cannot be accounted for in the models. Second, the delamination and development of gaps and cracks within the panel caused the degradation of stiffness values. However, for effective transverse stiffness in the minor strength direction as shown in Figure 7.7, only predicted values by Timoshenko beam theory with modified SCFs method fall into the range of measured values. This is due to the existence of middle layer parallel to grain, which leads to a small variation of SCF and dominates the effective shear stiffness in the minor strength direction. Shear analogy method only predicts close results with G/G_r ratio of 3, and underestimates the effective shear stiffness of the 3-layer CLT panel in the minor strength direction.

Moreover, the difference between shear analogy method and Timoshenko beam theory with modified SCFs method in predicting effective transverse shear stiffness is about 15% for the major strength direction regardless of G/G_r ratio, while difference in the minor strength direction increases from 20% to 60% with the increase of G/G_r ratio from 3 to 10. The findings verify the similar discrepancy found between measured and predicted values by shear analogy method in the previous study (Zhou et al., 2017). Based on the effective transverse shear moduli by planar shear tests and the effective shear stiffness values by modal tests, the Timoshenko beam theory with modified SCFs method seems to be more appropriate for predicting the effective shear stiffness of the 3-layer CLT in both strength directions than the shear analogy method.
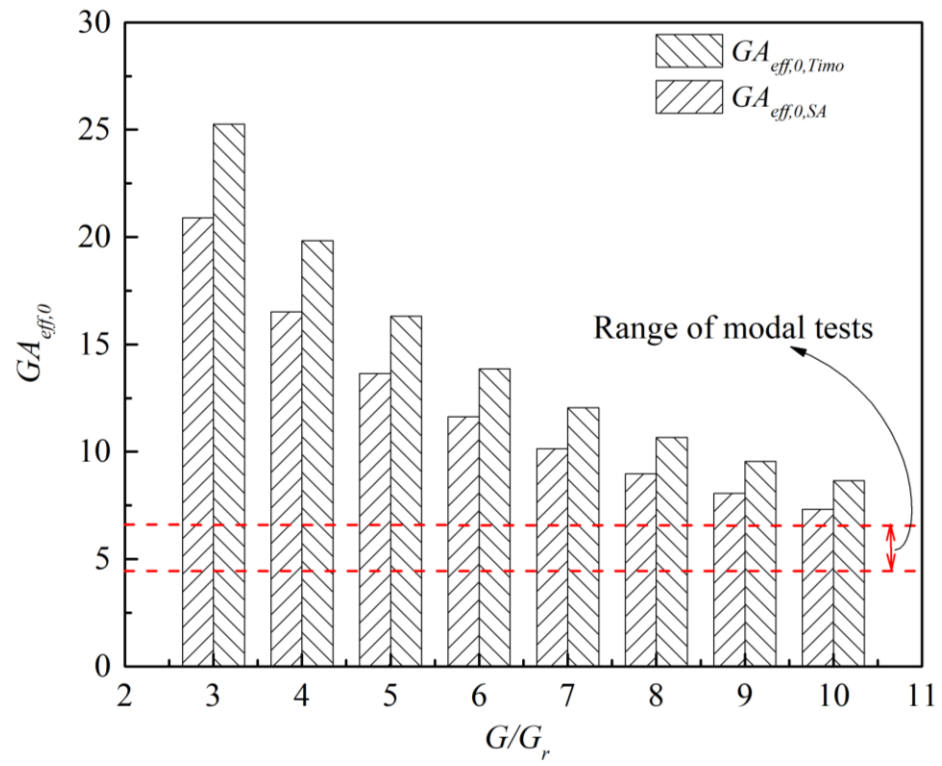
Figure 7.6 Predicted effective shear stiffness in the major strength direction with

different G/G_r ratios
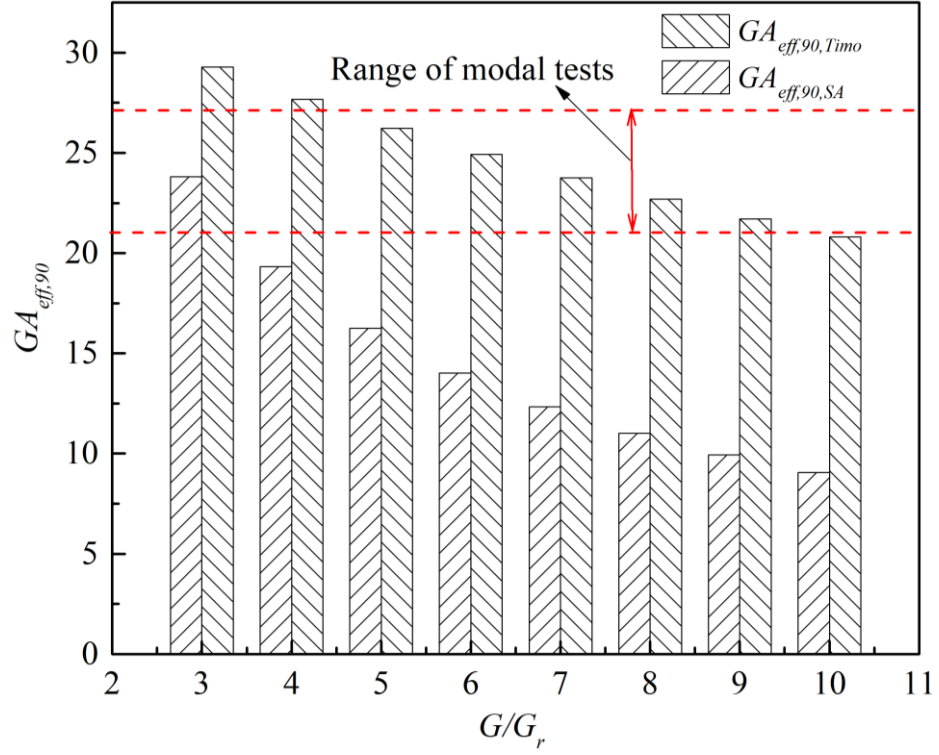
Figure 7.7 Predicted effective shear stiffness in the minor strength direction with different

G/G_r ratios

7.4 Conclusions

The validation of the elastic constants of the 3-layer CLT panel measured by the proposed

method in (Zhou et al., 2018) has been checked with static test results. The in-plane elastic

constants, namely E_x, E_y and G_{xy}, are verified to be sufficiently accurate for the 3-layer

CLT panels tested. The verification of transverse shear moduli, namely G_{xz} and G_{yz},

measured by modal tests has been conducted with the reference values measured by planar

shear tests. The effective transverse shear moduli of the 3-layer CLT panel match with

those measured by planar shear tests with a G/G_r ratio of around 7. The effect of shear

correction factor should be considered when the proposed method is applied to laminated composite materials with low transverse shear moduli for determining their elastic constants. Both shear analogy method and Timoshenko beam theory with modified SCFs have close predictions with measured effective shear stiffness of CLT in the major strength direction, while only the latter method is able to predict reasonably accurate effective shear stiffness in the minor strength direction.

References

APA (The Engineered Wood Association). (2017). *Standard for performance-rated cross-laminated timber*. ANSI/ APA PRG 320. APA - The Engineered Wood Association, Tacoma, WA, USA.

ASTM. (2015). *Standard test methods of static tests of lumber in structural sizes*. Designation: D198-15. American Society for Testing and Materials, West Conshohocken, PA, USA.

ASTM. (2011). *Standard test methods for structural panels in planar shear (rolling shear)*. Designation: D2718-00. American Society for Testing and Materials, West Conshohocken, PA, USA.

Bogensperger, T., Silly, G., & Schickhofer, G. (2012). *Methodenvergleich approximativer Nachweisverfahren für Brettsperrholz [Comparison of methods of approximate verification procedures for cross laminated timber]*. Report #: MMSM 2.2.3 sfem_mat, holz.bau forschungs GmbH, Institut für Holzbau und Holztechnologie, Technische Universität Graz, Graz, Austria.

Chui, Y. H., Gong, M. (2015). *Evaluation of planar shear properties of cross layer in massive timber panel*. Final Report #: WSTC2013-015, Wood Science and Technology Centre, the University of New Brunswick, Fredericton, NB, Canada.

Kreuzinger, H. (1999) Platten, Scheiben und Schalen - ein Berechnungsmodell für gängige Statikprogramme [Plate and shell structures. A model for common calculation tools]. *Bau Mit Holz, 1*, 34–39.

Niederwestberg, J., Chui, Y. H., & Gong, M. (2016). Influence of layer and laminate characteristics on shear properties of cross laminated timber and hybrids. In E. Josef,

W. Wolfgang, F. Alireza, & P. Martina (Eds.), *World Conference on Timber Engineering* (pp. 1081–1090). Vienna: TU-MV Media Verlag GmbH.

Stürzenbecher, R., Hofstetter, K., & Eberhardsteiner, J. (2010). Structural design of Cross Laminated Timber (CLT) by advanced plate theories. *Composites Science and Technology*, *70*(9), 1368–1379.

Schickhofer, G., Bogensperger, T., Moosbrugger, T. (2009). BSPhandbuch [CLT Handbook]. Graz: Verlag der Technischen Universität Graz.

Vlachoutsis, S. (1992). Shear correction factors for plates and shells. *International Journal for Numerical Methods in Engineering*, *33*(7), 1537–1552.

Wallner-Novak, M., Koppelhuber, J., Pock, K. (2014). Cross-Laminated Timber Structural Design: Basic design and engineering principles according to Eurocode (1st ed). Vienna: proHolz Austria.

Whitney, J. M. (1973). Shear correction factors for orthotropic laminates under static load. *Journal of Applied Mechanics*, *40*(1), 302–304.

Zhou, J., & Chui, Y. H. (2014). Efficient measurement of elastic constants of cross laminated timber using modal testing. In A. Salenikovich (Ed.), *World Conference on Timber Engineering*. Quebec City.

Zhou, J., Chui, Y. H., Gong, M., & Hu, L. (2016). Simultaneous measurement of elastic constants of full-size engineered wood-based panels by modal testing. *Holzforschung*, *70*(7), 673–682.

Zhou, J., Chui, Y. H., Gong, M., & Hu, L. (2017). Elastic properties of full-size mass timber panels: Characterization using modal testing and comparison with model predictions. *Composites Part B: Engineering*, *112*, 203–212.

Zhou, J., Chui, Y. H., Gong, M., & Hu, L. (2018). Effective bending and shear stiffness of cross laminated timber by modal testing: method development and application. Under submission.

CHAPTER 8 CONCLUSIONS AND RECOMMENDATIONS

8.1 Conclusions

This dissertation presented a series of studies on the development and application of vibration-based non-destructive techniques for material characterization and on-line quality control of engineered wood-based panel products. First, a fast and reliable NDT has been developed for the simultaneous measurement of elastic properties, namely the E values in two strength directions and in-plane G value, of full-size engineered wood-based panels based on the transverse vibration of orthotropic thin plate theory under the boundary condition of SFSF. Subsequently, an in-depth comparative study has been conducted on the proposed method and other existing vibration-based methods for future development of a standard testing method and an on-line NDT. Then the proposed method has been applied for *in situ* measurement of the elastic constants of industrial-size (up to 17 meters long and 3 meters wide) mass timber panels, mainly CLT panels, produced by three CLT manufacturers. The effects of material characteristics and production process on elastic properties were investigated and suggestions on quality control were provided. With these first-hand data, the accuracy of three prediction models used by engineers and researchers for CLT structural design were compared. Furthermore, the proposed method is further developed to identify the effective bending and shear stiffness values of CLT panels based on the transverse vibration of orthotropic Mindlin plate theory, with a genetic algorithm developed for the inverse problem. The transverse shear moduli were evaluated by modal tests with shear correction factors with planar shear test results as reference values. The following specific conclusions can be drawn from the whole research work.

1. The proposed vibration-based NDT method in Chapter 3 is able to identify elastic constants including E_x, E_y and G_{xy} of full-size engineered wood-based panels products. The results obtained represent the global effective elastic constants of a panel, which agree well with its static tests values. For strand and particle-based wood panel products such as OSB and LSL, the static test values from panel specimens have a better agreement with NDT test results, especially for E_y.

2. Boundary condition of SFSF is proved to be the most suitable over FFFF and SFFF for modal testing of full-size engineered wood-based panels, especially mass timber panels. The sensitivity analysis together with the sensitive frequency identification procedure are essential for a fast and reliable measurement.

3. The influences of edge bonding, gap and layup on E_x, E_y and G_{xy} and their variations of CLT panels as well as their prediction models have been found with *in situ* test results of 55 full-size panels. E_x is solely dependent on layup; E_y is mainly dependent on layup but is also influenced by edge bonding and gap size; G_{xy} is significantly affected by edge bonding and gap size. Non-edge bonding and gap size have a negative effect on both E_y and G_{xy} and lead to a large variation compared with edge bonded panels.

4. CLT prediction methods including *k*-method, gamma method and shear analogy method are validated for calculating effective bending stiffness of CLT panels with a large length-to-thickness ratio in the major strength direction, while shear analogy method could be a better choice in comparison to other two methods when CLT had a small length-to-depth ratio. The *k*-method also provides effective bending stiffness in the minor strength direction that was close to the value measured by modal test method.

230

However, the accuracy of *k*-method in prediction of effective bending stiffness in the minor strength direction was influenced by layup and edge bonding. Shear analogy method could include an over-estimated transverse shear effect for CLT with a small width-to-thickness ratio and leads to a much smaller prediction of E_y value.

5. For engineered wood-based panels with small transverse shear moduli or small length/ width to thickness ratios, the proposed vibration-based NDT method in Chapter 6 can be used for the determination of elastic constants including E_x, E_y, G_{xy}, G_{xz} and G_{yz}. The SCF values are critical for G_{xz} and G_{yz}, and should be carefully determined for laminated composites such as CLT. Planar shear test method is recommended for evaluation of transverse shear properties.

8.2 Recommendations

According to the above findings, the elastic constants of full-size structural panels measured by proposed NDT methods are recommended for establishing design values for structural design, especially for serviceability limit design. Edge bonding is recommended for CLT manufacturing as it can reduce the variations of mechanical properties and increase in-plane shear properties.

The following recommendations are given for future research considering the practical application and further developments of the proposed NDT methods.

1. For a plate that is not stiff enough to support itself when two edges in the width direction are simply supported or the maximum deflection caused by self-weight is too great, causing obvious bounces on the supports during impact tests, a proper clamping

system should be applied. Future research should focus on developing a suitable clamping system to simulate simple support or to introduce a compensation factor that quantifies the clamping effort on the measured frequencies.

2. The proposed NDT method in Chapter 3 is recommended for developing an on-line quality control system for mass timber panels for future research. The G_{xy} or related frequency value is suggested as an indicator for gap control and delamination detection.

3. For application of the proposed NDT method in Chapter 6 for laminated composites, the forward solution of free transverse vibration of laminated plates based on higher order plate theory is worth for direct measurement of transverse shear moduli. Improvements on the genetic algorithm are also recommended to increase computation efficiency.

Appendix I MATLAB Codes

Appendix I includes all the necessary MATLAB codes mentioned in this thesis work.

I. FRF Data Processing, Frequency Spectra and Mode Shape Plotting

The following MATLAB codes are used to import and process all the frequency response function (FRF) data in the format of '.txt' created by RT Pro Photon 6.33 for plotting frequency spectra of all impacts and mode shapes. The code is only capable with the data files created by RT Pro Photon 6.33, and modification is needed for other formats of data.

readtxts.m

```matlab
% Read all text files and reshape them for plotting frequency spectra and
% mode shape. Check working directory before running,
% the folder should have all the data to be processed.

close all;
clear all;
clc;

%% Import all data files, which contain the real and imaginary parts of each FRF
d = dir('*.txt');
n = length(d);
data = cell(1, n);
t = cell(1, n); % The whole data files
re = cell(1, n); % The total real parts
im = cell(1, n); % The total imaginary parts
m = cell(1, n); % The total magnitude parts

for k = 1:n
    filename = d(k,1).name;
    data{k} = importdata(filename);
end

for k = 1:n
    t{k}= data{k}.data;
end

T = cell2mat(t); %  The whole data files matrix

for k = 1:n
    re{k}= T(:,3*k-1);
end
```

```matlab
for k = 1:n
    im{k}= T(:,3*k);
end

RE = [T(:,1) cell2mat(re)]; % The real parts matrix
IM = [T(:,1) cell2mat(im)]; % The imaginary parts matrix

% Calculate the magnitude of each FRF
for k=1:n
    m{k}=sqrt(RE(:,k+1).^2+IM(:,k+1).^2);
end
M= [T(:,1) cell2mat(m)]; % The magnitude parts matrix

%% Plot the frequency spectra of all impacts
% Start point from 0.1 Hz to avoid fundamental frequency of the system
st=round(0.1/IM(2,1));
% End point of the spectrum
sp=round(max(T(:,1))/IM(2,1));

figure
subplot(2,1,1)
plot(M(st:sp,1), M(st:sp,2:n+1));
title('Frequency-Magnitude Spectra');
xlabel('Freq (Hz)');
ylabel('Magnitude (m/s2/N)');
axis tight;

subplot(2,1,2)
plot(IM(st:sp,1), IM(st:sp,2:n+1));
title('Frequency-Imaginary Spectra');
xlabel('Freq (Hz)');
ylabel('Imaginary (m/s2/N)');
axis tight;

disp('Manually pick the most obvious frequencies!')
```

234

mplot.m

```matlab
% Plot mode shape of a SFSF plate
clc;
disp('input the picked frequency value from frequency spectra');
freq = input('freq= ');
line = round(1+freq/IM(2,1));
C = IM(line,2:end);

BK = [0 0 0 0 0 0]'; % Simply supported edges, size depends on grid size
Ms= reshape(C,12,6)'; % Reshape based on grid size
MS=[BK Ms BK];

figure
mesh(MS)
grid off
axis off
```

ifreq.m

```matlab
% Select frequencies of interest from a single spectrum
close all ;
clear;
clc;

% Import data files
d = dir('*.txt');
disp(' Select the ith impact of interest ');
i=input('i= '); % Select the ith impact of interest

filename = d(i,1).name;
h=importdata(filename);

%Calculate magnitude
format long
hdata=h.data;
mag=sqrt(hdata(:,2).^2+hdata(:,3).^2);
% data file with freq, mag, imag
hnew=[hdata(:,1) mag hdata(:,3)];

figure
subplot(2,1,1)
plot(hnew(:,1),hnew(:,2));
title('Fre-Mag Spectrum');
xlabel('Freq (Hz)');
ylabel('Magnitude');
axis tight

subplot(2,1,2)
plot(hnew(:,1),hnew(:,3));
title('Fre-Im Spectrum');
xlabel('Freq (Hz)');
ylabel('Imaginary');
axis tight
```

II. Forward Solution and Sensitivity Analysis of a Thin Orthotropic Plate

The following MATLAB codes serve as the forward solution for calculating the natural frequencies of free transverse vibration of thin orthotropic rectangular plates based on the improved approximate expressions by Kim and Dickinson (1985). A sensitivity analysis code is also provided.

FreqSFSFthin.m

```matlab
function [ freqthin ] = FreqSFSFthin( a, b, h, rho, Ex, Ey, Gxy, vxy, m, n )
% Calculate the natural frequency of mode (m, n) of a thin rectangular
% orthotropic plate based on Kim and Dickinson (1985) with the input of
% length (a), width (b), thickness (h), density (rho) and elastic constants
% and mode indices (m, n). All inputs are in SI unit.
% Kim, C. S., and Dickinson, S. M. (1985). Improved approximate expressions
% for the natural frequencies of isotropic and orthotropic rectangular
% plates. Journal of Sound and Vibration, 103(1), 142-149.

%% Calculate the stiffness and rigidity
r=b/a;
vyx=vxy*Ey/Ex;
Dx=Ex*h^3/(12*(1-vxy*vyx));
Dy=Ey*h^3/(12*(1-vxy*vyx));
Dxy=Gxy*h^3/12;
D1=Dx*vyx;  % or D1=Dy*vxy
H=D1+2*Dxy;

%% Calculate natural frequency
% The following parameters had no physical meaning and can be found in Kim
% and Dickinson (1985).
% m is the number of nodal lines perpendicular to x direction.

Gx=m-1;
Hx=(m-1)^2;
Jx=(m-1)^2;
Kx=0; Lx=0; Mx=0;
Gxm=m+2-1;
Hxm=(m+2-1)^2;
Jxm=(m+2-1)^2;

% n is the number of nodal lines perpendicular to y direction.

if n==0;
   Gy=0; Hy=0; Jy=0; Ky=1.883; Ly=0; My=0;
   Gyn=1.506; Hyn=1.247; Jyn=5.013;
   Kyn=5.328; Lyn=0.182; Myn=3.584;
```

```
elseif n==1;
    Gy=0; Hy=0; Jy=12/pi^2;
    Ky=4.113; Ly=0; My=8*sqrt(3)/pi^2;
    Gyn=2.500; Hyn=4.666; Jyn=11.036;
    Kyn=5.624; Lyn=0.536; Myn=5.835;

elseif n==2;
    Gy=1.506; Hy=1.247; Jy=5.013;
    Ky=5.328; Ly=0.182; My=3.584;

elseif n==3;
    Gy=2.500; Hy=4.666; Jy=11.036;
    Ky=5.624; Ly=0.536; My=5.835;

else
    Gy=n-0.5;
    Hy=(n-0.5)^2*(1-2/pi/(n-0.5));
    Jy=(n-0.5)^2*(1+6/pi/(n-0.5));
    Ky=(2*n+3)^4/(4*n^2+4*n+5)/(2*n+1)/pi;
    Ly=(2*n-1)^4/(4*n^2+4*n+5)/(2*n+1)/pi;
    My=(4*n^2+4*n-3)*(12*n^2+12*n+7)/(4*n^2+4*n+5)/(2*n+1)/pi;
end

if n>=2;
    Gyn=n+2-0.5;
    Hyn=(n+2-0.5)^2*(1-2/pi/(n+2-0.5));
    Jyn=(n+2-0.5)^2*(1+6/pi/(n+2-0.5));
    Kyn=(2*(n+2)+3)^4/(4*(n+2)^2+4*(n+2)+5)/(2*(n+2)+1)/pi;
    Lyn=(2*(n+2)-1)^4/(4*(n+2)^2+4*(n+2)+5)/(2*(n+2)+1)/pi;
    Myn=(4*(n+2)^2+4*(n+2)-3)*(12*(n+2)^2+12*(n+2)+7)/(4*(n+2)^2+4*(n+2)+5)/(2*(n+2)+1)/pi;
end

Cij=(Dx/H)*Gx^4*r^2+(Dy/H)*Gy^4*(1/r)^2+2*(Hx*Hy+2*(Dxy/H)*(Jx*Jy-Hx*Hy));
Cin=(Dx/H)*Gx^4*r^2+(Dy/H)*Gyn^4*(1/r)^2+2*(Hx*Hyn+2*(Dxy/H)*(Jx*Jyn-Hx*Hyn));
Cmj=(Dx/H)*Gxm^4*r^2+(Dy/H)*Gy^4*(1/r)^2+2*(Hxm*Hy+2*(Dxy/H)*(Jxm*Jy-Hxm*Hy));
Eij=Hx*(Ky+Ly)*(2*(Dxy/H)-1)+4*(Dxy/H)*Jx*My;
Eji=Hy*(Kx+Lx)*(2*(Dxy/H)-1)+4*(Dxy/H)*Jy*Mx;
T=-(Kx*Ky+Lx*Ly)*(2*(Dxy/H)-1)+4*(Dxy/H)*Mx*My;
c=(Cmj*Eij-Eji*T)/(Cin*Cmj-T^2);
d=(Cin*Eji-Eij*T)/(Cin*Cmj-T^2);
Z=(Cij+c^2*Cin+d^2*Cmj-2*c*Eij-2*d*Eji+2*c*d*T)/(1+c^2+d^2);

Omegathin=(pi^2/(a*b))*sqrt(H*Z/rho/h); % Frequency in rad/s
freqthin= Omegathin/2/pi; % Frequency in Hz

end
```

Sensitivitythin.m

```matlab
% This M-file calculates the normalized sensitivities of a SFSF plate
clear
clc

syms Ex Ey Gxy vxy

%% Input information of a plate
a=5.45; % length, m
b=2.47; % width, m
h=0.102; % thickness, m
r=b/a; % side ratio
rho=520; % density, kg/m3
f20=6.912; % experimental fundamental frequency

%% Elastic constants to be evaluated
% Ex1 is calculated based on experimental natural frequency and the others
% are based on the its ratio to Ex, which can be places with exact values
% or predicted values or reported values.
Ex1=47.52*f20^2*a^4*rho/pi^2/h^2; % modulus of elasticity in x direction
Ey1=0.1*Ex1; % modulus of elasticity in y direction
Gxy1=0.06*Ex1; % in-plane shear modulus
vxy1=0.02; % major possion ratio
vyx1=vxy1.*Ey1./Ex1; % minor possion ratio

%% Sensitivity analysis
k=1;
for m=2:6
   for n=0:5
      freqs(k) = FreqSFSFthin( a, b, h, rho, Ex, Ey, Gxy, vxy, m, n );
      k=k+1;
   end
end

dfdEx=diff(freqs,Ex);
dfdEy=diff(freqs,Ey);
dfdGxy=diff(freqs,Gxy);
dfdvxy=diff(freqs,vxy);

X=[Ex1; Ey1; Gxy1; vxy1];
XX=zeros(4,(m-1)*(n+1));

for i=1:(m-1)*(n+1)
   XX(:,i)=X;
end

dfdEx1=subs(dfdEx,{Ex,Ey,Gxy,vxy},{Ex1,Ey1,Gxy1,vxy1});
dfdEy1=subs(dfdEy,{Ex,Ey,Gxy,vxy},{Ex1,Ey1,Gxy1,vxy1});
dfdGxy1=subs(dfdGxy,{Ex,Ey,Gxy,vxy},{Ex1,Ey1,Gxy1,vxy1});
dfdvxy1=subs(dfdvxy,{Ex,Ey,Gxy,vxy},{Ex1,Ey1,Gxy1,vxy1});
freqs1=subs(freqs,{Ex,Ey,Gxy,vxy},{Ex1,Ey1,Gxy1,vxy1});
freqsensitivity=eval([dfdEx1; dfdEy1; dfdGxy1; dfdvxy1].*XX./[freqs1; freqs1; freqs1; freqs1]);
% freqsensitivity is the normalized sensitivity, [X X X] array number
```

239

```matlab
% equals to (m-1)*(n+1)

freqsr=eval(freqs1); % frequency values
freqsort=sort(freqsr); % sort frequencies

freqmatrix=reshape(freqsr,n+1,m-1);
senEx=reshape(freqsensitivity(1,:),n+1,m-1);
senEy=reshape(freqsensitivity(2,:),n+1,m-1);
senGxy=reshape(freqsensitivity(3,:),n+1,m-1);
senvxy=reshape(freqsensitivity(4,:),n+1,m-1);

% Pick the first nth frequency, here n=15
freqsn=freqsort(1,1:20);

% Find the corresponding frequency indices and sensitivities
I=[];
J=[];
Sens=[];
for i=1:length(freqsn)
    [r,c]=find(freqmatrix==freqsn(1,i));
    sEx=senEx(r,c);
    sEy=senEy(r,c);
    sGxy=senGxy(r,c);
    svxy=senvxy(r,c);
    Sens=[Sens; sEx sEy sGxy svxy];
    I=[I; c]; %m
    J=[J; r]; %n
end

% Frequency indices
ind=[I+1 J-1]; % mode (m, n)

disp('The first 15th frequencies with mode indices and normalized frequency sensitivities to Ex, Ey, Gxy
and vxy:')
freqmode=[freqsn' ind Sens];
open freqmode;
```

SensitivitythinMCS.m

```matlab
% This M-file calculate the normalized sensitivities of a SFSF plate with
% Monte Carlo Simulation with the uncertainty of each elastic constant
clear
clc

syms Ex Ey Gxy vxy

%% Input information of a plate
a=2.44; % length, m
b=1.22; % width, m
h=0.011; % thickness, m
r=b/a; % side ratio
rho=617; % density, kg/m3

%% Random sampling with normal distribution
Ex0=1;
Ex1=Ex0.*(0.9+rand(1000,1)*0.2); % modulus of elasticity in x direction
Ey1=0.5.*Ex0.*(0.8+rand(1000,1)*0.4); % modulus of elasticity in y direction
Gxy1=0.3.*Ex0.*(0.8+rand(1000,1)*0.4); % in-plane shear modulus
vxy1=0.3*(0.9+rand(1000,1)*0.2); % major possion ratio
vyx1=vxy1.*Ey1./Ex1; % minor possion ratio
X=[Ex1'; Ey1'; Gxy1'; vxy1'];

%% Sensitivity analysis
k=1;
tic;
for m=2:5
    for n=0:3
        freqs(:,k)= FreqSFSFthin( a, b, h, rho, Ex, Ey, Gxy, vxy, m, n );
        k=k+1;
    end
end

dfdEx=diff(freqs,Ex);
dfdEy=diff(freqs,Ey);
dfdGxy=diff(freqs,Gxy);
dfdvxy=diff(freqs,vxy);

dfdEx1=subs(dfdEx,{Ex,Ey,Gxy,vxy},{Ex1,Ey1,Gxy1,vxy1});
dfdEy1=subs(dfdEy,{Ex,Ey,Gxy,vxy},{Ex1,Ey1,Gxy1,vxy1});
dfdGxy1=subs(dfdGxy,{Ex,Ey,Gxy,vxy},{Ex1,Ey1,Gxy1,vxy1});
dfdvxy1=subs(dfdvxy,{Ex,Ey,Gxy,vxy},{Ex1,Ey1,Gxy1,vxy1});
freqs1=subs(freqs,{Ex,Ey,Gxy,vxy},{Ex1,Ey1,Gxy1,vxy1});

for i=1:((m-1)*(n+1))
    freqsen(:,(4*i-3):4*i)=[dfdEx1(:,i) dfdEy1(:,i) dfdGxy1(:,i) dfdvxy1(:,i)].*X'./[freqs1(:,i) freqs1(:,i) freqs1(:,i) freqs1(:,i)];
    i=i+1;
end

sensta=[min(freqsen); mean(freqsen); max(freqsen)];
senmatrix=[sensta(:,1:4);sensta(:,5:8);sensta(:,9:12);sensta(:,13:16)];
```

241

```
time=toc

for i=1:((m-1)*(n+1))
    s(i,1)=sensta(2,4*(i-1)+1);
    s(i,2)=(sensta(3,4*(i-1)+1)-sensta(1,4*(i-1)+1))/2;
    s(i,3)=sensta(2,4*(i-1)+2);
    s(i,4)=(sensta(3,4*(i-1)+2)-sensta(1,4*(i-1)+2))/2;
    s(i,5)=sensta(2,4*(i-1)+3);
    s(i,6)=(sensta(3,4*(i-1)+3)-sensta(1,4*(i-1)+3))/2;
    s(i,7)=sensta(2,4*(i-1)+4);
    s(i,8)=(sensta(3,4*(i-1)+4)-sensta(1,4*(i-1)+4))/2;
    i=i+1;
end

open s
```

III. Inverse Identification of Elastic Constants for a Thin Orthotropic Plate

The following MATLAB code is able to identify the elastic constants, namely E_x, E_y, and G_{xy}, of a thin orthotropic plate with experimental natural frequencies of primary modes (2, 0), (2, 1) and (2, 2) based on an iterative process. Additional experimental natural frequencies of higher pure bending modes in the width direction such as mode (2, 3) can be added to the iteration depended on sensitivity analysis results. The coupled effects of two or three elastic constants on one frequency mode is considered in the iteration, which can be modified based on sensitivity analysis results. The function file of 'FreqSFSFthin.m' is needed for the following M-file.

Inverseplate.m

```
% Simultaneous measurement of bending and in-plane shear moduli of an
% orthotropic thin wood-based panel under SFSF boundary condition

clc
clear
%% Input information of a plate
a=3.96; % length, m
b=1.02; % width, m
h=0.133; % thickness, m
r=b/a; % side ratio
rho=520; % density , kg/m3
f20=15.344; % Experimental frequency of the first bending mode in length
f21=31.063; % Experimental frequency of thefirst torsional mode
f22=289.156; % Experimental frequency of the first bending mode in width
%f23=; % Experimental frequency of the second bending mode in width can be
% included if the sensitivity of f22 is not large enough.
freqt=[f20 f21 f22]; % Can also be freqt=[f20 f21 f22 f23]

%% Initial guesses of elastic constants
Ex=47.52*f20^2*a^4*rho/pi^2/h^2; % modulus of elasticity in x direction
Ey=0.2*Ex; % modulus of elasticity in y direction
Gxy=0.05*Ex; % in-plane shear modulus
vxy=0.02; % major possion ratio OSB 0.23 MDF 0.33 CLT 0.35
vyx=vxy*Ey/Ex; % minor possion ratio

%% Iteration
TotalDiff=1;
t=1;
% The limit of TotalDiff is depended on goodness of data and is suggested
```

```matlab
% to be less than 0.05.
while (TotalDiff>=0.01)
    for i=1:t

        Dx=Ex*h^3/(12*(1-vxy*vyx));
        Dy=Ey*h^3/(12*(1-vxy*vyx));
        Dxy=Gxy*h^3/12;
        D1=Dx*vyx;  % or D1=Dy*vxy
        H=D1+2*Dxy;
        k=1;

        % m and n depend on the selection of frequency combination
        for m=2
            for n=[0 1 2]
                freq(k)= FreqSFSFthin( a, b, h, rho, Ex, Ey, Gxy, vxy, m, n );
                k=k+1;
            end
        end

        fdiff=freq-freqt;
        delta=(freq-freqt)./freqt;

        if delta(1)>0.001
            Ex=0.999*Ex;
        elseif delta(1)<-0.001
            Ex=1.001*Ex;
        else
            Ex=Ex;
        end

        if delta(2)>=0.001
            Gxy=0.999*Gxy;
            Ex=0.9999*Ex; % COUPLED
        elseif delta(2)<=-0.001
            Gxy=1.001*Gxy;
            Ex=1.0001*Ex; % COUPLED
        else
            Gxy=Gxy;
            Ex=Ex;
        end

        if delta(3)>=0.001
            Ey=0.999*Ey;
            Gxy=0.999*Gxy; % COUPLED
        elseif delta(3)<=-0.001
            Ey=1.001*Ey;
            Gxy=1.001*Gxy; % COUPLED
        else
            Gxy=Gxy;
            Ey=Ey;
        end

        TotalDiff=(sum(abs(fdiff)))/sum(freqt);
        t=t+1;
```

```matlab
    end
end

%% Display results
disp('The iteration count is')
disp(t)
freq
freqt

disp('The frequencies selected were f20 f21 f22 f23. ')
disp('Absolute frequency differences (Hz):')
disp(fdiff)

disp('Relative frequency differences in percent:')
disp(sprintf('% 0.3f%% ',delta*100))

TotalDiff=sprintf('%2.3f%%', sum(abs(fdiff))/sum(freqt)*100);
disp('Total relative frequency difference in percent:')
disp(TotalDiff)

disp('Elastic constants estimated (MPa):')
Ex=sprintf('% 0.0f',Ex/1e6)
Ey=sprintf('% 0.0f',Ey/1e6)
Gxy=sprintf('% 0.0f',Gxy/1e6)
```

IV. Forward Solution of a Mindlin Orthotropic Plate

The forward solution for free transverse vibration of a moderate thick (Mindlin) rectangular orthotropic plate with boundary condition of SFSF is adopted from Liu and Xing (2011). The MATLAB codes provided by Xing and Liu (2015) has been adopted and modified as the forward solution. The following MATLAB codes are necessary for obtaining the exact frequency solution. The function files 'SolutionCoef.m', 'eigen.m', 'F.m' are cited from Xing and Liu (2015), and are needed for solving the characteristic frequency equations by 'freqmn.m'. 'Rigidity.m' calculates the stiffness and rigidities of the plate. The M-file 'ExactMindlin.m' is used to calculate the natural frequency of a specific mode (m, n) of a rectangular Mindlin orthotropic plate under boundary condition of SFSF. To be noted, m is equal to ($m+1$) in the codes for thin plates.

SolutionCoef.m

```
function [g1,h1]=SolutionCoef(p,q,D,g)

D1 = D(1); D2 = D(2); D3 = D(3); C1 = D(4);
C2 = D(5); h = D(6);  J = h^2/12;

s1=(D1*p^2)/C1 - (D3*p^2)/C2 - (J*g)/C1 + 1;
s2=p^2/C2 - (J*g)/C2 + 1;
s3=(D3*g)/(C1*C2) - (D3*p^2)/C2 + 1;

g1 = (s3 - (D3*q^2)/C1)/(q^2/C1 + s1);
h1 = (s3 - (D3*q^2)/C1)/(s2 - (D3*q^2)/C1 + (D2*q^2)/C2);
end
```

eigen.m

```matlab
function [q,r,s]=eigen(X,p,coef)
% coef=[b,Omgi,BC,D];
    K=length(coef); D=coef(4:K); g=X;
    D1 = D(1); D2 = D(2); D3 = D(3); C1 = D(4); C2 = D(5); h = D(6); J=h^2/12;
    % The coefficients of equation: a*x^3+b*x^2+c*x+d = 0
    s1=(D1*p^2)/C1 - (D3*p^2)/C2 - (J*g)/C1 + 1;
    s2=p^2/C2 - (J*g)/C2 + 1;
    s3=(D3*g)/(C1*C2) - (D3*p^2)/C2 + 1;
    s4=- C1*p^2 + g;
    a=-D2/C1;
    b=(C1*(D2*s4 - C2^2*s2 + C2^2*s3 + C2*D3^2*p^2) - C2*D3^2*s4)/(C1^2*C2) - (D2*D3*p^2 +
C2*D2*s1)/C2;
    c=(D2*s1*s4 - C2^2*s1*s2 + C2^2*s1*s3 + C1*D2*p^2*s3 - C2*D3*p^2*s2 - C2*D3*p^2*s3)/C2 +
(s4*(s2 - D3*s1))/C1;
    d=s2*(C1*s3*p^2 + s1*s4);
    % The roots of equation: y^3+p*y+q = 0
    p = (c - b^2/(3*a))/a; q = (d + (2*b^3)/(27*a^2) - (b*c)/(3*a))/a;
    dt=sqrt((q/2)^2+(p/3)^3); t=q/2;
    p1=(-t+dt)^(1/3); p2=(-t-dt)^(1/3);
    omg1=(-1+1i*sqrt(3))/2; omg2=(-1-1i*sqrt(3))/2;
    y1=p1+p2; y2=omg1*p1+omg2*p2; y3=omg2*p1+omg1*p2;
    % The roots of equation: a*x^3+b*x^2+c*x+d = 0
    x1=y1-b/(3*a); x2=y2-b/(3*a); x3=y3-b/(3*a);
    q=sqrt(x1); r=sqrt(x2); s=sqrt(x3);
end
```

F.m

```
function F=F(X,coef)
% Characteristic equations for SFSF
b=coef(1); p=coef(2); BC=coef(3); K=length(coef); D=coef(4:K); v = D(7);
[q,r,s]=eigen(X,p,coef);
[g1,h1]=SolutionCoef(p,q,D,X);
[g2,h2]=SolutionCoef(p,r,D,X);
[g3,h3]=SolutionCoef(p,s,D,X);

% Boundary conditions (BC): 1-FF(sym), 2-FF(anti)
switch BC
   case {1,2}
     d1 = g1*v*p^2 + h1*q^2; d2 = g2*v*p^2 + h2*r^2;
     d3 = g3*v*p^2 + h3*s^2; e1 = (g1 + h1)*p*q;
     e2 = (g2 + h2)*p*r; e3 = (g3 + h3)*p*s;
     f1 = (1 - h1)*q; f2 = (1 - h2)*r; f3 = (1 - h3)*s;

     if BC == 1
       F = - d1*cos(b*q)*(e2*f3 - e3*f2) + ...
           d2*cot(b*r)*sin(b*q)*(e1*f3 - e3*f1) - ...
           d3*cot(b*s)*sin(b*q)*(e1*f2 - e2*f1) ;
     else
       F = -d1*sin(b*q)*(e2*f3 - e3*f2) + ...
           d2*cos(b*q)*tan(b*r)*(e1*f3 - e3*f1) - ...
           d3*cos(b*q)*tan(b*s)*(e1*f2 - e2*f1) ;
     end
end
```

freqmn.m

```matlab
function [freq, X] = freqmn( m, n, a, b, rho, h, D, D6, X)
% Calculate the frequency of a specific mode (m, n)

% Identify m and n to be odd or even,
% Boundary conditions (BC):
% 1-FF(symmetrical mode, m=odd/even, n=even), 2-FF (antisymmetric mode)
if bitget(m,1) == 1 && bitget(n,1) == 0
    BC=1;
elseif bitget(m,1) == 0 && bitget(n,1) == 0 && n>0
    BC=1;
else
    BC=2;
end

Omgi=m*pi/a;
coef=[b,Omgi,BC,D];

M=10000;
errx0=1e-6;
errf0=1e-6;

for j=1:M
    F0=F(X,coef);
    dh=abs(X)*1e-4;
    J=(F(X+dh,coef)-F(X,coef))/dh;
    dX=-J\F0;
    errx=norm(dX)/(norm(X)+eps); errf=norm(F0);
    if errx<errx0 && errf<errf0
        X=X+dX;
        break;
    else
        X=X+dX;
    end
end

X=real(X);
% omega=sqrt(X*D6/rho/h);   % frequency in rad/s
freq=sqrt(X*D6/rho/h)/2/pi; % frequency in Hz
end
```

249

Rigidity.m

```matlab
function [D,D6,J] = Rigidity( ElasticConstants,mu12,k13,k23,h )
% Calculating rigidities
E1=ElasticConstants(1);G12=ElasticConstants(2);E2=ElasticConstants(3);
G23=ElasticConstants(4);G13=ElasticConstants(5);
mu21=E2*mu12/E1;
nu=1-mu12*mu21;
D11=E1*h^3/(12*nu);
D12=E1*h^3*mu12/(12*nu);
D22=E2*h^3/(12*nu);
D21=E2*h^3*mu21/(12*nu);
D66=G12*h^3/12;
C44=k23*G23*h;
C55=k13*G13*h;

D1=D11/D66;
D2=D22/D66;
D3=(D12+D66)/D66;
D6=D66;
C1=C55/D66;
C2=C44/D66;
J=h^2/12;
D=[D1,D2,D3,C1,C2,h,mu12];
end
```

ExactMindlin.m

```matlab
% Natural frequency of an orthotropic Mindlin plate under SFSF boundary
% condition
clear;
clc;

% Material constants for orthotropic plates
a=3.96;% length, m
width=1.02; % width, m
b=width/2;
h=0.133; % thickness, m
k13=0.24; % k13 for G13 pi^2/12 0.3323
k23=0.23;  % k23 for G23 pi^2/12 0.8670
E1=9400e6; % E value in the major strength direction, Pa
E2=2400e6; % E value in the minor strength direction, Pa
G12=450e6; % Inplane shear modulus, Pa
G13=200e6; % transverse shear modulus of 13 plane, Pa
G23=500e6; % transverse shear modulus of 23 plane, Pa
mu12=0.02; % Poisson¡¯s ratio
rho=520; % Density, kg/m3
%f0=input('f0= ');
ElasticConstants=[E1 G12 E2 G23 G13];

[D,D6,J] = Rigidity( ElasticConstants,mu12,k13,k23,h );

Frequency= [];
t=1;
for m=1
   for n=0
      % Initial value based on thin plate
      [omegathin, freqthin] = FreqSFSFthin( a, width, h, rho, E1, E2, G12, mu12, m, n );
      X=rho*h*omegathin^2/D6/(m+1);
      % X=rho*h*(f0*2*pi)^2/D6;
      [freq, X]=freqmn( m, n, a, b, rho, h, D, D6, X);
      while freq>freqthin
         X=X*0.9;
         freq=freqmn( m, n, a, b, rho, h, D, D6, X);
      end
      Frequency(t,1)=freq;
      t=t+1;
   end
end

open Frequency
```

V. Inverse Identification of Elastic Constants for a Mindlin Orthotropic Plate

The inverse identification of elastic constants for a rectangular Mindlin plate with SFSF boundary condition is realised by M-file 'InverseMindlin.m' and function files 'FreqFit.m' and 'DeltaDiff.m'. The objective function is coded in 'FreqFit.m'. The 'DeltaDiff.m' function file calculates the difference between each experimental and calculated natural frequency and its total difference. The 'InverseMindlin.m' file includes a genetic algorithm for the optimization process. The 'ga' function embedded in MATLAB is called in InverseMindlin.m.

FreqFit.m

```matlab
function [ TotalDiff ] = FreqFit( ElasticConstants )
% Fitness function for genetic algorithm optimization
% E1=ElasticConstants(1);G12=ElasticConstants(2);E2=ElasticConstants(3);
% G23=ElasticConstants(4);G13=ElasticConstants(5);

global a b h rho freqexp mu12 k13 k23 mm nn

% Material constants
[D,D6,J] = Rigidity( ElasticConstants,mu12,k13,k23,h );
% Initial guess based on measured frequency
X=rho*h*(2*pi*freqexp).^2/D6;

k=1;
for m=mm
  if m==1
    ns=nn;
  else
    ns=0;
  end
  for n=ns
    freq= freqmn( m, n, a, b, rho, h, D, D6, X(k));
    freqcal(k,1)=freq;
    k=k+1;
  end
end

delta=(freqexp-freqcal)./freqexp;% use ^2 to speed up
TotalDiff=sum(abs(delta));

end
```

DeltaDiff.m

```matlab
function [ freqcal, delta ] = DeltaDiff(ElasticConstants)
% Calculate the difference between experimental frequencies and predicted
% frequencies in percentage and the total absolute difference
global a b h rho freqexp mu12 k13 k23 mm nn
% Material constants
[D,D6] = Rigidity( ElasticConstants,mu12,k13,k23,h );
% Initial guess based on measured frequency
X=rho*h*(2*pi*freqexp).^2/D6;

k=1;
for m=mm
   if m==1
      ns=nn;
   else
      ns=0;
   end
   for n=ns
       freq= freqmn( m, n, a, b, rho, h, D, D6, X(k));
       freqcal(k,1)=freq;
       k=k+1;
    end
 end
delta=(freqexp-freqcal)./freqexp;
TotalDiff=sum(abs(delta));

end
```

InverseMindlin.m

```matlab
clear;
clc;

%% Material constants for orthotropic plates
global a b h rho freqexp mu12 k13 k23 mm nn
 a=3.15; % Length
 width=1.06; % Width
 b=width/2;
 h=0.103; % Thickness
 rho=520; % Density
 f10=19.959; % First bending mode in length
 f11=27.695; % First torsional mode
 f12=96.771; % First bending mode in width
 f13=246.277; % Second bending mode in width
 f14=447.601; % Third bending mode in width
 f20=65.781; % Second bending mode in length
 f30=124.922; % Third bending mode in length

%% Choose frequency combinations
mn=1;
switch mn
    case 1
        freqexp=[f10 f11 f12 f13 f20]';
        mm=[1 2];
        nn=[0 1 2 3];
    case 2
        freqexp=[f11 f13 f14 f20 f30]';
        mm=[1 2 3];
        nn=[1 3 4];
    case 3
        freqexp=[f10 f11 f12 f13 f14 f20 f30]';
        mm=[1 2 3];
        nn=[0 1 2 3 4];
    otherwise
        warning('Error! Not included.');
end

%% Initial values of elastic constants
 mu12=0.02; % Poisson's ratio
 k13=0.312; % Shear correction factor k13 for G13
 k23=0.873; % Shear correction factor k23 for G23

%% Input bound constraints of elastic constants
% EG0=[E1 G12 E2 G23 G13];
lb=[11000 230 500 200 100]*1e6;
ub=[12000 300 600 300 300]*1e6;

%% Single objective optimization
nvars=5;
options = gaoptimset;
% Modify options setting
```

```matlab
options = gaoptimset(options,'PopulationSize', 100);% Population size
options = gaoptimset(options,'Generations', 20); % Stopping criteria, maximum generation
options = gaoptimset(options,'CrossoverFraction', 0.6); % Crossover fraction
options = gaoptimset(options,'TolFun', 1e-3); % Function tolerance
options = gaoptimset(options,'FitnessLimit', 0.02); % Stopping criteria, maximum fitness limit
options = gaoptimset(options,'CrossoverFcn', {  @crossoverheuristic 1.2}); % Crossover function: heuristic
options = gaoptimset(options,'MutationFcn', @mutationadaptfeasible); % Mutation function: adaptive
feasible
options = gaoptimset(options,'Display', 'iter');
options = gaoptimset(options,'PlotFcns', {  @gaplotbestf @gaplotscores });
[ElasticConstants,TotalDiff] = ga(@FreqFit,nvars,[],[],[],[],lb,ub,[],[],options);
[ freqcal, delta ] = DeltaDiff(ElasticConstants);
EG=ElasticConstants/1e6; % MPa
disp('Estimated Ex Gxy Ey Gyz Gxz (MPa):')
disp(sprintf('% 0.0f ',EG))
disp('Experimental and calculated frequencies using optimized E and G:')
disp(sprintf('% 0.3f ',freqexp'))
disp(sprintf('% 0.3f ',freqcal'))
disp('Relative differences between experimental and calculated frequencies:')
disp(sprintf('% 0.3f ',delta'))
disp('Sum of relative difference:')
disp(sprintf('% 0.3f ',TotalDiff'))
```

Appendix II Experimental Natural Frequencies of All Panel Specimens

The experimental natural frequencies together with dimension and density information of all panel specimens are presented in the following tables.

Table II.1 Experimental natural frequencies of full size CLT, OSB and MDF panels in Chapter 3

Panel #	Density (kg/m^3)	Length (m)	Width (m)	Thickness (mm)	Frequency (Hz)			
					f_{20}	f_{21}	f_{22}	f_{23}
CLT 1	520	5.50	2.15	103	7.656	9.844	27.81	68.13
CLT 2	520	5.25	2.15	103	8.25	10.63	29.13	69.63
OSB 1	614	2.44	1.22	11.65	2.813	7.50	28.44	59.05
OSB 2	611	2.44	1.22	11.22	2.813	7.188	26.88	56.88
OSB 3	632	2.44	1.22	10.45	2.813	7.50	29.06	56.25
OSB 4	613	2.44	1.22	10.79	3.125	7.188	29.69	56.56
OSB 5	619	2.44	1.22	11.06	2.813	7.50	27.81	57.50
MDF 1	696	2.46	1.24	15.7	2.813	8.125	31.25	67.50
MDF 2	689	2.46	1.24	15.7	2.813	8.438	30.94	68.13
MDF 3	703	2.46	1.24	15.7	2.813	8.281	30.94	67.19
MDF 4	690	2.46	1.24	15.7	2.813	8.057	31.25	67.19
MDF 5	706	2.46	1.24	15.7	2.813	7.813	30.63	68.44

Table II.2 Experimental natural frequencies of OSB and DOSB panels in Chapter 4

OSB Panel #	Density (kg/m³)	Frequency-FFFF (Hz)			Frequency-SFFF (Hz)				Frequency-SFSF (Hz)		
		f_{20}	f_{11}	f_{20}	f_{11}	f_{21}	f_{02}	f_{31}	f_{20}	f_{21}	f_{22}
1-1-1	606	28.748	27.832	75.623	15.930	39.550	52.734	86.610	13.001	30.945	95.581
1-1-2	614	29.663	28.931	78.552	16.663	41.748	50.903	89.360	13.367	32.227	100.708
1-2-1	609	28.283	25.500	76.172	15.747	39.185	51.086	86.240	13.184	31.311	96.863
1-2-2	625	29.663	28.381	78.735	16.663	41.382	55.298	89.360	13.180	32.230	98.510
2-1-1	621	27.649	26.733	74.341	15.381	39.917	50.537	85.510	12.634	30.945	96.130
2-1-2	623	27.832	26.917	75.256	15.564	39.002	49.987	85.880	12.817	31.311	96.497
2-2-1	579	27.649	26.733	73.608	14.465	38.369	50.537	84.230	12.451	30.396	91.919
2-2-2	622	29.297	27.466	75.623	15.564	40.283	50.900	88.990	13.180	31.490	95.210
3-1-1	605	25.452	24.353	68.481	14.648	36.255	47.058	78.000	11.536	28.015	86.426
3-1-2	648	26.733	25.269	70.862	14.832	37.720	50.171	81.670	12.085	29.114	91.553
3-2-1	644	26.917	25.818	71.960	14.648	37.537	50.171	81.480	12.085	29.663	92.835
3-2-2	632	26.733	25.818	73.425	14.465	37.354	48.340	81.670	12.268	29.663	90.088
4-1-1	639	27.650	26.180	73.060	15.381	39.734	50.537	85.510	12.634	30.579	91.553
4-1-2	622	26.184	24.902	69.031	13.550	36.255	47.607	80.380	11.719	28.381	90.271
4-2-1	594	27.100	26.001	72.327	15.015	38.269	51.270	83.130	12.451	30.212	93.384
4-2-2	597	26.917	25.635	71.411	14.099	37.354	49.622	81.120	12.085	29.114	89.722
5-1-1	606	27.283	26.917	74.707	14.832	38.269	55.481	84.960	12.634	30.945	95.032
5-1-2	618	26.920	26.550	73.240	13.733	38.452	54.199	84.780	12.451	30.396	92.102
5-2-1	627	28.015	26.917	76.172	14.465	39.002	56.213	86.430	12.817	31.494	97.595
5-2-2	627	28.381	27.100	75.989	14.125	39.000	54.199	84.560	12.817	29.846	94.666
DOSB Panel											
1	623	21.719	41.406	180.547					21.719	41.406	180.547
2	628	19.063	39.531	176.238					19.063	39.531	176.238
3	654	20.313	41.172	160.781			/		20.313	41.172	160.781
4	623	19.688	48.828	177.969					19.688	48.828	177.969
5	630	20.859	42.188	160.234					20.859	42.188	160.234

Table II.3 Experimental natural frequencies of MDF and DMDF panels in Chapter 4

MDF Panel #	Density (kg/m³)	Frequency-FFFF (Hz)			Frequency-SFFF (Hz)				Frequency-SFSF (Hz)		
		f_{20}	f_{11}	f_{20}	f_{11}	f_{21}	f_{02}	f_{31}	f_{20}	f_{21}	f_{22}
1-1-1	702	23.621	29.114	93.384	16.296	38.09	61.16	80.38	10.986	31.311	108.948
1-1-2	694	23.987	29.663	93.750	15.930	38.09	60.42	80.75	10.803	30.579	116.821
1-2-1	685	23.438	29.297	93.201	15.560	36.80	59.51	80.38	10.803	31.128	110.046
1-2-2	702	23.438	29.480	93.567	16.113	38.09	60.79	80.93	10.620	30.579	110.200
2-1-1	678	23.620	29.480	92.285	16.113	38.09	62.62	81.12	10.620	31.128	105.652
2-1-2	677	23.621	29.663	94.116	15.747	37.72	61.16	80.02	10.803	31.860	110.413
2-2-1	702	23.438	29.114	91.187	15.747	37.72	61.52	79.47	10.620	31.494	108.582
2-2-2	699	23.804	29.297	92.835	16.479	38.82	62.81	81.85	10.803	32.227	110.962
3-1-1	691	23.987	30.212	94.849	16.663	39.18	64.46	82.76	11.169	32.593	111.694
3-1-2	686	23.804	30.029	95.032	16.846	39.55	63.08	82.95	10.986	32.593	111.145
3-2-1	718	24.350	30.210	95.030	15.930	39.00	61.16	78.37	10.986	32.227	114.258
3-2-2	715	23.804	29.297	95.032	16.113	38.82	62.62	80.38	10.990	31.860	113.700
4-1-1	675	23.254	28.198	88.074	15.930	36.99	60.06	78.19	10.254	29.480	104.187
4-1-2	678	23.254	28.381	88.623	16.296	38.27	61.71	79.10	10.254	28.198	103.272
4-2-1	699	23.438	29.663	97.595	16.663	38.82	63.17	83.13	10.620	31.677	114.807
4-2-2	709	23.438	29.846	97.595	16.663	39.00	63.35	78.55	10.620	31.677	112.610
5-1-1	707	23.438	29.297	92.102	16.480	38.27	60.61	78.55	10.803	32.593	112.061
5-1-2	714	24.350	30.210	94.850	16.846	39.92	63.54	82.95	10.986	32.593	114.075
5-2-1	707	23.990	30.030	93.930	16.480	38.64	62.07	82.03	10.986	32.776	113.525
5-2-2	697	23.620	29.297	91.553	16.200	38.72	62.71	81.30	10.803	32.044	110.413
DMDF Panel											
1	715	44.688	54.063	175.781					18.969	55.313	207.406
2	710	42.344	51.250	163.438					18.438	52.971	188.188
3	700	42.031	51.406	165.625			/		17.500	53.125	188.594
4	695	41.563	49.219	155.000					17.578	51.016	193.125
5	718	42.188	50.630	162.656					16.719	52.188	202.500

Table II.4 Experimental natural frequencies of mass timber panels in Chapter 5

Panel #	Density (kg/m^3)	Length (m)	Width (m)	Thickness (mm)	Frequency (Hz)		
					f_{20}	f_{21}	f_{22}
C-78-3s-1	523	4.86	2.47	78	7.324	9.384	23.94
C-97-3s-1	520	5.02	2.47	97	8.194	9.888	18.72
C-105-3s-1	520	9.95	2.47	105	2.197	5.081	21.96
C-105-3s-2	520	6.85	2.47	102	4.669	8.331	25.45
C-105-3s-3	520	5.45	2.47	102	6.912	9.247	26.23
C-105-3s-4	520	2.95	2.47	102	18.87	19.34	30.51
C-105-3s-5	520	3.21	2.47	105	18.63	19.10	34.65
C-105-3s-6	520	11.10	2.47	105	1.717	4.646	22.64
C-105-3s-7	520	6.45	2.47	105	5.31	7.645	23.53
C-131-5S-1	523	4.87	1.02	134	11.38	30.88	289.13
C-131-5S-2	525	4.87	1.02	134	11.25	31.13	285.90
C-131-5S-3	525	4.87	1.02	134	11.50	30.50	291.30
C-175-5s-1	520	15.98	2.47	175	1.328	4.852	63.72
C-175-5s-2	520	17.70	2.47	175	1.053	4.166	61.66
C-175-5s-3	520	17.70	2.47	175	1.075	4.211	60.79
C-175-5s-4	520	17.70	2.47	175	1.063	4.211	61.25
C-175-5s-5	520	17.70	2.47	175	1.099	4.257	61.39
C-175-5s-6	520	17.70	2.47	175	1.075	4.166	62.67
C-175-5s-7	520	17.70	2.47	175	1.099	4.211	61.78
C-175-5s-8	520	16.40	2.47	175	1.236	4.761	64.36
C-175-5s-9	520	4.00	1.57	171	18.16	22.19	147.9
C-175-5s-10	520	17.70	2.47	175	1.087	4.074	61.02
C-175-5s-11	520	17.70	2.47	175	1.053	4.126	60.65
C-175-5s-12	520	17.70	2.47	175	1.099	4.211	62.26
C-220-7S-1	539	8.30	1.00	217	6.226	21.51	499.8
C-220-7S-2	535	8.30	1.00	218	6.317	20.78	487.5

Panel #	Density (kg/m³)	Length (m)	Width (m)	Thickness (mm)	Frequency (Hz)		
					f_{20}	f_{21}	f_{22}
A-3s-120-1	436	6.50	0.90	119	7.073	20.35	169.6
A-3s-120-2	427	6.50	0.90	119	6.836	21.64	176.1
A-3s-120-3	437	6.50	0.90	119	7.188	20.94	168.4
A-3s-120-4	443	6.50	0.90	119	7.266	20.66	163.2
A-3s-120-5	431	6.50	0.90	119	6.992	21.05	170.6
A-3s-120-6	426	6.50	0.90	119	6.758	21.21	172.9
B-3s-100-1	440	10.55	2.30	100	2.06	5.31	32.31
B-3s-120-1	440	10.35	3.00	120	2.43	5.45	21.20
B-5s-100-1	440	11.05	3.00	100	1.69	4.00	30.88
B-5s-100-2	440	11.05	3.00	100	1.66	3.94	29.94
B-5s-100-3	440	12.65	2.80	100	1.25	3.44	33.38
B-5s-100-4	440	12.65	2.80	100	1.22	3.44	33.88
B-5s-100-5	440	12.65	2.80	100	1.25	3.56	34.06
B-5s-100-6	440	11.05	2.80	100	1.69	4.19	33.88
B-5s-100-7	440	12.65	2.50	100	1.31	3.81	43.25
B-5s-120-1	440	13.25	2.30	120	1.44	4.81	46.63
B-5s-150-1	440	9.40	2.44	150	3.81	8.69	47.06
B-5s-160-1	440	9.35	2.50	160	4.03	9.13	49.94
B-5s-160-2	440	10.15	2.30	160	3.44	8.88	57.75
B-5s-160-3	440	10.35	2.80	160	3.25	7.63	42.13
B-5s-160-4	440	8.05	3.00	160	5.44	9.38	37.38
B-5s-200-1	440	13.75	2.50	200	2.13	6.94	80.13
B-7s-220-1	440	5.57	1.98	220	15.39	22.85	99.88
B-7s-220-2	440	12.00	2.95	220	3.38	7.94	49.81
B-8s-300-1	440	7.40	2.50	300	12.13	20.55	82.17
D-3s-40-1	446	6.02	2.01	40	2.625	4.875	15.969
D-3s-40-2	442	6.02	2.01	40	2.578	5.098	16.406
D-3s-40-3	437	6.02	2.01	40	2.617	4.961	2.617
D-3s-55-1	439	4.00	2.01	55	7.246	10.98	36.09

Appendix III Identification of Elastic Properties of Laminated Strand Lumber

A full-size Laminated Strand Lumber (LSL) panel with a length of 2.44 m, a width of 1.22 m and a thickness of 38.2 mm was tested by the proposed method in Chapter 3. The LSL panel was made from strands of aspen with a moisture content of 12% and a density of 725 kg/m^3. The elastic constants obtained by modal test is listed in Table III.1.

Table III.1 Elastic constants of a LSL panel

Methods	E_x (MPa)	E_y (MPa)	G_{xy} (MPa)
Plate Vibration	10733	2227	1599
Beam vibration[*]	12280	1917	/
Static[*]	11331	1350	/

[*]: Cited from (Niederwestberg et al. 2016), which conducted the beam vibration and static bending tests of the same LSL panel.

Curriculum Vitae

Candidate's full name: Jianhui Zhou

Universities attended: Bachelor of Engineering in Wood Science and Engineering, South China Agricultural University, 2011

Master of Engineering in Wood Science and Technology, South China Agricultural University, 2014

Publications:

Zhou, J., Chui, Y.H., Gong, M., Lin, H. (2017). Comparative study on measurement of elastic constants of wood-based panels using modal testing: choice of boundary conditions and calculation methods. *Journal of Wood Science*, 112, 203-212.

Zhou, J., Chui, Y. H., Gong, M., Lin, H. (2017). Elastic properties of full-size mass timber panels: Characterization using modal testing and comparison with model predictions. *Composites Part B: Engineering*, 112, 203-212.

Zhou, J., Chui, Y.H., Gong, M., Lin, H. (2016). Simultaneous measurement of elastic constants of full-size engineered wood-based panels by modal testing. *Holzforschung,* 70 (7), 673–682.

Zhou, J., Hu, C., Ma, X., & Guo, X. (2014). Finite element modeling and experimental validation of radio frequency heating (RFH) of curved laminated wood-based panels. *Holzforschung*, 68 (6), 699–705.

Zhou, J., Zhou, H., Hu, C., & Hu, S. (2013). Measurements of thermal and dielectric properties of medium density fiberboard with different moisture contents. *BioResources*, *8*(3), 4185-4192.

Zhou, J., Hu, C., Hu, S., Yun, H., & Jiang, G. (2012). Optimization of hinge configuration of furniture doors using finite element analysis. *BioResources*, *7*(4).

Zhou, J., Hu, C., Hu, S., Yun, H., Jiang, G., & Zhang, S. (2012). Effects of temperature on the bending performance of wood-based panels. *BioResources*, *7*(3), 3597-3606.

Zhou, J. H., Hu, C. S., Hu, S. F., Yun, H., Jiang, G. F., & Zhang, S. K. (2012). Analytical solution and FEM simulation of transient heat transfer for the heating of medium density fiberboard. *Transactions of Materials and Heat Treatment*, *33*(5), 143-148. (In Chinese)

Wang, Z., Dong, W., Wang, Z., **Zhou, J.**, Gong, M. (2018). Effect of macro characteristics on rolling shear properties of fast-growing poplar wood laminations. *Wood Research*, 63 (2), 227-238.

Wang, Z., **Zhou, J.**, Dong, W., Yao, Y., Gong, M. (2018). Influence of technical characteristics on the rolling shear

properties of cross laminated timber by modified planar shear tests. *Maderas-Cienc Tecnol*, 20 (4), 1-19.

Liao, Y., Tu, D., **Zhou, J.**, Zhou, H., Yun, H., Gu, J., Hu, C. (2017). Feasibility of manufacturing cross-laminated timber using fast-grown small diameter eucalyptus lumbers. *Construction & Building Materials,* 132, 508–515.

Wang, Z., **Zhou, J.**, Gong, M., Chui, Y. H., & Lu, X. (2015). Evaluation of modulus of elasticity of laminated strand lumber by non-destructive evaluation technique. *BioResources*, 11(1), 626-633.

Hu, C., Jiang, G., **Zhou, J.**, Xiao, M., & Yi, Z. (2013). Effects of thickness of the heat-treated wood specimen on water-soluble extractives and mechanical properties of merbau heartwood. *BioResources*, *8*(1), 603-611.

Hu, C., Jiang, G., Xiao, M., **Zhou, J.**, & Yi, Z. (2012). Effects of heat treatment on water-soluble extractives and color changes of merbau heartwood. *Journal of wood science*, *58*(5), 465-469.

Hu, S., **Zhou, J.**, Yun, H., Hu, C. (2011). Detection of sound knots and dead knots on sugi timber using grey level co-occurrence matrix parameter. *Wood Processing Machinery*, 5. 11-15. (In Chinese)

Wang T.J., **Zhou J.H.**, Zhu Y. et al. (2009). Overview of the furniture related standards and its trends. *Guangdong Forestry Science and Technology*. 25 (6): 100-105. (In Chinese)

Conference Presentations:

Zhou, J., Niederwestberg, J., Chui, Y., Gong, M. (2018). Bending properties of innovative multi-layer composite laminated panels. In *the 15th World Conference on Timber Engineering*, Seoul, Korea.

Niederwestberg, J., **Zhou, J.**, Chui, Y., Gong, M. (2018).

Shear properties of innovative multi-layer composite laminated panels. In *the 15th World Conference on Timber Engineering*, Seoul, Korea.

Niederwestberg, J., **Zhou, J.**, Chui, Y. (2018). Strain distribution

of 5-Layer composite laminated panels using digital imaging correlation technique. In *the 15th World Conference on Timber Engineering*, Seoul, Korea.

Zhou, J., Chui, Y., Schickhofer, G., Frappier, J. (2016).

Elastic constants of cross laminated timber panels of industrial size: non-destructive measurement and verification. In *the 14th World Conference on Timber Engineering*, Vienna, Austria.

Zhou, J., Chui, Y. (2015). Influence of boundary conditions on measurement of elastic constants of engineered wood-based panels using modal testing. In *the 19th International*

Nondestructive Testing and Evaluation of Wood Symposium, Rio de Janeiro, Brazil.

Zhou, J., Chui, Y. (2014). Efficient measurement of elastic constants of cross laminated timber using modal testing. In *the 13th World Conference on Timber Engineering*, Quebec City, Canada.

Niederwestberg, J., **Zhou, J.**, Chui, Y. (2014). Influence of boundary conditions in modal testing on evaluated elastic properties of mass timber panels. In *the 13th World Conference on Timber Engineering*, Quebec City, Canada.

Zhou, J., Niederwestberg, J., Chui, Y., Hu, C. (2014). Determination of elastic constants of cross laminated timber (CLT) by modal testing. In *the 12th Pacific Rim Bio-Based Composites Symposium*, Beijing, China.

Hu, C., **Zhou, J.**, Zhu, J. Y. (2014). Some key issues on manufacturing curved wood-based furniture components using radio frequency heating. In *the 12th Pacific Rim Bio-Based Composites Symposium*, Beijing, China.